Study respecting the design, development and supply of a domestic communications satellite system : interim report

Table of Contents

INTRODUCTION

This material constitutes the Interim Report on the contract raised under Department of Industry Requisition Number 4296-37 and Treasury Board Number 681847 entitled "Study Respecting the Design, Development and Supply of a Domestic Communications Satellite System". This report concerns the Phase I activities in respect to the system and satellite trade-off studies and the preliminary design of a selected spacecraft.

The first portion of the report consists of two sections, the first of which concerns the total system analysis and particularly the relationship between the satellite capabilities and the ground terminal requirements. Section two contains the data concerning the potential launch vehicles as provided by their respective manufacturers, and an analysis of the missions in respect to the launch phases, telemetry and command constraints, etc.

Section three reports the trade-off studies towards, and the preliminary designs of, the respective spacecraft systems. Thus section three initally discusses some of the possible trade-offs available within the vehicle and shroud constraints and the various communications capabilities resulting. This section then presents preliminary design data in regard to the antenna, the transponder, and the tracking, telemetry and command systems.

The succeeding parts of section three describe the design and specification of the various spacecraft systems or area of major design concern e.g. weight and thermal aspects. The final portion of the section contains the preliminary layouts and general configuration of the selected preliminary design.

It may be noted that this interim report is a summary of the Phase I Studies and does not include the details of the derivations upon which these data are based. Further it must be kept in mind that because of various approximations and assumptions, much of the information is most useful in comparisons between different spacecraft subsystems and configurations. Refinements of these data can only be done by detailed examination of a selected design. Notwithstanding this, it is believed that most of the approximations err on the conservative side.

PART I

DESIGN CONSIDERATIONS

Although the basic satellite parameters for the Canadian domestic satellite have been defined in the Department's work statement, RCA Victor has undertaken a number of system studies related to the overall performance and requirements which, in general, support the Department's choice of satellite parameters. However, some of these studies indicate that for optimum system performance, certain satellite parameters should be modified.

SUMMARY

From this preliminary study, the following conclusions can be drawn and will be confirmed in the final report.

a) The specified orbit inclination inaccuracy of $\pm 0.2^{\circ}$ should be reduced to $\pm 0.1^{\circ}$. This improved inclination control is easily attained and will result in lower degradation due to pointing errors for the small fixed antenna stations. This in turn will permit a smaller antenna size to achieve the required communications performance.

b) It appears feasible to use a 32 foot diameter "fixed" antenna with an uncooled paramp. of 100°K noise temperature to provide high quality television performance (55 db video signal to weighted RMS noise) including a separate sound carrier. The G/T which can be achieved with this arrangement is about 29 db which results in a downlink carrier-to-noise ratio of about 19 db. This performance assumes satellite ERP of 34 dbW at the satellite antenna beam edge.

c) If large antennas are used to provide a G/T ratio of 40.7 db, it is feasible to carry up to 1500 voice channels. A station with a G/T ratio of 36.7 db can carry up to 1200 channels.

d) The cost differential between a fully tracking station and non-tracking station is very large.

1. Systems Analysis

In establishing a synchronous satellite system, careful consideration must be given to total performance objectives of the system, i.e. traffic requirements, channel capacity, operational objectives, etc. Trade-off studies must be made to determine the most practical and economical system. RCA Victor is currently engaged on such studies with a view towards obtaining optimum system performance.

The following pages contain discussions on the various factors which influence the choice of overall system parameters. The discussions are centred largely

on the satellite and the small receive-only stations since overall system performance is established mainly by these two elements. The main communication and control stations will have large diameter antennas, large G/T ratios and will be fully steerable. There will therefore, be no system performance limitations due to these stations.

1.1 Factors affecting Performance

a) Satellite Drift

Drift Mechanisms: A satellite in orbit is subject to perturbations which cause the inclination, eccentricity and subpoint longitude of an initially perfect synchronous orbit to change. The dominant forces are radiation pressure and variations in the gravitational field. The variations in the gravitational field are caused by the asphericity of the earth and the gravitational fields of the sun and moon. The effect of radiation pressure is to cause a circular orbit to become eccentric and then circular again each year. Triaxiality of the earth causes the satellite to oscillate about the minor axis of the earth's equator. Points of stable equilibrium occur at 74°E and 106°W longitude, and the initial drift rate depends on the distance from the stable points, the maximum occurring halfway between the stable and unstable points.

The major effect of the sun and moon is to increase the orbit inclination. The sun causes an increase of 0.27 degrees/year, and the increase due to the moon varies with the inclination of the moon's orbit to the equatorial plane. The effect of the moon on orbit inclination varies from 0.48 degree/year to 0.68 degree/year, with an 18.6 year period. The effect of sun and moon together, in 1972, will be about 0.91 degree/year and will decrease to 0.75 degree/year in 1978, as discussed in Section 2 on Mission Analysis.

Effect on System Performance: As viewed from the surface of the earth, the motion of an inclined synchronous orbit is a "figure eight", traced each sidereal day. For an inclination of 0.1 degrees, the width of the "figure eight" is vanishingly small, and the height, as seen from the earth, depends on the latitude and relative longitude of the earth station and satellite subpoint. Eccentricity of the orbit also causes a diurnal variation, in this case, it is a longitudinal drift of $\pm 2e$ and where e is the eccentricity of the orbit. Longitudinal drift caused by triaxiality has no diurnal variation, and if uncorrected, would librate about 106°W longitude with a period (of the order of years) dependent on the initial position.

Assuming that the satellite can be kept on station within 0.1 degree in longitude and inclination drift, the largest angular excursion will be 0.156° from nominal position for most stations in Canada, decreasing

somewhat for northern stations. For a tracking antenna satellite drift will not lead to a reduction in system gain, however, for a non-tracking antenna the gain reduction depends on the beam width. Figure 1-1 shows the attainable G/T (gain-to-noise temperature ratio) for conditions of maximum drift. Combinations of maximum longitude and inclination drift occur for a small fraction of the time and the degradation due to drift is treated as a fade in section 1.1(d).

b) Small Earth Station Pointing Errors

It is assumed that all earth stations except the large diameter main communication and control stations will have non-steerable antennae. These antennae will, however, be capable of manual positioning to provide coverage of the visible synchronous belt. These earth stations will thus be subject to degradations in receive C/T (carrier-to-noise temperature ratio) due to antenna pointing errors. These errors can be divided into two parts:

i. error due to satellite position movement,

ii. error due to earth station initial adjustment errors and environmental disturbances.

The effect on receive system performance of satellite station tracking errors is described in 1.1 a). The initial antenna positioning error is largely a matter of the time and effort expended; with a reasonable amount of effort it should be possible to position the antenna so that this initial set-up error is negligible.

Environmental conditions which affect pointing accuracy include:

i. wind induced errors,

ii. errors due to reflector surface deformations caused by ice and snow loads,

iii. variations in refractive bending.

None of these contributions is expected to affect significantly the receive C/T with the possible exceptions of ice and snow loads. With antennae of about 30 ft. diameter wind induced errors can be kept very small without resorting to costly antenna structures. The refractive bending variations are maximum at the lowest elevation angles (5°) but even here they will be small compared to the antenna beamwidth. Degradation due to ice and snow loads may be significant in some parts

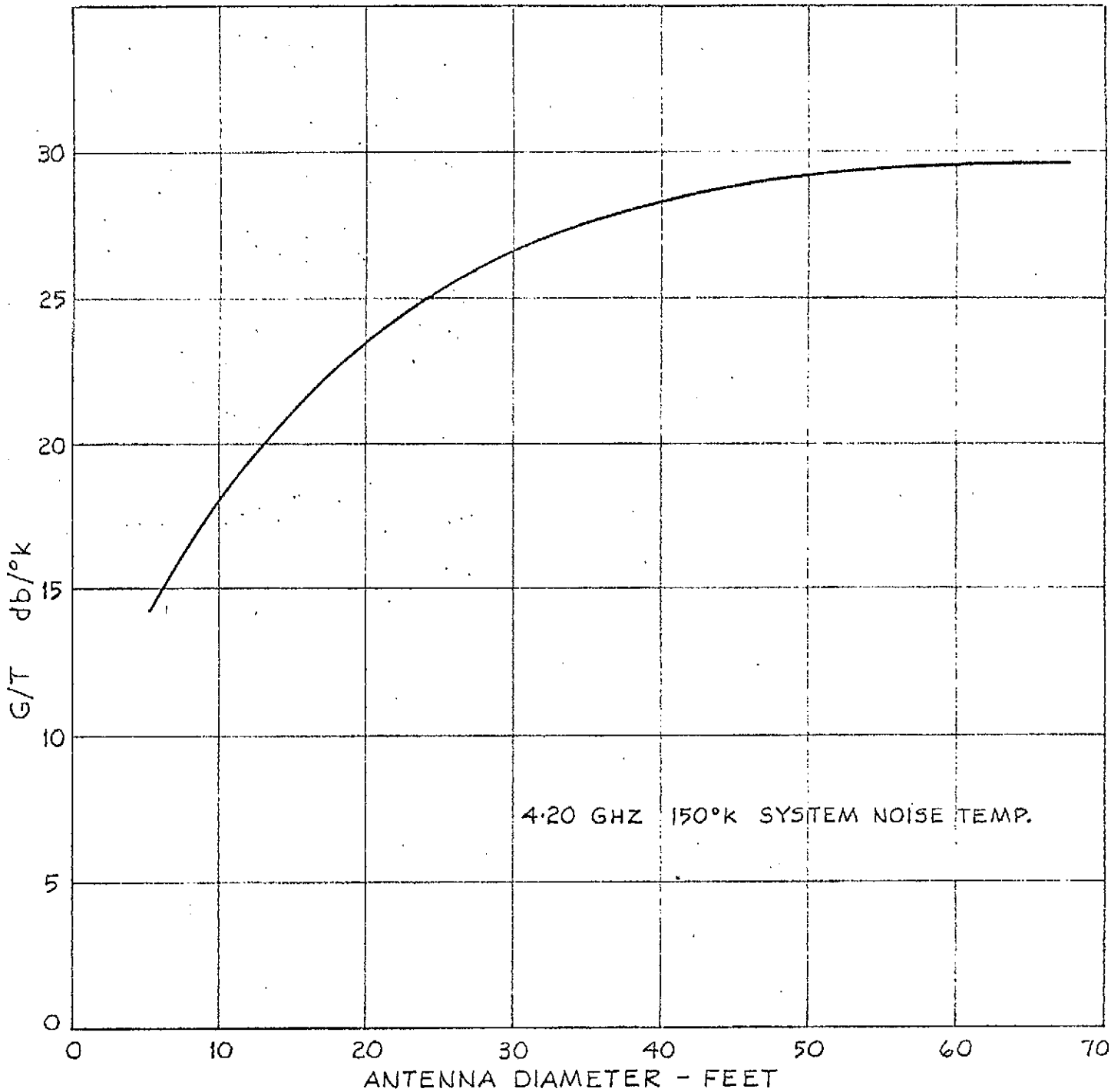

FIG. 1-1

MINIMUM EFFECTIVE G/T FOR NON-TRACKING ANTENNA VS. SIZE.

SATELLITE STATION KEEPING ± 0·1 DEGREE IN DRIFT AND INCLINATION.

of the country, particularly northern Canada, and design of earth stations for these regions must take cognizance of this environment. Special deicing and snow removal techniques may be required for these stations. In summary, "small" earth station pointing errors will generally be small and will not significantly affect station performance.

c) Path Loss

Calculation of earth station performance at any particular site must take into account the path loss between the satellite and the earth station. Two components contribute to total path loss: free space attenuation, which varies with slant range to the satellite, and atmospheric attenuation, which varies with elevation angle. Both slant range and elevation angle are functions of earth station latitude and of the relative longitude of the earth station and satellite sub-point. Figure 1-2 shows the total path loss at 4 GHz a function of longitudes and latitudes in Canada.

Canada, with much territory at high latitudes will experience considerable variation in path loss with site location. The peak difference will be about 0.7 db so this factor must be taken into account when plotting the effective beam coverage of Canada. The combination of the projected antenna beam contours and path loss will result in contours of equal flux density. This is described in more detail in Section 1.6.

d) Fading Distribution

Calculations of station performance on a statistical basis must include C/T degradations due to all environmental conditions. The major contributor to fade, for both large and small stations, is rainfall. Obviously, this will vary widely across the country. Rainfall data shows that maximum annual rainfall occurs along the coast of British Columbia while maximum short term rainfall intensity occurs in southern Ontario. Central Alberta and the Atlantic coast also have relatively high short term rainfalls.

Prediction of station fade due to rainfall can only be estimated since the data available on total weather patterns for a given location is limited. Fade calculation requires a knowledge of rainfall intensity distribution as well as the mean width and height of a rainstorm. In general, high intensity rainfalls occur over relatively small areas while low rainfalls or drizzle can be tens of miles in extent.

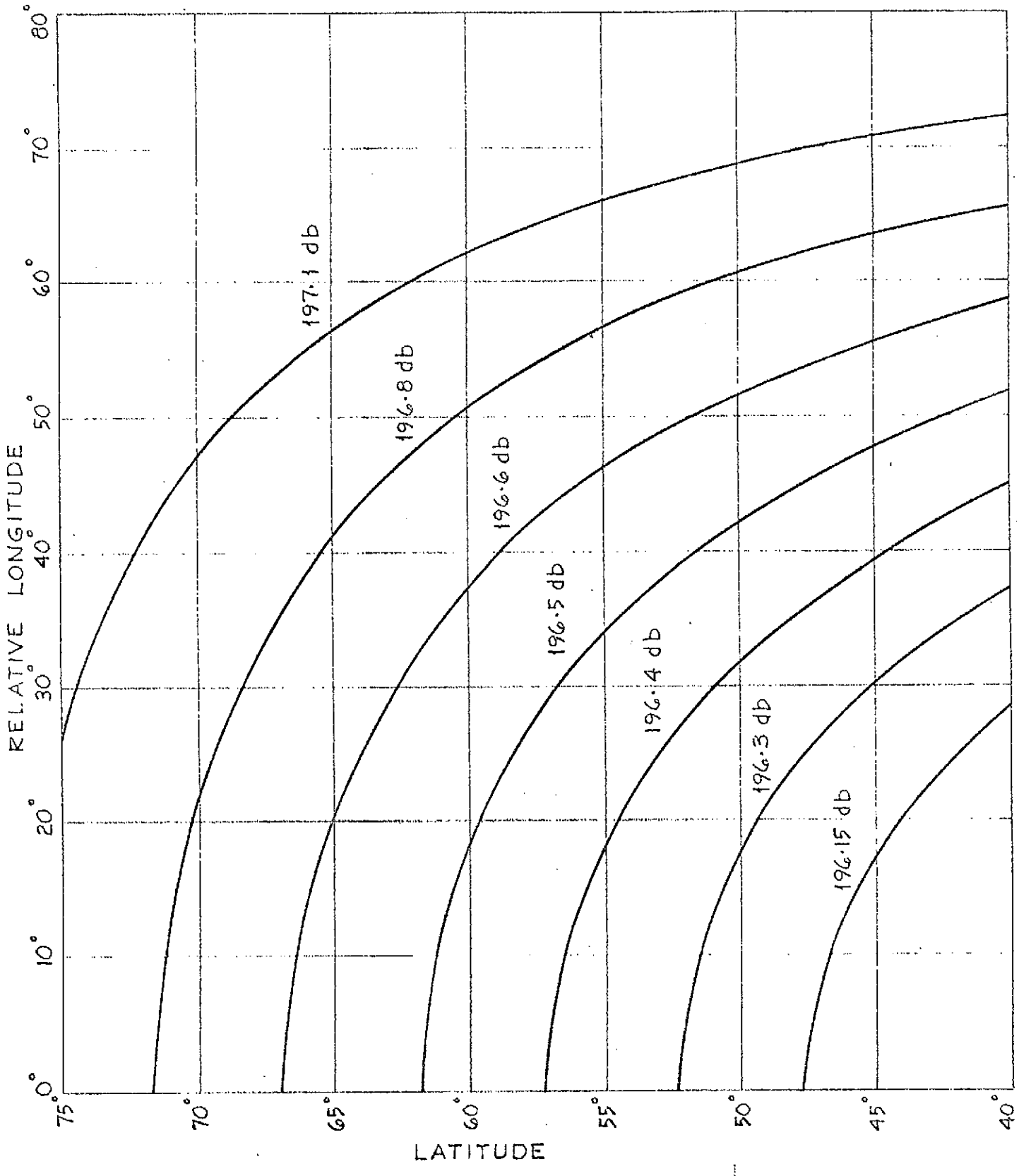

FIG. 1-2

TOTAL PATH LOSS IN db VS. SITE LOCATION

4.0 GC.

The presence of a rainfield in front of an earth station antenna degrades system performance in two ways: the rainfield acts as an attenuator and directly reduces incoming signal strength, and this attenuation further deteriorates the system performance by increasing the overall receive noise temperature.

Figure 1-3 shows a fade distribution curve for a typical small earth station located in southern Canada. Assumptions made for the derivation of this curve include:

i. Total annual rainfall approximately 50 inches.

ii. Station system noise temperature in clear weather = 150°K

iii. Overall receive C/T is degraded 1 db due to up-link and satellite noise plus a further 1 db due to adjacent satellite and terrestrial interference.

It can be seen that station fade due to rainfall is acceptable and will not impose any limitations on the design of the small earth stations. Fade due to wind or refractivity variations will be second-order compared to rainfall.

In addition to the fade due to weather, the receive C/T at any particular location will experience fluctuations caused by inaccuracies in satellite position keeping and antenna pointing. The worst earth station location from an overall fade point of view will be for points at the nominal beam edge in the eastern and western regions. Overall receive system fade for such a station is shown in Figure 1-4, the reference signal level being based on a satellite EIRP of 34 dbW at the nominal beam edge. This curve has been derived by a convolution of the individual fading curves due to rainfall, satellite pointing inaccuracy and satellite position keeping accuracy. The overall fade distribution assumes the following:

i. Satellite EIRP at the 8 1/2° x 3 1/4° beam edge is 34 dbW (optimum as shown in 1.6 b).

ii. Satellite antenna pointing accuracy is $\pm$ 0.5° each axis; 3-sigma gaussian distribution.

iii. Earth station is located at a position 4.25° - 0.5° (3-sigma) east or west of the nominal beam centre.

iv. Earth station antenna pointing error degradation (30 ft. diameter non-tracking antenna) assumes all satellite positions $\pm$ 0.1° longitude and $\pm$ 0.1° inclination, are equally probable.

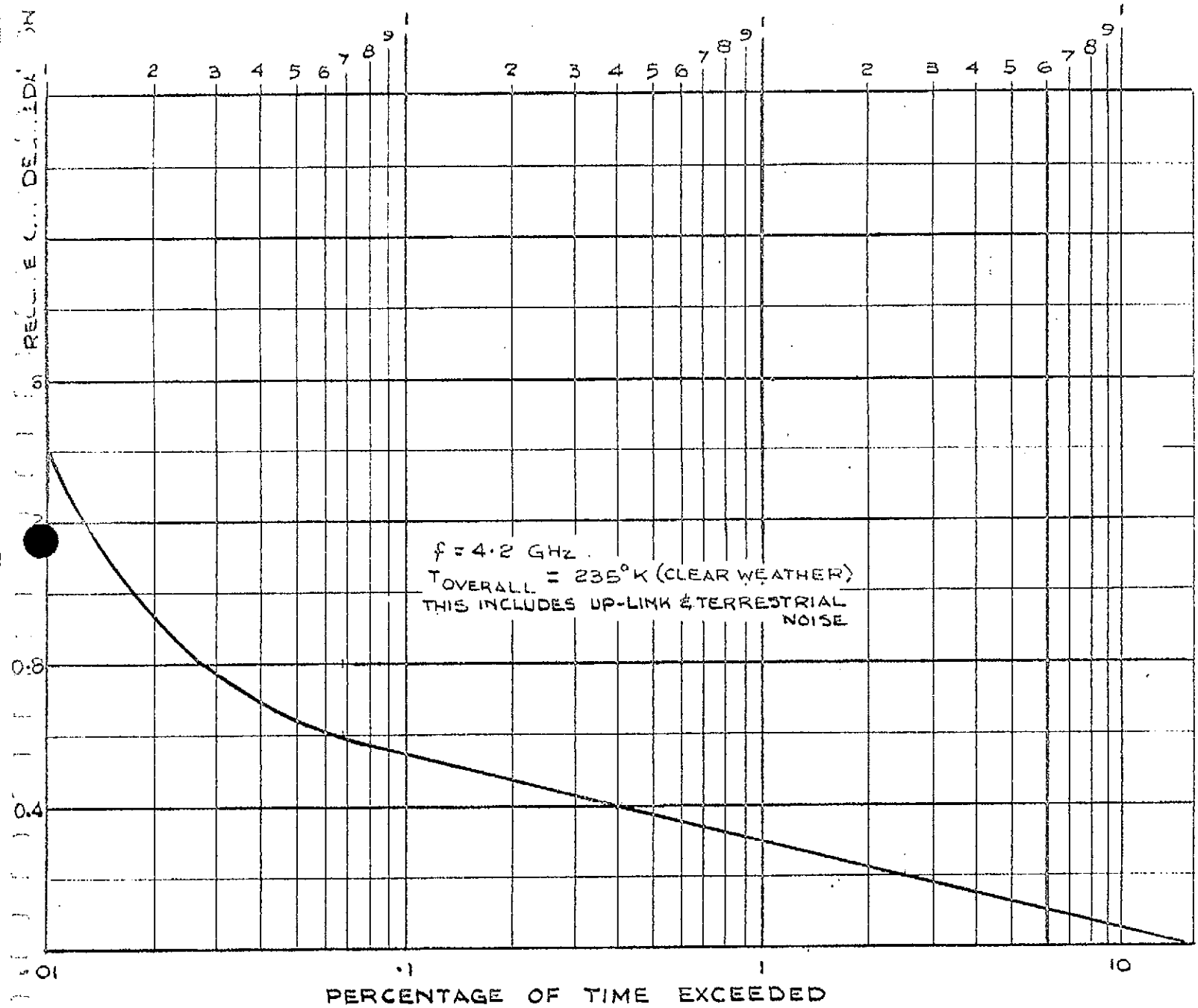

FIG. 1-3

TYPICAL EARTH STATION FADE FOR SOUTHERN CANADA

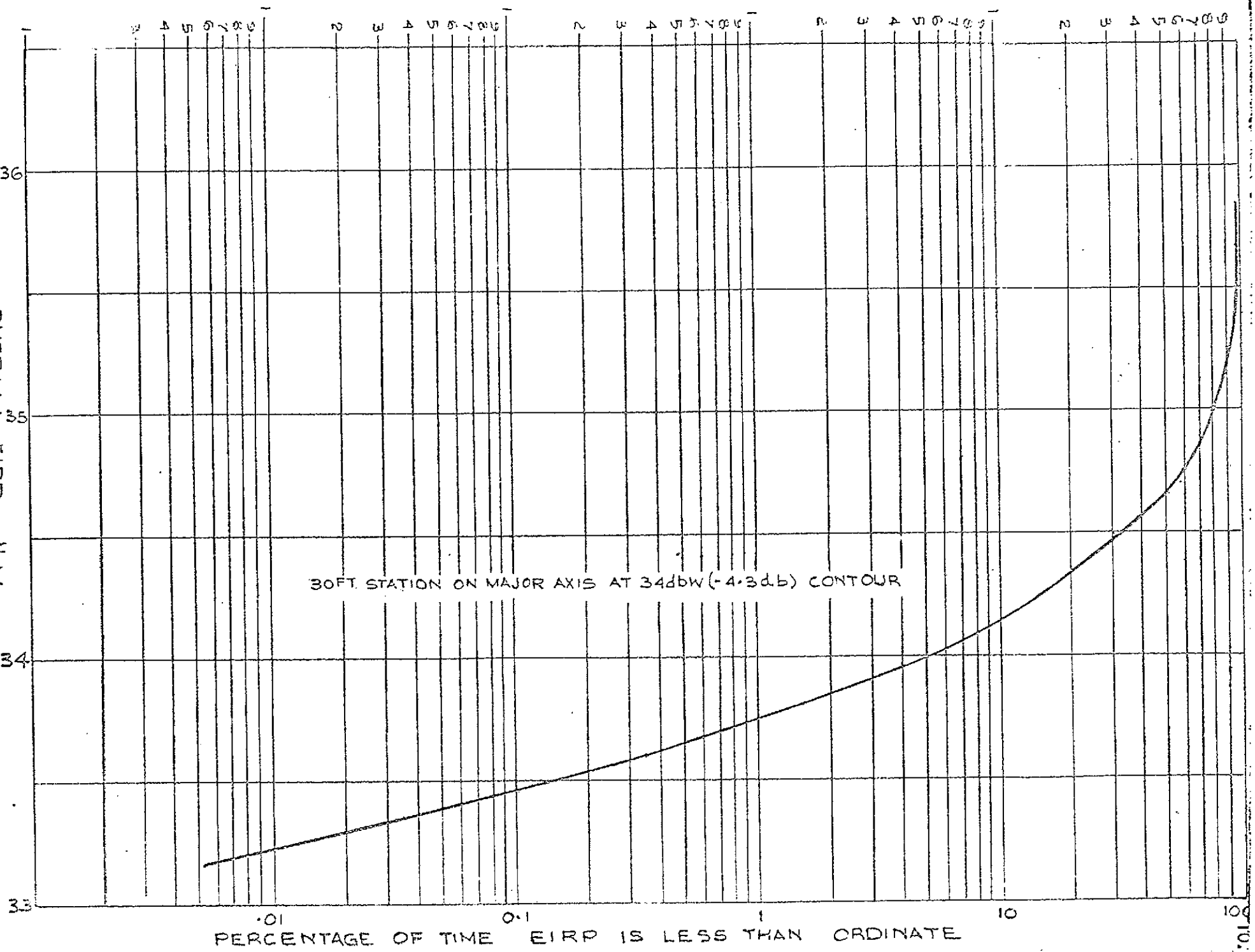

FIG. 1-4

EARTH STATION FADE DUE TO RAINFALL + SATELLITE POINTING + SATELLITE DRIFT

v. Rainfall fade distribution curve in Figure 1-3 applies.

The composite fade curve does not include the effects of initial earth station antenna positioning error, wind induced pointing errors, refractivity errors and errors due to snow or ice loads. As stated previously, however, these errors are expected to be of second order magnitude compared to the primary errors.

e) Noise Objectives and Budgets

In order to determine overall system parameters, the basic overall noise requirements must be defined. These requirements can be divided into three sections: telephony channel video and video programme. The following requirements have been used as a basis for calculation.

Telephony	7500 pWp for the worst channel
Video	55 db peak to peak for high quality (47 db nominal quality)
Programme	57 db psophometric at +9 dbmO

From these requirements the following noise budgets can be used:

Telephony:	Multiple Carrier Operation	Trunk Operation
Adjacent satellite interference	1000 pWp	1000 pWp
Terrestrial Link interference	1000 pWp	1000 pWp
Up-path Thermal	1000 pWp	1000 pWp
Intermodulation	1500 pWp	1000 pWp
Down-path Thermal	3000 pWp	3500 pWp
TOTAL	7500 pWp	7500 pWp

Video (High Quality):

Adjacent satellite interference effect in baseband	S/N = 65 db
Terrestrial link interference effect in baseband	S/N = 65 db
Up-path thermal 6 db below down path thermal	S/N = 63.1 db
Down path thermal noise	S/N = 57.1
TOTAL	S/N = 55 db

f) Earth station Noise Temperature

Earth station system noise temperature objectives are dependent on the desired station G/T ratio. For the main communication and control stations with a G/T ratio of 36 to 40.7 db it is necessary to use cooled parametric amplifiers to achieve the lowest possible noise temperature. Typically stations in this category can achieve system noise temperatures of about 70°K.

For the small TV receive-only stations with a G/T requirement of 27 - 30 db uncooled paramps. can be used. Stations of this type would be expected to have system noise temperatures of about 150°K. These paramps. will of course be more reliable and simpler to maintain than the cooled paramps. These stations will also be less subject to rainfall fade since the increase in system noise temperature due to rainfall will be less significant than for a low noise station.

g) Sun Outage and Eclipse Operation

Solar Transits and Eclipses: Near the vernal and autumnal equinoxes the sun has a number of undesirable effects on both the space and earth segments of the system: the sun's apparent path causes it to pass behind the satellite as seen by an earth station, and to pass behind the earth as seen by the satellite. The transit of the sun through the earth station beam causes the receive system noise temperature to approach that of

the sun. The passage of the sun behind the earth eclipses the sun from the satellite for which the present study envisages storage cells of sufficient capacity to enable two channels to operate during an eclipse. Fortunately eclipses occur during the hour after local midnight at the satellite subpoint and thus at a time when traffic would be relatively light for most of the country. The moon can also pass behind the satellite and cause an increase in receiver noise, however, the temperature of the moon is about 236°K and the increase in noise temperature should be within the station margin.

Total eclipse of the sun by the moon, as seen by the satellite will occur with about the same frequency as a total eclipse at a given spot on earth, but will last slightly longer. This is such a rare event that it can be considered negligible in comparison with eclipses of the sun by the earth.

The sun also causes system degradation by another mechanism. This occurs when the sun comes sufficiently close to the satellite's receive antenna beam to cause an increase in the up-link noise temperature budget. Assuming a satellite noise figure of 7 db, the worst case degradation gives a noise figure of 9 db. This occurs twice a year, just before the autumn eclipse and just after the spring eclipse. The degradation becomes progressively less on days preceding and succeeding the day of worst case occurrence. This type of degradation will have negligible effect on system performance.

Duration of Eclipses: Satellite eclipses by the earth are highly predictable, and tables have been computed to give in umbra, penumbra and time of occurrence for any arbitrary circular orbit[1]. In general, eclipses occur once per day for 43 days in the spring and 43 days in the autumn, with the longest eclipse (69 minutes) occurring on or about March 22 and September 22.

Duration of Solar Transits: Solar transits of the earth station antenna cause fading so deep, that it must be considered a communication outage. RF energy from the sun is not constant and during "disturbed" sun activity the RF level at 4 GHz can be 20 or 30 times greater than the "quiet" sun level. For the majority of the time however, "quiet" sun conditions prevail. At this time the 4 GHz flux level at the earth's surface will be approximately 2×10^{-20} watts/M^2-Hz. In this situation a 60 foot antenna with low sidelobe levels will experience a degradation greater than 3 db for 6 minutes on the worst day, and 5 1/2 minutes and 2 minutes of the two days preceding and succeeding the

1 "Tables for Eclipse Times of an Earth Satellite of Arbitrary Circular Orbit", T. Szirtes, September, 1967, RCA Space Systems, Montreal

worst day. This will happen two months per year, and represents an outage on each of ten days per year. Figure 1-5 is a time distribution curve of the G/T degradation for 60 foot and 30 foot antennas with low sidelobe levels. It is unlikely that these outages would be acceptable to the satellite users. A number of methods for eliminating the outage or reducing it to an acceptable level are discussed below.

i. Earth station antennae can be spaced approximately 500 to 1500 miles apart, depending on antenna size, so that the sun is not in the beam width of both antennae simultaneously. As this would require twice as many terminals, in addition to the microwave hops to connect them to the distribution centre this solution has little to recommend it.

ii. Two satellites can be orbited, and each station can have two antennae per receiver terminal. System costs will not be doubled by this approach since any system must have an orbiting backup satellite if long service disruptions due to satellite failure are to be avoided, and thus there are no extra costs in the space segment. For each receive station only an extra antenna and perhaps paramp are required. The remainder of the receive system can be common to both antennae. This, nevertheless represents a substantial increase in system costs.

For low cost receive only stations, reduced outage time can be achieved by moving the earth station antenna to the second satellite when the sun comes into the region of the first satellite. A preliminary investigation reveals that acceleration rates of $2^{o}/sec^{2}$ and velocities of $2^{o}/sec$ can easily be obtained with the type of antennae envisaged with an unsophisticated positioning system. A very low cost servo is required as it is not a tracking system and can be pre-programmed. Mechanical brakes would hold the antenna at each position. For satellites 6 degrees apart this would cause a 5 second outage, and for satellites 12 degrees apart, this outage would be 7 seconds. If the station is initially using the westernmost satellite, the outages can be kept to one during the day and one at some convenient time at night.

1.2 Orbital Slot Utilization

Our views on using the stationary orbit efficiently have been published* and a copy of the paper is attached. The primary conclusion of the paper is that satellites with identical RF channels can be spaced

* D. Jung, "Defining System Considerations for Canadian Domestic Satellites", Electronics and Communications, June 1968

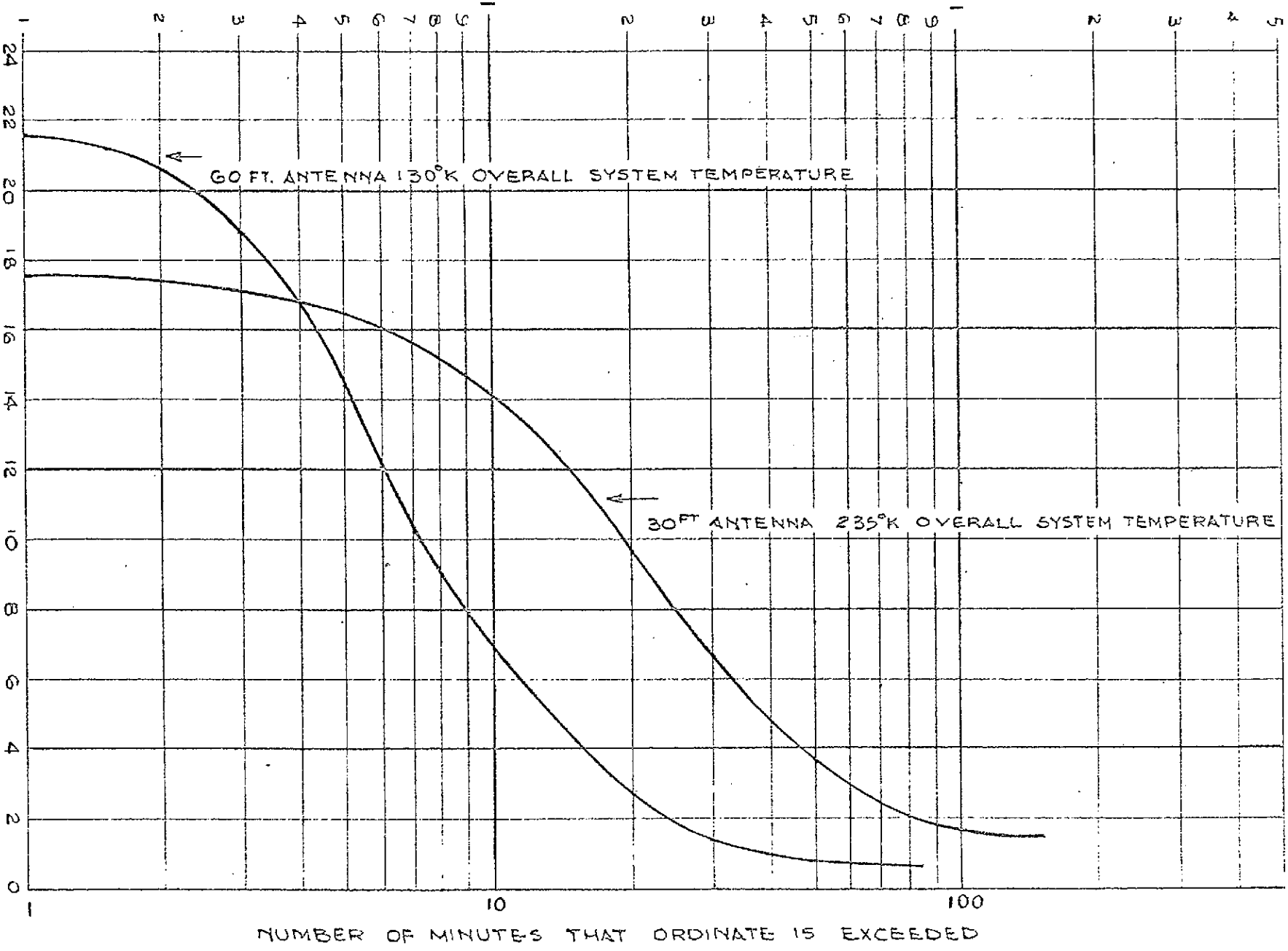

FIG. 1-5

DEGRADATION DUE TO SOLAR RADIATION - WORST MONTH

about 6° apart but if frequency interleaving is applied to adjacent satellites, the spacing can be reduced to about 3°. A proposed frequency plan is shown in Figure 1-6. No tolerances for satellite drift, antenna gain, ERP, etc., were allowed for determining the approximate spacing. However, for a practical system some allowance must be made and a factor of 7/6 appears satisfactory. This will provide a satellite spacing of 7° for the co-channel case and 3.5° for the interleaved case.

Interleaving can also be used for RF channels using multiple carriers. For example, assume that 4 carriers, each carrying 60 channels are transmitted on RF Channel No. 1 of plan A, and assume 1500 channels are transmitted on RF Channel No. 1 of plan B. The worst case interference is caused by one of the 60 channel carriers interfering with the 1500 channel carrier at the worst frequency. but fortunately the satellite ERP of the 60 channel carrier is about 16 db less than that of the 1500 channel carrier. Therefore, the interference in this case will be no more than that caused by 1500 channel carrier into an interleaved 1500 channel carrier.

It should be noted that in the proposed frequency plan, it is found that adjacent RF channels should be crossed polarized in the up link in order to simplify the satellite design. For example, all the odd channels on plan A might be vertically polarized and the even number channels might be horizontally polarized.

1.3 Overall Communications Performance

a) Television

The television performance can be calculated from the following formula:

$$S/N = 10 \log (3/2\ C/kT\ \ \Delta f^2/f_m^3) + 6 + 13$$

where $S/N = \frac{\text{peak-to-peak}}{\text{rms noise}}$ picture in db

C/T = carrier to noise temperature ratio
k = Boltzman's Constant
Δf = peak video signal deviation
f_m = top video frequency
6(db) = rms signal to p-p picture conversion factor
13(db) = pre-emphasis and weighting factor

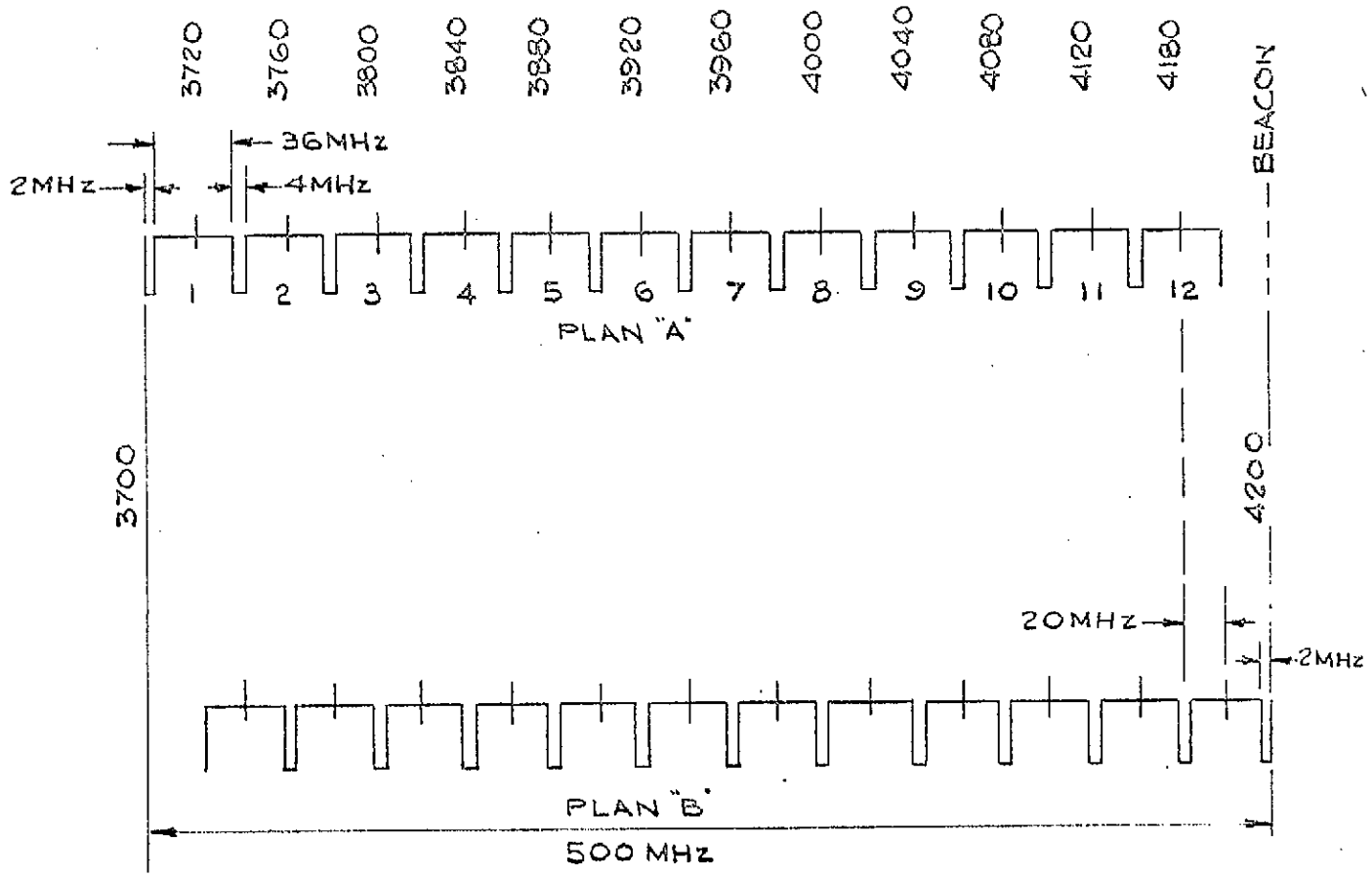

FIG. 1-6

PROPOSED FREQUENCY PLAN FOR ADJACENT SATELLITES.

The C/T is determined from the following assumptions:

ERP at 3 db beam edge	34 dbW
Path Loss at 5°	197.1 db
Isotropic Power	-163.1 dbW

$C/T = -163.1 + G/T$ (db)

The deviation (Δf) is determined from the Carson's Rule bandwidth formula as follows:

$$B = 2(\Delta f + f_m)$$

where B is the receiving bandwidth.

The receive bandwidth has assumed two values 36 MHz and 32 MHz for this calculation. The smaller bandwidth would allow for a program channel to be transmitted adjacent to the video carrier which is the envisaged scheme. With an earth station of 29 db G/T, this bandwidth would give a down path carrier to noise ratio of 19.5 db. It should be noted that some deviation is required for energy dispersal which will affect the transmission bandwidth. This has been considered and is reflected in the results given here.

These parameters can now be substituted into the above equation from which the curves of Figure 1-7 of signal to noise vs. values of G/T were plotted.

b) Telephony

The telephony performance can be calculated from the following formula:

$$S/N = 10 \log \quad C/kT \quad \frac{\Delta f^2}{f_m^2} \quad \frac{1}{2b} \quad + P + W$$

where $S/N = \frac{\text{rms test tone}}{\text{rms noise}}$ in db

C/T = carrier to noise temperature ratio
k = Boltzman's Constant
Δf = test tone peak deviation
f_m = top channel frequency
b = baseband channel bandwidth = 3.1 kHz
P = pre-emphasis advantage for top channel = 4 db
W = psophometric weighting factor = 2.5 db

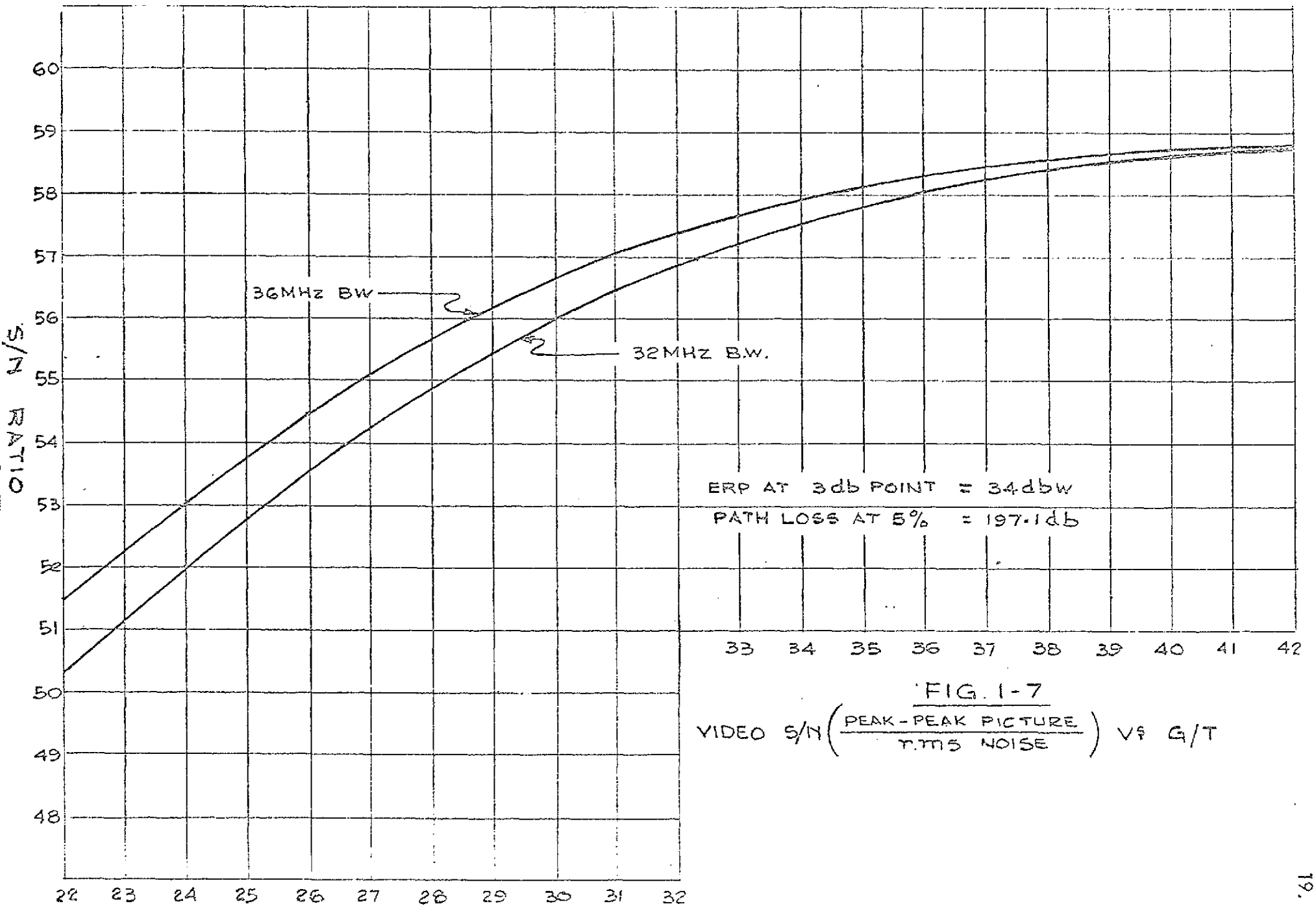

FIG. 1-7

VIDEO S/N $\left(\frac{\text{PEAK-PEAK PICTURE}}{\text{r.m.s NOISE}}\right)$ VS G/T

Using the same ERP, path loss and bandwidth as used in the video calculation, we can derive the optimum number of channels that can be transmitted assuming a receive station G/T. If two carriers are transmitted via the same transponder the bandwidth should be reduced by half to 18 MHz and the ERP per carrier reduced accordingly. For these two cases it is assumed that earth stations with a G/T of 40.7 would be receiving the signal. For the case of telephony communication to northern stations. it is assumed that multiple-carrier operation will be utilized with at least 4 carriers in the assigned RF channel. Furthermore, because of multiple carrier intermodulation, the spacing of the four carriers would have to be non-uniform thereby reducing the bandwidth available for each carrier. Therefore the maximum number of channels that can be carried has been calculated for a fixed bandwidth.

A summary of the telephony calculations is shown in Table 1.

TABLE 1

No. of Carriers per Transponder	No. of Channels; per Carrier	Bandwidth per Carrier (MHz)	Station G/T (dbW/°K)
1	1500	36	40.7
2	600	18	40.7
4	60	4.5	27
4	72	5.4	27
4	84	6.4	27
4	96	7.6	27

c) Summary of Carrier-to-Noise Temperature Ratios

The following table outlines the required C/T ratios required for system operation. The uplink C/T ratio is that required at the satellite based upon 1,000 pWp for telephony and a signal to noise ratio of 63.1 db for video. Similarly, the down-link contribution is based upon 3,000 pWp for telephony and a signal to noise ratio of 57.1 db for video. The overall C/T ratio is based upon 7,500 pWp for telephony and a signal to noise ratio of 55 db for video.

Up-path fades are not considered here because it is envisioned that some form of ground station ERP compensation will be available.

No. of Carriers per RF Channel	Capacity	C/T (dbW/°K) per carrier		
		Up-Link	Downlink	Overall
1	TV	- 129.0	- 135.0	- 137.1
4 to 6	60 channels	- 139.1	- 143.9	- 147.8
2	600 channels	- 123.2	- 128.0	- 131.9
1	1500 channels	- 117.6	- 122.4	- 126.3

1.4 Typical TV Receive Earth Station Requirements

An examination of the data given in the preceding paragraphs enables the tentative establishment of small earth station parameters. Consider the high quality TV receive-only station where the receive S/N ratio objective is understood to be 55 db or greater for 99 percent of the time. Calculations of the overall communications performance Figure 1-7, Part 1.3) shows that this S/N ratio can be achieved with an earth station G/T of 28.2 db. This is based on an EIRP of 34 dbW and a path loss of 197.1 db (5° antenna elevation angle). The fading distribution curve (Figure 1.4, Part 1.1 d)) shows that a station located at the beam edge will see an effective satellite EIRP of 33.75 dbW or greater for 99 percent of the time. It will therefore be assumed that the required earth station G/T is 28.5 db. For a station with an uncooled parametric amplifier, the overall earth station noise temperature will be about 150°K. We have therefore:

Required Earth Station G/T ratio	28.5 db
Earth Station Noise Temperature	150°K = 21.8 db/°K
Required Earth Station Gain	50.3 db

With a shaped reflector and Cassegranian antenna optics, this gain can be achieved with a 30 foot antenna. A 32 foot antenna is chosen for the small receive stations in order to have a design margin of 0.5 db on the required communications performance. The above calculations are based on the worst case condition at the satellite beam edge. All other stations located inside the beam will have extra margin on the required communication performance because of higher EIRP values.

A 32 foot antenna appears to be a near optimum choice for the TV receive station for several reasons, namely:

i. This size antenna will enable high quality TV performance with 55 db S/N ratio to be achieved with a 19 db C/N ratio

ii. A 32 foot diameter is near the minimum acceptable size from the point of view of adjacent satellite interference if high density utilization of the synchronous orbit belt is to be achieved.

iii. Fixed antennae with manual positioning capabilities can be utilized. Relatively small signal degradation due to satellite drift will be experienced.

For the nominal quality TV receive station, a simplification can be achieved through the use of tunnel-diode amplifiers at the receiver front end. These units are more reliable and lower in cost than parametric amplifiers. They also have a higher noise temperature but will still enable a receive S/N ratio of 47 db to be achieved.

1.5 Relative Cost of Earth Stations vs G/T

Earth station costs will cover a very wide range depending on the antenna size, G/T ratio, tracking or non-tracking antennae, the number of receivers and transmitters, site location and access, etc. It is beyond the scope of this study to make an accurate estimate of the station costs for the ground network. However, in order to obtain some indication of the probable costs for the entire system, budgetary costs for typical earth stations have been established.

Costs have been estimated for two types of station; the main communication ;and control stations and the TV receive only stations. All stations are priced on the basis of a single antenna; if two antennae are used prices will increase by some factor less than 2 depending on the degree of redundancy desired. The equipment assumed for each type of station is as follows:

a) Main Communication Station (95 ft. or 60 ft. Antenna):

QTY.	
1	Antenna, fully tracking with autotrack facility
2	Cooled Parametric Amplifiers
6	Low Power (1 KW) transmitters
8	Receivers (delivering video signals)
1	Control, Monitoring and Test Facility
1	Telemetry and Command System

b) TV Receive Only Station (40 ft. or 30 ft. Antenna):

Qty	
1	Antenna, manually positioned, partially steerable
2	Uncooled Parametric Amplifiers
3	Receivers

Not included in price estimates are:

- Cost of land
- Buildings and civil works
- Primary Power
- Deicing

Figure 1-8 shows the relative costs of the two types of station with a 30 ft. TV receive station cost normalized to 1.0. The specific antenna sizes and G/T ratios analyzed are:

Antenna Diameter	G/T Ratio
95 ft.	40.7 db
60 ft.	36.7
40 ft.	31.5
30 ft.	29

The absolute cost of the 30 ft. station installed will be in the order of $400,000. The remaining stations are scaled accordingly.

In summary, we emphasize again that these prices are "ball-park" values. The figures for the small stations may in fact be conservative since price reductions for large quantity supply of equipments should be achievable. Antenna suppliers have indicated that no special strengthening is required for Arctic locations although special steel, resulting in a 10% increase in antenna cost, might be necessary. Deicing might be required in most locations but this represents less than 5% of total station costs.

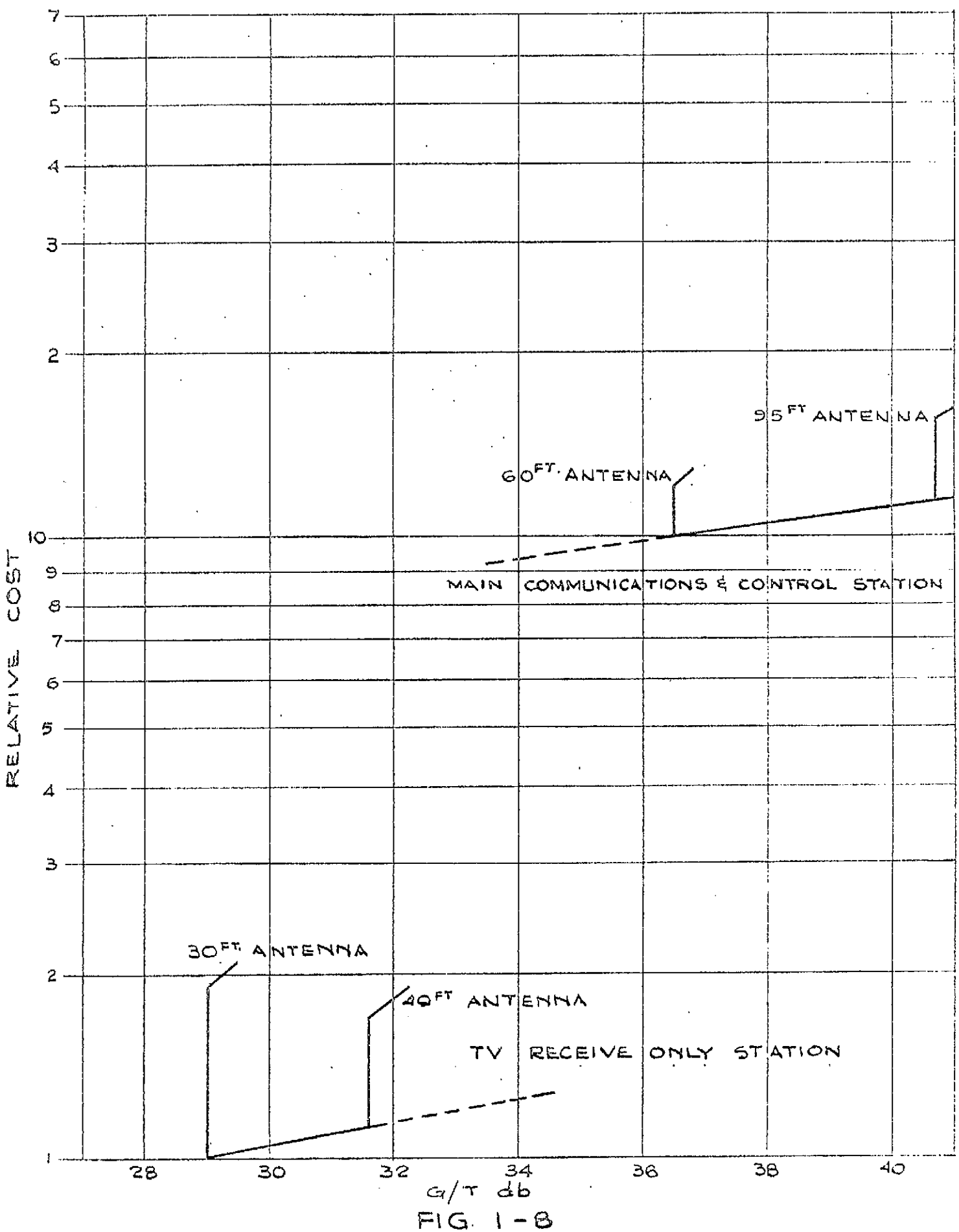

FIG. 1-B

EARTH STATION RELATIVE COST Vs G/T

1.6 Earth Coverage by Satellite Antenna

a) Philosophy:

For a satellite of a given weight whose main purpose is the distribution of television, the prime function of the antenna or indeed of the whole satellite is to cover the area of Canada with a suitable signal level on the largest possible number of channels. In a broad sense there is a weight trade-off between antenna size and power system size that would give a minimum total weight if the communications function were to provide only point-to-point trunk communications. In the limit then, the antenna beam could be made as small as possible consistent with the attainable pointing accuracy. It is probable that the minimum weight would occur when the sum of solar array and battery weights nearly equalled that of the antenna and portions of the pointing system. For the problem of large area coverage it becomes clear very quickly that this weight optimization cannot be achieved. With the present solar array and battery technology the weight of these components is far greater than that of the antenna that just covers the required area. It would be folly for example to increase the beam size thereby reducing antenna size and weight, for the increase in power system weight necessary to offset the reduction in antenna gain would greatly outweigh the antenna reduction by perhaps a ratio of three to one.

To achieve the highest antenna gain possible becomes then a problem of fitting the smallest practical antenna patterns of ellipses or circles, to a projection of Canada as seen from the orbital arc. The limits of this arc from 80°W to 120°W are set by the lowest practical ground station antenna elevation angle which is taken as 5°.

The next steps in the choice of beam size and pointing depend on the satellite location in the orbital arc and on the attainable angular pointing accuracy.

Although a single satellite location may be optimum for best antenna gain the actual antenna design chosen should be acceptable for a reasonable range of locations such as a 20° arc that would contain the main and protection satellites. The angular dimensions of the beam determined in this way must then be increased by an amount set by the expected angular pointing error which is taken as $\pm$ 0.5° in the N-S and E-W sense.

For the early part of this study the work statement specification of a 3 db beam width of 4° x 8° with beam centre EIRP 37 dbW has been interpreted as follows: The EIRP towards any point in Canada will not be less than 34 dbW. For the final refinement of beam design path loss variations due to slant range and atmospheric loss will be considered and the requirement will be interpreted in terms of a minimum flux density for any point in Canada.

b) Area Coverage Optimization:

Figure 1-9 is a projection of Canada as seen from a satellite location at 90°W longitude and 0° latitude. On this projection beam shapes appear as true ellipses and the selection of a minimum area ellipse can be made on a manual trial and error basis or by an iterative computer calculation. For the initial study program however, an existing computer program was used to plot the coverage contours of various beams onto a map of Canada. Various satellite and beam centre locations were used as inputs and a close approach to an optimum beam was selected by inspection for a best fit. The results of this are shown in Figure 1-10 which gives the projection of a $2.25^\circ \times 7.5^\circ$ beam from 84° W longitude aiming at 89°W longitude and 51° N latitude.

c) Effect of Pointing Error:

To offset the effect of the anticipated $\pm$ 0.5 degree pointing error the minimum beam size must be increased by the amount of the error as a first approximation. The resulting $3.25^\circ \times 8.5^\circ$ beam is plotted in Figure 1-11, where the beam centre has been displaced from its nominal position by 0.5° in both N-S and E-W senses. The inner contour then represents the locus of the beam edge for the expected pointing error and is equivalent to the coverage area defined by the $2.25^\circ \times 7.5^\circ$ undisturbed beam. The importance of beam pointing error on antenna gain is shown in Figure 1-12 where change in beam dimensions and the resulting change in gain is shown as a function of pointing error.

d) Optimization of Antenna Gain at the Beam Edge:

When the minimum angular size of the beam has been selected it is necessary to decide what point is to be taken on the gain function of the antenna as the beam edge. This antenna gain function depends on the illumination function and two cases have been chosen for optimization, namely a cosine squared illumination and a lambda function illumination. The procedure is to write the expression for the gain as a function of angle and beam width and to differentiate the expression with respect to beam width and set to zero.

For comparison Figure 1-13 shows the gain as a function of angle of two cosine squared illumination antennae, with the 3 db beam width of one equal to the 4.34 db beam width of the other.

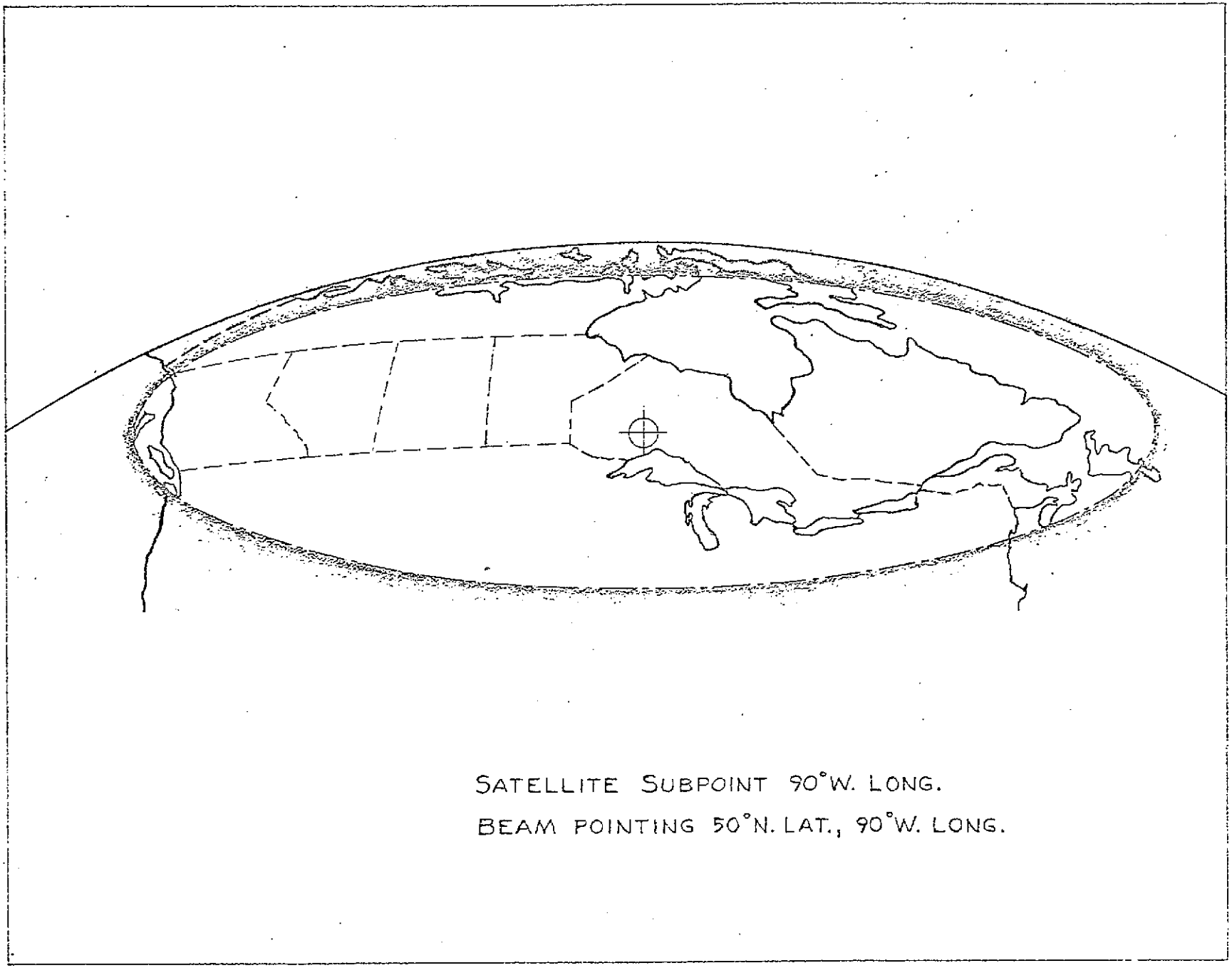

FIG. 1·9
CANADA AS VIEWED FROM SATELLITE

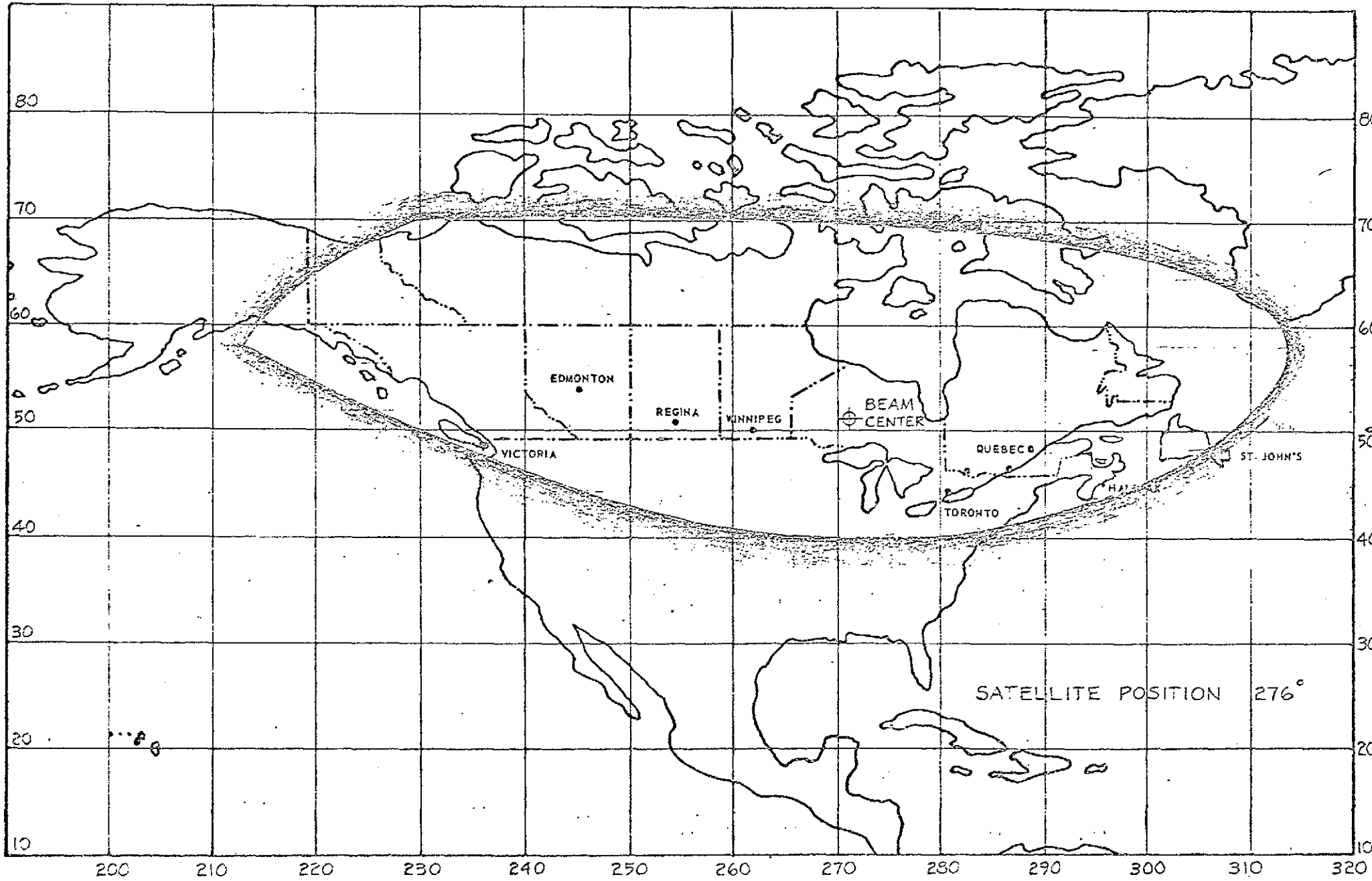

FIG. 1·10

2·25 × 7·5° BEAM COVERAGE

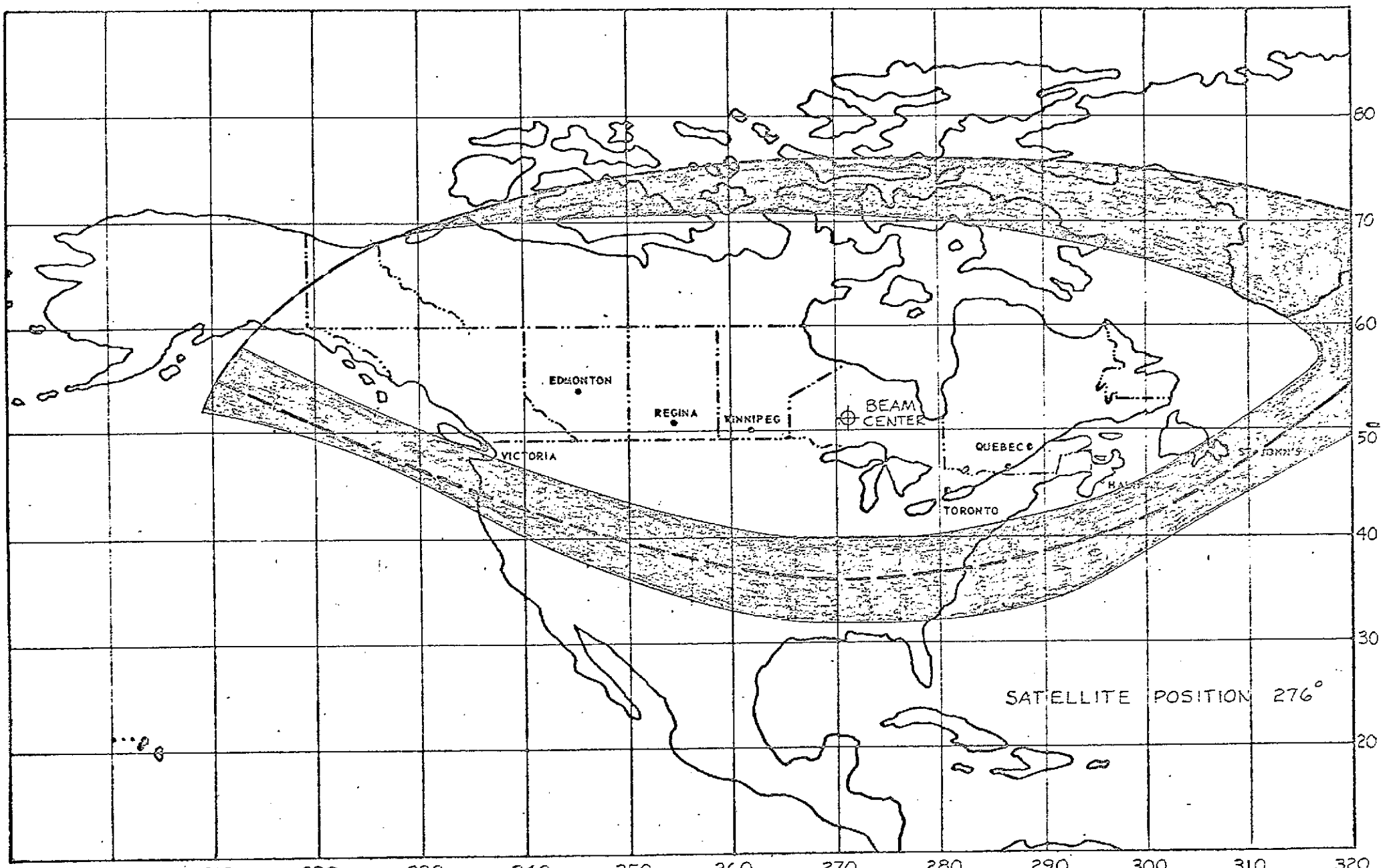

FIG. 1·11
3·25 × 8·5° BEAM COVERAGE
INCLUDING POINTING ERROR

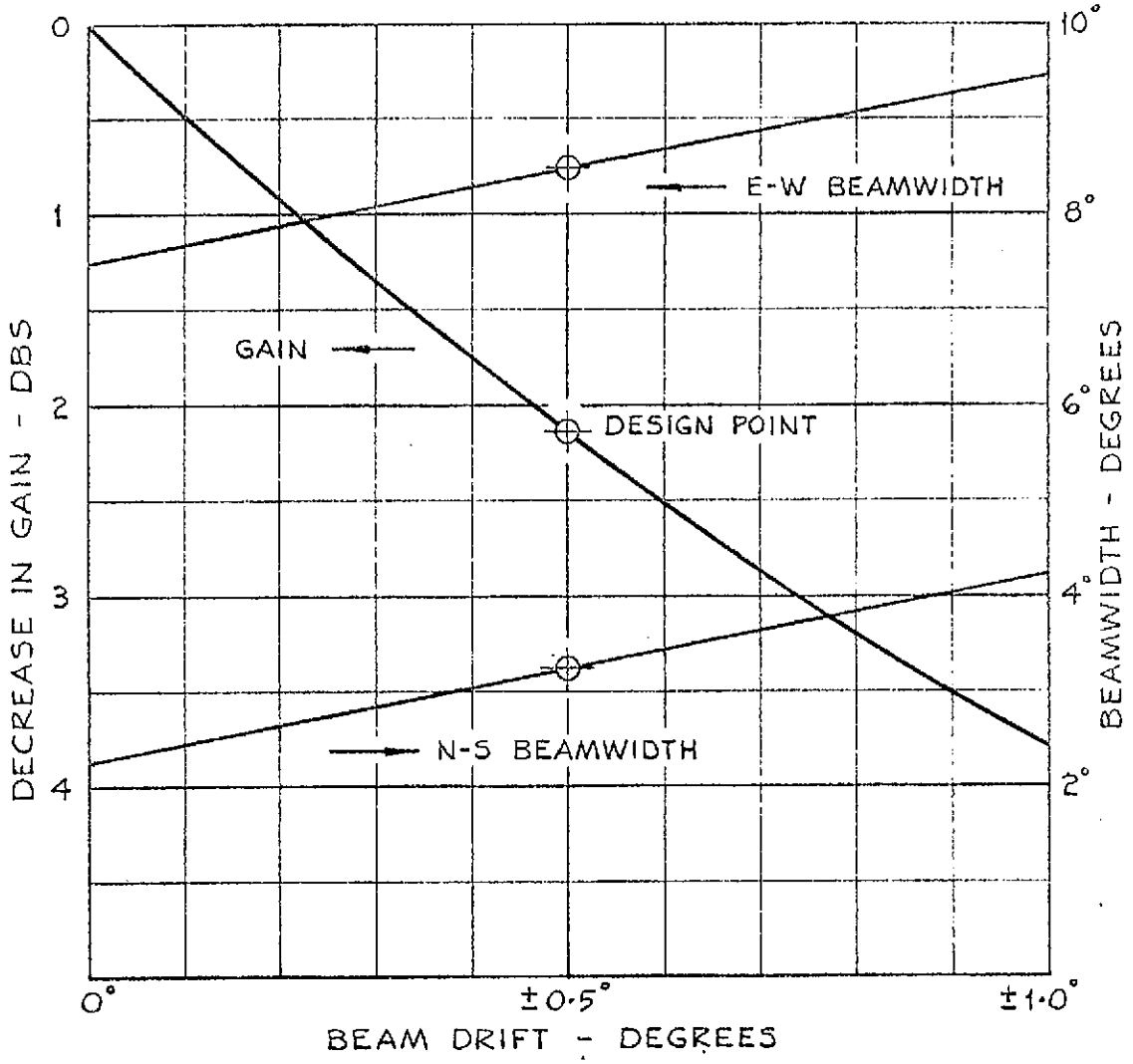

FIG. 1·12

ANTENNA GAIN AS A FUNCTION OF POINTING ERROR.

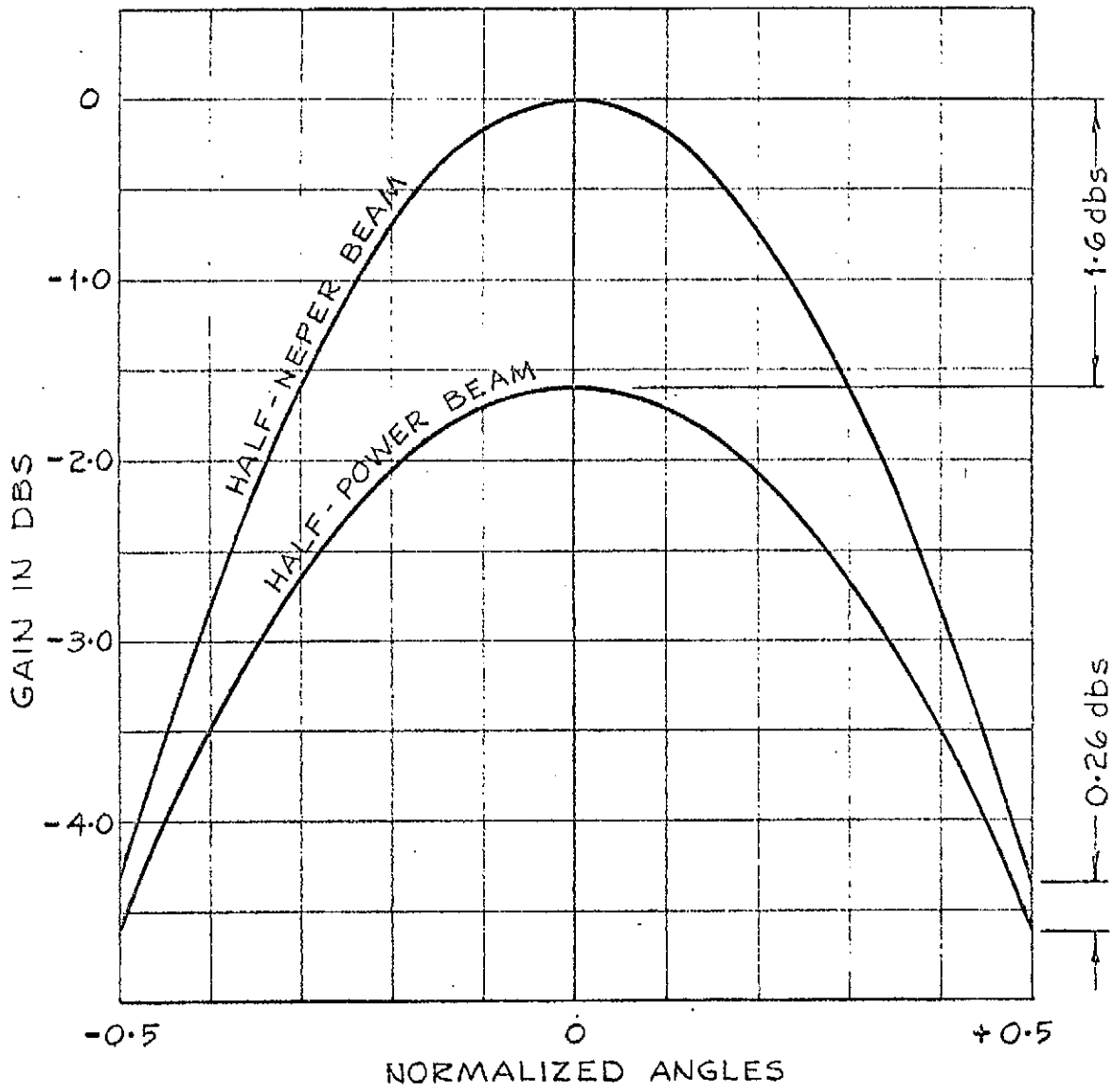

FIG. 1·13

COMPARISON OF HALF POWER AND HALF NEPER BEAMWIDTH.

The optimization procedure is illustrated in Figure 1-14 which is a plot of the antenna gain vs the antenna beamwidth. The antenna beamshape in the main lobe was assumed to be parabolic- gain in dbs $(\theta/\theta a)^2$ - and the half-neper beamwidth was normalized to the required angular coverage. Similarly the antenna gain is normalized to the beam center gain of the optimum antenna. Starting from a very small beam, Go, the gain at beam center is high but the edge of the coverage area sits very low on the beam pattern and has therefore very little gain (Ge). As the beam is widened, Go decreases at a rate of 2 db/db but Ge goes through a maximum of -4.34 dbs (1/2 Neper). With further widening of the beam both Go and Ge decrease monotonically.

Similar curves can be drawn for other beam shapes created by different illumination functions, e.g., Ge has a peak value of -4.03 dbs referred to optimum Go, for a lambda function illumination.

e) Effect of Frequency on Beam Size:

As the frequency of operation increases the beam size decreases while the gain on beam axis increases. It can be shown that these effects counterbalance each other if the beam size is chosen according to the optimization described above. This is true over the 500 MHz band from 3700 MHz to 4200 MHz, for which all the preceding discussions apply, but does not apply to the operation of the antenna as a 6 GHz receiving antenna. For this band it will be necessary to defocus the antenna or control the illumination in such a way as to produce a beam of nominally the same size as the 4 GHz beam.

f) Effect of Slant Range on Coverage:

For each point on the earth within sight of the satellite, a particular slant range and elevation angle are associated which together define both the free space loss and the atmospheric loss. This information can be shown parametrically as a function of station longitude and latitude relative to the satellite (Figure 1-2). It can also be combined with an assumed antenna beam size and shape, such as that previously derived, to generate contours of equal flux density on the earth. This is shown in Figure 1-15 for a $3.25^\circ \times 8.5^\circ$ beam with cosine squared illumination, including the effects of beam pointing error, where the flux contours are taken relative to the beam axis.

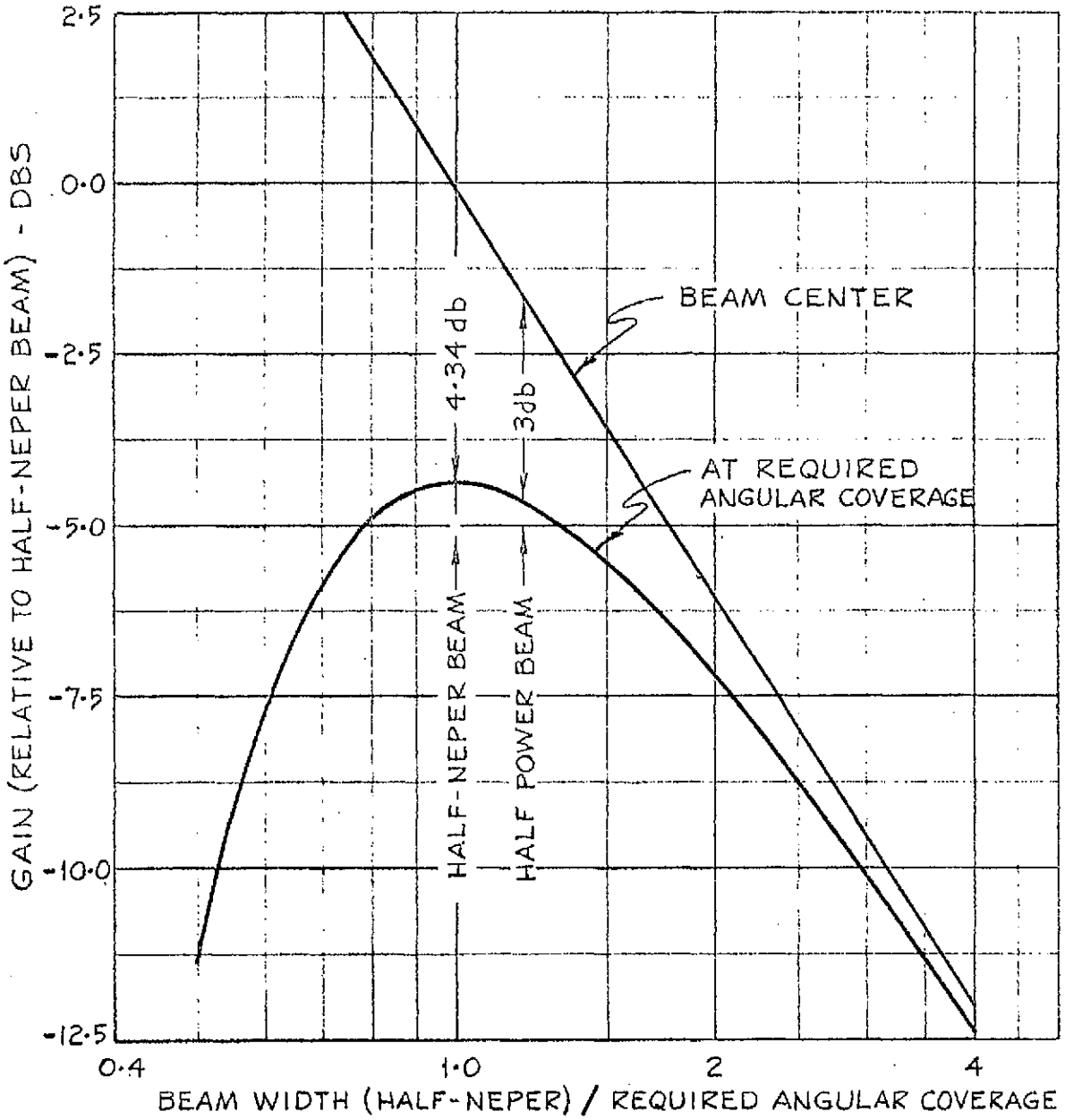

FIG. 1·14

OPTIMIZATION OF BEAM EDGE GAIN.

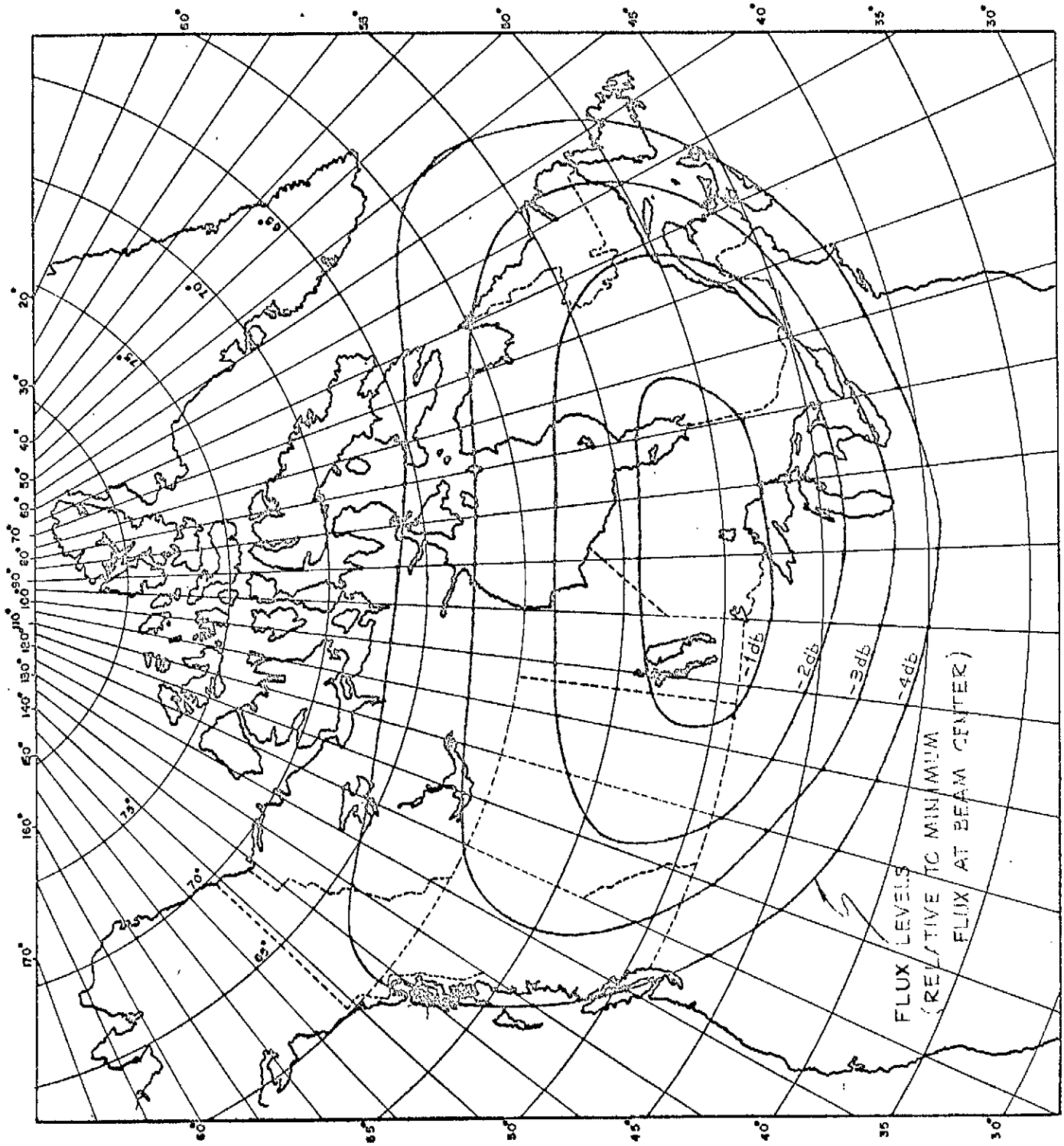

FIG. 1·15

FLUX DENSITY CONTOURS

3·25 × 8·5° BEAM INCLUDING POINTING ERRORS.

g) Items of Further Study:

To provide the final optimization of beam size and shape before detailed preliminary design of antenna is begun, three additional problems will be studied.

i. The beam size will be optimized for twist or rotation about its main beam axis. This may have some effect on the size and position of the optimum orbital arc.

ii. The beam shape may be altered to maximize the flux at beam edge by tapering the illumination function. This will have the effect of increasing the beam edge gain and reducing the beam centre gain giving a flatter beam shape with steep sides.

iii. The effects of range and atmospheric loss will be used to optimize the final beam size and pointing.

2.0 Mission Analysis

2.1 Launch Vehicles

Two potential launch vehicles are available for the Canadian Comsat Mission--one being the Thor-Delta ($DSV\text{-}3L^2$) built by McDonnell Douglas and the other being the Atlas/Burner II built by General Dynamics/Boeing. Both of these vehicles are presently being examined in detail to determine their mission capabilities, fairing development status, and booster development status. The description of each configuration is contained in the following sections.

2.1.1 Thor-Delta ($DSV\text{-}3L^2$)

Figure 2-1 shows the general configuration of the $DSV\text{-}3L^2$. The $DSV\text{-}3L^2$ is basically the same as the DSV-3L except that six strap-on solid motors are used on the booster instead of three. This configuration has recently been given a hardware contract go-ahead by NASA with the first launch scheduled in May, 1969. The total booster is made up of three stages. The first stage is the DSV-2L-1B with strap-on solids (6 Castor II). The second stage is improved Delta, and the third stage is the TE-364-3 solid motor.

Douglas is currently performing a booster capability study to determine how much payload weight can be placed in a transfer orbit up to a synchronous equatorial apogee. Based upon preliminary results, the maximum payload weight is 1005 pounds, including the interstage structure between the booster and payload. The interstage structure with all its separation equipment weighs a nominal 40 pounds. Therefore, the net payload weight into orbit is 965 pounds.

For the particular trajectory at which this booster capability exists, the orbit inclination is 28.7 degrees, which means that the payload must supply a V capability of 6040 ft/sec to circularize the orbit at synchronous altitude. This particular trajectory does not completely satisfy all the present radio guidance constraints; however, it is expected that a modification will be made to the guidance antennas which will permit this trajectory to be flown. This type of modification has already been incorporated into Thor-Agena launch vehicles.

The present fairing being used by the Thor-Delta is too short to incorporate the communications antenna and the required solar array for optimum six channel designs. Douglas has proposed to develop a new fairing with the same diameter but approximately 263 inches long.

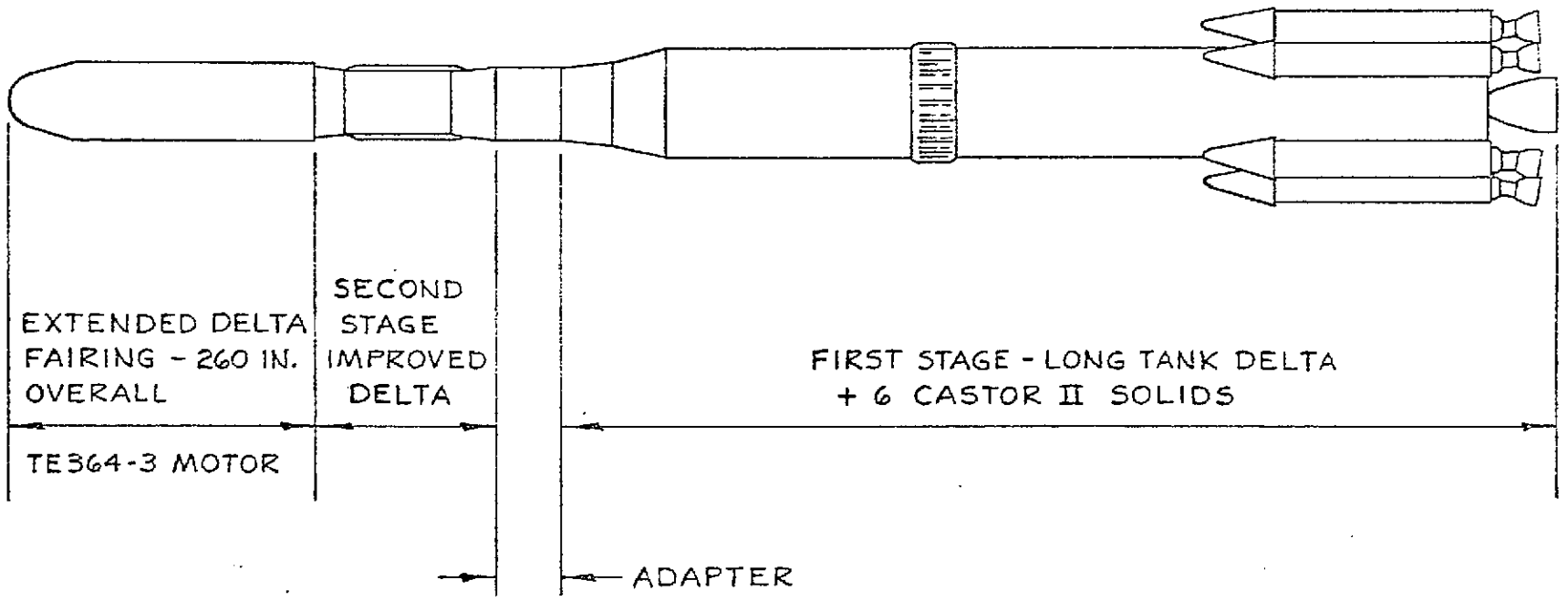

FIG. 2-1

THOR-DELTA LAUNCH VEHICLE DSV 3L[2]

An outline of this fairing together with the present one, is shown in Figure 2-2. The weight of the improved fairing is 675 pounds. This increased weight was included in the calculation of the net payload weight into orbit.

Another important booster performance parameter is the total orbit dispersion produced at synchronous altitude due to booster errors. This dispersion must be removed by the payload through the use of its own propulsion system. A significant effort is underway to determine what this booster dispersion is so that a ΔV allotment can be assigned to this payload. At the present time, definitive data is not available to determine what this number should be. Based upon an error covariance matrix received from Douglas, the velocity dispersion could be as high as 500 ft/sec. However, it is expected that proper trajectory biasing and optimization will reduce this number. Therefore, a nominal ΔV of 300 ft/sec is currently being used in the design which corresponds to the Intelsat III dispersion, which flies on a similar type booster.

2.1.2 Atlas Burner II

The Atlas-Burner II is a relatively new booster combination which is scheduled for its first launch in August, 1968. This configuration is shown in Figure 2-3. The Atlas portion is the standard SLV-3A and the Burner II stage is the same stage flown on six Thor-Burner boosters, all of which were successful. The Burner II stage includes a strap-down inertial guidance with a programmer and velocity meter which enables this payload to be accurately injected into its transfer orbit. This is in contrast to the Thor-Delta which relies on the booster for attitude reference and injection into a transfer orbit by a spun-up last stage. This type of injection by Burner II produces a total booster dispersion equivalent to an error of 180 ft/sec at synchronous apogee which is considerably better than the Thor-Delta. This smaller booster dispersion is equivalent to about 8 pounds of booster payload because of the smaller quantity of hydrazine required.

The Atlas-Burner II is capable of placing a payload weight of 1005 pounds into a transfer orbit up to a synchronous equatorial altitude. This number is coincidently the same as the Thor Delta except that the interstage structure has already been subtracted. For the type of trajectory flown by the Atlas-Burner II (a bi-elliptic orbit transfer), the required velocity to inject into a circular synchronous orbit is 6090 ft/sec.

Because of the size of the Cansat, the standard Burner II fairing would have to be extended approximately 140 inches, thereby increasing the fairing weight up to 790 pounds. This type of modification is relatively simple; a similar type modification has already been made for the launch in August.

PRESENT

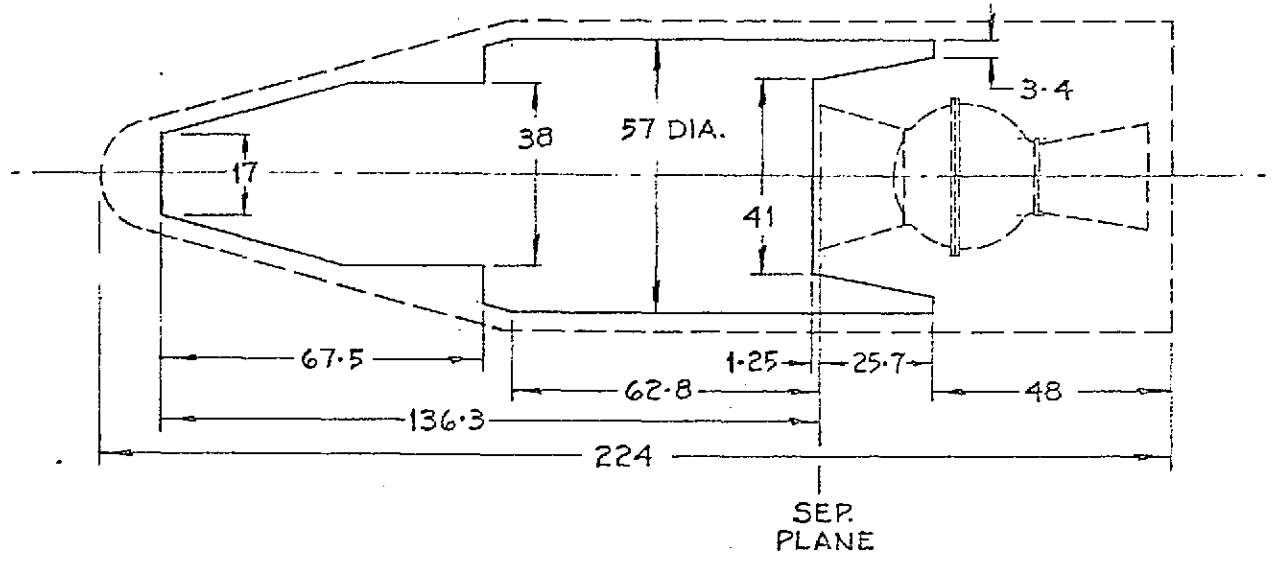

IMPROVED (PROPOSED)

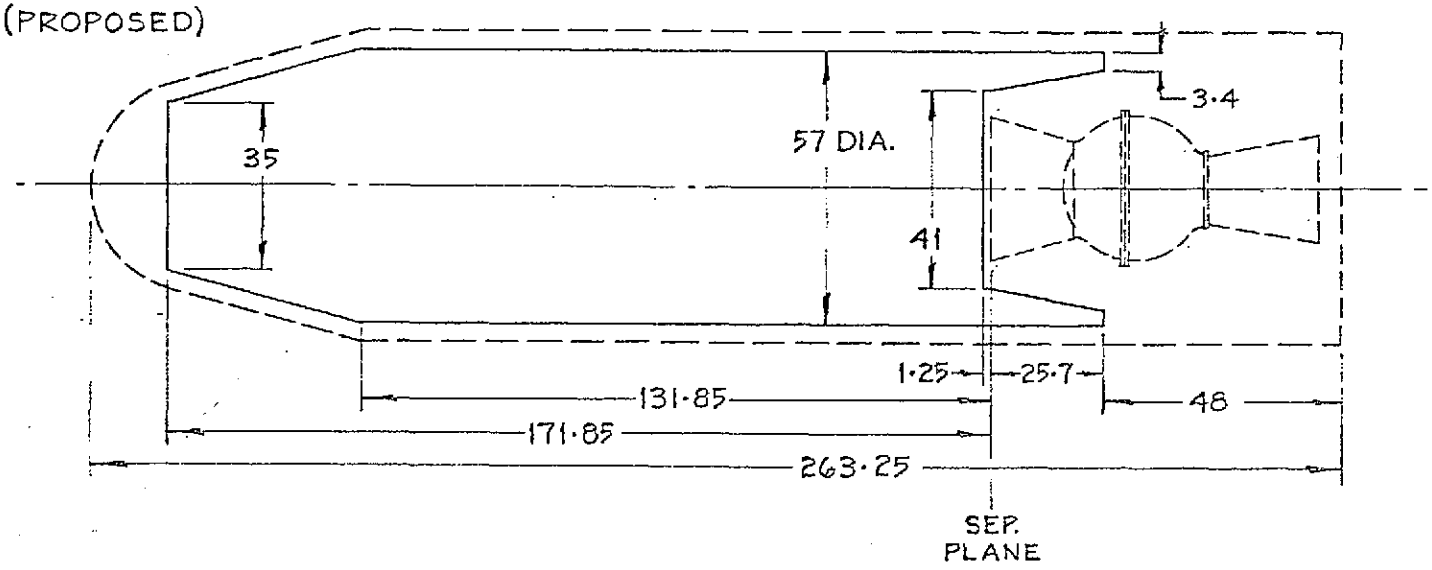

FIG. 2·2

THOR-DELTA FAIRINGS

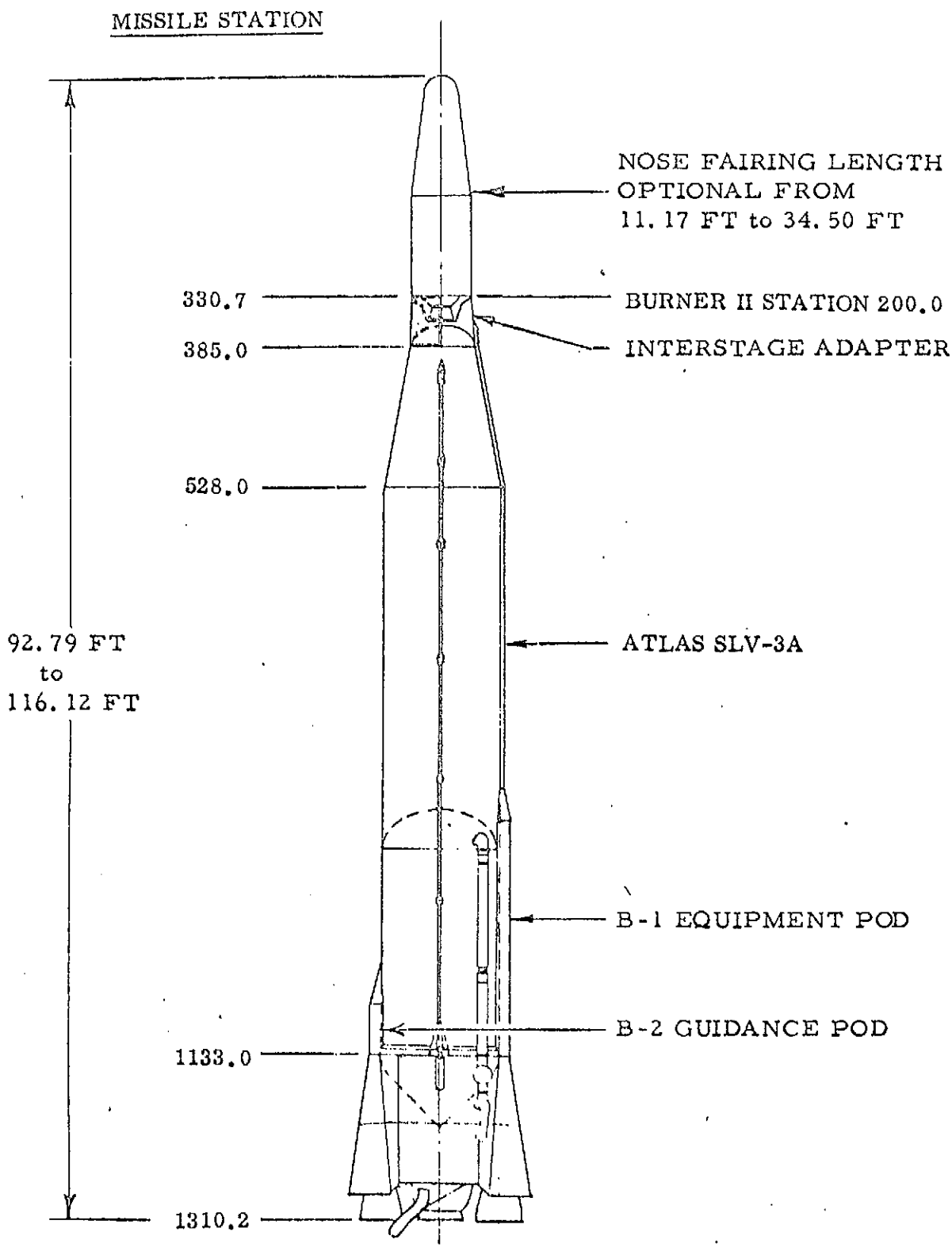

Figure 2-3 Atlas SLV-3A/Burner II with 65-Inch Diameter Nose Fairing

2.1.3 Performance Comparison of Thor-Delta and Atlas-Burner II

	Thor-Delta	Atlas-Burner II
Weight into transfer orbit	1005	1005
Interstage structure	40	0
Net weight into transfer orbit	965	1005
Solid motor weight	531	553
Hydrazine propellant	69	62
Net useful payload into orbit	365	390

Therefore, the net useful payload difference between the two boosters is 25 pounds.

2.2 Launch Constraints

2.2.1 Mission Sequencing Plan

A particular sequence of events will be followed in order to place CANSAT into a synchronous, equatorial orbit at approximately 100°W longitude (midway between the eastern and western Canadian boundaries). The events are outlined below and discussed in more detail in subsequent sections.

- o Lift-off

  Lift-off will take place from ETR. Two launch vehicles are currently being considered for use with CANSAT; Thor-Delta manufactured by Douglas and an Atlas/Burner II manufactured by General Dynamics and Boeing. (The Atlas configuration is SLV-3A).

- o Transfer to Synchronous Altitude

  The Thor/Dalta executes lift-off, coasts to the first southerly equatorial crossing and injects the CANSAT into a transfer ellipse with apogee at synchronous altitude.

  Two ascent modes are available with the Atlas/ Burner II configuration. The first is a Hohmann transfer from a 100 n.mi. circular parking orbit, and the second is a bi-elliptic ascent. Both of these modes (which are elaborated on in a later section) use a transfer ellipse with apogee at synchronous altitude.

- The Drift Orbit

  When CANSAT has coasted to apogee of the transfer ellipse, an apogee injection maneuver is performed to place CANSAT into a nearly circular, equatorial drift orbit. The drift orbit is required because, in general, the longitude at apogee on the transfer will not coincide with the desired stationary longitude. In order to obtain a more favourable initial longitude in the drift orbit, it may be desirable to delay the apogee injection maneuver until the second or third (or even later) apogee crossings. Each revolution in the transfer orbit takes about 10.5 hours and shifts the longitude of apogee westward by approximately 158^{o}.

- Final Positioning

  When CANSAT reaches the proximity of the desired stationary longitude, a final positioning maneuver will be performed to circularize the orbit (remove the drift velocity), and position CANSAT at the desired stationary longitude.

- Station Keeping

  Due to the ellipticity of the earth and the perturbations of the sun and moon, CANSAT will drift in longitude and latitude from the location at which it was originally positioned. Thus, periodic station keeping maneuvers will be required to maintain the spacecraft's position. These maneuvers will control longitudinal drift and orbit inclination build-up (latitude drift).

- Attitude Control

  During its lifetime, CANSAT will require periodic reorientation to its nominal attitude, due to the combined effects of magnetic moments, gravity torques, solar pressure torques, etc.

2.2.2 Launch Ascent Phase

Two types of elliptical transfer trajectories can be used to establish a synchronous equatorial orbit, depending on the flexibility of the launch vehicle. The usual mode of ascent is the Hohmann transfer (left side of Figure 2-4). The initial burn of the launch vehicle establishes a low altitude circular parking orbit.

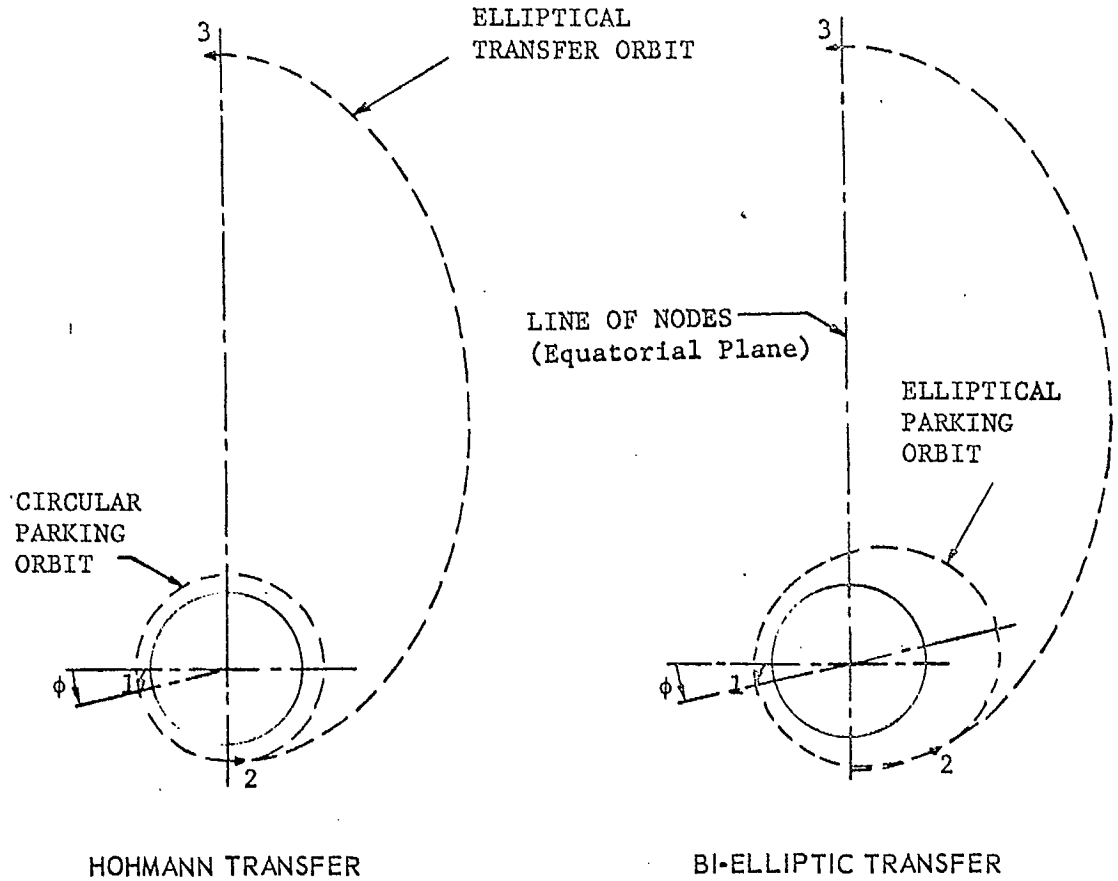

1 – First Burn to Establish Parking Orbit

2 – Second Burn to Establish Transfer Orbit

3 – Third Burn for Final Injection and Plane Change. ϕ = Boost Range Angle

Figure 2.4 – Launch ascent profiles for synchronous equatorial orbits

Upper stage burn at the desired nodal point provides the velocity to establish an elliptical transfer with apogee over the equator at synchronous altitude. The third burn is performed at apogee to simultaneously remove the inclination and circularize the final orbit.

When a non-restartable launch vehicle is used with greater capability than required to reach the initial low altitude parking orbit, the remaining impulse is lost, since the booster cannot restart to augment the transfer vehicle burn at the node of the parking orbit. The bi-elliptic* non-coincident line of apsides transfer technique (right side of Figure 2-4) uses the full boost vehicle capability to establish an elliptical parking orbit with perigee located at boost burnout. The transfer burn occurs at the point where the elliptical parking orbit and the elliptical transfer orbit are tangent. A final burn is then used for plane change and circularization at synchronous altitude.

2.2.3 Positioning Sequence

In order to attain the desired altitude, CANSAT will be injected into a transfer orbit, having a perigee of about 100 n.mi. (parking orbit altitude), and having nominal apogee altitude corresponding to synchronous altitude h = 19,323 n.mi. If a non-restartable launch vehicle is used, the bi-elliptic transfer mode discussed in section 2.2.2 may be adopted. For either of these techniques, the nominal inclination of the transfer orbit depends upon launch azimuth, the latitude of the launch site, and the specified plane change (if any) carried out at the epoch of injection into the transfer orbit.

Once CANSAT has reached apogee on the transfer orbit, an "apogee burn" is carried out which serves the purpose of injecting the satellite into an equatorial drift orbit. The nominal longitude at which the apogee burn is carried out depends upon the longitude of the equatorial crossing at which the transfer orbit is initiated, the period of the transfer orbit, and the number of revolutions in the transfer orbit prior to performance of the apogee burn. Figure 2-5 shows the variation in longitude at which the apogee burn may be carried out for a launch azimuth 93° from ETR for the first northerly and southerly equatorial crossings and for the first six revolutions in the transfer orbit. Since the longitude at which the apogee burn is carried out will not, in general, correspond to the desired stationary longitude (in the vicinity of 100°W), the drift orbit will be designed to enable the satellite to drift to the desired stationary longitude in a specified time period.

---

* Bi-elliptic is used here to mean cotangential transfer.

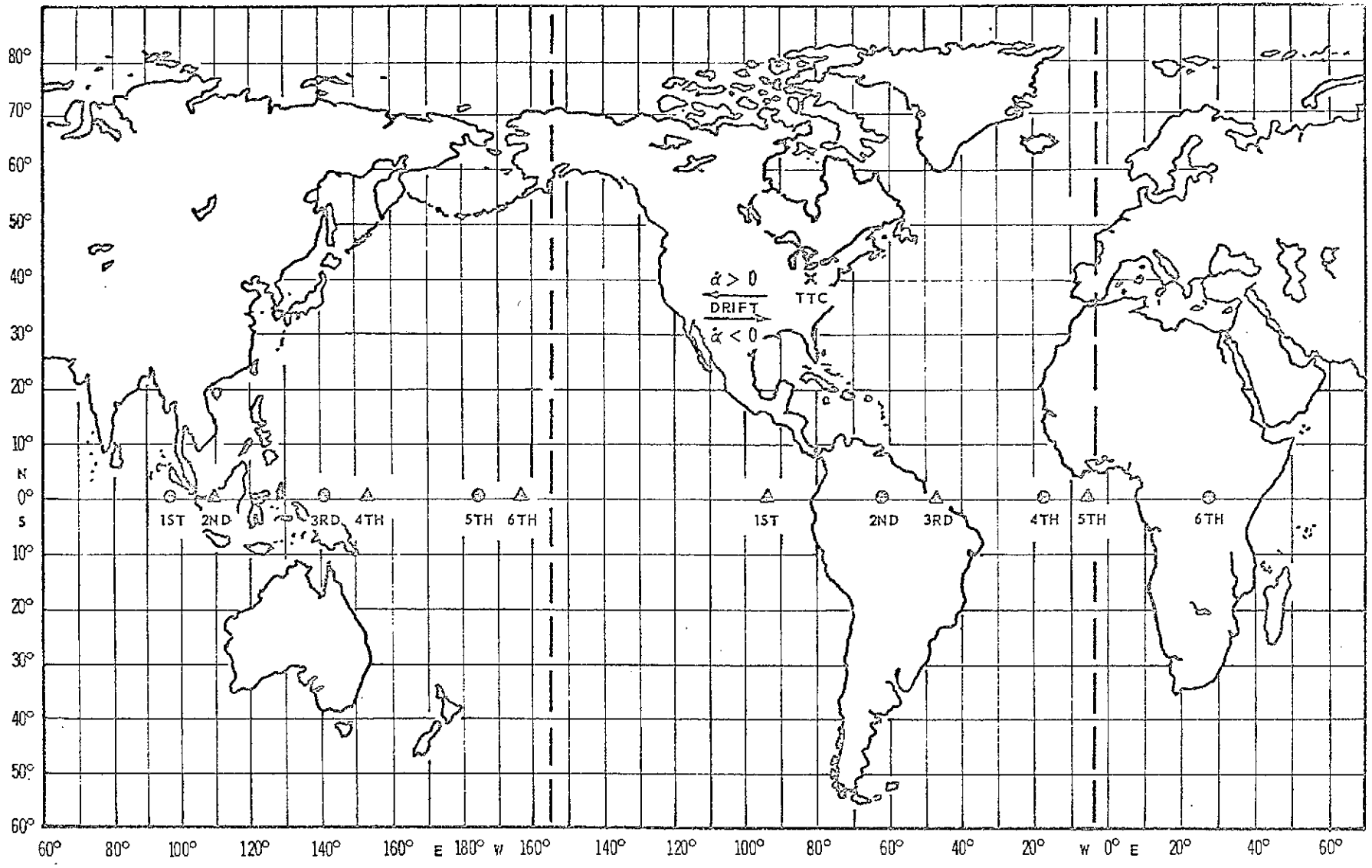

Figure 2.5 – Successive apogees of a transfer ellipse resulting from perigee burn at first ▲ northerly ● southerly equatorial crossing

The selection of the actual mission sequence will be predicted on the constraints that:

- Apogee motor firing as well as trim maneuvers due to launch vehicle injection errors, etc, and station keeping maneuvers will be carried out from a command station located in Canada in the close proximity of 80°W longitude and 40°N latitude.

- Tracking of CANSAT for the purpose of station keeping as well as positioning (during the entire drift phase) will be carried out from Canadian based tracking stations.

These constraints impose the restriction that the apogee burn must be carried out at longitudes which are visible to the ground station. Acceptable regions for the apogee burn are contained within the vertical dashed lines of Figure 2-5.

In addition, the latter constraints require that the drift direction be such that the satellite can be acquired by the ground station at all times during the drift phase and station keeping phases.

Several possible ascent sequences are suggested by Figure 2-5. In general, it will be desirable to inject into the transfer orbit from either the first northerly or first southerly equatorial crossing. In fact, various launch vehicle operational constraints may require that injection be made at the first southerly crossing. When injection is made at the first southerly corssing, it follows from Figure 2-5 that a desirable sequence of events is as follows:

- Enter the transfer orbit at the first southerly equatorial crossing.

- Remain in the transfer orbit until arrival at the second apogee (in the vicinity of 60°W). Or alternately, remain in the transfer orbit until the fourth apogee is reached (in the vicinity of 20°W).

- Carry out a biased apogee burn at the second (or fourth) apogee on the transfer orbit which results in a drift orbit with westward drift.

- o Upon completion of the apogee burn, the satellite will be tracked to determine its orbit. Subsequently, trim maneuvers will be carried out to remove any launch vehicle injection errors, etc.

- o At a specified epoch during the drift phase, the final positioning maneuver will be performed which will position CANSAT at the desired stationary longitude.

This mission sequence has the distinct advantage of a backup mode, i.e., if the apogee burn cannot be carried out at the second apogee, then an apogee burn at fourth apogee can be carried out without violating any mission constraints.

The apogee burn is characterized by an impulsive velocity change, ΔV, and firing angle, γ (defined as the acute angle between the apogee burn vector and the equatorial plane) which depend upon the inclination of the transfer orbit, i, and the drift rate, $\dot{\alpha}$. Figures 2-6 and 2-7 present values of ΔV and γ as functions of i and $\dot{\alpha}$. The values of ΔV and γ corresponding to $\dot{\alpha} = 0$ characterize the apogee burn required to enter an equatorial synchronous orbit. Values of ΔV and γ corresponding to values of $\dot{\alpha} > 0$ characterize the apogee burn required to enter a specified equatorial drift orbit (westward drift).

In particular, selection of an apogee burn which results in a drift rate $\dot{\alpha}$ = 5 deg/day would enable final positioning at the stationary longitude (100°W) to be accomplished in about 8 days from the time of apogee burn at the second apogee, or in about 16 days from the time of apogee burn at the fourth apogee.

Figure 2-8 presents a graph showing the hydrazine required for final positioning at the desired stationary longitude. If the apogee burn is carried out at the second apogee, the longitudinal drift is about 40° in 8 days ($\dot{\alpha} = 5.0$). Similarly, if the apogee burn is carried out at the fourth apogee, the longitudinal drift is about 80° in 16 days ($\dot{\alpha} = 5.0$). In both cases, the hydrazine required for the final positioning maneuvers is 48 ft/sec.

2.2.4 Station Keeping

Once CANSAT has been positioned at its desired stationary longitude, in the vicinity of 100°W, it will tend to drift in longitude; primarily due to the ellipticity of the equator. In addition, CANSAT will drift in latitude; primarily due to the combined effect of luni-solar perturbations. The proposed station keeping capabilities for CANSAT are $\pm$ 0.10° in longitude and $\pm$ 0.10° in latitude for a five year duration. As indicated in the System Analysis Section this is an improvement over the work statement and is a desirable trade off.

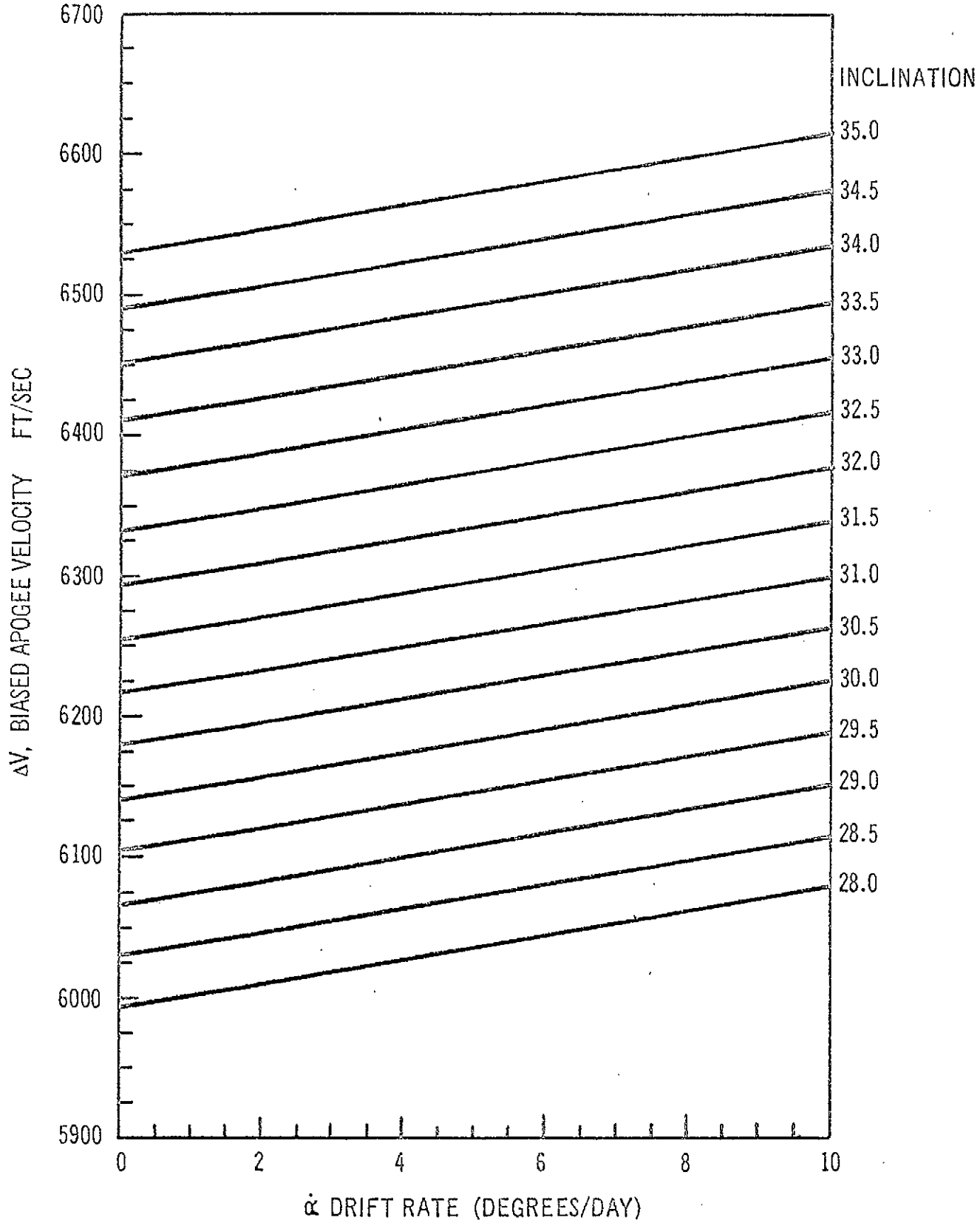

Figure 2.6 – Apogee burn ΔV versus drift rate

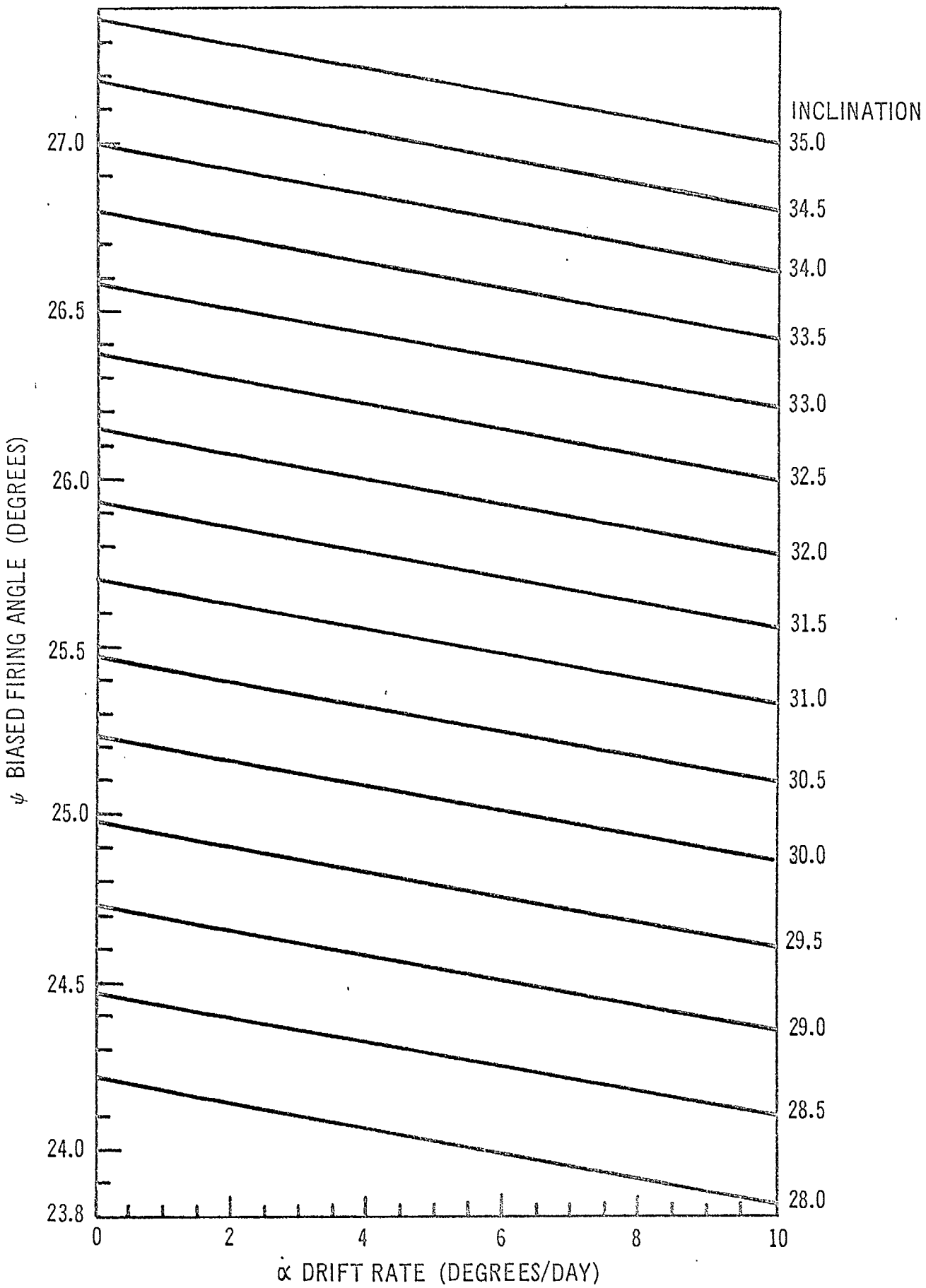

Figure 2.7 – Apogee burn firing angle versus drift rate

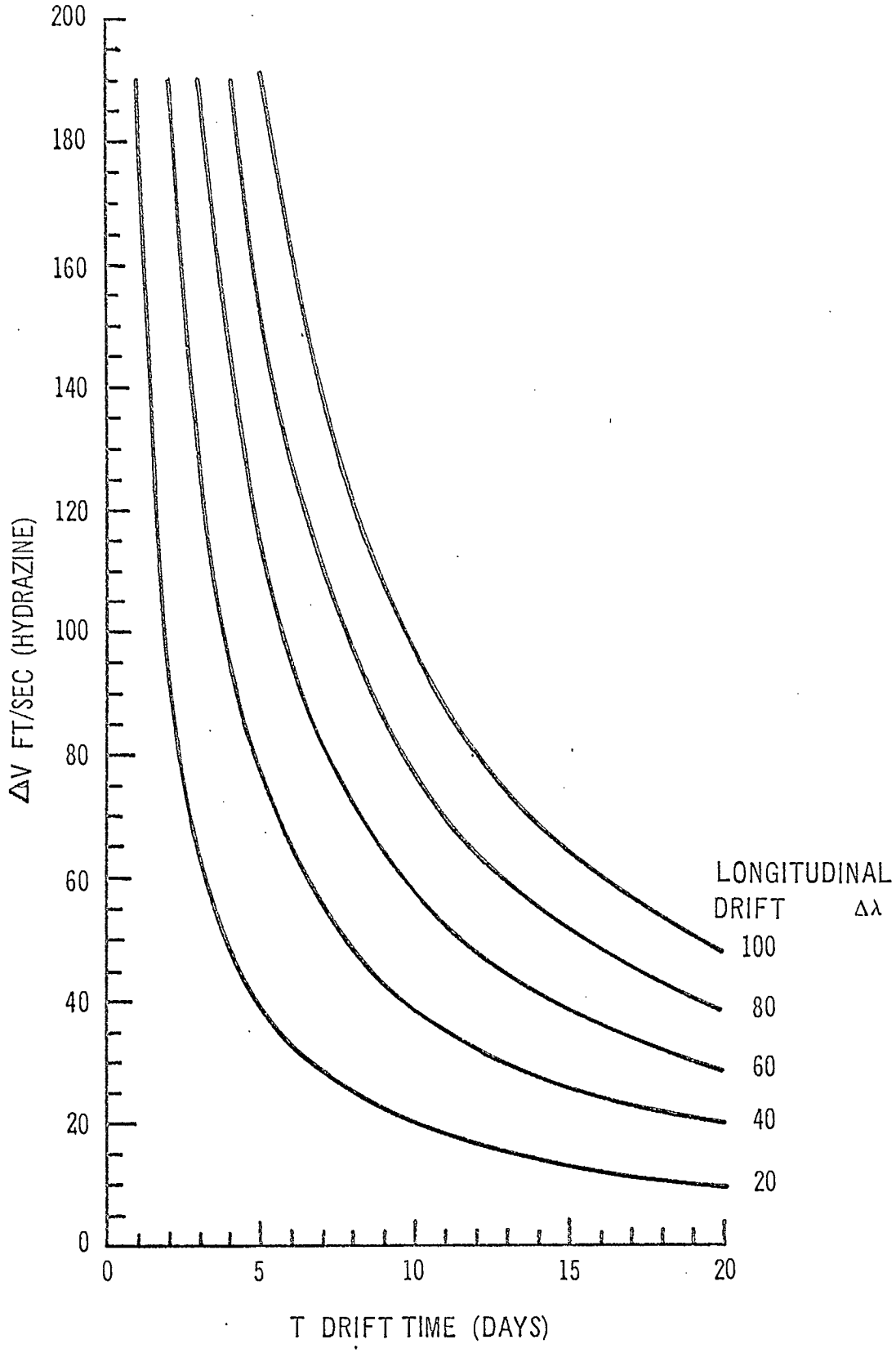

Figure 2.8 – Velocity required for final positioning maneuver

The longitudinal station keeping will be carried out by use of radial thrustors (hydrazine). The satellite will be allowed to drift in longitude until the first extreme of the tolerance band is reached, at which time an impulse will be applied of magnitude ΔV_1 (see Figure 2-9) which reverses the drift direction. The time required for drift from the stationary position to the first extreme of the tolerance band is T_1 (see Figure 2-10). The application of ΔV_1 enables CANSAT to drift to the opposite extreme of the tolerance band and then return to the point of application of ΔV_1. The time required for drift through one complete cycle is T (see Figure 2-10). Once CANSAT has reached the first encounter of the tolerance band limit, an impulse of magnitude ΔV is applied (see Figure 2-9) which enables CANSAT to drift through one complete cycle in T days. Subsequent application of ΔV with periodicity T will maintain the limit cycle within the deadband of $\pm$ 0.10°. The total impulsive ΔV_T, required for five years of longitudinal station keeping, is shown in Figure 2-11.

The latitude of the satellite will vary over its operational lifetime due to the inclination build-up caused by the combined effect of lunar-solar perturbations and the oblateness of the earth. The rate at which inclination builds up is dependent upon the position of the moon's line of nodes and, hence, varies from year to year. A graph showing rate of change of inclination as a function of time is presented in Figure 2-12. The graph shows that, for the years 1971 $\frac{1}{2}$ to 1976 $\frac{1}{2}$, the rate of change of inclination of an initially equatorial orbit decreases almost uniformly from about $\frac{di}{dt}$ = 0.91 deg/yr to $\frac{di}{dt}$ = 0.79 deg/yr. The total inclination build up for the five year lifetime is the area under the $\frac{di}{dt}$ curve between the dashed lines. If it is noted that a velocity increment of 176 ft/sec is required to remove one degree of inclination, it follows from Figure 2-12 that the total ΔV budget required to remove the five year inclination build-up (1971$\frac{1}{2}$ to 1976$\frac{1}{2}$) is ΔV = 747 ft/sec. The periodicity with which latitudinal station keeping maneuvers must be carried out depends upon the latitude tolerance of 0.10°. The time required for an inclination build-up of 0.10° varies from about 40 days in 1971 to about 46 days in 1976. Latitudinal station keeping will be carried out by use of the axial thrustors (hydrazine).

2.25 Attitude Reorientation Maneuvers

The spin axis of CANSAT will require periodic reorientation to its normal position, which is perpendicular to the equatorial plane with the antenna end of the spacecraft pointing north. The first reorientation arises after apogee motor firing has occured, and the desired drift orbit has been achieved. This spin axis reorientation will require an angular change capability of 114°. In addition, the spacecraft spin axis will vary, due to the combined effect of:

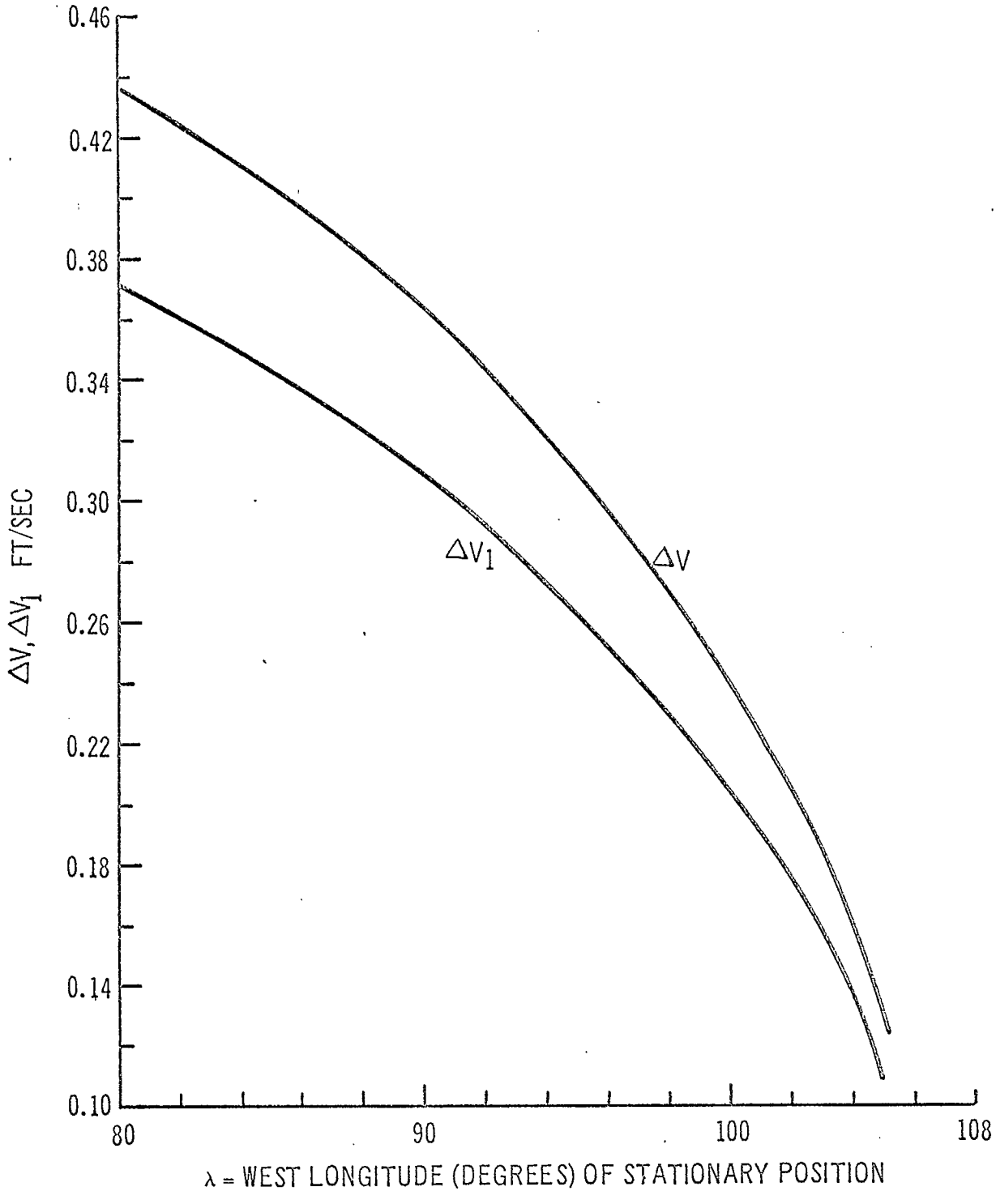

Figure 2.9 – ΔV_1 = Velocity impulse required for first longitudinal station keeping maneuver

ΔV = Velocity impulse required for subsequent longitudinal station keeping maneuvers, deadband = ± 0.10 degrees

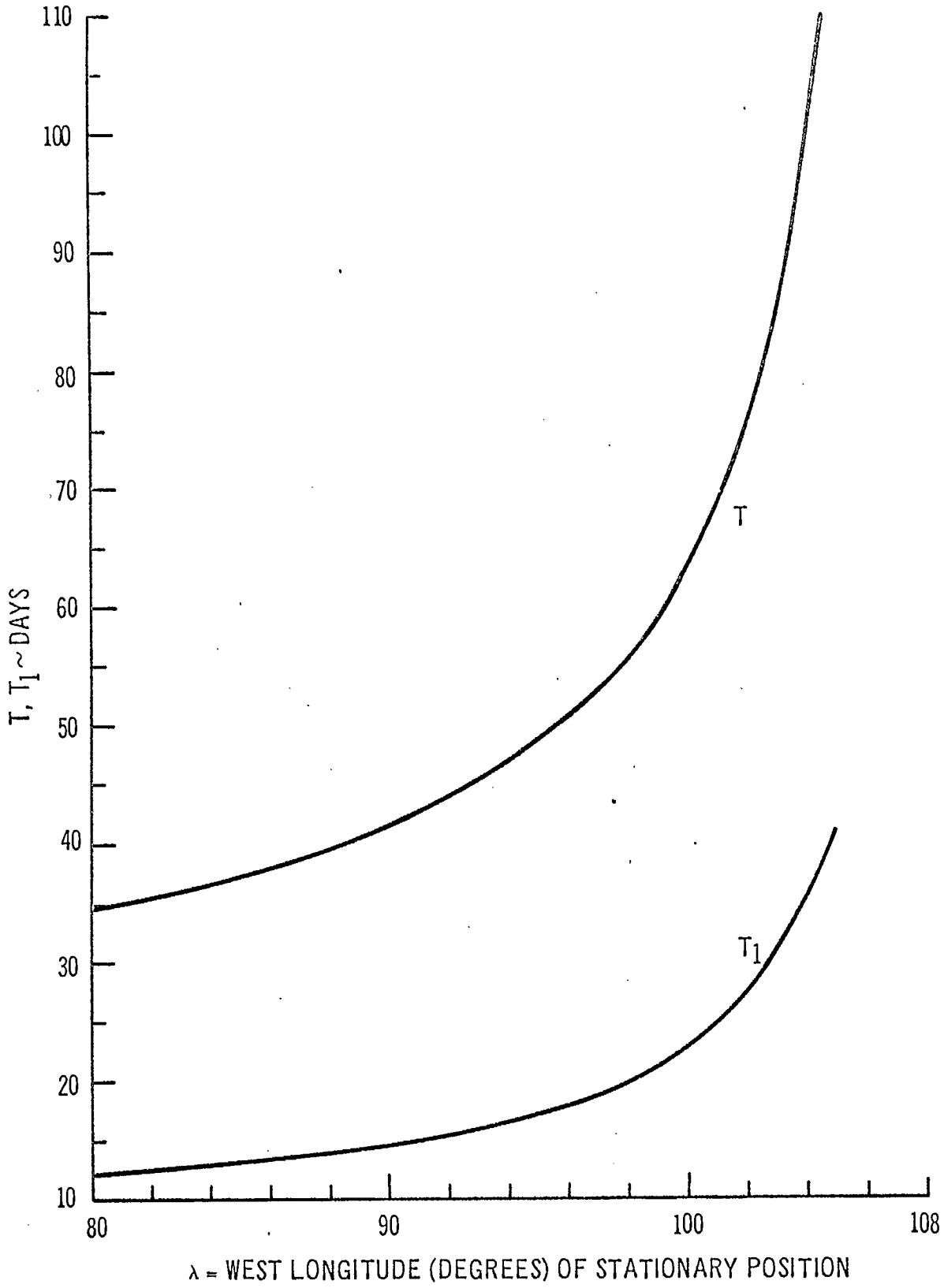

Figure 2.10 – T_1 = Drift time from stationary position to first longitudinal station keeping maneuever
T = Time between subsequent longitudinal station keeping maneuvers

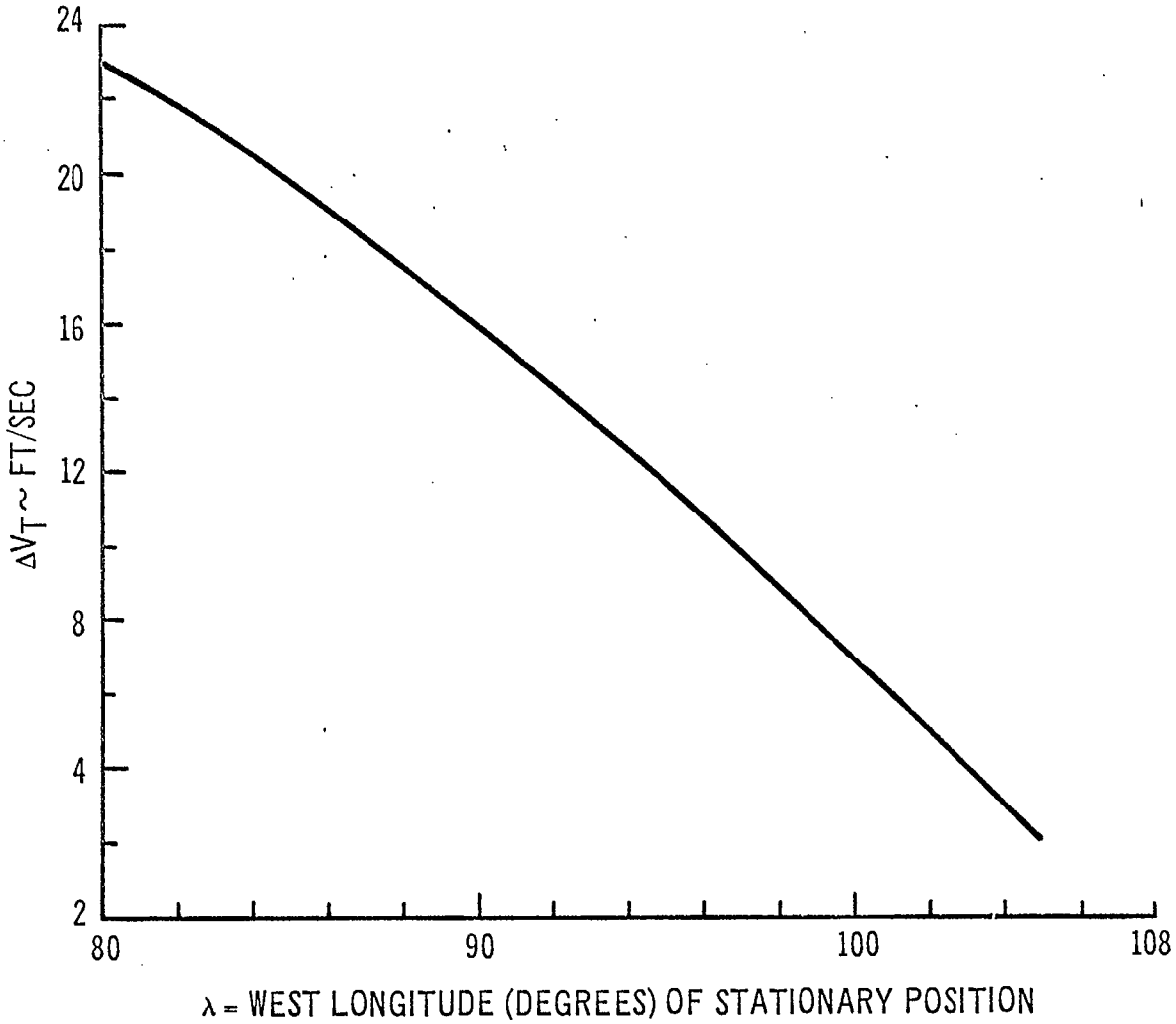

Figure 2.11 – Total ΔV required for five years of longitudinal station keeping, with deadband of ±0.10 degrees

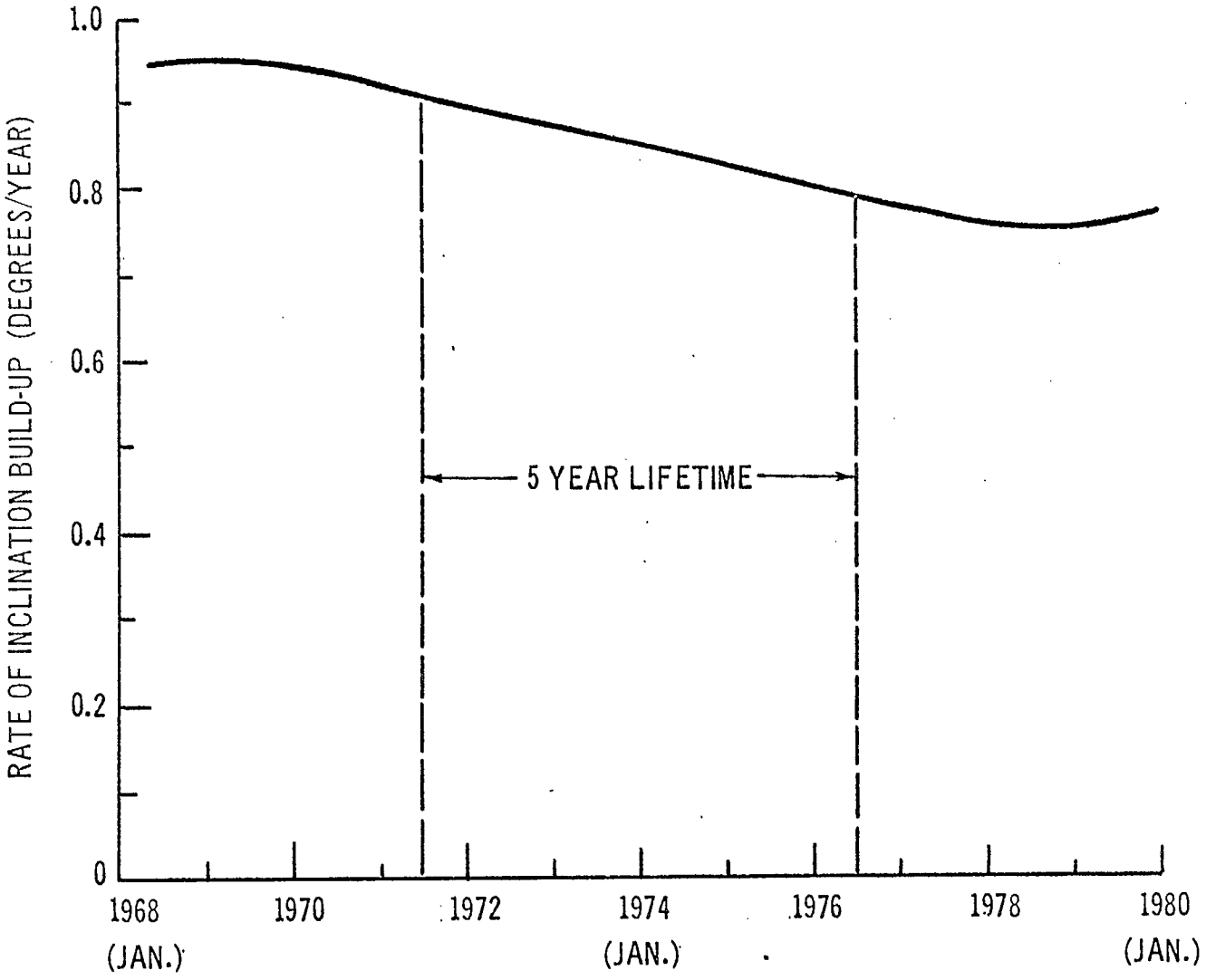

Figure 2.12 – Rate of change of inclination due to the combined effect of luni-solar and asphericity perturbations

- o Torque due to solar pressure: this torque is proportional to the distance between the center of mass and the center of solar pressure.

- o Torque due to magnetic moment: great care is exercised to assure a maximum of magnetic cleanliness in the spacecraft.

- o Torque due to gravity: since the gravity torque on the satellite is proportional to the angle between the spin axis and orbit normal and since the spin axis is kept within 0.50^{o} from the orbit normal, the influence of this torque on the attitude of the spacecraft is negligible.

- o Attitude error due to misalignment of the apogee motor, dynamic unbalance of the spacecraft, wobble and nutation.

The ΔV corresponding to a change of β radians in the attitude of the spacecraft spin axis is given by

$$\Delta V = \frac{I\omega}{mr_o}\beta$$

where I represents the moment of inertia of the spinning section of the spacecraft about its spin axis; ω is the spin rate; m is the mass of spacecraft; and r_o is radial distance from the spin axis to the axial thrustor. For the CANSAT design, the above equation takes the form

$$\Delta V = \begin{cases} 0.112\beta^{o} \text{ at booster separation} \\ 0.178\beta^{o} \text{ after apogee motor burn} \end{cases}$$

The initial reorientation maneuver of $\beta^{o} = 114^{o}$ will require ΔV = 20 ft/sec. Subsequent attitude reorientation maneuvers required to correct spin axis variation due to solar pressure, magnetic moments, gravity torques, misalignment of the apogee motor and dynamic unbalance of the spacecraft are estimated to require, at most, ΔV = 20 ft/sec. Hence, the total attitude control budget is estimated to be, at most, 40 ft/sec for the five year operational lifespan of CANSAT.

2.26 Total Hydrazine Requirement

In summary, the preliminary design indicates that the total hydrazine required to maintain CANSAT within the specified tolerances for a five year operational life-span is as follows:

ΔV required for:

o removal of 99% probable space vehicle injection errors	181 ft/sec, Atlas-Burner II
	300 ft/sec*, Thor-Delta
o final positioning maneuver	48 ft/sec
o latitudinal station keeping	748 ft/sec
o longitudinal station keeping	8 ft/sec
o attitude control of spacecraft spin axis	40 ft/sec
Totals, Atlas-Burner II	1025 ft/sec
Thor-Delta	1144 ft/sec*

2.2.7 Tracking Analysis Study

A study has been conducted to determine the accuracy with which CANSAT can be tracked in a circular synchronous orbit. Two distinct tracking modes have been considered: angles only tracking and angle range tracking.

CANSAT was assumed to be placed at 100° W longitude and tracking stations were assumed to be placed as indicated in Table 2.1.

Table 2.1

Station	Longitude	Latitude
P_1	135° W	43° N
P_2	152° W	23° N
P_3	158° W	15° N
Q_1	40° W	37.5° N
Q_2	65° W	43° N
Q_3	77° W	23° N

The stations labeled P are located west of the CANSAT subsatellite point and those labeled Q are east. These stations have been used in pairs in various combinations to track CANSAT.

* This value is an assumed dispersion error after a proper trajectory biasing technique has been used. Without biasing the error could be as high as 500 ft/sec. A detailed study will be made after booster dispersion data is received from the booster contractor.

The error model shown in Table 2.2 is based upon information contained in Reference 1.

Table 2.2

Tracking Study Error Model

	Noise (1σ)	Bias (1σ)
Azimuth, Elevation	0.005^{o}	0.02^{o}
Range	40 ft.	60 ft.
Station Location		
Latitude, Longitude	---	0.28×10^{-3} deg
Height	---	131 ft.
(Earth's gravitiational constant)	---	8.2×10^{-7} $(\frac{\sigma_\mu}{\mu})$
C_{22}	---	2.15×10^{-9}
S_{22}	---	1.93×10^{-8}

The results of the tracking study are shown in Table 2.3. For comparison, both angle only measurements and angle range measurements were made at each ground station. Tracking periods of 2 days and 10 days at the rate of 2 points per hour for each measurement are shown. The entries in Table 2.3 are the 1σ error in the drift rate determination expressed in degrees per day, σ_D, and the 1σ error in the longitude determination expressed in degrees, σ_λ.

Table 2.3

Tracking Accuracy

Stations	Measurements	2 Days of Tracking		10 Days of Tracking	
		σ_D	σ_λ	σ_D	σ_λ
P_1, Q_1	A, E	.00325	.0138	.00651	.0133
P_2, Q_2	A, E	.00325	.0141	.00652	.0137
P_3, Q_3	A, E	.00275	.0121	.00650	.0118
P_1, Q_1	A, E, R	.00056	.00036	.00056	.00033
P_2, Q_2	A, E, R	.00056	.00033	.00056	.00030
P_3, Q_3	A, E, R	.00056	.00035	.00057	.00032

The pair of ground stations P_1, Q_1 are close to the location of the proposed CANSAT ground stations. It is seen that the accuracy is nearly insensitive to the placement of the ground stations. These results may be interpreted in the following way: the quoted value is the standard deviation of the normally distributed parameter being estimated. For example, in the case of stations P_1 and Q_1, tracking for 10 days with angle measurements, the probability that the satellite longitude estimate differs from the true longitude by more than 0.0266° is 0.045. The probability of being more than 0.04° in error is 0.003. The advantages of range measurements are a more accurate longitude determination and a more rapid drift rate determination. However, the accuracy achieved with angle tracking seems sufficient for the planned mission.

Based upon the results shown in Table 2.3, it is concluded that ranging information is not required for the CANSAT mission, thereby simplifying both the ground stations and satellite design.

REFERENCE

[1] "Evaluation of Antenna Pointing Accuracy", D.C. Buchanan, RCA Internal Correspondence, 10 June 1968.

PART II

Trade-offs and Preliminary Design

3.1 Constraints

The following list gives the various constraints, assumptions and guidelines that were used in the tradeoff study.

	DSV3L[2]	Atlas Burner II
Payload weight in transfer orbit	965	1005
Shroud	existing or new with same diameter	new, based on existing
Solar array	Based on Intelsat III panels	Based on Intelsat III or new
Minimum No. RF Channels daylight	4	4
Minimum No. Channels eclipse	2	2
Minimum EIRP at edge of country	34 dbw	34 dbw
Pointing error	$\pm 0.5^{\circ}$	$\pm 0.5^{\circ}$
Polarization	Down Link Linear E-W	Down Link Linear E-W

3.1.1 Spacecraft Tradeoffs

The most important tradeoff considered at the beginning of the study is the budgeting of the available payload weight to maximize communications capacity. As a starting point a transfer orbit payload weight of 950 pounds was used (as given in the work statement). As more up to date vehicle and subsystem numbers were generated the power and weight budgets were revised to maintain the largest possible fraction of payload weight dedicated to the basic communications function, while maintaining a reasonable margin for weight growth. Before the complete antenna beam optimization had been performed as described in Section 1.6 it was possible to make trial weight and power budgets based on the tentative specifications of the work statement and the weights and powers of subsystems and components from the Intelsat III spacecraft. Workable if somewhat conservative assumptions of antenna gain and circuit losses were made to determine the TWT power requirements per RF channel, and DC power calculated

using current TWT and power supply efficiencies.

To give flexibility in the weight evaluation of several candidate spacecraft configurations, TWT RF output per channel was used as a convenient parameter. This is consistent with the variations that may occur in the assumed antenna gain and circuit losses, and with the possible lowering of minimum EIRP depending on earth station assumptions.

3.1.2 Configurations Considered

(1) Existing Delta Shroud

Within the existing Delta shroud the largest antenna of suitable beam size that will fit within the tapered portion has been described in Reference 1. The largest solar array can be taken somewhat optimistically as 61 inches long with a 55 inch diameter. The antenna gain at beam edge and the derived power level per channel indicates a maximum of four daylight channels. This configuration is space limited and some of the weight margin may be used to provide full eclipse operation and greater TWT redundancy.

(2) Modified Delta Shroud

For this option no shroud restriction is placed on solar array height or antenna height, the array diameter is assumed fixed however at 55 inches. The largest solar array is used in conjunction with the highest gain antenna that covers Canada subject only to payload weight limit.

(3) Atlas Burner II Shroud

For this option no shroud restriction was assumed and it is probable that the existing Intelsat III solar array diameter would be maintained and the length of array and antenna height subject to weight limits only.

3.1.3 Weight and Power

Figure 3-1 is a typical plot of array power as a function of TWT RF power output per channel for both a 6 channel and a 4 channel configuration.

Ref. 1 A Canadian Satellite to serve Canada's Domestic Communictions Requirements RCA Space Systems, September 1967

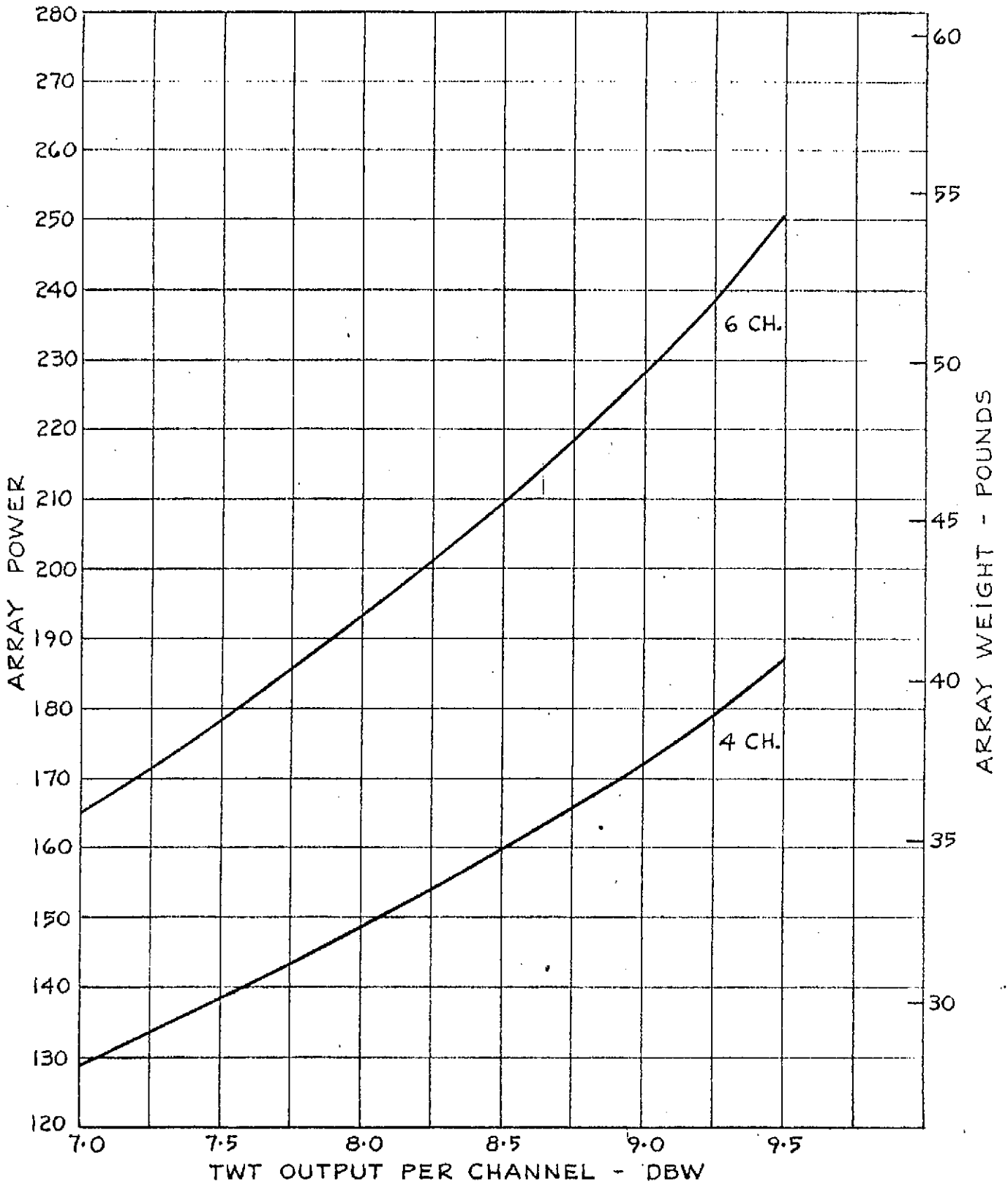

FIG. 3·1

ARRAY POWER VS. TWT OUTPUT

Figure 3-2 is a plot of battery capacity in watt hours as a function of TWT RF power per channel with all other loads assumed constant and an eclipse of 72 minutes.

Combining the information from figures 1 and 2 and using the best available estimates of solar array and battery specific weights we get a combined weight curve as shown in Figure 3.3 for various candidate configurations.

3.1.4 Beam Size and EIRP

Figure 3-4 is a graph showing combinations of NS and EW beam dimensions which give equal antenna gain according to the equation

$$Go = 45.85 - 10 \log \theta_{NS}\ \theta_{EW}$$

where Go = Beam centre gain

θ_{NS} = Beam width in N-S direction

θ_{EW} = Beam width in E-W direction

If we assume that the optimum beam will have a gain at the edge one half neper (4.34 db) below the beam center and further assume 2 db circuit loss between the TWT and antenna port, we can plot EIRP at beam edge with TWT output per channel as a running parameter. When the angular dimensions of the coverage area are shown as limits we can then see the minimum TWT output per channel required to produce a given EIRP at beam edge.

3.1.5 Eclipse Operation

To maximize the number of communications channels available during normal sunlit operation it is necessary to keep eclipse capacity to a minimum (2 ch.) thereby keeping battery weight to a minimum.

It is interesting to observe that considerable excess solar array capacity exists at equinox (eclipse season) because of perpendicular illumination, and is more than adequate to recharge batteries for the maximum number of eclipse channels. This can be explained by the long period available for recharge ($\approx$20 hours). In practice the solar array size need only be increased by a small amount to account for a trickle charge to maintain battery charge and temperature during non eclipse times.

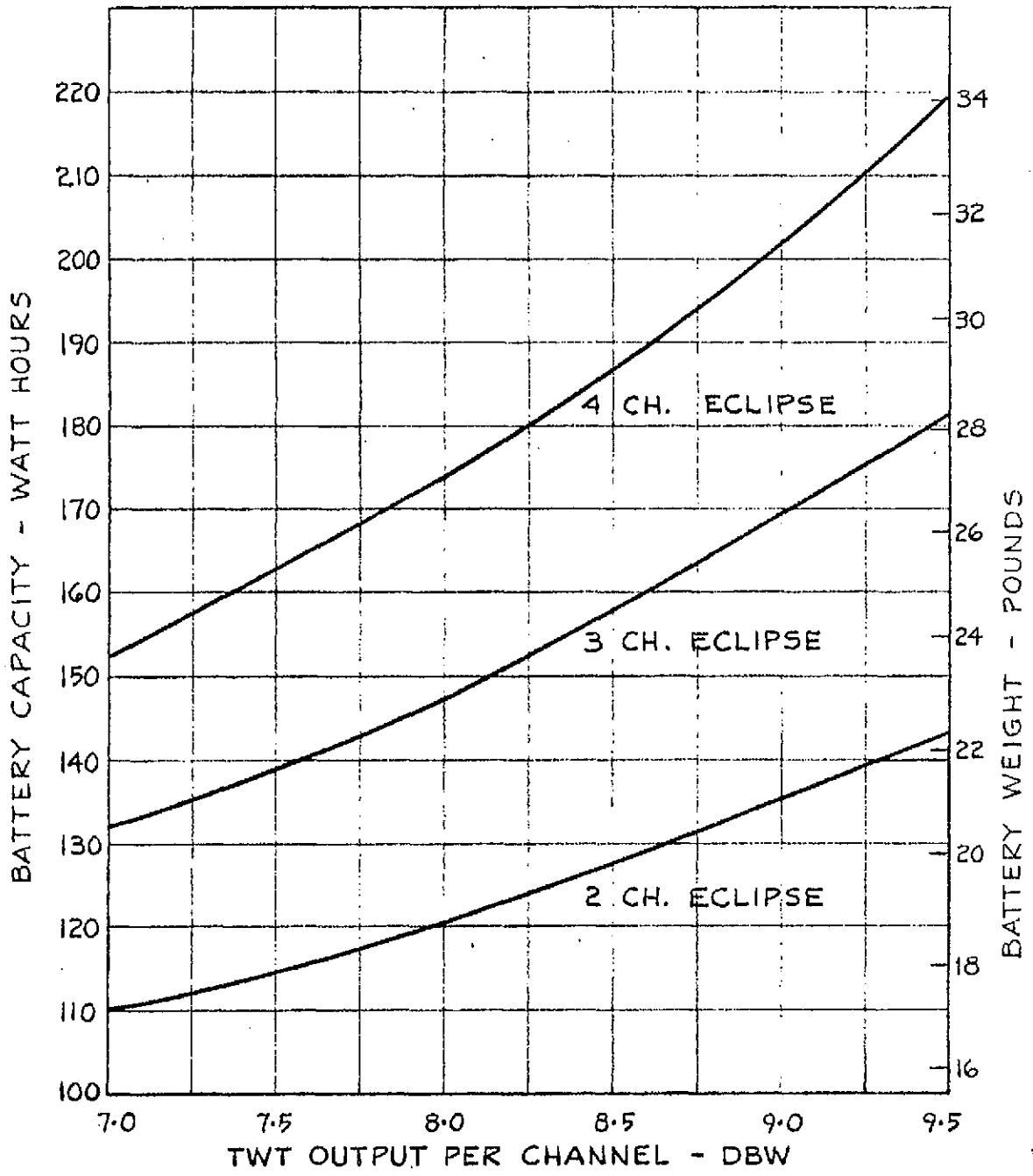

FIG. 3·2

BATTERY CAPACITY VS. TWT OUTPUT

ECLIPSE TIME 72 MINUTES

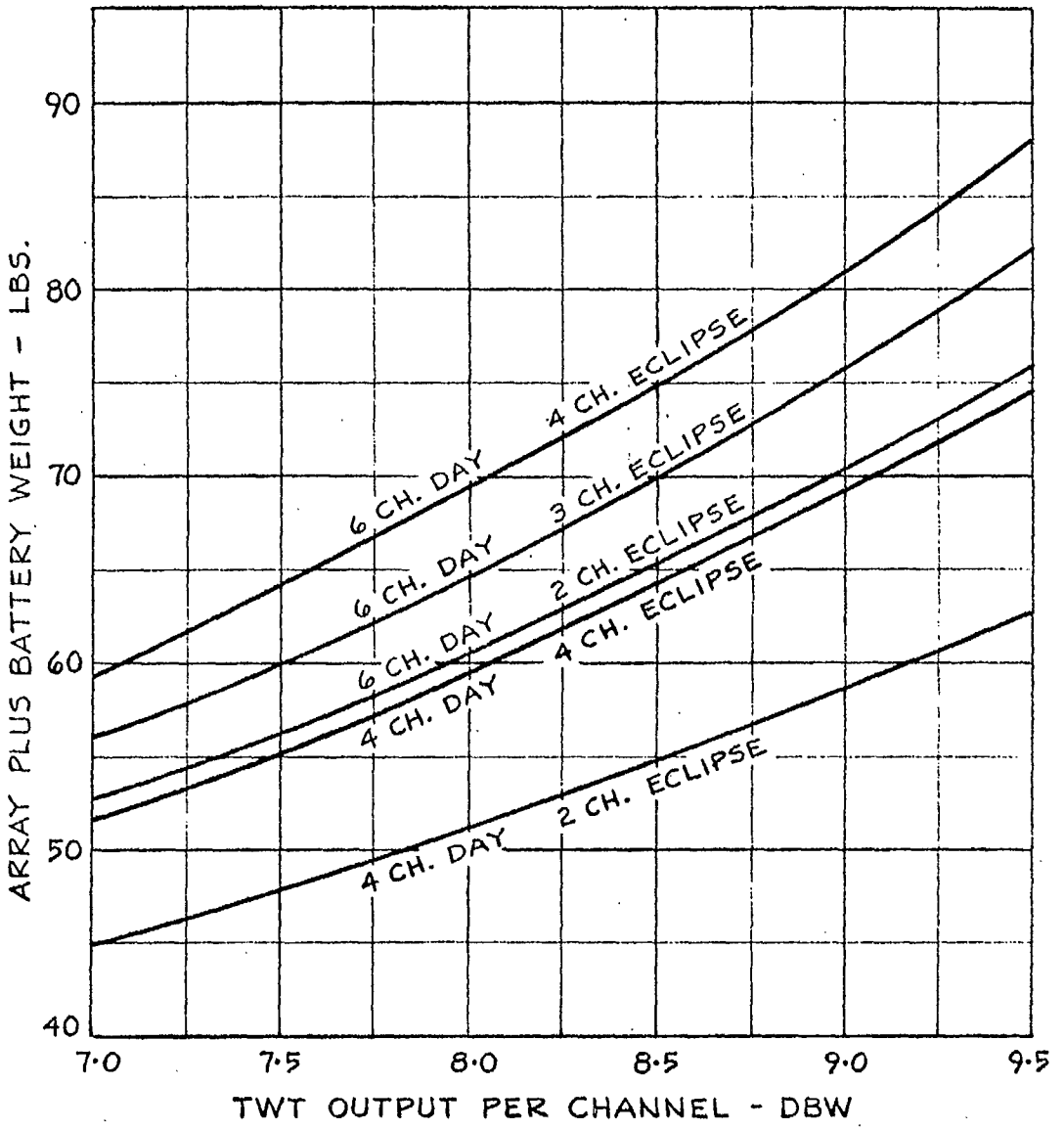

FIG. 3·3

SOLAR ARRAY PLUS BATTERY WEIGHT VS. TWT OUTPUT PER CHANNEL.

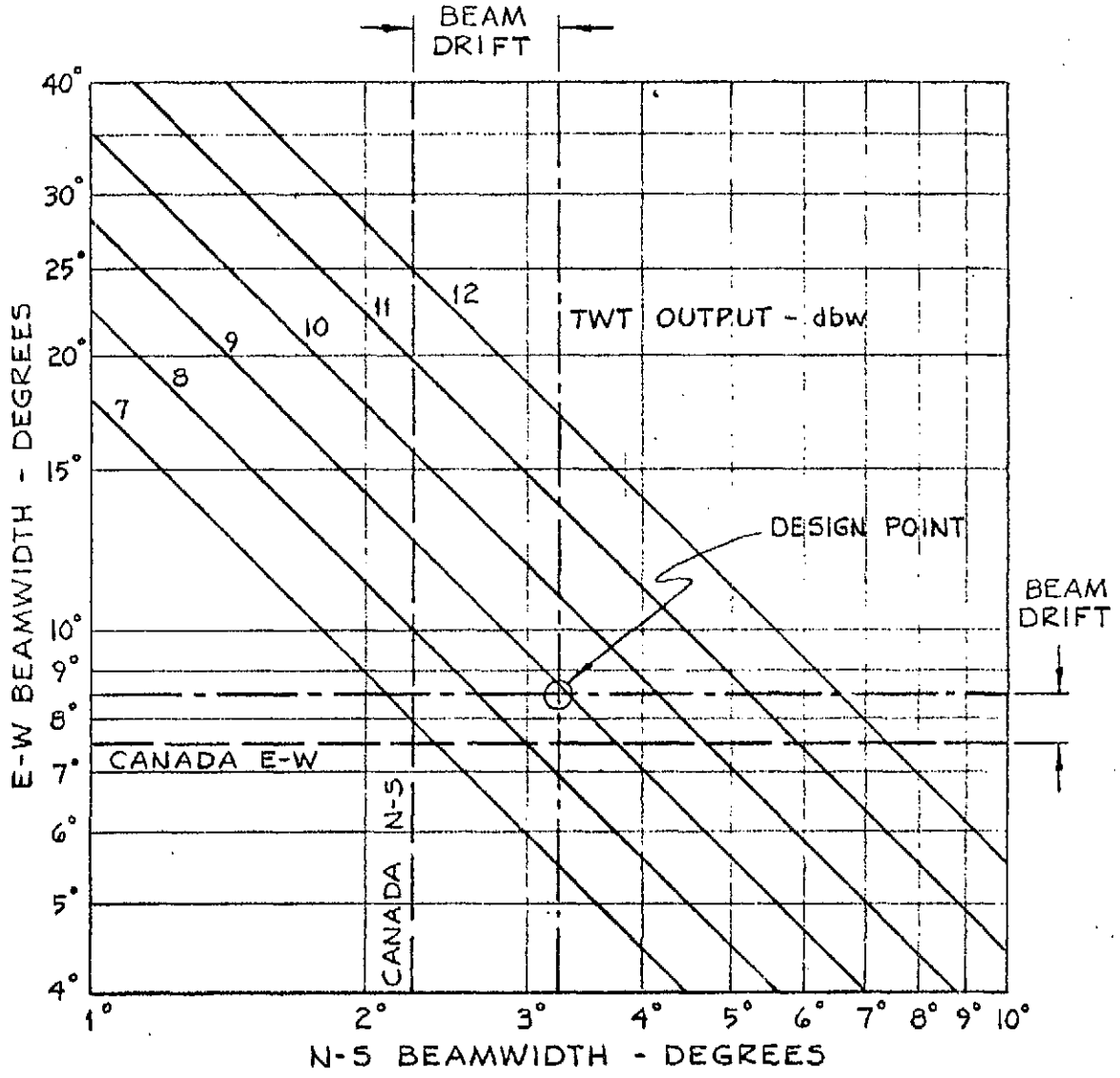

FIG. 3·4

REQUIRED TWT POWER AS A FUNCTION OF BEAM SIZE.

ASSUMPTIONS:

GAIN AT BEAM EDGE = $41.51 - 10 \log \theta_a \theta_b$

EIRP " " = 34 dbw

3.1.6 Station Keeping Considerations

No consideration is given to trading off fuel for longitude station keeping as this function, as well as spin axis maintenance, is essential. The largest portion of the secondary propulsion fuel is needed for correcting orbital inclination drift. This weight could be used alternatively for extra communications channels, increased ERP, operational lifetime, or for increased reliability through redundancy, if earth station designs could be economically adapted to the resulting satellite oscillations in latitude ($\approx \pm 2.5^{\circ}$).

The drift of theorbital plane which is the cause of the problem is regular and predictable, so some consideration could be given to fuel savings by a combination of initial inclination biasing and a limited number of corrections. The pertinent expressions are:

$$V_N = V_T \cdot \frac{N}{N+1}$$

and

$$C_N = \frac{Ct}{N+1}$$

where V_N = velocity increment for N corrections

V_T = total velocity increment for complete removal of inclination

N = Number of corrections

C_N = Peak inclination error associated with N corrections

C_T = Peak initial inclination error (assumed one half of the total uncorrected drift over the satellite lifetime).

The technique is shown graphically in Figure 3.5. Figure 3-6 shows the total amount of secondary propulsion fuel required to stay within stated limits, with spacecraft lifetime as a parameter.

For the present earth station technology no economic solutions exist for the problem of limited steering capability to accommodate a satellite of uncontrolled or moderately limited inclination (say $\pm 2.5^{\circ}$). As can be seen from the figures, no significant fuel savings acrue when the inclination error is small and the number of corrections large. The ground station philosophy has been then to demand as accurate as

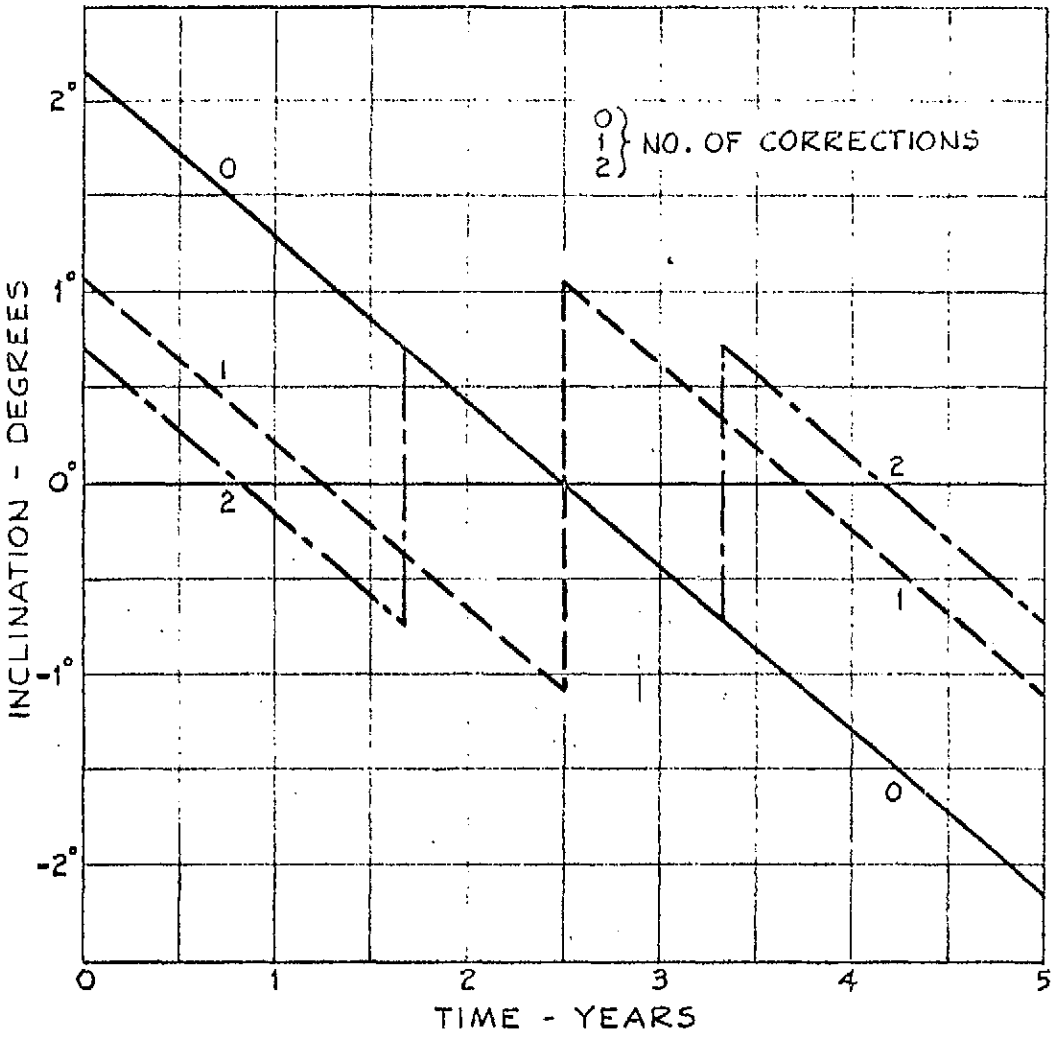

FIG. 3·5
INCLINATION HISTORY VS. NO. OF CORRECTIONS

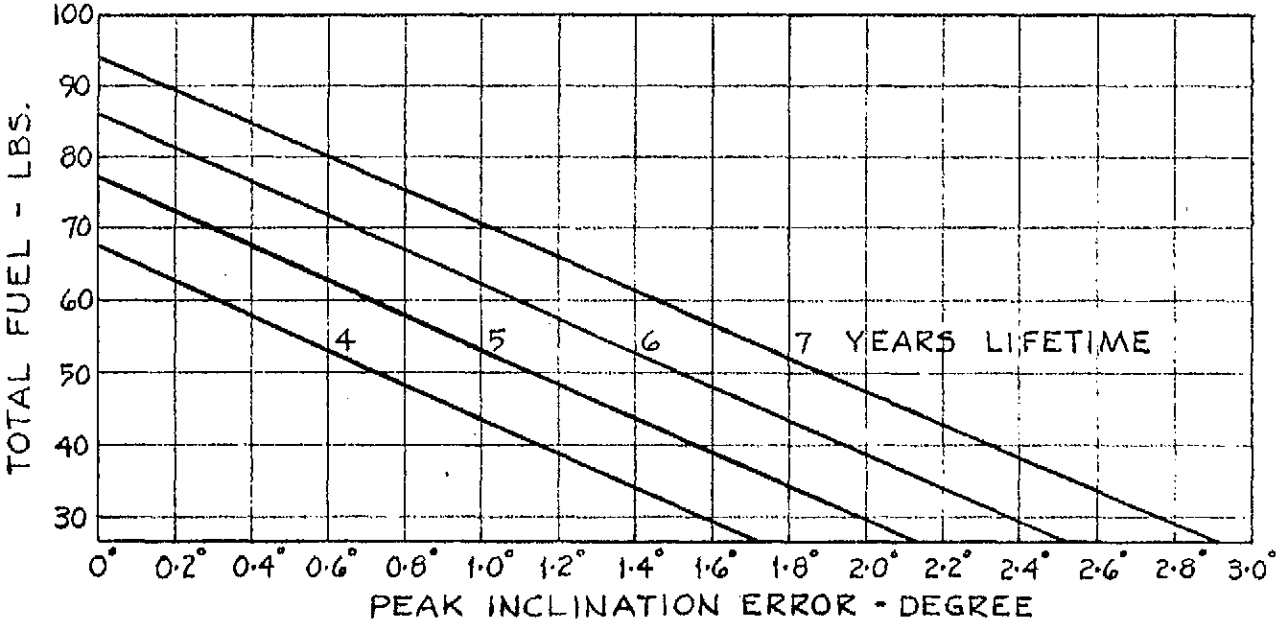

FIG. 3·6

TOTAL FUEL REQUIREMENTS VS. INCLINATION ERROR AND LIFETIME.

possible satellite station keeping to permit use of relatively large (30') non steered antennas. No extra fuel pensalty is paid for this accuracy and it becomes mainly a problem of obtaining accurate tracking information from the control stations. Without inclination correction there would be a small but significant penalty in the spacecraft antenna gain which depends on the peak orbital inclination because the beam would have to be increased in the NS sense by the amount of the peak to peak latitude excursion ($\approx 5^{o}$). It can be mentioned parenthetically that much scope for ingenuity exists in the area of economical TV receiving stations for this satellite system.

3.1.7 Frequency and Polarization Considerations

From reasonably detailed considerations of spacecraft transponder filter design requirements, it is concluded that alternate channels should have opposite sense polarization. This is true whether all channels are in one satellite, as Intelsat IV, or half in one satellite and half in a second satellite occupying the same orbital slot as is proposed here. The same reasoning applies also for linearly or circularly polarized satellites. Where the adjacent channel protection is achieved by frequency filtering alone, a very difficult filter design must be assumed which becomes impractical at 4 GHz because of group delay and temperature problems. Even at an IF of several hundred MHz, filters are still troublesome. If polarization isolation at beam center can be used to give 12 to 15 db of adjacent channel rejection, then filter problems are very much reduced and the prospects of an all RF design becomes more practical. This is considered advantageous because of the simpler configuration of the all RF transponder.

The transmission to ground would be with all channels of the same polarization. Adjacent satellite orbital slots would use the opposite sense of polarization taking advantage of any polarization discrimination that the ground station antenna sidelobes may provide on transmission or reception. For calculation of interference from adjacent satellites into an earth station, which determines satellite spacing, it is assumed that all interfering satellites are illuminating the same area as the desired one. It is assumed that no advantage is gained by polarization discrimination in the ground station sidelobes but an isolation of about 15 db would be obtained by offsetting adjacent satellite frequencies by one half a channel bandwidth.

Table 3.1.1 shows several possible combinations of frequency and polarization plans of which plan 3 is the preferred one. Here both up and down links of adjacent satellites would operate on interleaved frequency plans with opposite senses of polarization. This plan is optimum if no advantage is claimed for polarization

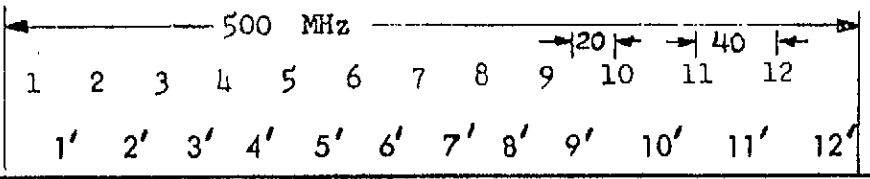

Channel Nos		Channel Nos
1	Orbit Location A	6 up
		4 down
	Orbit Location B	6 up
		4 down
2	Orbit A	6
		4
	Orbit B	6
		4
3	Orbit A	6
		4
	Orbit B	6
		4
4	Orbit A	6
		4
	Orbit B	6
		4
5	Orbit A	6
		4
	Orbit B	6
		4

Table 3.1.1

ALTERNATIVE FREQUENCY AND POLARIZATION PLANS

discrimination. Other plans such as #5 with all up links of one polarization offer the same performance. The point to be made is that if polarization discrimination to adjacent satellites does not exist, then complete flexibility exists in a choice of polarization plans, and a plan is chosen which gives maximum benefit to satellite and ground station design without affecting system compatibility.

3.1.8 Ground Station Considerations

With all transmissions from one satellite location of the same polarization, the low noise front end of the ground receiver would be the same for any number of received channels. If reception from an oppositely polarized satellite is required it would probably be done by manually changing the connection between the low noise amplifier and the appropriate port of the feed assembly.

If it becomes necessary to transmit both polarizations frome one antenna while receiving all channels, such as from a central station originating more than six programs, then it would be necessary to provide a transmit-receive frequency duplexer at one port of the orthogonal coupler. This would increase the system receiving temperature by a few degrees Kelvin.

3.1.9 Linear or Circular Polarization

Circular polarization has the advantage that a greater variety of antenna and feed systems are available as design choices. A rotating feed system is possible, that is one without the losses of a rotary joint, illuminating a despun mirror or combination of reflecting surfaces. Such a system is not possible with linear polarization as relative rotation between a linear feed and a mirror would produce rotating linear polarization. A rotating circular waveguide joint supporting orthogonal circular modes is attractive because of its low loss compared to a coaxial rotary joint. Figure 3.7 shows several methods of transferring signals between the despinning and despun portions of the satellite, for both add and even channel satellites where it is assumed that;

(1) up and down links are linearly polarized

(2) all down links are vertically polarized for the initial Canadian system

(3) there are six channels per satellite.

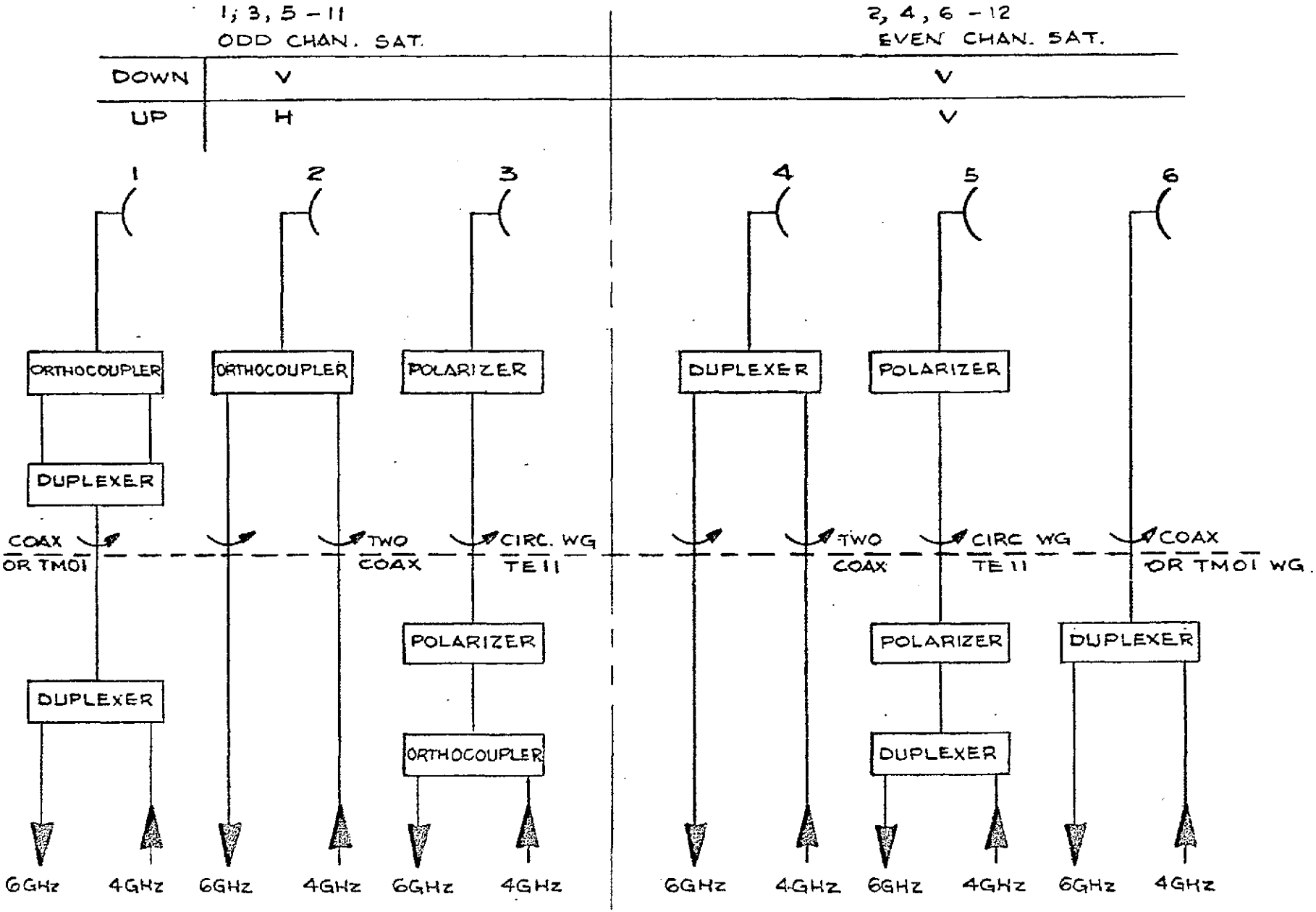

FIG. 3.7

ALTERNATIVE FEED METHODS FOR A SIX CHANNEL SATELLITE WITH DESPUN ANTENNA (LINEAR POLARIZATION)

Figure 3-8 shows alternative feed methods for a circularly polarized satellite.

Construction of the satellite antenna feed system with circular polarization is more complex than linear because of the polarizer that is necessary to convert from linear to circular. At the same time the use of linear polarization prevents the possibility of using circular waveguide with a low loss waveguide rotary joint. This occurs because

(1) Two orthogonal linear polarizations cannot pass through a rotating waveguide joint and

(2) It is impractical to use two polarizers to convert from linear to circular and back again after a waveguide rotary joint.

The polarization plans discussed here are naturally adapted to a six or three channel satellite configuration. The four channel minimum requirement configuration is not as well suited to the alternating polarization plan because one of the three satellites necessary to develop an orbital slot would have to carry both odd and even channels though not necessarily adjacent in frequency. See Table 3.1.2.

If linear polarization is used method 2 Figure 3.7 using two coaxial rotary joints is preferred for the odd channel satellite. For even channel satellite method 6 using a single coax rotary joint is preferred. For circular polarization some question still exists about the possibility of achieving bends in a circular waveguide supporting the TE11 mode. If it is feasible, then the odd satellite would use method 7 and the even, method 9.

3.1.10 Selected Sapcecraft Configurations

Table 3.1.3 summarizes the key characteristics of several candidate spacecraft of which the 6 channel day and 2 channel eclipse configuration is the preferred one for the DSV3L[2] launch vehicle with modified fairing, and the same version with extended life and reliability as the preferred version for the Atlas Burner II vehicle.

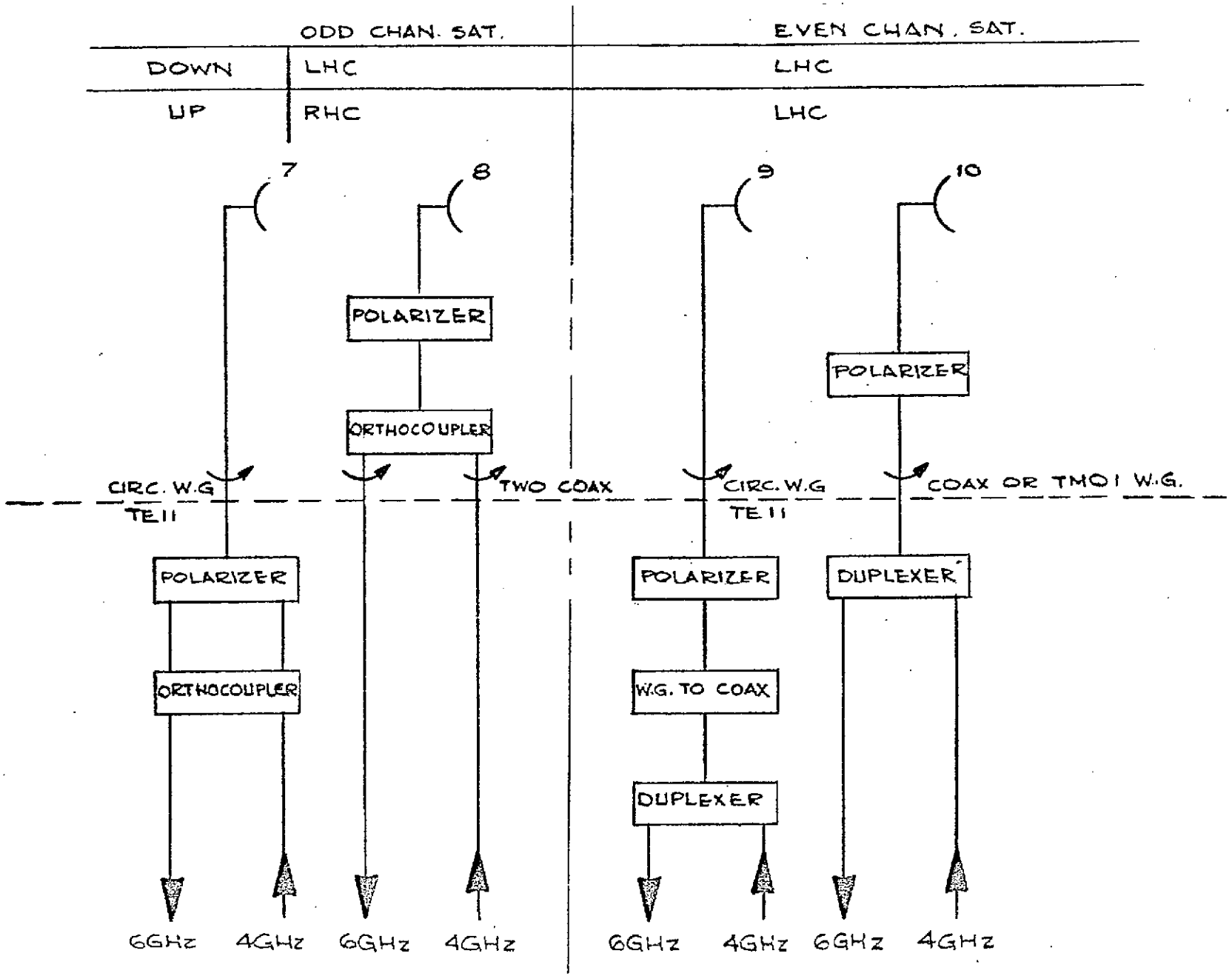

FIG. 3.8

ALTERNATIVE FEED METHODS FOR A SIX CHANNEL SATELLITE WITH DESPUN ANTENNA (CIRCULAR POLARIZATION)

CHANNEL NOS.	1	2	3	4	5	6	7	8	9	10	11	12	
SAT. 1.	↑						↑		↑		↑		PLAN 1
SAT. 2.		→		→		→						→	
SAT. 3			↑		↑			→		→			
SAT. 1	↑		↑		↑						↑		PLAN 2
SAT. 2						→		→		→		→	
SAT. 3		→		→			↑		↑				
SAT. 1					↑		↑		↑		↑		PLAN 3
SAT. 2		→		→						→		→	
SAT. 3	↑		↑			→		→					

TABLE 3.1.2

ALTERNATIVE FREQUENCY AND POLARIZATION PLANS FOR A FOUR CHANNEL SATELLITE

	Existing Delta Fairing		Modified Delta Fairing		Atlas Burner II		
RF Channels day	4	4	6	4	6	6	6
RF Channels eclipse	2	4	2	4	2	4	6
EIRP Beam edge	34	34	34	34	34	34	34
Beam Size (3db)	3.3 x 8.6	3.3 x 8.6	2.7 x 7.0	2.7 x 7.0	2.7x 7.0	2.7 x 7.0	2.7 x 7.0
Array Weight lbs	39.7	39.7	49.5	37.5	49.5	49.5	49.5
Battery Weight	22.1	33.5	21	31.5	21	31.5	42
Lifetime Yrs	6	5	5	6	6	5	5
Number of OP TWTs	8	6	6	6	9	9	6
Prob of Survival 4 Ch.	.642	.683	.723	.618	.698	.741	.723
Prob of Survival Full	.642	.683	.344	.618	.591	.656	.344
Weight Margin	37	43.6	37.1	36.6	39.1	39.6	41.1
Limitation	DC Power	DC Power	Weight	Weight	Weight	Weight	Weight

Table 3.1.3

3.2 Antenna

The requirement for the antenna on the Cansat satellite is to exceed a minimum specified power level over the surface of Canada. It must do this in a manner which is most economical in terms of satellite weight and power requirements. This is somewhat different than normal antenna designs where maximum gain on axis is required and the optimum configuration must be determined.

The actual antenna gain is given by the expression $G = \mathcal{E}\frac{4\pi A}{\lambda^2}$ which becomes:

$G = \frac{\pi^2 \mathcal{E} a b}{\lambda^2}$ for an elliptical aperture and

$G = \frac{4\pi \mathcal{E}^2 a b}{\lambda^2}$ for a rectangular aperture.

Where $\mathcal{E}$ is aperture efficiency

a is the major dimension and

b is the minor dimension of the aperture

The 3 db beam widths are $\Theta_{a3} = \frac{K\lambda}{a}$, $\Theta_{b3} = \frac{K\lambda}{b}$

in the directions of the major and minor axis respectively where the proportionality constant K is the same in the two directions but differ from rectangular to circular and for different illumination tapers.

Eliminating a and b the gain becomes

$G = \frac{\pi^2 \mathcal{E} K^2}{\Theta_{a3}\,\Theta_{b3}}$ elliptical and

$G = \frac{4\pi \mathcal{E}^2 K^2}{\Theta_{a3}\,\Theta_{b3}}$ rectangular

Since Θ_{a3} and Θ_{b3} are fixed by geometrical considerations it is necessary only to maximize the product $G\,\Theta_{a3}\,\Theta_{b3}$ which can be considered a figure of merit for antennae of this type.

Using published* values of gain and beam width for different illumination tapers, the products $G\Theta_{a3}\,\Theta_{b3}$ have been calculated and plotted in Figure 3.9 as a function of the first side lobe level. The figure of merit varies from a low of 9.7 for uniform illumination to a high of 12.4 for $\left(\text{Cos}\ \frac{\pi x}{2}\right)^4$ illumination with side lobe levels ranging

* Silver S., Microwave Antenna Theory and Design
Volume 12, Radiation Laboratory Series

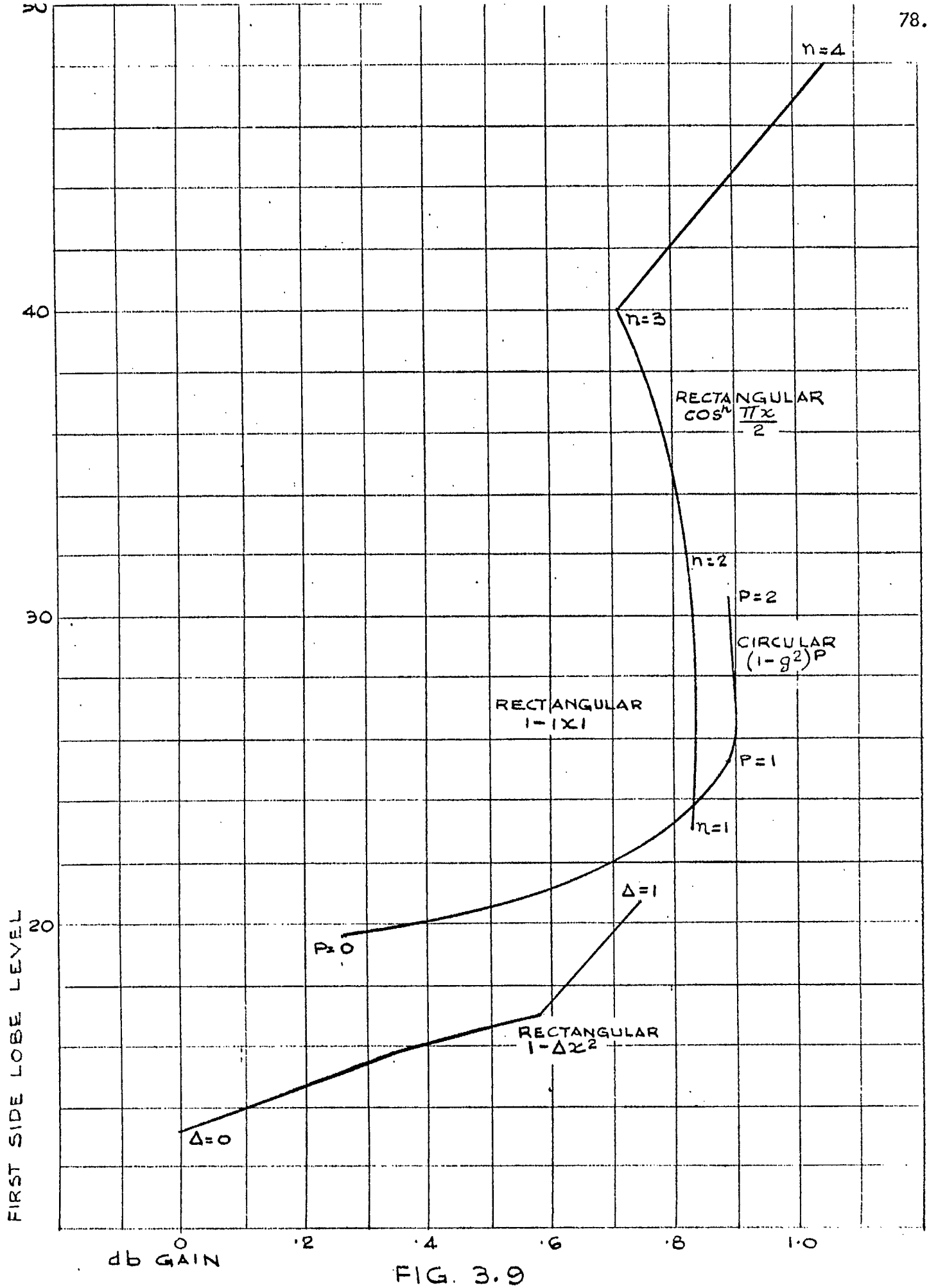

FIG. 3.9

GAIN IMPROVEMENT COMPARED TO A RECTANGULAR APERTURE WITH UNIFORM ILLUMINATION OVER A SPECIFIED ANGULAR COVERAGE

between 13.2db for uniform to 48 dB for $(\text{Cos}. \frac{\pi x}{2})^4$. This graph stresses the fact that the less energy radiated into the side lobes the more will be available for the main lobe and every effort should be directed towards reducing the level of the side lobes, and preventing loss due to spill over. While a rectangular aperture with $(\text{Cos} \frac{\pi x}{2})^4$ illumination is the best it would require the antenna to be made so perfectly that the 48 db side lobe levels are maintained. It is preferable to aim at side lobe levels between 20 and 25 db which are more easily attainable. Two tapers look reasonable, a circular aperture with $1 - \rho^2$ taper and Cos $\frac{\pi x}{2}$ taper with a rectangular aperture.

The specifications calls for a power level of 37 dbw to be radiated onto the surface of Canada. This can be done with a low gain antenna and high transmitter power or a high gain antenna and low transmitter power. Weight calculations have indicated that the minimum satellite weight occurs when the highest gain antenna is used consistent with the required ground coverage. The minimum beam widths required to adequately cover Canada have been determined by a series of computer calculations described in Section 1.6. These minimum angles are 3.25 degrees N-S and 8.5 degrees E-W.

In addition to finding the optimum illumination taper for the aperture it is necessary to determine the antenna size to give maximum gain at the edge of the required coverage. In this way the required transmitter power is a minimum.

For a circular aperture with $1 - \rho^2$ illumination the maximum gain at the edge of the coverage occurs when the field strength is 4.03 db below the maximum. For a rectangular aperture with Cos $\frac{\pi x}{2}$ illumination the corresponding figure is 4.03 db below the beam peak. The following table summarizes the results for these two antennae.

	Circular	Rectangular
U at edge of coverage	2.29	.682 π
Aperture width for 3.25° beam (inches)	76.8	71.9
Aperture width for 8.5° beam (inches)	29.4	27.5
Theoretical gain (db)	33.97	34.44
Efficiency loss (db)	1.25	1.83
Net gain (db)	32.72	32.61
Beam edge below peak (db)	-4.03	-4.0
Gain at edge of coverage (db)	28.69	28.61

The circular aperture illumination has a slight margin of superiority in gain at the expense of a slightly higher antenna. However, the lack of the square corners may make it easier to fit within the shroud. The final dimensions of the antenna may be adjusted depending upon the illumination taper actually obtained.

Three antenna configurations have been investigated in detail. The structure, support feed and feed line have been designed for each and the antennas are compared on the basis of total weight and net loss. The three antenna configurations are 1) offset segment of a parabola of revolution. 2) Center fed parabola of revolution, 3) double reflector antenna system. These configurations are described in more detail in the following paragraphs.

3.2.1 Offset segment of a parabola of revolution (Figure 3.51).

This has a number of attractive features as well as some difficult design problems. The antenna has no aperture blockage because the feed horn is outside the aperture area. In addition the feed line from the satellite is minimum resulting in lowest losses: Undesirable electrical features are the assymetric aperture illumination and the poorer cross polarization performance compared to a symmetically fed parabola of revolution. This configuration presents some difficult mounting problems. A focal length of 42 inches is about optimum. With a shorter focal length the upper tip interferes with the shroud and with a longer focal length very little space is available behind the reflector for support structure. In addition the configuration presents difficult thermal design problems to prevent excessive thermal distortions due to temperature differences parts of the support structure. Additional weight would be necessary to balance the despun platform.

3.2.2 Center fed parabola of revolution, (Figure 3.52A)

This configuration offers adequate space to design a rigid light weight and thermally stable support structure. In addition, because a shorter focal length can be cased, the antenna can be positioned so that no additional weights are required for balancing purposes. The antenna has good cross polarization characteristics but has larger losses due to the long feed line and some blockage.

3.2.3 Double reflector antenna (Figure 3.52B).

A standard cassegrain utilizing a parabola and hyperbola of revolution is difficult to design for this application, both because of the large beam widths involved and the large aspect ratios in aperture dimensions. It has the same attractive features as the second configuration with a slightly shorter feed line.

The subreflector blockage is greater than the blockage of the horn in antenna two. It is however possible to shape the subreflector to accomplish illumination control. In this way it is possible to radiate the energy normally blocked by the subreflector and to control the illumination taper for optimum performance. In this way much of the loss due to blockage can be eliminated. Some loss remains due to the degradation in pattern because of the hole in the illumination.

3.2.4 Bandwidth

The satellite communication band is a full 500 MHz between 3.7 and 4.2 GHz for the down link and between 5.925 and 6.425 GHz for the up link. The antenna and feed system must handle the full 500 MHz band at both up and down frequencies. In addition, a duplexer must be provided to isolate the receiver from the transmitter signal. The 500 MHz band is divided into twelve 40 MHz bands. A plan for allocating these bands is described in section 3.1. As described in that section one satellite would transmit channels 1,3,5----11. With the up link polarized at right angles to the down link while a second satellite at the same location in space would transmit channels 2,4,----12 with the up and down links polarized in the same direction. Thus on one satellite a polarizer is used to isolate the up and down link while in the second satellite a diplexer is used.

3.2.5 Polarization

The preferred polarization from the antenna stand point is E-W for the 4 GHz down link and either N-S or E-W for the 6 GHz up link. This preference is slight and the alternate polarization for the 4 GHz down link could be used. However, the horn and duplexer are designed on the assumption that the 4 GHz down link is polarized E-W.

3.2.6 Feed Methods

The various methods by which the up and down links can be taken through the rotary joint are presented in section 3.1. The two preferred configurations for the two satellites carrying the even and odd frequency bands respectively are reproduced in figure 3.10.

3.2.7 Efficiency

The theoretical gain of the antenna given by $\frac{4\pi A}{\lambda^2}$ is reduced by the efficiency of the aperture distribution η_A and a number of other losses which must be evaluated. The first loss is spillover loss, i.e., that part of the feed horn pattern which is not intercepted by the reflector

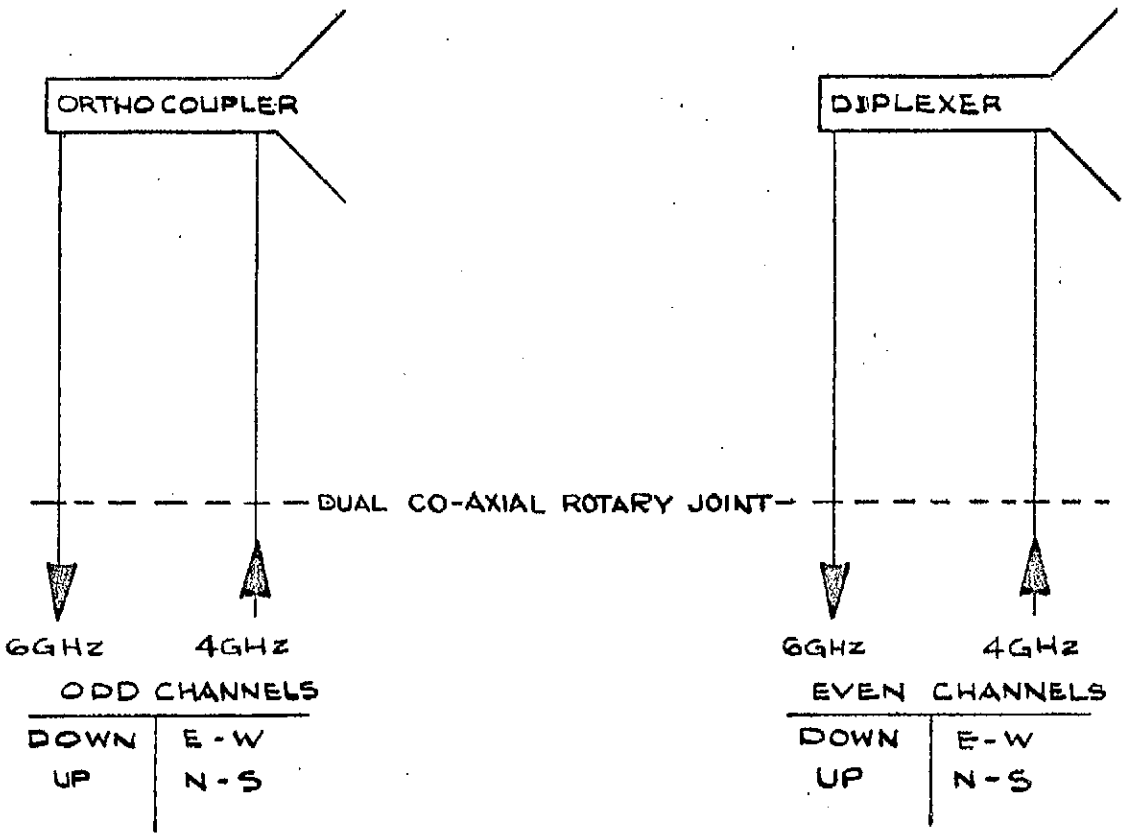

FIG. 3.10

PREFERRED DUPLEXER CONFIGURATIONS FOR LINEAR POLARIZATION SYSTEMS.

surface. This includes back lobe energy from the horn. If a sub-reflector is used most of this loss occurs at the subreflector η_{SS}, but a small additional amount occurs at the main reflector η_{SM}. If any obstruction occurs within the aperture then on additional loss of energy occurs. This is divided into two parts, the loss due to the reduction in radiated energy η_{BE} and the loss in gain due to pattern degradation η_{BP}. The first part is recoverable by properly shaping the subreflector, the second part is not recoverable. The support structure for the horn or subreflector contributes the blockage loss η_{BQ}. Random deviations in surface contours cause a loss in gain η_{PM} due to scattering into the side lobes. Loss in gain η_{PF} also occurs due to phasing errors caused by the phase center of the horn being of finite size. The above losses are caused by geometrical errors and are associated with the antenna gain. The remaining losses are associated with the feed line, they are mismatch loss in the feed horn η_{RF}, absorption loss in the horn η_{LF}, ortho coupler or duplexer loss η_{CC}, waveguide loss η_{LL}, waveguide to coax transition loss η_{WC}, and finally the rotary joint loss η_{RJ}. Additional losses associated with the transmitter filtering and multiplexing are also shown.

The following table summarizes the performance of the three antenna configurations giving the estimates losses and the estimated net gains at beam edge as well as the weight estimates of the antenna and its associated support structure.

4 GHz Antenna Losses in db for Three Antenna Configurations with elliptical aperture 76.8 x 29.4 inches and illumination tapers $1 - \rho^2$.

Antenaa		1 Offset Feed Horn	2 Center Feed Horn	3 Shaped Subreflector
Distribution efficiency	η_A	1.25	1.25	1.25
Spill over main reflector	η_{SM}	1.10	1.00	0.25
Spill over subreflector	η_{SS}	-	-	1.00
Energy blockage	η_{BE}	-	0.11	-
Blocked pattern degradation	η_{BP}	-	0.06	0.54
Support Blockage	η_{BQ}	-	0.20	-
Surface inaccuracies Sd = .003"	η_{PM}	0.10	0.10	0.20
Phase center errors	η_{PF}	0.07	0.07	0.07
Total Antenna loss		2.52	2.79	3.31
Reflection loss in feed	η_{RF}	0.04	0.04	0.04
Absorption loss in feed	η_{LF}	0.03	0.03	0.03
Line length inches		30	80	80
Line loss waveguide	η_{LL}	0.05	0.11	0.07
Rotary joint lossq	η_{RJ}	0.30	0.30	0.30
W.G. to coax trans.	η_{WC}	0.10	0.10	0.04
Ortho coupler or diplexer	η_{CC}	0.10	0.10	0.10
Total feed loss		0.56	0.62	0.58
Filter and multiplexer loss		1.10	1.10	1.10
Total Loss		4.18	4.51	4.99
Theoretical antenna gain		33.97	33.97	33.97
Theoretical gain at beam edge -4.03		29.94	29.94	29.94
Net gain at beam edge		25.76	25.43	24.95
Beam edge power with 9 dbw TWT		34.76	34.43	33.95

3.2.8 Support

The antenna support structure must fullfil a number of rather stringent requirements. It must maintain the antenna dimensions and keep it pointing in the correct direction, have minimum weight, withstand the launch environment, and not interfere with the shroud during launch. In addition the despun platform must be balanced about the axis of the spacecraft, and finally it must be thermally stable so that temperature differentials do not distort the antenna or change the beam direction excessively.

Because of these conflicting requirements the final selection of the antenna configuration has not been made at this time. The study of all three types will be continued in parallel until the overall advantage of one configuration becomes clear.

A detailed description of the mechanical and thermal aspects of the antenna and antenna support are given in the section (3.10) on structures and in the thermal section (3.9).

3.3 The Transponder

3.3.1 Introduction

The transponder, for the purpose of this report, is defined as the electronics package which accepts signals from the rotary joint in the frequency band 5925-6425 MHz and delivers amplified signals to the rotary joint in the frequency band 3900-4200 MHz. It therefore excludes components associated with the antenna, viz, the polarizer, the orthogonal coupler or the duplexer and the rotary joint itself.

The transponder consists basically of an amplifying chain with some means of translating the 6 GHz band to the 4 GHz band. With the proposed scheme the transponder amplifies only the communications signals and is devoid of any function in the command and telemetry area.

3.3.2 Input Carrier Level to the Transponder

The uplink carrier-to-noise temperature or C/T ratios were calculated and summarized in section 1.3 (c) and are repeated here.

No. of Carriers per RF Channel	Capacity	C/T (dbW/°K) per carrier	C dbw (per carrier) T = 1830°K
4 to 6	60 channels	-139.1	-106.5
2	600 channels	-123.2	- 90.6
1	1500 channels	-117.6	- 85.0
1	TV	-129.0	- 96.4

(The effective input noise temperature of the satellite is esimated to be about 1830°K). It can be seen there is a significant variation in the level at the input to the transponder between the TV and 1500 channel telephony carrier. In order to keep the level between the various types of carriers at a relative constant value in order to simplify the design of the transponder, more stringent requirements are assumed to be placed on earth station ERP at the present time. It is the intent to further study this aspect in depth during the second half of the study and perhaps increase the amount of gain control in the satellite as a compromise between transponder design problems and earth station requirements.

Selection of Preamplifier

A Tunnel Diode Amplifier (TDA) has been chosen as the pre-amplifier for its low noise capability and its essential simplicity. A noise figure of 5 dbs can be achieved with a 6 GHz TDA. The TDA therefore bridges the gap between the very low noise parametric amplifiers (NF: 1-3 db) and transistors, when they become available. Furthermore, the subsequent amplifying devices contribute substantially to the overall noise figure of the transponder and hence there is no advantage in using the lowest noise figure preamp.

Transponder Output

The output capability of the transponder may also be derived from system considerations. Based on trade-off studies described elsewhere it appears that an antenna with beamwidths of 8.5° East-West and 3.25° North-South and an effective beam-edge gain of approximately 26 to 27 dbs will be used. The effective gain, which is adjusted for the losses in the antenna circuitry and the rotary joint, is referred to the bottom end of the latter.

Assuming that the ERP directed towards the beam edge stations will be +34 dbw, the output of the transponder will have to be +8 dbw (ERP-gain) maximum. The circuit loss between the final amplifier of the transponder and the input to the antenna would be approximately 1.0 db consisting mostly of the output multiplexer loss. The final amplifier output would therefore have to be +9 dbw or 8 watts.

Selection of Output Amplifier

The main criterionfor the selection of the output amplifier is the DC to RF power conversion efficiency. The obvious candidate therefore is a Travelling Wave Tube (TWT) amplifier which has an overall efficiency of about 28% including power supply and other losses. Space qualified TWT's with 8 watts output and a saturated gain of 42 dbs are available.

3.3.3 Interstage Amplification: RF vs IF

With a broadband TDA as the 6 GHz multicarrier amplifier and a saturated TWT as the 4 GHz single carrier output amplifier, there are three functions to be performed by the interstage amplifiers:

i. translating the 6 GHz band to the 4 GHz band

ii. separation of the 36 MHz wide channels for individual amplification by the TWT output stage

iii. additional amplification.

All three functions can be provided with either a scheme utilizing Intermediate Frequency (IF) amplifiers or with RF amplifiers as shown in Figure 3.11.

The main advantage of the IF scheme is that amplification is easily available and hence losses in the branching network are of no consequence. As a result filters with very steep skirt selectivities can be built in reasonable volume and weight. The same applies to group delay and loss equalizers. The disadvantages are that a high IF ($>$ 500 MHz) has to be used if preselection at 6 GHz is to be avoided, the number of local oscillator sources is large, and most important of all a high level upconvertor is needed to provide sufficient drive for the output TWT. This creates a serious spurious and intermodulation problem.

The main advantages of the RF scheme are its simplicity with a lower parts count and the requirement ot a single translating L.O. source. Wide-band amplifiers are also easily available. The main disadvantage is the size and weight of the branching network, this being dictated by the amount of loss which can be tolerated.

3.3.4 Drivers for the Power Amplifiers

The driver stage has to deliver 0.5 mW (-3 dbm) per channel to the input of the individual power amplifiers (gain 42 dbs) to give a saturated output of 8 watts (9 dbw). Three types of driver amplifiers were considered.

i. Tunnel Diode Limiter-Amplifiers (TDLA): An overdriven TDA acts as a saturating amplifier and can be made to deliver outputs of the order of -10 dbm. With balanced configurations and better diodes this output limit can perhaps be raised a few dbs. The use of TDLA's would therefore require i) increase in the power amplifier gain and ii) separate drivers for each PA. TDLA's are only suitable for channels dedicated to single carrier operation (e.g. trunk message) and hence would not be suitable for a mixed traffic satellite.

ii. Transistor Amplifiers: Presently the commercially available transistor amplifiers (class A, linear operation) have an output of +5 dbm and a top frequency of 3.5 GHz. Talks with manufacturers of these units indicate that commercial units operating up to 4.2 GHz should be available in the near future. The estimates of this time vary between 3 to 18 months.

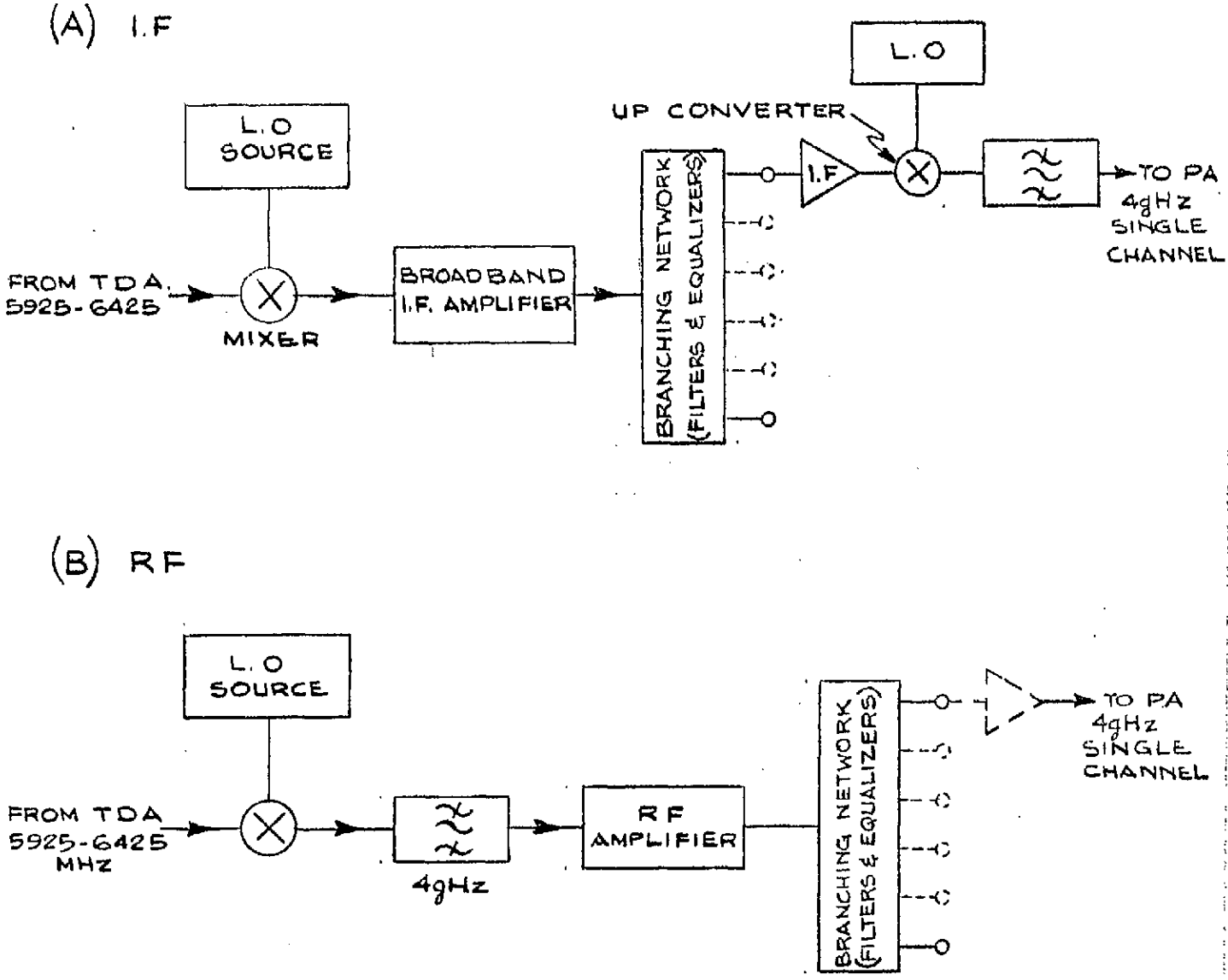

FIG. 3:11

INTERSTAGE AMPLIFICATION

The transistor amplifiers appear very attractive as drivers because of their wide dynamic range - low noise figures combined with high outputs - and the inherent wide bandwidths. They would be ideal to bridge the gap between the usable TDA outputs (-20 to -30 dbm) and the required drive level for PA's. An added advantage would be increased reliability associated with solid state circuits and an overall reduction in amplifier-power supply weight.

An open mind would be kept to include any advances in technology which might make the transistor amplifiers available before the hardware phase is launched.

iii. TWT driver amplifiers: A low-noise TWT amplifier has been selected as the best available driver at present. A weight vs number of drivers trade-off has been made (Fig. 3.12) on the assumption that the same type of branching networks would be used for any number of drivers and that all the drivers can be run off the same power supply. The weight tradeoff also included a penalty for DC power consumption. It indicates that a single TWT driver configuration is the least weight solution, however, two drivers do not constitute a large penalty. Individual TDLA's are also marked on the trade-off curve for 6 driver configuration as a comparison.

Overall Transponder Design

Amplifier Chain

The proposed transponder, shown in Figure 3.13 , utilizes redundant wideband amplifying chains up to the output stage. The output stage consists of an individual Travelling Wave Tube (TWT) power amplifier for each of the six channels used in the satellite. It is assumed that the redundancy provided by the "Sun Outage" satellite in the next orbit location and the graceful degradation of the overall output channels will provide sufficient reliability at the capacity required for good system performance.

There are four stages of amplification, all at microwave frequencies, and one frequency translation. The preamplifier is a low-noise Tunnel Diode Amplifier, followed by a Translator (pumped by a L.O. at 2225 MHz) which shifts the uplink 6 GHz common carrier frequency band to the 4 GHz down-link band. Another TDA (4 GHz) completes the preamplifier chain. The preamplifier chain has a redundant spare which can be switched into the circuit by ground command. The preamplifier chain is fully 500 MHz wide and has no filtering functions except those associated with the frequency translator.

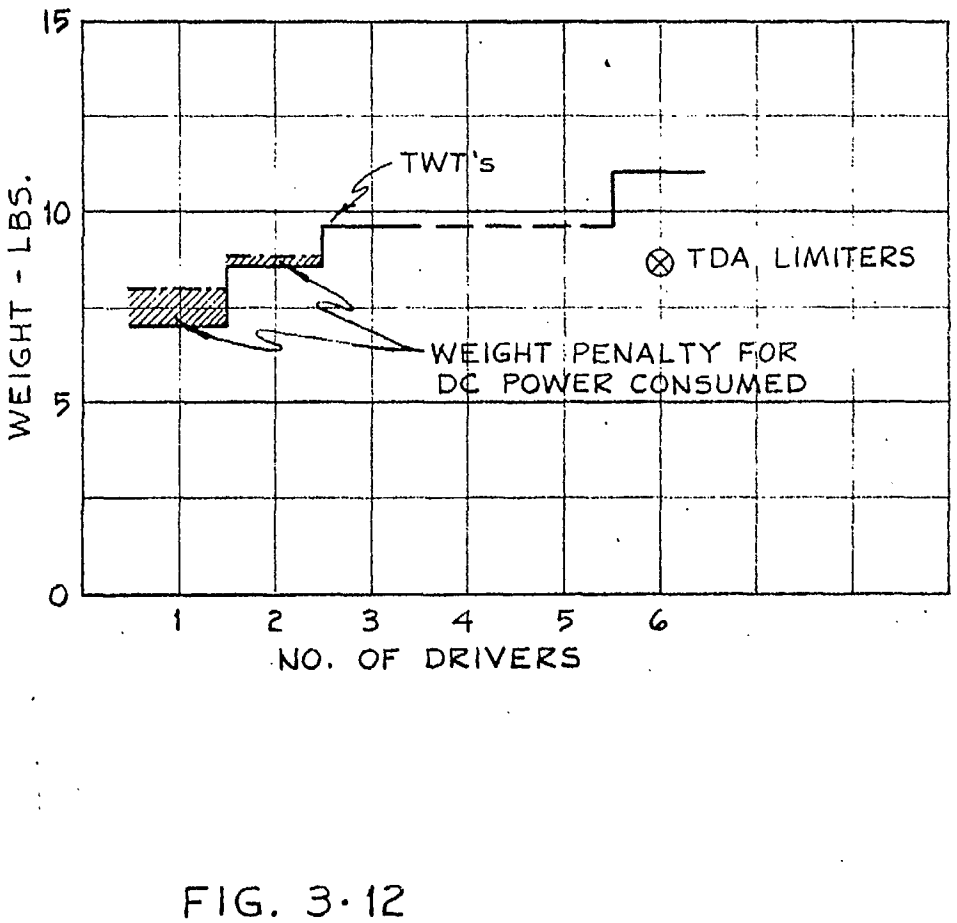

FIG. 3·12

WEIGHT TRADEOFF FOR DRIVER STAGE + BRANCHING NETWORKS

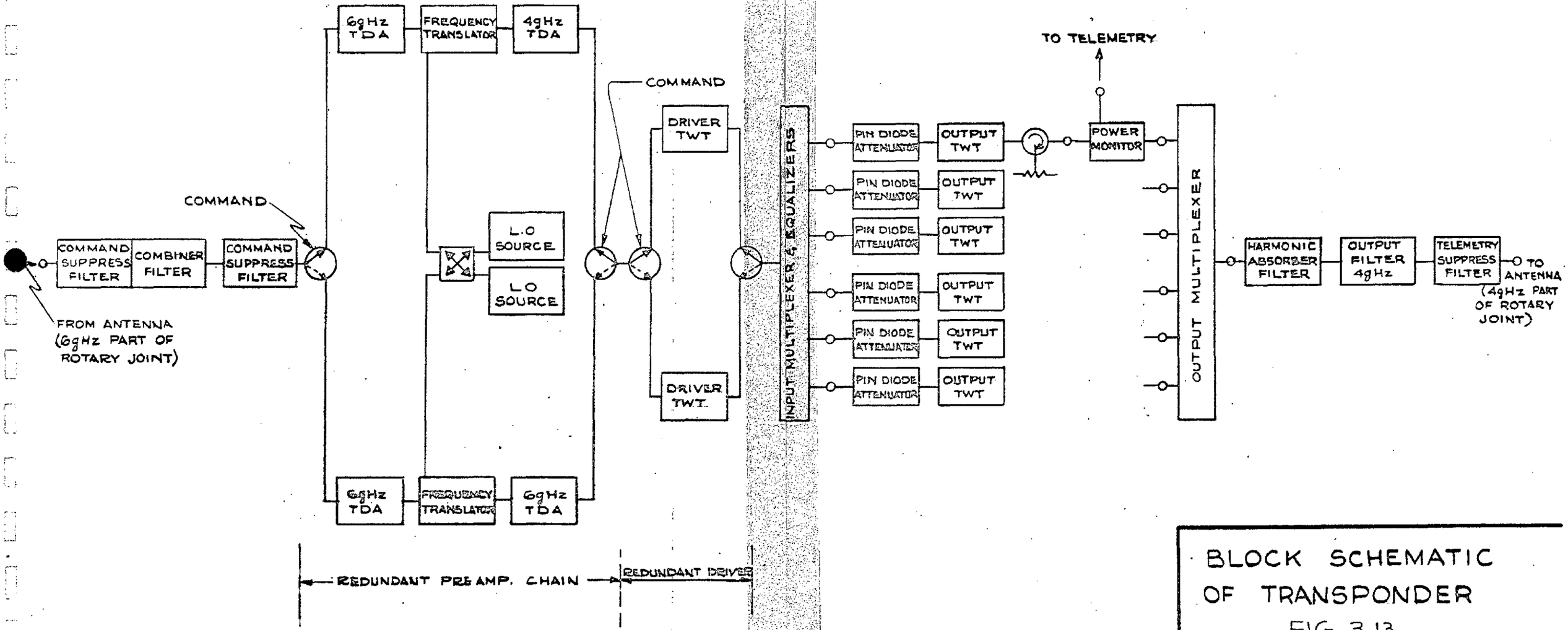

BLOCK SCHEMATIC OF TRANSPONDER

FIG. 3.13

A single wideband TWT, with a redundant switchable spare, is proposed as a driver amplifier for all six output stages, since this is the least weight solution. Present indications, albeit based on insufficient and extrapolated data, are that the carrier to intermodulation ratio (C/I) can be kept to a sufficiently low level with a TWT backoff of 16 to 18 dbs. Schemes utilizing two TWT drivers and proper selection of channels have been studied to circumvent the intermod problem. Since there is a weight penalty associated with two drivers, the present preference is for the proposed single driver scheme. However, experimental verification of the intermodulation predictions would be made before a final design is arrived at.

Another attractive possibility is individual transistor drivers for the six output TWTs. If such units become available in the near future, the transponder design can be adapted without too much modification.

The output power amplifier stage uses high-efficiency TWT's with a saturated output of 8 watts. For multicarrier operation within a RF channel, TWT backoff can be provided by pin-diode attenuators at ground command. The output of each TWT is monitored and telemetered down to ground.

Filtering

Besides the amplifier chain, the transponder also has a large number of passive filtering devices which serve various functions.

i. Input Bandpass and Output Band Filters: The main function of these filters is to prevent the 4 GHz output signal and its Spurii (in the 6 and 8 GHz band) from entering the amplifier chain. Subsidiary functions for the input filter are to exclude out of band, signals from Earth from reaching the preamplifier and for the output filter to reduce radiation of spurious signals.

ii. Command and Telemetry Suppression Filters: Since the transponder is devoid of any T & C function, these filters are utilized to prevent the command signal entering the transponder and to suppress any radiation from the transponder in the telemetry band.

iii. "Comb" Filter: The satellite will be using either the even or the odd channels in 12 channel frequency plan covering 500 MHz. For an odd channel satellite the only isolation for even channels is due to polarization discrimination and this may be limited to 12 - 15 dbs.

It may be necessary to reduce the power in the even channels even further in order to keep the intermodulation low. It is therefore proposed to use a filter consisting of notches tuned to the even channel frequencies which will pass the required channels.

iv. Input Multiplexer: Functionally the input multiplexer is a one input, six output device which selects the appropriate 36 MHz wide RF channel and diverts it to the proper output amplifier. Since it is the main frequency selective element in the transponder it must also provide sufficient isolation for the adjacent channels. Because of this narrow band filtering, the multiplexer will introduce large parabolic group delay component in each channel. It is intended, therefore, to provide a single section RF equalizer on each channel to partially compensate the group delay.

v. Output Multiplexer: The output multiplexer will combine the six outputs from the power amplifiers into one port. Since the channels are 36 MHz wide but spaced 80 MHz apart the output filters can be made fairly wide and hence would have low group delay.

vi. Harmonic Suppression Filter: This filter will suppress the radiation of 8 GHz, the 2nd harmonic frequency, from the output TWT.

Work Under Progress

i. Mixed Traffic Transponder

As indicated in Section 3.32 there is a large difference between the minimum (C/T) ratios required for different type of traffic. Various transponder configurations are presently being studied in conjunction with the earth station parameters to evolve a compromise solution. The extremes of this trade-off study are on one hand a fixed gain transponder with variable ERP from Earth Stations and on the other hand a completely flexible, variable gain transponder which allows the ground station ERP to be minimized consistent with the system requirements.

ii. Intermodulation & Crosstalk

Intermodulation products created by non-linearities in the TDA's, the translator and most of all in the TWT drivers are being studied to evolve the proper operating levels for each unit. Crosstalk produced by AM/PM conversion and gain and group delay slopes is also being studied.

iii. Group Delay Distortion

The group delay caused by the various filters in the transponder will produce distortion in the transmitted signal. Only part of this distortion is correctible on ground. Optimum combinations of filters and onboard equalizers are therefore being studied.

Reliability

Considerations of power and weight trade-offs apart, there are two ways of providing a "minimum of 4 channels" in the transponder. Configuration A (Figure 3.14a) utilizes six TWTs with one RF channel each and no switched redundancy. The capacity at start is six RF channels and degrades with time. Configuration B (Figure 3.14b) utilizes six TWTs in which 4 are active and the other two act as switched standbys on a one for two basis. The capacity at start is 4 RF channels and is maintained at 4 RF channels as long as there are less than two failures in either half.

Besides the fact that Configuration (A) provides more ERP because of the absence of switches, it would be more reliable because it provides in effect a complete "any two for any other four type" of redundancy. The transponder previous to the TWTs is common to both configurations and that its probability of survival is assumed to be 0.961 at 5 years lifetime. The probability of 4 channels being available at the end of 5 years has been computed as follows:

	Prob. of Survival of 4 Channels		
	$p = 0.1$	$p = 0.12$	$p = 0.2$
Configuration A	0.945	0.935	0.867
Configuration B	0.915	0.888	0.775

where p: probability of one TWT failure at 5 years lifetime.

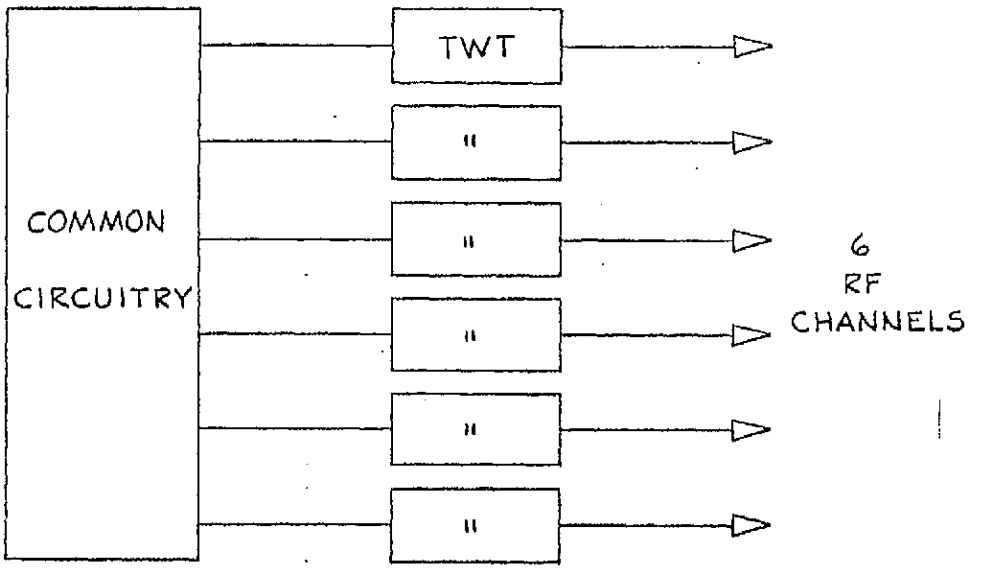

CONFIGURATION A

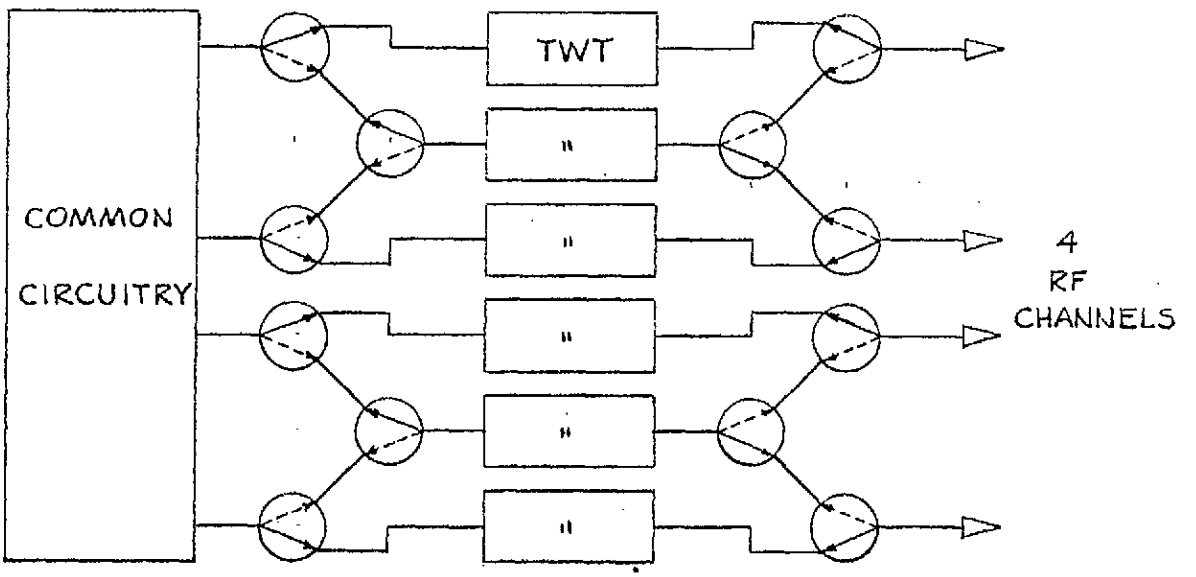

CONFIGURATION B

FIG. 3·14
OUTPUT TWT CONFIGURATIONS

3.4 TTC System

3.4.1 Concept of the Telemetry, Tracking and Command System

General

This section deals with the results of an inquiry into the Telemetry, Tracking and Command requirements for the proposed Canadian Communications Satellite. These requirements have been considered within the general guidelines for the overall Space System as outlined by the Canadian Government.

The study has proceeded to the point whereby the basic TTC requirements can be reasonably stated insofar as the spacecraft concept is maintained in its present configuration. Detailed performance analyses have, however, not been made at this time and this is the region wherein the effort is presently centered.

The concept of the TTC system has evolved from these basic considerations:

a) reliability and continuity of equipment operations

b) accuracy of command execution

c) relatively slow telemetry data rate requirements

d) use of telemetry and command during the transfer orbit, and to-station maneuvering of the spacecraft

e) freedom from interference

f) standardization of technique and equipments

g) freedom from intermodulation problems with the communications system

h) simplicity of equipment and operational procedures

i) provision of a tracking carrier thereby permitting precision angle tracking

With these considerations in mind, a system operating, as required, almost entirely in the 4 GHz and 6 GHz common carrier shared bands is presently visualized.

Beacon Consideration

The command signals from earth-to-satellite will be transmitted in the 6 GHz band while the telemetry and tracking signals from satellite-to-earth will be transmitted in the 4 GHz band. Operation in these bands satisfies many of the above considerations, but raises one problem: that of acquisition and tracking during launch, and the "to-station" maneuvering wherein the precise location of the satellite may not be known, in which case the rather narrow beamwidth of 4 GHz antennas of the size envisioned for earth terminals may make acquisition difficult.

To guard against potential problems, a 136 MHz Beacon transmitter will be provided. This beacon would be turned off after the spacecraft is placed "on-station".

Carrier Modulation

FM is envisioned for main carrier modulation in the up link and PM for main carrier modulation in the down link. The use of angle modulation in both up and down links permits a reduction in power requirements and some degree of assistance in rejection of spurious interference. The specific use of PM in the down link provides a residual carrier for tracking purposes.

Subcarriers

Where appropriate, subcarrier operating specifications and performance capabilities established by the IRIG references should be used. These subcarriers will generally be FM modulated, but the use of PSK for telemetry signals is not precluded and is currently under study.

Reliability and Continuity

Two parallel command and telemetry chains are envisioned. Starting with the command system we have:

1. Command

a) The two command receivers, each driven by half of the available received command power, are available and always powered. Failure of one receiver will not effect the operation of the other.

b) The two command decoders supplied will each be driven by the output from both receivers. The loss of one receiver will not affect the decoder operation. Either receiver can then drive either decoder. The decoders will both be always powered.

c) The decoder outputs will be paralleled. Loss of one decoder will not effect command capability.

and for the telemetry system:

2. Telemetry

a) Two separate but identical encoders will be provided, but only one will be on at a time, selectable on command.

b) The transmitter will be a dual channel phased system so that the RF signal outputs can be added to boost the output power by 3 db. Dual capacity will be used during launch and tracking and telemetry for "to-station" maneuvering.

c) Either of the transmitters can be turned off to conserve power. The 3 db power loss resulting will be subtracted from margin only, therefore, the specified performance should still be available most of the time.

d) At least one transmitter will be on to ensure that a tracking beacon is available at all times. Automatic transfer from one channel to the other in the event of failure should be provided.

Coding

1. Command

The preferred command coding is tone digital (binary commands on one tone) using an PDM coding scheme.

2. Telemetry

Multiplexing of housekeeping and verification signals is preferably PCM.

Verify Before Execution

The command procedure which requires verification of a transmitted command stored in the decoder before the execution of that command, is selected for this system. This procedure does not reduce the probability of incorrect transmission of the command but does increase operational reliability by the identification and correction of erroneous commands before they are executed. This is considered to be a very desirable characteristic for an operational satellite communication system.

System Description Summary

A block diagram illustrating the command and telemetry system interconnections with each other, and with the rest of the spacecraft, is shown in figure 3.16.

NOTES:-
1. RF LINES SHOWN THUS ━━━
2. COMMAND LINES SHOWN THUS ——
3. POWER LINES SHOWN THUS – – – – ——
4. POWER SWITCHING NOT SHOWN
5. CLOCKING INPUTS TO ENCODERS NOT SHOWN

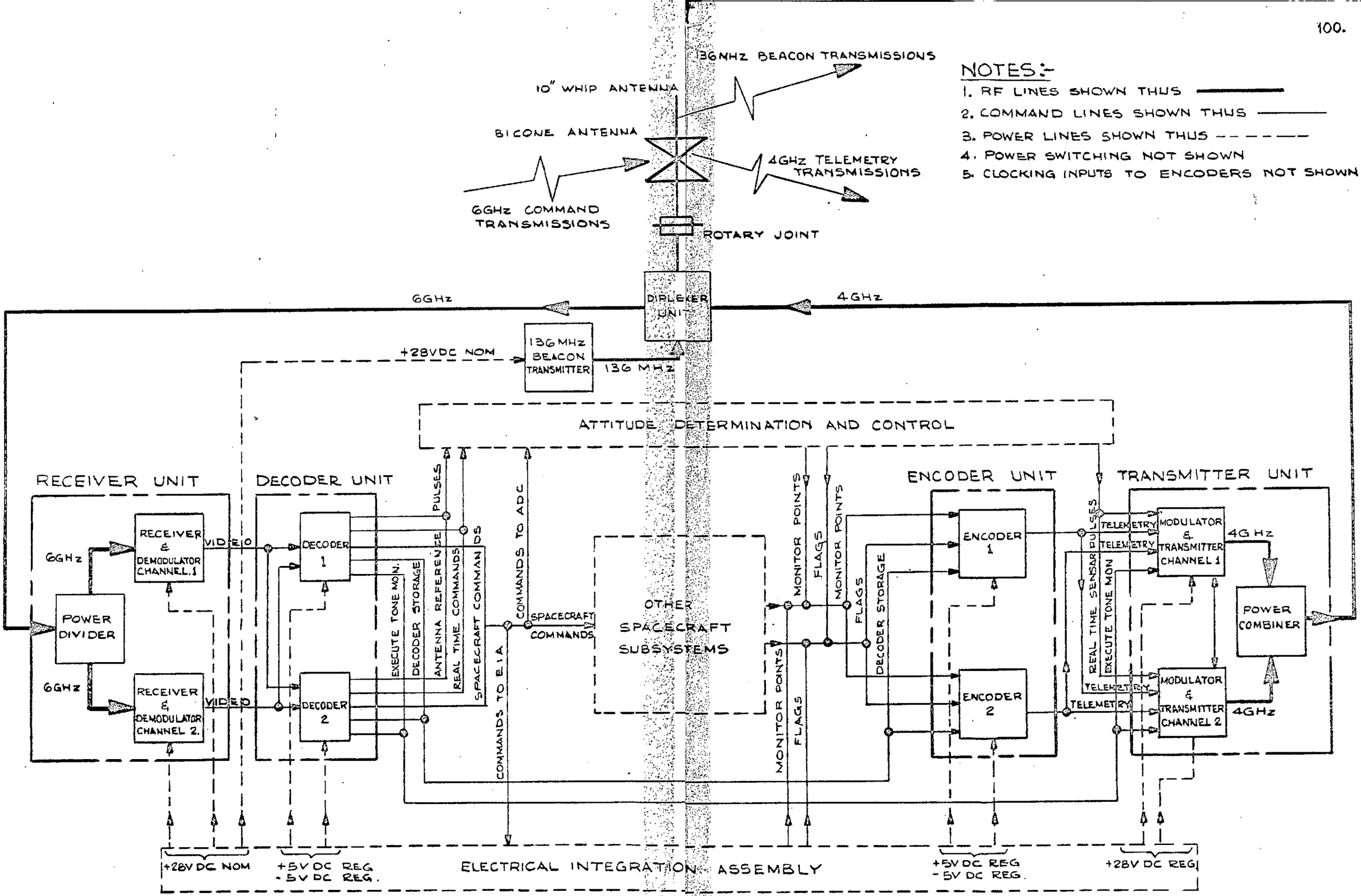

FIG 3.16
BLOCK DIAGRAM OF TTC SYSTEM

3.4.2 Command Signal Characteristics

General

Commands to the spacecraft are required to serve many purposes. Basically, these purposes may be listed as follows:

i. those through which the spacecraft is instructed to assume the proper attitude during the initial "to-station" maneuvering

ii. those which operate the station-keeping thrusters on the spacecraft to correct for small variations in spacecraft drift.

iii. those which are used to place the spacecraft in the proper operational mode

iv. those which are used to provide the attitude and control circuits with artificial earth sensor pulses in the event of a specific failure (see Sec. 3.6)

These are now discussed with a view to establishing the command signal characteristics. Following this is a discussion of command texts and formats.

Type S Commands

Most operational commands to the spacecraft simply require that the equipment on board be switched into a particular configuration. Thus, for example, the number of communications TWT's in operation at a given time is determined by commanding the required number "on".

The command is transmitted in a binary coded format and identified in the spacecraft decoder. Once identified and accepted, the command appears as a discrete pulse on the appropriate output terminal of the decoder. Since this pulse sets the spacecraft into a specific configuration, it is designated as a type S pulse. It may be used to set a mechanical latching relay, or a flip-flop, as necessary.

Type R Commands

During those times in which to-station maneuvering, or station-keeping operations, are in progress, the command system must be used to operate the on-board thrusters which in turn operate on the spacecraft orbital or attitude characteristics. These thrusters are placed to fire axially (e.g., along the spin axis) or radially (normal to the spin axis). Complete spatial control of the spinning spacecraft is achieved by correct timing of the thruster firing.

The commands to fire thrusters are sent in real time, and are in the form of a continuous tone. As long as the tone is present, the thrusters will fire. They will cease firing upon disappearance of the tone.

The tones themselves may be continuous, lasting as little as 50 milliseconds or as long as several minutes, or they may be intermittent occuring for short intervals of time at the spacecraft rate of revolution. The exact form depends upon the requirements for thrust.

These commands being sent in real time, are designated as Type R.

Note that in order for a Type R command to be accepted, a Type S command must first be transmitted to set the spacecraft into a configuration so that the Type R command will operate the correct thruster.

Type C Commands

One specific failure involving earth sensors, coupled with the interference of the sun with the operation of the other earth sensor, requires the replacement of the earth sensor pulse signal by an artificial earth pulse (AEP) generated by earth-based equipment at the command location.

These artificial earth pulses must be transmitted continuously as long as the sun interference is present, a type C command.

As in the case of type R commands, this type C command requires prior transmission of the appropriate type S command to set the spacecraft into the proper configuration.

A summary of the command listings by Type is given below:

Command Types	R	S	C	Execute
Command and Telemetry		8		2
Attitude Determination and Control	6	8	1	
Communications System		35		
Power System		7		
Totals	6	58	1	2

This list is provisional only and may undergo further revisions as requirements become further refined and confirmed.

Command Text

A command text requires two parts: first an address, and then a command. The address simply permits a specific spacecraft to respond to the command so that only one spacecraft in a conceptual network will be affected.

A practical command text for the Canadian communications satellite is one consisting of 12 bits transmitted in serial form. The first 5 bits are reserved for addressing while the remaining seven are reserved for the command proper. Figure 3.17 shows the text format.

The use of 5 bits in the address allows 32 different addresses. Not all would be required in a given system therefore redundant bit codes can be used for protection against false addressing.

The 7 bits in the command part of the text permits a capability of 128 commands. Part 3.4.1 shows that at present, slightly less than half of this capability is presently assigned.

The 12 bit text fits nicely into two words of the 6 bit PCM system that is contemplated for the telemetry system and represents a good interface characteristic for command verification, via telemetry.

Command Code for Type S Commands

The command code selected is PDM/FM. A single tone will be keyed on and off in accordance with the command text requirements. A "narrow" pulse will represent a "0" and a "wide" pulse will represent a "1".

The procedure follows that established by NASA for the Tone Digital System, a bit occupying 72 cycles of a sub-carrier oscillator wave. A "1" will occupy 1/2 of this, or 36 cycles, while a "0" will occupy 1/4, or 18 cycles.

One modification is to provide a synch tone which will precede the command text starting 3 bit intervals before the command text and lasting only 2 1/2 bits. Following the command text, the sub-carrier will remain off for 3 bits, signifying the end of the command, before a second command can be sent. Thus, one command can be sent every 18 bits or for every 1296 Hz. Assuming a command rate of 72 bits/second, then the tone frequency is 5184 Hz.

The command code format is shown in figure 3.18.

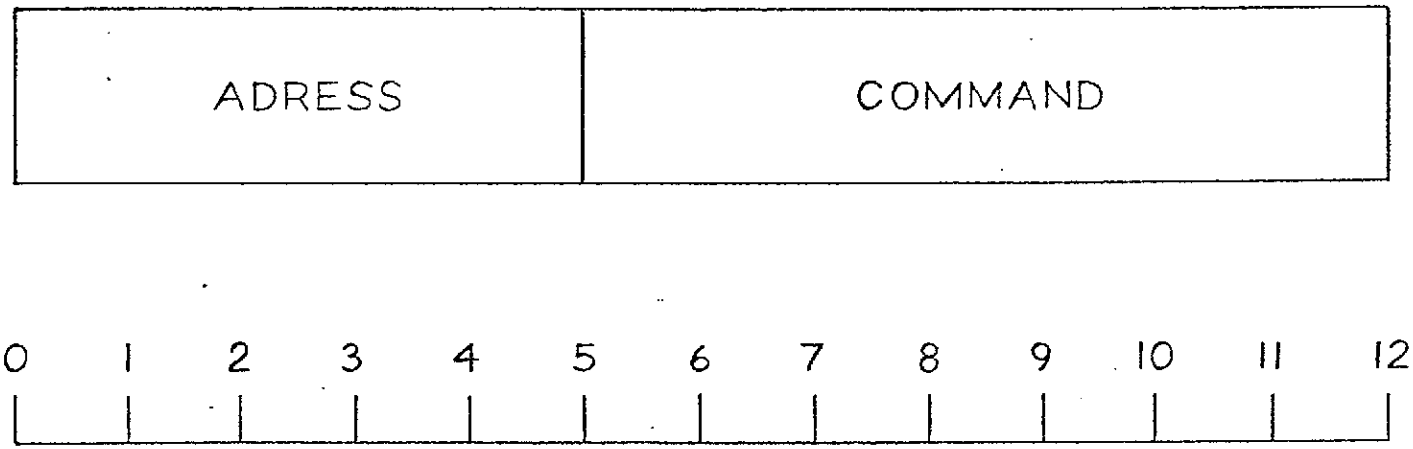

FIG. 3.17
COMMAND TEXT

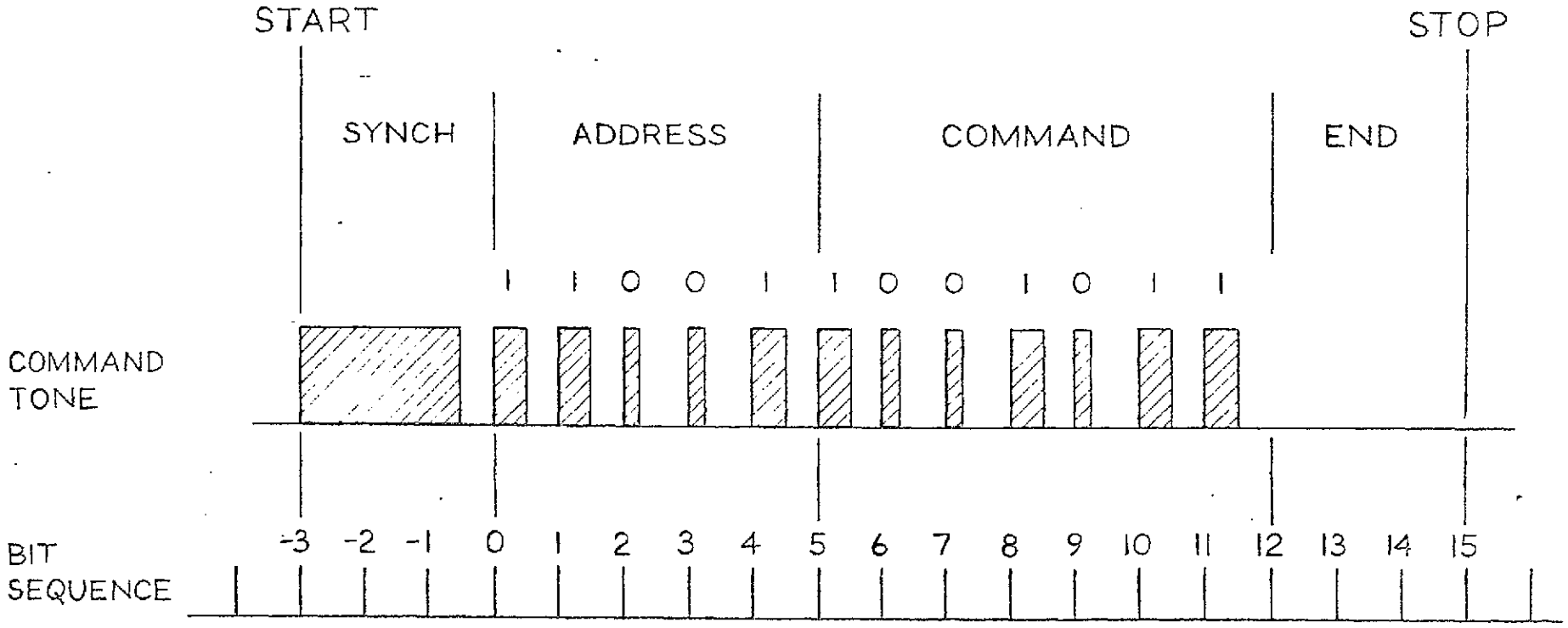

FIG. 3.18
COMMAND CODE FORMAT

Command Execute for Type S Commands

The execute command will be a single tone burst at a frequency harmonically unrelated to the command tone frequency beginning at the second bit after the address tone has been completed. The fact that a command pulse bit is missing after the address will indicate the imminence of the execute tone.

The execute tone will last for about 83 milliseconds, or 6 bits, occupying the second word slot of the Command Text interval.

The execute format is shown in Figure 3.19.

Command Signal Baseband

The three tones comprising the command signal format may be represented as shown in Figure 3.20.

The exact frequencies have not yet been decided upon but in the previous part of this section it has been suggested that the tone frequency for the command text be 5184 Hz.

3.4.3 Telemetry Channel Characteristics

General

The telemetry system channels may be subdivided into the following general categories:

a) Housekeeping signals
b) Flags
c) Sensor signals
d) Command verification
e) Spacecraft signature

A brief discussion of these categories now follows.

Housekeeping Signals

The operating conditions and environment of the spacecraft will be assessed from sample measurements performed on the major electrical, thermal, etc, parameters of the spacecraft. The sample rate need not be too high, as variations of these parameters will ordinarily not occur very rapidly. However, there must be a sufficient number of parameters sampled so that a proper diagnosis of the spacecraft state (not status!) can be made.

The telemetry channels which include these measurements, will be termed housekeeping channels.

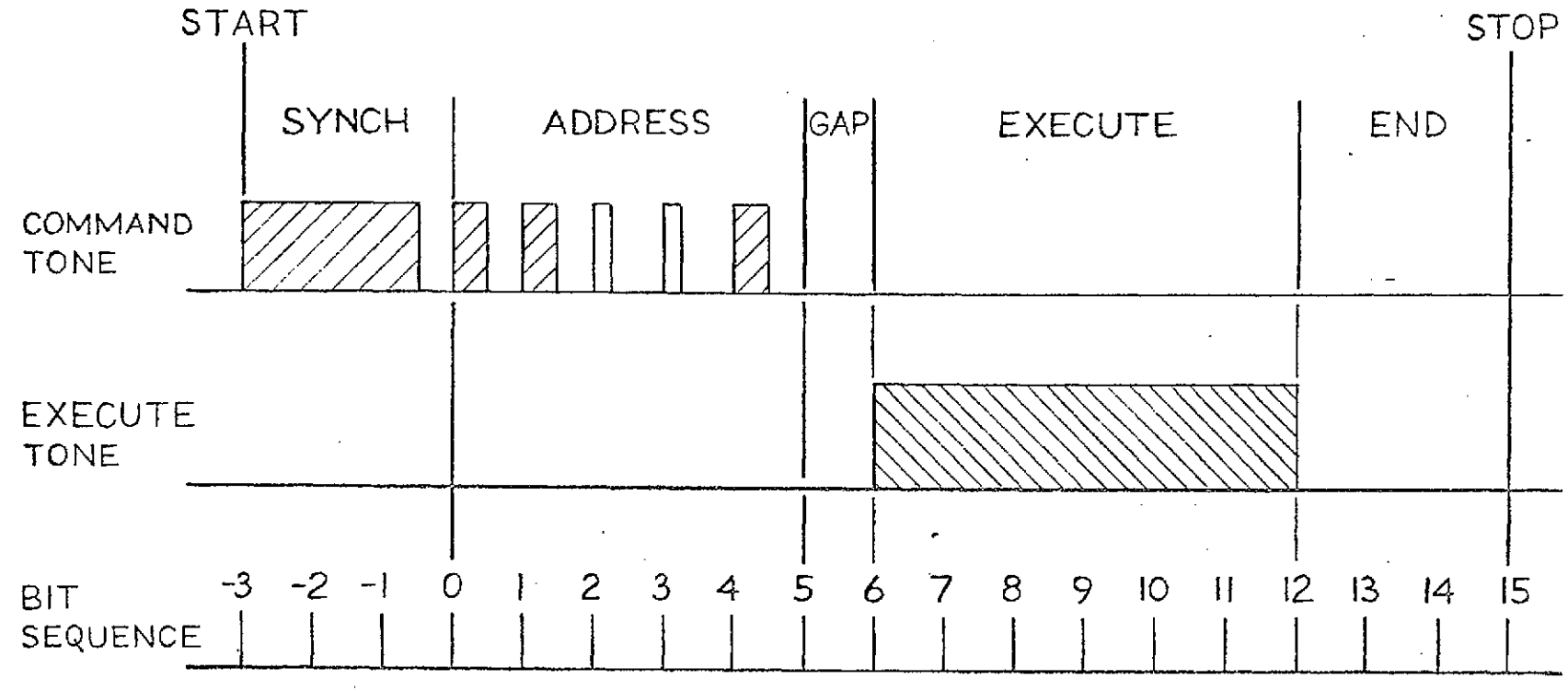

FIG. 3.19 COMMAND EXECUTE FORMAT

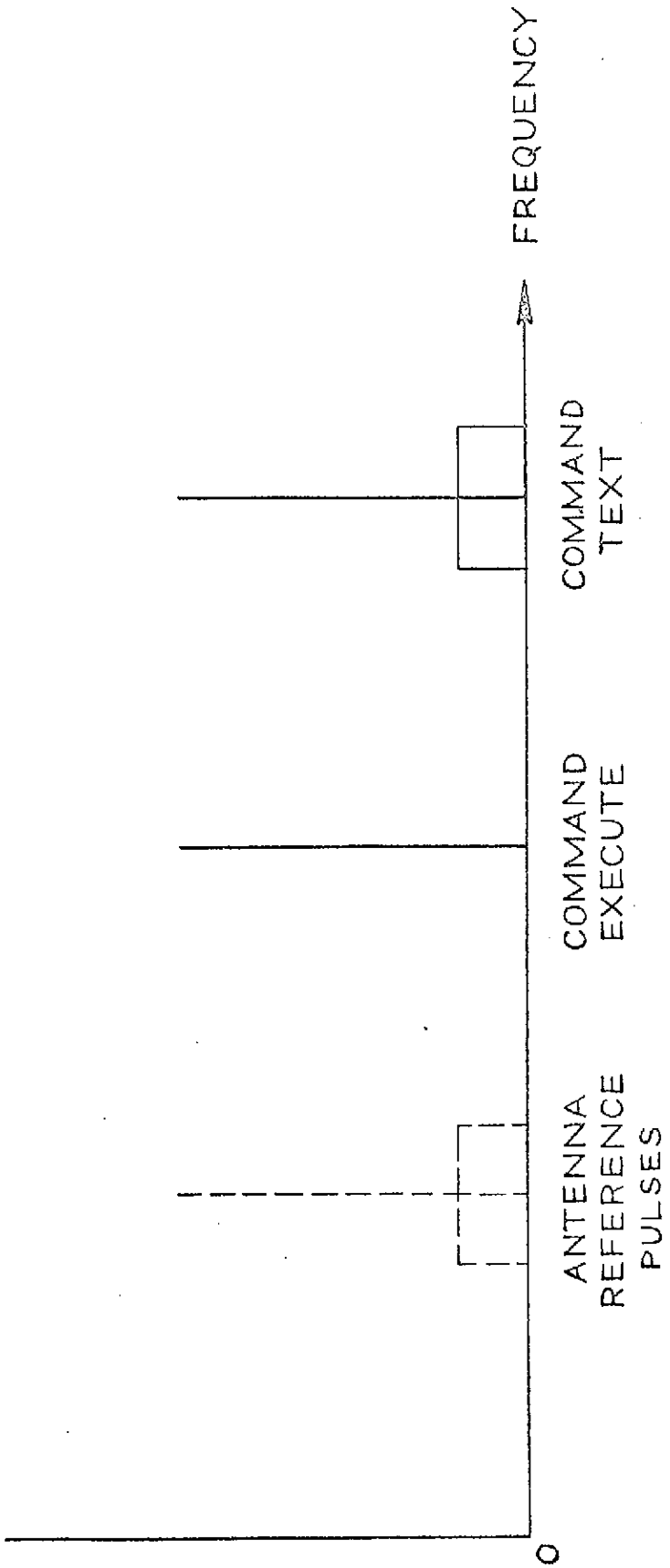

FIG. 3.20
COMMAND SIGNAL BASEBAND

Flags

The indicated flexibility of the spacecraft will permit selection of many configurations. For proper operational control, therefore, some type of "quick-look" facility should be provided to give operators an immediate appreciation of the configuration. This is an important consideration particularly during eclipse.

For that reason, status information indicating on/off or connected/disconnected status by means of a single binary digit will be provided. These indicators will be called "flags".

Command Verification

The present command concept is that a command instruction received by the spacecraft will not immediately be executed but will be stored in the command decoder. The contents of the store will be telemetered back to the ground station to permit the operator to verify that the command has been understood correctly by the spacecraft's decoder. After such verification the operator can then instruct the spacecraft to execute the stored command.

Command verification thus becomes an important part of the telemetry system and will be transmitted at rates reasonable for good operational practices.

As a further check, real time verification of the execute command is contemplated.

Spacecraft Signature

As the number of emitting spacecraft increases, the requirement for identification of each spacecraft becomes more important. Each spacecraft is therefore assumed to have, in some specific portion of the telemetry channel assignment, a unique "signature" consisting of a binary number, or other format. The signature will be transmitted at least once per sub-frame.

Listing of Telemetry Channels

The basic flexibility of the communications system and the operational necessity of monitoring spacecraft status imposes a heavy demand for telemetry capability. In all, some 7 digital, 78 analogue, 56 "flags" and 5 real time telemetry signals, as shown below, are necessary for proper monitoring.

Summary of Telemetry Channels

Data Sample Interval	Digital 1 sec	Digital 4 sec	Analogue 32 sec	Flag 4 sec	Real Time
Command and Telemetry	4	5	10	4	1
Attitude Determination and Control			2	2	4
Position and Orientation			8	1	
Communications Systems			49	23	
Power System			9	5	
Totals	4	5	78	38	5

Telemetering Options for Pulses

It is a requirement to telemeter to earth the earth and sun sensor pulses either in real time, or else process the sensor pulses in "on-board" circuitry and then telemeter the reduced data to earth in coded form. The real time option has the merit of simplicity, but because the real time channels must have maximum information capacity all the time yet the pulses exist for only a small fraction of the time, the spectrum utilization will be rather inefficient. The second option involving on-board processing increases the spacecraft complexity, but decreases the channel capacity requirements hence improves spectrum efficiency.

Despite the spectrum efficiency considerations, the present choice is in the direction of simplicity. If the resultant transmitter power requirements should prove to be excessive in relation to the benefits gained, then the question of on-board processing will be reviewed.

Real Time Signal Combinations

For complete monitoring the following signals are required:

1 Earth Sensor pulses from first earth sensor
2 Earth Sensor pulses from second earth sensor
3 Antenna reference pulse
4 Sun sensor pulses

If any of the real time signals can be combined, the total number of real time channels can be reduced. An examination of the signals reveals that the following probably can be done:

a) since earth sensors are redundant, and only one will be used in operation, only one set at a time, selectable on command need be transmitted.

b) the antenna reference pulse signal can be directly added to the earth sensor pulse signal, since the times of occurence do not coincide in on-station operation, nor is there any real operational difficulty during coincidences which might occur during "off-station" times *

c) sun-sensor pulses cannot be added directly to earth sensor signals since they will periodically coincide with earth sensor pulses and will cause difficulty in signal analyses.

Thus, the requirements may be reduced to two real time channels: one for earth sensor pulses combined with antenna reference pulses, and the second for sun sensor pulses.

Operation with One Failed Earth Sensor

For most of the time, operation is possible with either of the two available earth sensors. However, the sun will interfere with the operation of an individual earth sensor. When this occurs to the only operating sensor, normal operation becomes impossible. The procedure taken to circumvent this problem is to by-pass normal on-board loop. The telemetered antenna reference pulse received at the groundstation is used with special circuitry to generate "Artificial Earth Pulses" which are transmitted to the satellite via the command link. The satellite is commanded to accept these pulses in lieu of the real earth sensor pulses. The ground circuitry is adjusted so that the timing of the artificial earth pulses when received at the satellite is the same as it would be if the real earth pulses were available. It may be noted that in this failure mode, no additional telemetry requirements are necessary (save, perhaps, for confirmation of the artificial earth pulse command execution) however, some additional command capability is required.

* For example, during orbital maneuvers and loss of "on-station" lock due to eclipse operation with a failed battery

PCM Technique for Analogue Signals and Flags

In a PCM system, the magnitude of the sample to be transmitted is first adjusted, or "quantized" to the closest level of a hierarachy of discrete values. Thus, at the receiving end of the telemetry system, the sample magnitude need only be established as being one of the expected levels of the discrete set values, not as a continuous set.

It is proposed to measure to within 2% to 5%. Neglecting noise effects, the required number of discrete levels for a 2% accuracy is 50. A convenient bit rate to satisfy this is 2^6 or 64. For our purposes, therefore, a basic PCM system using 6 bits per analogue channel and 1 bit per flag channel is considered.

The approximate minimum word rate can be determined as follows:

Digital - 4 words/second	=	128 words/32 seconds
Digital - 5 words/4 seconds	=	40 words/32 seconds
Analogue - 78 words/32 seconds	=	78 words/32 seconds
Flag - 38 bits/4 seconds	=	51 words/32 seconds
Total	=	297 words/32 seconds.

Since the flags and some of the digital words are transmitted at a 4 second rate, a subframe interval of 4 seconds is established. With analogue data transmitted at 32 second intervals, we have, using sub-commutation

8 subframes in one frame.

The 1 second digital words can be accommodated by supercommutation.

The basic 297 words in 32 seconds is equivalent to 37 1/8 words in one sub-frame. Allowing for expansion, and adjusting the word rate, a basic sub-frame format is established, as shown in figure 3.24. Here an 8 x 6 format comprising 48 words at a rate of 12 words per second is used. At 6 bits per word, the bit rate is 72 bits per second (equal to the command bit rate).

The first 5 words are taken up with the synchronizing words, the sub-frame identifier word (requiring, actually, only 3 bits for 8 sub-frames) and the spacecraft signature.

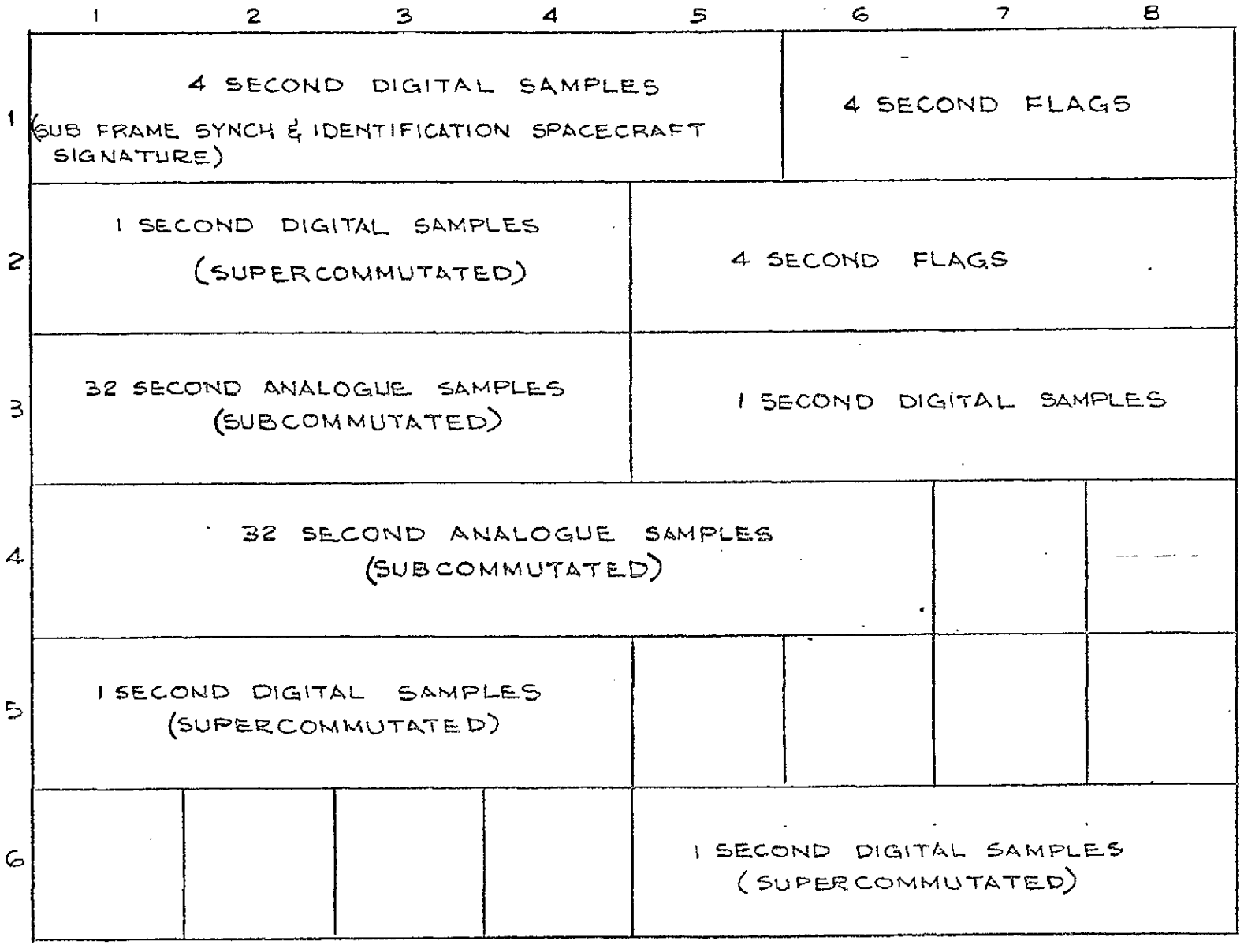

FIG. 3.24

PCM TELEMETRY SUB FRAME FORMAT

Telemetry Signal Baseband

A frequency division multiplex scheme is recommended to transmit the PCM encoded telemetry channel and the two real time channels simultaneously. The adoption of IRIG standardized FM modulated sub-carriers is a practical solution to the requirements and is assumed to be used. The exact sub-carrier frequencies involved have not yet been established, however, and further refined considerations of signal characteristics and link requirements are in process to establish the most practicable assignment of frequencies.

The execute tone from the command system, for any command received, identified and accepted by the command decoder, will also be telemetered in real time for operational monitoring purposes.

Thus a simplified baseband signal spectrum for the telemetry baseband is shown in figure 3.25. Note that the assignment of sub-carriers is only tentative and may, through some further analysis, be reassigned.

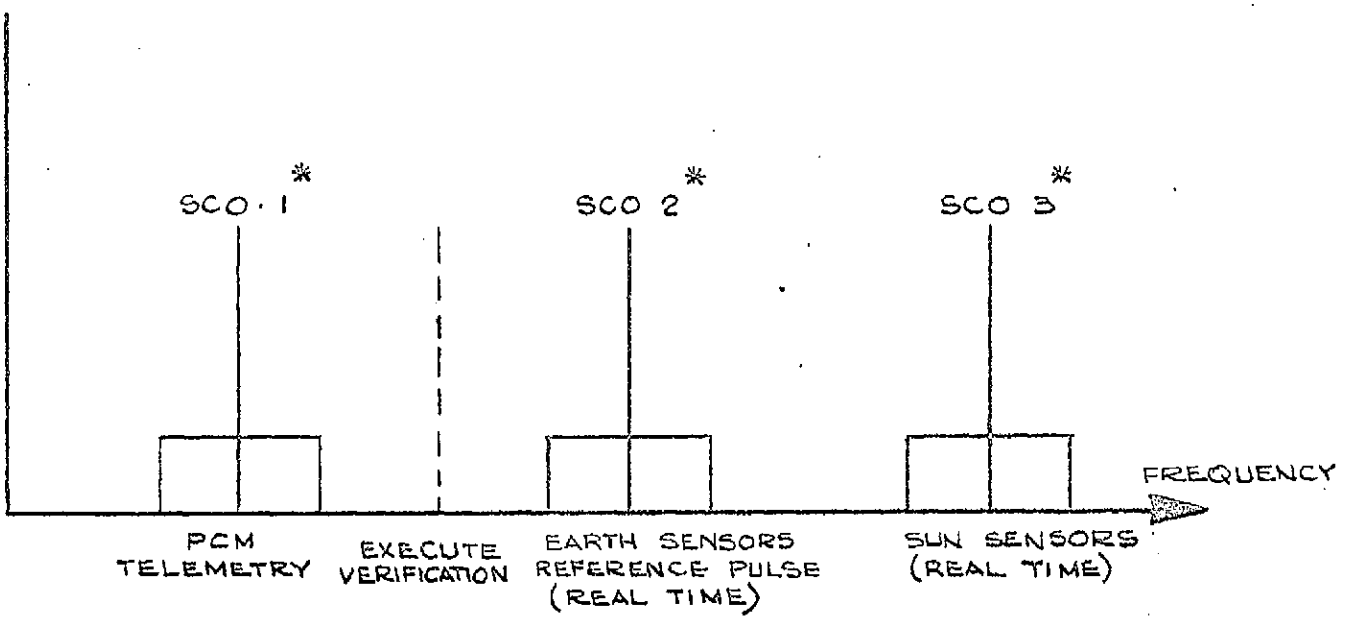

* ASSIGNMENT OF SUB-CARRIERS ONLY TENTATIVE

FIG. 3.25

TELEMETRY BASEBAND SPECTRUM

Table 3.1

General TTC Concept

Parameter	Specification	Comments
Configuration	Self-Contained	The telemetry and command system will be completely separate electrically and mechanically from the Communications system.
Protection	Redundancy	Two complete telemetry and command signal paths will be available. See separate discussion in the Command Table 3.2 or the Telemetry Table 3.3 for additional details.
RF Links	Frequency Bands	Telemetry operation will be in the 4 GHz common carrier band with an optional beacon provided in the 136 MHz band. Command operation will be in the 6 GHz common carrier band.
Standards	IRIG	Where applicable the systems will adhere to the appropriate IRIG standards unless technical constraints or operational requirements dictate otherwise. Thus IRIG subcarrier recommendations will follow IRIG standardization where practicable.
	NASA	NASA Aerospace Standards will primarily apply to the characteristics of emissions of the optional 136 MHz Beacon Signal only. The beacon emissions will meet these requirements.
	CCIR	The 4 GHz and 6 GHz RF emissions will conform to CCIR recommendations.
Antenna	Omnidirectional	Omnidirectional coverage is required for telemetry and command. It is felt that an omnidirectional toroidal beam such as provided by a bi-cone antenna is a good compromise.
Tracking	Equipment	A separate (from telemetry) 4 GHz beacon transmitter will not be used for the primary system. Since the telemetry baseband will phase modulate the main carrier, a residual carrier will be present to be used for tracking. Phase lock carrier tracking receivers are envisioned for use on the ground. The optional 136 MHz beacon will not be modulated but will serve primarily to assist in locating the satellite (following the launch and insertion into the transfer orbit) to within the precision necessary for acquisition and tracking using the 4 GHz equipment.

Table 3.2

Command Concept

Parameter	Specification	Comments
Operating Frequency	6 GHz Band	The command signal should preferably be located at either band edge of the 5.925 GHz to 6.425 GHz common carrier band. (See Section 3.1)
Main Carrier Modulation	FM	FM is recommended to reduce the possibility of spurious signals giving commands and to simplify command receiver designs.
Channel Requirements *	58 Basic	These set the systems in the spacecraft into the desired configuration. They are On/Off, selection, etc., commands.
	2 Real Time	These primarily operate the thrusters in real time. They are used in conjunction with attitude and control and station keeping.
	1 Continuous	This is the channel for the artificial earth pulse. It is required only in certain failure modes.
	3 Execute and Reset	These are special check or clearing functions in the decoder.
Concept	Verify Before Execute	The transmitted command is stored in the decoder and the contents of the store are telemetered to earth. The ground operator verifies that the command in the store is correct then he may instruct the satellite using the execute command to effect the stored command.
Command System	Tone Digital	A command in binary digit form transmitted either as a PDM code on a single tone or as '1's or '0's on two separate tones, it is the recommended system for command.
Main Carrier Baseband	Multiplexed Signal	Will consist of a) the tone bursts necessary for command b) In one specific failure mode, artificial earth pulses would also be continuously transmitted. c) The execute command would also be present on a separate tone after command verification.

* Present Listing Only.
The final requirements may be different because of revisions.

Table 3.2 (Continued)

Parameter	Specification	Comments
Bit Rate	Tone Digital	The exact rate is not yet established.
	Real Time - as required	The thruster operation will dictate this.
Decoding	Pulses of 50 msec.	These pulses operate relay drives to set latching relays. This is for the basic commands.
	Variable pulses	These are of the length required for thruster operation.
Ranging Tones	None	The present concept is to fix the satellite positions using angle tracking techniques only.
Equipment	Receiver	Solid state, double conversion IF with approximately 10.7 MHz used for the second IF. Both IF local oscillators to be developed by frequency multiplication of a single LO crystal.
	Decoder	Solid state using micrologic circuitry, etc., as necessary to reduce weight, increase reliability etc. The "tree" principal should be used to localize failures, should they occur.
Redundancy	Receivers	Two electrically separate (but packaged in the same enclosure) receivers will be used. Both receivers will be on always, and the output of either will be sufficient to drive the decoders. The failure of one receiver will have no effect on the operation of the other, or the decoders.
	Decoders	Two electrically separate (but possibly packaged in the same enclosure) decoders will be used. Both will be powered simultaneously. Each will have a signal from both receivers. Either decoder can thus work with either receiver. Only 1 decoder is necessary for operation.
Receiver Noise Figure	10 db	Exclusive of the effect of power splitting for the two receiver channels or the effect of cable losses, etc., between the antenna and the receiver terminals.

Table 3.2 (Continued)

Parameter	Specification	Comments
Receiver Bandwidth	200 kHz	Adjusted as necessary to allow for a) doppler shifts during initial positioning maneuvers b) Long term drifts of oscillators and equipments on-board the space satellite over the life-time of the satellite.
Receiver Dynamic Range	Not yet established	The dynamic range will be established from MDS to the highest level (plus safety margin) which could conceptually be obtained during the test, checkout and prelaunch phase of the program.
Receiver Selectivity	Out-of-band Rejection	The receiver selectivity will enable the receiver to work normally in the presence of strong communication signals, or other signals, plus a reasonable safety margin.
Antenna	Omnidirectional	A bi-cone antenna mounted on the despun section of the satellite will provide a 40° toroidal omnidirectional pattern suitable for command capability to the spacecraft during the critical transfer orbit phase.

Table 3.3

Telemetry Concept

Parameter	Specification	Comments
Operating Frequency	Telemetry - 4 GHz	The telemetry RF signal should preferably be located near either band edge of the 3.7 GHz to 4.2 GHz common carrier band. (See Section 3.1).
	Tracking - 4 GHz	Primary tracking will be accomplished using the residual carrier in the telemetry RF signal. Modulation parameters will be chosen to insure an adequate residual carrier power to permit acquisition as well as tracking.
	Tracking - 136 MHz	An optional 136 MHz beacon may be provided to provide initial acquisition and tracking. This requirement depends to a large extent on the launch vehicle dispersions and on the satellite controlling agency, and is under study.
Main Carrier Modulation	PM	Phase modulation results in a residual carrier being available for tracking purposes. The phase deviation index has not been determined but would typically be from 0.5 to 1.4 radians peak.
Channel Requirements*	9 Digital	These are for synchronization, subframe identification and spacecraft signature purposes
	78 Analogue	These are for generally housekeeping data purposes.
	38 "Flags"	These are either "on" or "off". They include command verification signals, if a tone command system is used. They correspond to 1 bit of information.
	2 Real Time	The 2 real time channels are combined from 5 signal sources as follows: Channel 1 - either of two earth sensor pulses plus antenna reference pulse Channel 2 - sun sensor pulses

* Present Listing Only. The final requirements may be different because of revisions.

Table 3.3 (Continued)

Parameter	Specification	Comments
Main Carrier Baseband	Multiplexed Signal	Will consist of three IRIG subcarriers. The exact baseband configuration is still the subject of investigation.
Subcarrier Modulation	FM	This is the conventional modulation technique as established by the IRIG recommendations. Standard practices will be followed as practicable.
Sampling Rate	Max. 1 sec.	Used where the bandwidth of the signal to be telemetered warrants it, or where excessive time delays cannot be tolerated (such as command verification)
	4 Sec.	Sub-frame rate
	Min. 32 sec.	General housekeeping rate
Telemetry Encoding	Tentatively PCM	Tentative bit rate - 72 bits per second word rate - 12 words/second bits/word - 6
Ranging Tones	None	The present concept is to fix the satellite positions using angle tracking techniques only.
Equipment	Transmitter	Solid state, using UHF or microwave transistors followed by efficient (as far as the state-of-the-art permits) multipliers.
	Encoder	Solid state micrologic circuitry, etc., as necessary to reduce weight, increase reliability, etc.
Transmitter Redundancy	Dual Channel	Two electrically separate transmitters (packaged, however, into a single unit) each providing half the total power will be provided. Dual operation will be available and the signals will be phased so that they can be directly added to provide maximum power. One or the other transmitter may be independently turned off and in that case the output power will be reduced in half. The margin will be greater than 3 db so that single transmitter operation will simply reduce, but will not eliminate, the margin.

Table 3.3 (Continued)

Parameter	Specification	Comments
		Fail-protection will be provided for single transmitter operation to energize the stand-by transmitter should the operating one fail.
Encoder Redundancy	Two Encoder Channels	Only one or the other of the two encoders will be operating at a time. But either will be able to drive either transmitter. Switchover in case of failure may not be automatic, since encoder failures are not easily identified by sensing equipment. However, automatic switchover could be provided in the event of certain types of power failures, etc. Further, loss of an encoder does not by itself affect the basic communications operations or capabilities.
Transmitter Power	300 mW @ 4 GHz	This is a first estimate of power level requirement for one channel only (600 mW if both transmitters are operating).
	2-5W @ 136 MHz	The exact power requirement is still to be evaluated.
System Temperature	Design Level 200°K	This enables the use of low-noise but uncooled receivers to be used on ground for the tracking and telemetry functions.
Spacecraft Antenna	Omnidirectional 40° toroidal (4 GHz)	A Bi-cone antenna mounted on the despun section of the satellite will provide the required patterns. The 40° toroidal pattern will permit reasonable contact between satellite and ground during the initial maneuvering to-station.
	Omnidirectional (136 MHz)	10" whip antenna located on top of the micro-wave bi-cone antenna.

3.5 Positioning and Orientation System

3.5.1 Function

The positioning and orientation system will provide the following functions:

Initial orbital corrections resulting from launch vehicle injection errors, off nominal apogee motor performance and removal of drift velocity.

Attitude maneuvers and spin axis adjustments

Stationkeeping corrections at periodic intervals over the satellite lifetime to maintain a synchronous, equatorial orbit.

Initial orbital corrections and stationkeeping are accomplished by firing the axial thrusters in a continuous mode and firing the radial thrusters in a pulsed mode, thus providing the necessary velocity increment for orbit inclination and longitudinal drift corrections. Attitude maneuvers and spin axis corrections are accomplished by firing the axial thrusters in a pulsed mode of approximately 80 ms. per pulse.

3.5.2 Description

The design concept for the P and O subsystem is identical to that currently used for Intelsat III communications satellite system. A schematic of this subsystem is presented by Figure 3.26. The propellant is mono-propellant hydrazine, which is catalytically decomposed by Shell 405 catalyst.

The subsystem consists of two separate subassemblies each with its own fill and drain, instrumentation, and radial and axial thrusters supplied from an opposed pair of fuel tanks. The subassembly fuel feed lines are interconnected by a normally closed pyrotechnic valve. Actuating this valve in the event of the failure of a thruster propellant valve in the closed position makes available all the remaining propellant to any of the remaining operable thrusters. Both radial and axial thrusting capability is thereby maintained.

Propellant orientation is maintained by vehicle spin, and expulsion is accomplished by blowdown of the nitrogen gas in the pre-pressurized ullage space. Nitrogen is selected as the pressurant due to its negligible solubility in hydrazine and its reduced leakage potential when compared to helium. Pressure transducers in the propellant feed lines provide an indication of tank pressure. Each subassembly has a fill and drain provision for fueling, pressurizing and, if necessary, draining the subassembly. It is anticipated

FIGURE 3.26
POSITIONING AND ORIENTATION

SYSTEM SCHEMATIC

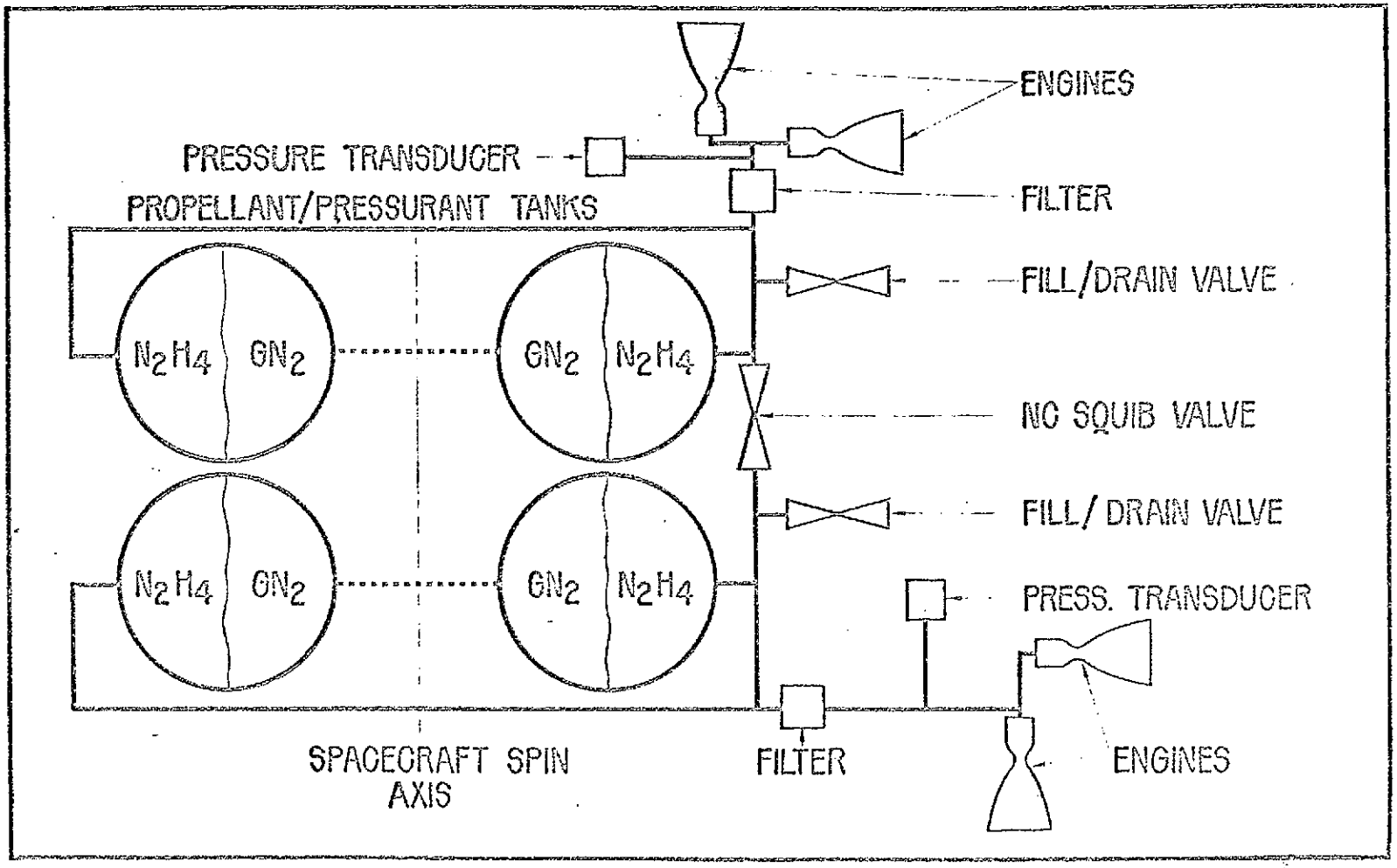

that an all-welded construction will be provided to eliminate any possible sources of leakage which would exist with mechanical joints. Also, the routing of the propellant and pressurant lines and tank configuration and orientation will be such as to permit complete draining of the system on the ground without the necessity of spinning up the satellite.

3.5.3 Operating Characteristics

The P and O subsystem will be controlled by a ground station, which transmits commands for selection of the thruster to be fired, the firing mode (whether continuous or pulsed), and pulse duration. Initial tank pressures will be approximately 600 psia and expulsion pressures at the end of life will be approximately 200 psia, which correspond to thrust levels of approximately 4.1 to 1.7 pounds respectively. Thus, measurement of tank pressure provides a means for pre-determining the firing duration required to achieve the desired total impulse, and for monitoring the propellant quantity remaining in the tanks.

3.5.4 Propellant Quantity

Based on a preliminary requirement for a total velocity increment of 1144 ft/sec, a total hydrazine propellant quantity of 71 pounds was determined to be required, for a spacecraft total weight in the transfer orbit of 965 lbs. This propellant weight was based on an average specific impulse of 225 seconds and includes a 3 percent allowance for expulsion efficiency, cold starts, and cosine losses due to radial thruster operation during initial positioning maneuvers. Figure 3.27 presents the variation of specific impulse in the continuous mode as a function of tank pressure, which has been determined by testing of the Intelsat III thrusters.

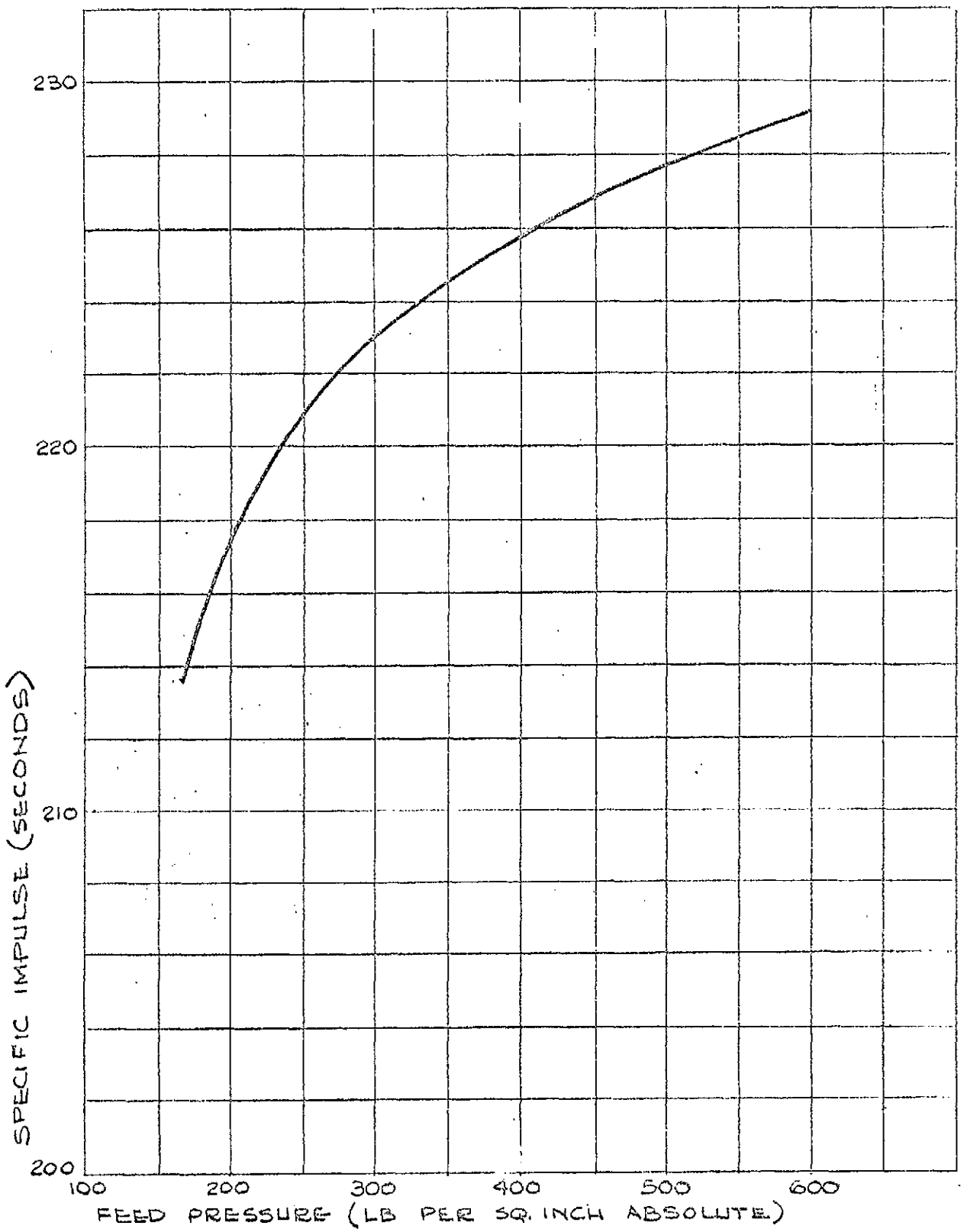

FIG. 3.27

POSITION & ORIENTATION SYSTEM PERFORMANCE - CONTINUOUS MODE FIRING.

3.6 Attitude Control and Antenna Despin Systems

3.6.1 Introduction

The Attitude Control and Antenna Despin Systems provides capabilities for performing the following functions:

Spin-axis attitude determination in both transfer and synchronous orbits

Initial positioning, stationkeeping and spin-axis attitude control

Antenna despin and pointing

These functions involve on-board as well as ground station equipment. The design employs techniques similar to the ones developed for Intelsat III, which provide maximum degrees of simplicity and reliability. The overall block diagram of the Attitude Control and Antenna Despin Subsystems showing the corresponding functional organizations is given in Figure 3.28.

Spin axis attitude determination is made using sun and earth sensors, the outputs of which are telemetered to the ground. The function counter processes the sensor information and provides indication of spin axis attitude. The satellite is equipped with two radial and two axial thrusters. These thrusters are actuated by ground command to control the satellite as follows:

Reorientation and Attitude Control

Pulsed operation of axial thrusters; pulses are timed to precess the satellite spin axis in the proper direction.

Correction of Orbital Inclination

Continuous operation of axial thrusters.

Initial Positioning and Stationkeeping

Initial positioning may be performed by continuous operation of the axial thrusters prior to satellite reorientation, or by pulsed operation of the radial thrusters after reorientation. Stationkeeping is performed by pulsed operation of the radial thrusters.

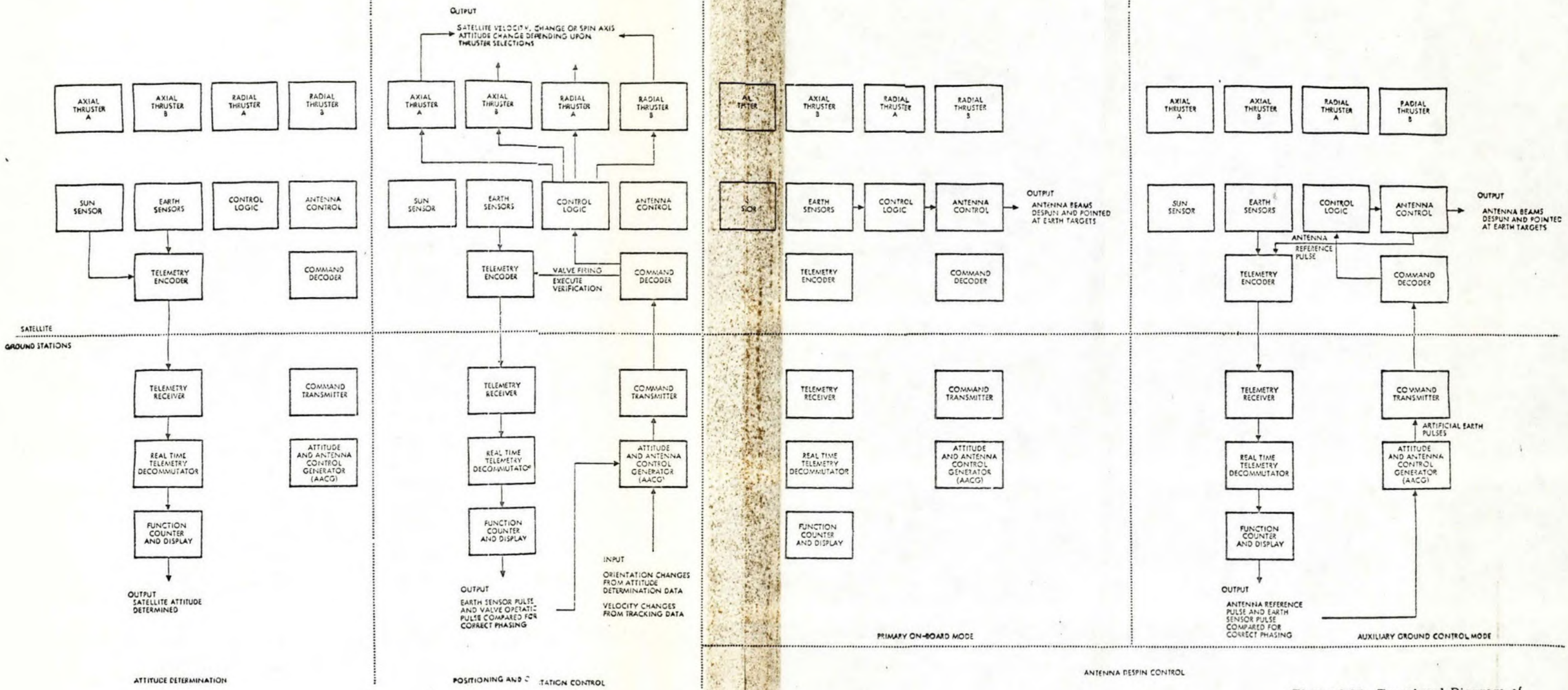

Figure 3.28 Functional Diagram of Positioning and Control Operations

The ground station attitude and antenna control generator (AACG) provides pulses at the proper time to the command encoder and transmitter which transmit the thruster valve commands to the satellite. Selection of the proper valve is accomplished by the command link. The AACG generates the pulses at the precise time required by measuring the time interval between reception of earth sensor pulses and telemetered valve operate pulses and by adjusting the transmission time of the valve operate pulses to obtain the desired interval.

Both on-board and ground antenna despin control alternatives are provided. On-board control is achieved by providing an earth reference pulse at the satellite rotational rate to the antenna control electronics. This once-per-revolution pulse synchronizes the generation of antenna waveforms to point the antenna beam at the earth target.

Ground antenna control is accomplished by first selecting the ground control mode using the command system and then transmitting artificial earth pulses (AEP) to the satellite at the satellite's rotational rate. The AEP's control the antenna beam in the same manner as the on-board control.

The timing of the AEP transmissions must, of course, be controlled to point the antenna beam at the earth. This is accomplished by comparing and adjusting the time interval between reception of an antenna reference pulse (ARP) and earth sensor (ES) pulse and adjusting the AEP transmission time for the proper ARP-ES interval. This latter function is performed by the attitude and antenna control generator (AACG) at the ground station. The desired ARP-ES pulse time interval is a manual input to the AACG unit, which then generates AEP pulses at the correct time and sends these pulses to the command encoder for transmission to the spacecraft.

Ground control will be required only when one earth sensor has failed and the sun or full moon are in the other earth sensor field-of-view and very close the edge of the earth.

3.6.2 Attitude Control System

The Attitude Control System consists of a sun aspect sensor, two passive earth sensors, control logic electronics and valve driver electronics. With these elements the subsystem provides:

Sensor information to ground stations from which the satellite's attitude and rotational position can be determined during transfer and final orbits.

An earth reference pulse to the antenna for use as a position reference in pointing the antenna beam toward the center of the earth.

Electronic power amplification for energizing the propulsion solenoid valves in response to ground commands for positioning and orientation.

A block diagram illustrating the system configuration is shown in Figure 3.29.

3.6.2.1 System Description

A dual earth sensor and sun sensor system provides ground determination of spin-axis orientation. An accuracy of at least ± 1.2 degrees after no more than 1/2 hour of continuous observation, and $\pm$ 0.6 degrees after no more than 2 hours of observation during transfer and final orbits, can be readily achieved. Two redundant earth horizon sensors and a sun aspect sensor permit satellite attitude and rotational position to be determined on the ground to an accuracy of $\pm$ 0.34 degree (3σ) with respect to the local vertical and the sun line. This accuracy is achieved within an observation period of 10 minutes on either the transfer or final orbits.

The earth sensors are the primary source of spin-axis attitude information. The optical axes of these two sensors are arranged in a "V" configuration with the plane of the "V" containing the spin axis (Figure 3.30). Each earth sensor sweeps across the earth once per satellite revolution and produces a pulse coincident with the instant of crossing the earth's horizon.

Under normal conditions, spin-axis attitude with respect to the local vertical can be determined accurately and rapidly on the ground by measuring the interval between the leading edge horizon contacts of the two earth sensor beams. When such contact times fail to coincide, spin axis displacement can be computed and then corrected by ground command. In the unlikely case that one of the earth sensors should fail, the same attitude information can be obtained by measuring the interval between leading and trailing horizon pulses from the operating earth sensor. This interval, which affords a measure of the earth's chord scanned by the sensor, is then compared with a nominal value based on the accurately known fixed orbital altitude. The earth sensor data will not be degraded during eclipses.

The leading edge horizon pulses from the earth sensors are conditioned in the control logic unit for use by the despin antenna electronics. Rotational speed of the antenna beam with respect to the satellite is then controlled by the frequency of earth pulses. Beam position is controlled to a fixed offset angle with respect to the earth sensor optical axis in phase with the earth horizon reference pulse. This angle is mechanically preset for the earth's chord length as scanned by the sensor at orbital altitude.

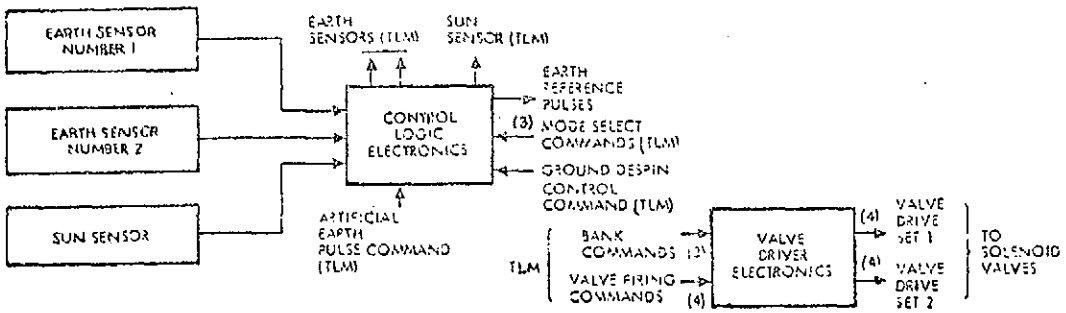

Figure 3.29 Attitude Control System Block Diagram

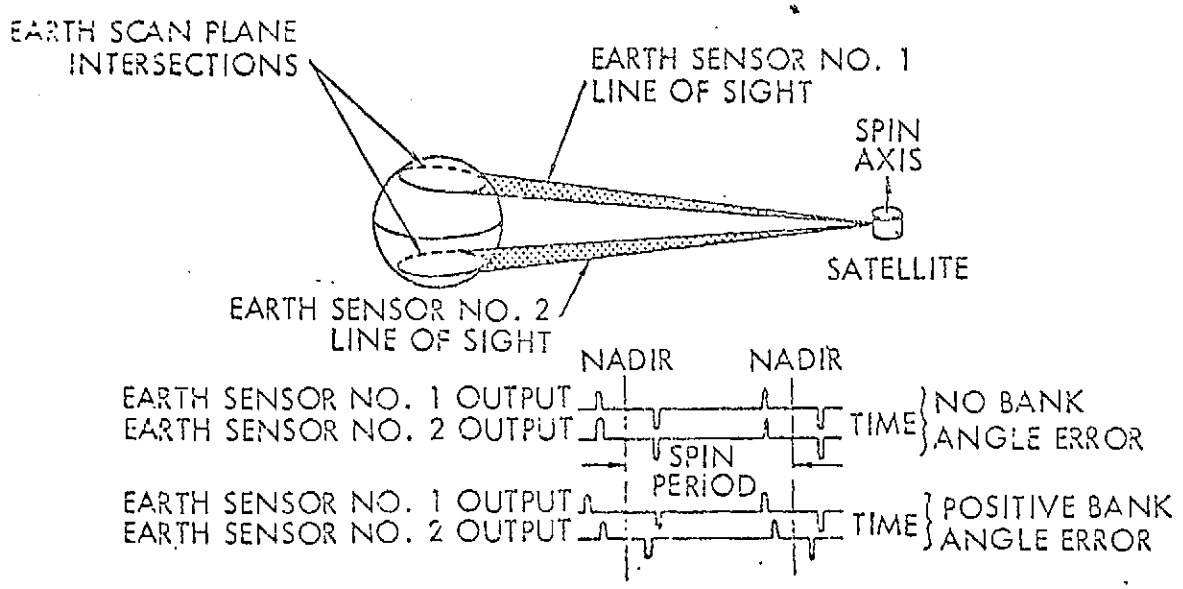

Figure 3.30 Earth Sensor

Ground control of antenna beam rotation position and speed is also provided by substituting artificial earth reference pulses transmitted from the ground in place of the onboard earth sensor pulses for antenna despin control. Position bias capability is provided in the Despin Control System for offsetting the antenna up to a maximum of ± 3 deg upon command.

3.6.3 Antenna Despin System

The Antenna Despin System supports and positions the antenna system in order to point the beams at a specific point on the earth. Its main components are a motor drive assembly and its associated control electronics.

3.6.3.1 Motor Drive Assembly

The motor drive assembly is illustrated in Figure 3.31. The basic bearing inner diameter is dictated by the required shaft inner diameter to allow for coaxial RF feed cable clearance and torsional stiffness. It is desired to keep the torsional resonant frequency of the drive system above 40 Hz to avoid any undesirable interaction between the control system and the drive mechanism. The actual bearing size is chosen to withstand the launch load. The outer race of the antenna and bearing is fitted in the housing and preloaded axially outward by a light spring. The spring is installed in a manner which will allow sufficient axial play on the shaft to compensate for differential contraction between the housing and shaft when the assembly cools down to the minimum expected ambient. The spring preload is sufficient to locate the shaft firmly and is well below the minimum thrust capacity of the bearing for 5 years operation at 115 rev/min and maximum achievable reliability.

The lubricant is a low vapor pressure organic liquid with metall-organic additives. It is applied in a thin film on all bearing surfaces and is impregnated into the ball separator, which has a specified 25 percent porosity in order to provide it with the necessary lubricant capacity. The lubricant and application method bear the designation Vac-Kote by Ball Brothers Research Corporation who developed the process for use on the Orbiting Solar Observatory series of satellites.

Lubricant replenishment is accomplished by oil stored in porous nylon reservoirs located on both sides of each bearing. Oil in the reservoirs out-gasses slowly until equilibrium is reached between the oil-coated surfaces of the assembly and the oil vapor in the closed compartment. As an oil molecule is lost by evaporation from any surface, it is replaced by one

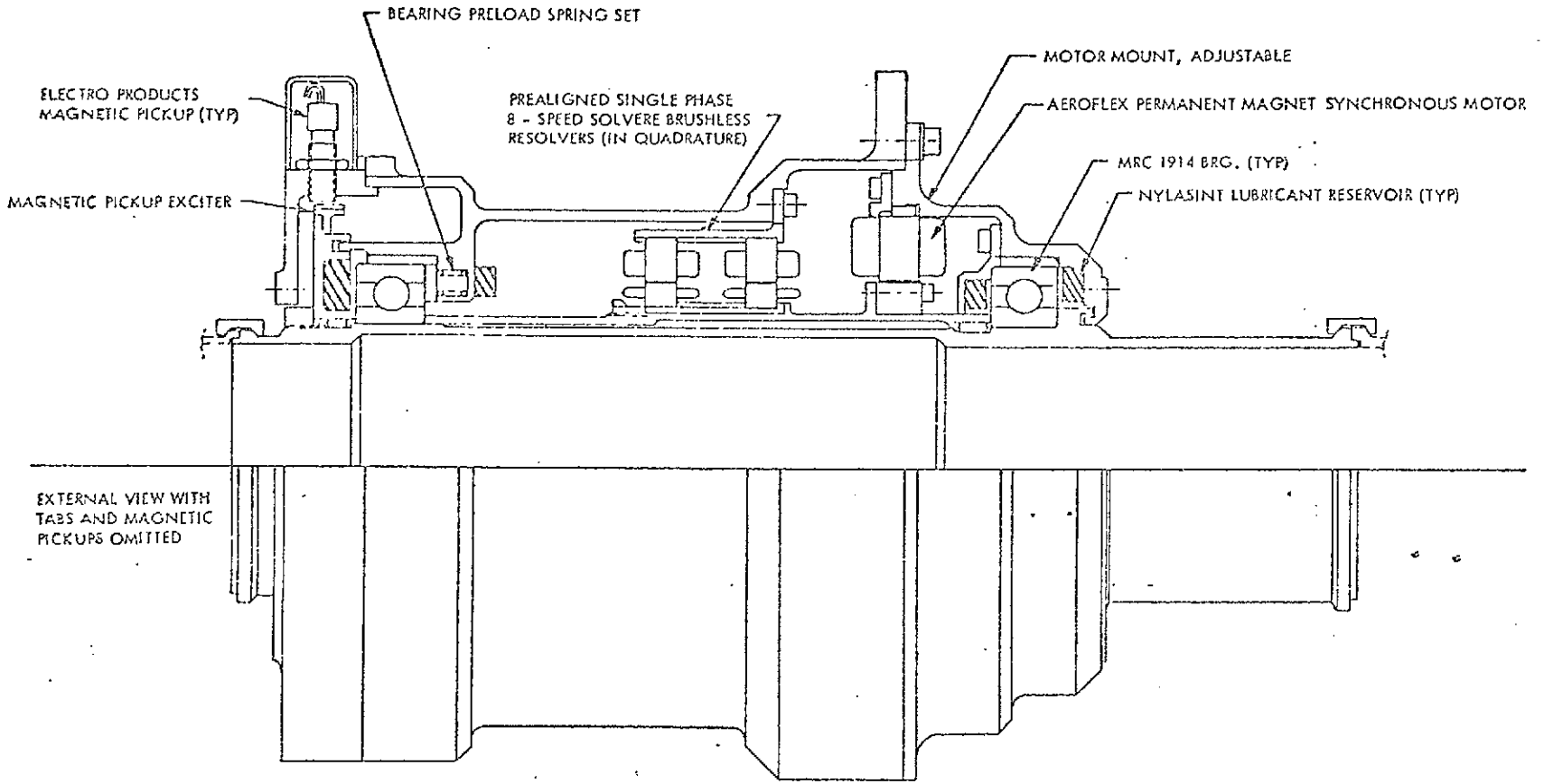

Figure 3.31 Motor Drive Assembly

striking and being captured by the temporarily depleted area. At equilibrium there is a continuous interchange of lubricant molecules between the bearing surfaces, the space around them, and the oil-coated internal walls of the assembly. Oil molecules finding their way through the labyrinth seals are replaced by molecules from the reservoirs. The thin lubricant films which this system employs have been proven capable of lubricating lightly loaded ball bearings at moderate speeds and temperatures by hundreds of space-rated components operating successfully for many thousands of hours.

The dc brushless torque motor used to drive the despin mechanism employs a rotary transformer type resolver which, when properly aligned, acts to commutate the synchronous permanent magnet motor. This effect is obtained by the use of an integrally mounted motor, resolver and rotary transformer. The resolver and rotary transformer are actually combined into a single unit. The resolver has an input winding which is excited at 1000 Hz and two output windings which have an output proportional to the input at the input carrier frequency modulated with a trigonometric function of the angular position of the rotor. The rotor is a variable reluctance element with shorted windings, whose turns and winding distribution are controlled to obtain an optimum modulation wave shape on the output winding and a desired phase relationship between the two windings. Schematically, the resolver is shown in Figure 3.32. This figure also shows the relationship between input and output signals where $\emptyset$ is an electrical phase shift between the carrier frequency input and output and θ is the angular position of the rotor. The motor, whose rotor is on the same shaft as the resolver rotor, is a permanent magnet two-phase synchronous motor having 8 pole pairs. The magnet is of Alnico 9 which has the highest energy product of the common magnet materials and has a magnetization force of 1600 oersteds, thus exhibiting extremely good stability which ensures minimum degradation during satellite life. The motor is energized from the demodulated resolver outputs as shown in Figure 3.33.

The direction or rotation and peak torque per unit power is controlled by the relative positions of the resolver and motor stators. This position is mechanically fixed such that the stator rotating field in the motor always leads the rotor rotating field by $\pi/2$ electrical radians.

The output from the resolver is demodulated and power amplified to drive the corresponding motor sine and cosine windings. The torque speed curves for this combination very closely approximate those of a dc torquer. This motor offers the same advantages in starting and controlling as well as in electrical efficiency, mechanical size, and weight.

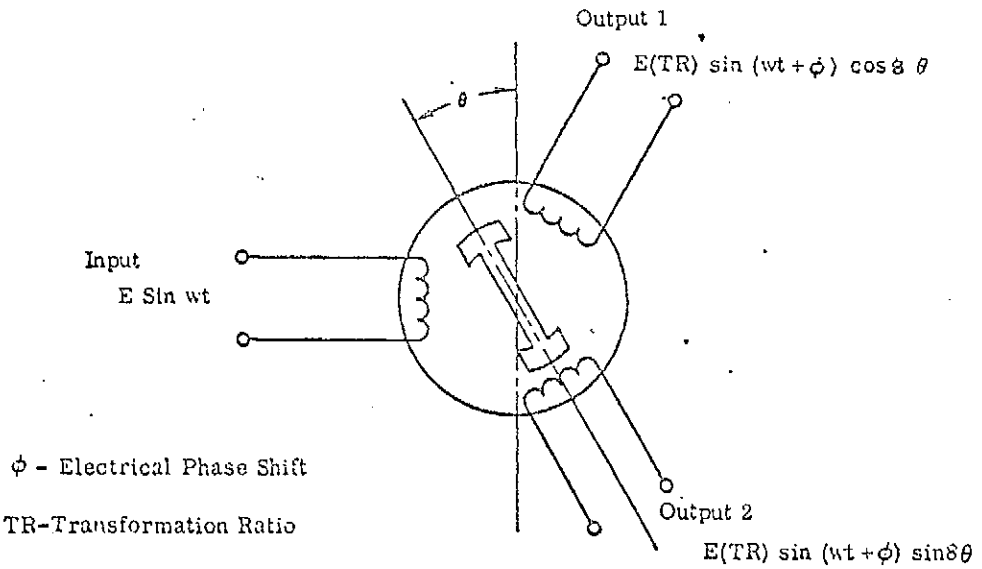

Figure 3.32 Resolver Diagram

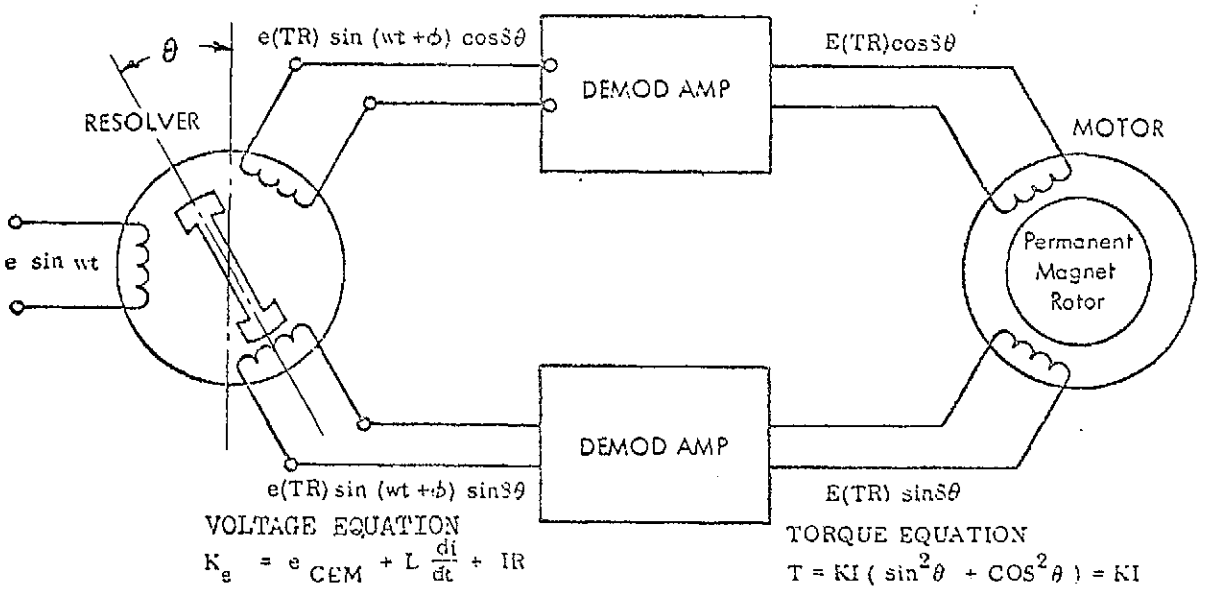

Figure 3.33 Motor-Resolver Block Diagram

The motor drive assembly also provides the once-per-revolution signal for antenna pointing and a reset signal from a magnetic pickup operating in conjunction with a single steel tooth on the rotor. Rate Feedback is provided from a third magnetic pickoff which operates with 180 precision machined teeth on the rotor.

3.6.3.2 Control Electronics

The control circuitry for despinning and stabilizing the antennas with respect to the earth are shown in the functional block diagram of Figure 3.34. The system comprises the following major functional blocks.

Earth sensors and earth reference select switches

Phase detector

Tachometer network

Acquisition network

Auxiliary despin mode control

Brushless motor resolver combination

a) Earth Reference Select Logic

Either of two earth sensors mounted on the spinning satellite body provides the basic pointing reference for the despun antenna. An alternate mode of antenna control uses an artificial earth pulse supplied by ground command. The earth reference select switches permit the selection of an earth reference pulse from either earth sensor or from the real-time command output identified as the artificial earth pulse (AEP). Two commands are required to control the selection: the earth sensor select and the AEP select.

Also, this block contains the circuitry required to threshold the raw earth sensor output signals and provide a square wave output pulse suitable for use by the phase detector.

b) Phase Detector

The phase detector compares the time phasing of the earth sensor output with that of the antenna position output as sensed by a magnetic pickup. The operation of the phase detector is illustrated in Figure 3.35, and its output is a sample-and-hold indication of the relative phase of the two signals.

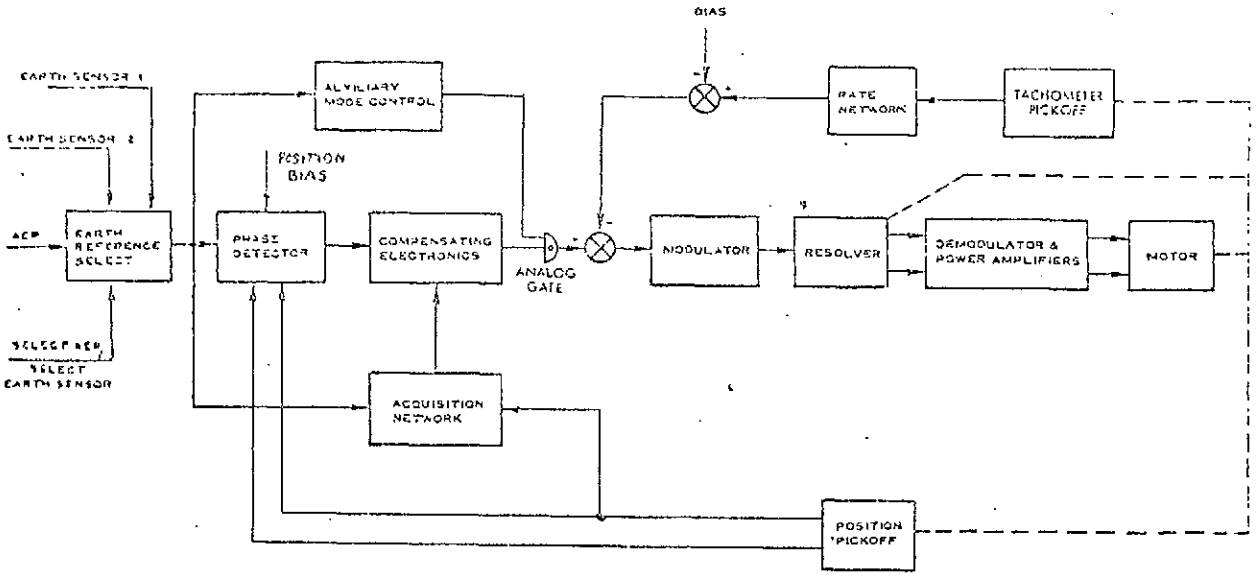

Figure 3.34 Control Electronics Block Diagram

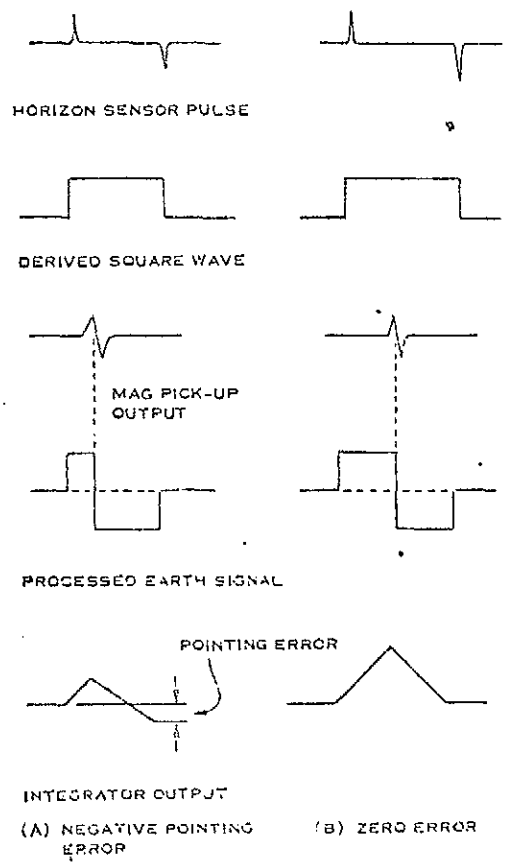

Figure 3.35 Phase Detector Operation

The phase detector has provision for rejecting signals generated when the IR sensor views the moon. Rejection is accomplished on the basis that the earth sensor output pulse from the moon is shorter than from the earth. The phase detector output is inhibited unless the pulse from the earth sensor is at least as long as one-half the length of the normal earth pulse.

During those periods when the sun or the moon will appear in the field of view of the primary sensor, normal operation is achieved by switching to the output of the alternate, identical earth sensor. If one of the sensors fails, normal operation can be obtained with the other sensor and the use of the AEP mode during times of visibility of the sun or moon.

The phase detector provides also capability for biasing the antenna position upon ground command. This is accomplished by introducing an initial condition voltage on the integrator used to sample and hold the modified sensor pulses.

c) Tachometer and Position Feedback

Antenna position with respect to the spinning spacecraft is referenced through the use of two magnetic pickoff units and a ferromagnetic tooth attached to the antenna shaft. The first pickoff unit operates as a prime reference while the second unit is mounted 180 degrees from the prime to accomplish sign inversion for the control circuitry. Antenna relative rate information is derived from a third magnetic pickoff mounted on the drive housing adjacent to a multiple tooth ferromagnetic disk.

It was found that for high precision applications tachometer feedback was required to eliminate the effect of drag friction. In the development of the mathematical model of the dc torque motor and the rotating element, it was established that bearing friction varied by as much as $\pm$ 100 percent of the average friction level, with frequency components related to motor speed and the number of balls in the bearings. The use of the resolver introduced additional disturbances due to anomalies in the sine and cosine outputs. Several tachometer schemes were investigated.

In the selection of a tachometer feedback loop, both analog resolvers and incremental digital encoders were considered.

It was concluded that the incremental digital encoder represented a lighter mechanical assembly, and, by using a magnetic pickup transducer with a slotted disk encoder, the weight, power, mechanical tolerance, sensitivity, and volume requirements could be minimized.

The slotted wheel encoder and magnetic pickup (MPU) combination output is in the form of a pulse train, the frequency of which is related directly to rotor speed. To avoid the need for a digital frequency lock loop and phase detector, the processing technique adapted converts the pulse train to a speed proportional signal with a form analogous to the output of a tachometer. This method is simple in principle and design. Operation is described in conjunction with the timing diagram in Figure 3.36.

Figure 3.36A shows a nominal output from the MPU. Each zero crossing is made to initiate a monostable multivibrator resulting in the output waveform as shown in Figure 3.36B. This latter waveform contains speed information in its average value. The rate network serves the dual purpose of filtering the tachometer ripple and providing adequate compensation for the rate loop.

d) Acquisition Network

In the system used for normal mode despin control the output of the phase detector is ambiguous during acquisition. Therefore a velocity loop is synthesized which when connected to an integrator drives the system to the correct relative speed. The position loop becomes unambiguous and aids the velocity loop once the relative speed differential is within the capability of the phase detector. In the actual implementation, the acquisition network is disconnected whenever the error output is below a silicon diode threshold to accomplish a lower drift sensitivity to the acquisition network.

The acquisition network consists of a speed differential indication circuit which is as shown in Figure 3.37. The earth sensor output triggers a monostable multivibrator to generate a speed dependent signal as described earlier for the tachometer operation. This signal is compared to the output from a similar circuit operated by the reference MPU. The output error is proportional to the speed differential, after filtering. The linearized transfer function is shown in Figure 3.37.

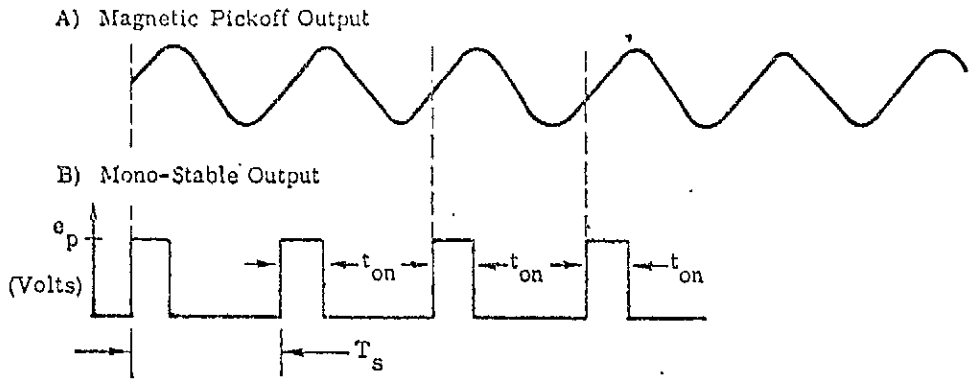

Figure 3.36 Tachometer Signal Processing, Timing Diagram

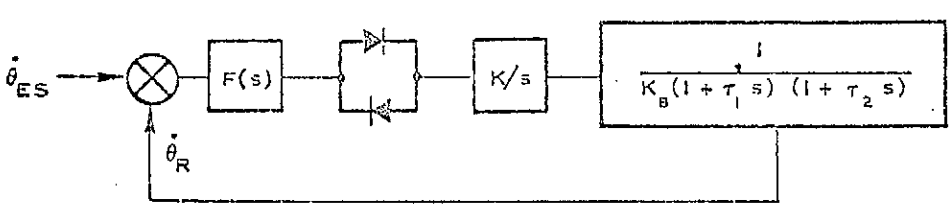

Figure 3.37 Acquisition Network Block Diagram

3.7 Electrical Power System

3.7.1 Introduction

This section of the report describes the electrical power system design and internal power system tradeoffs, concentrating almost exclusively on the maximum performance satellite configuration which has 6 transponders operating in sunlight and 2 in eclipse. The study has been based primarily on using currently available hardware and proven techniques. This approach is essential in view of the critical weight problem and the consequent need for realistic and accurate system design and analysis. Within the present state of the art, the configuration which is best able to provide the required life and reliability at an acceptable weight is one in which energy is derived from an array of silicon solar cells and eclipse operation is provided by a battery of nickel-cadmium cells.

3.7.2 Outline of Principle Design Problems

3.7.2.1 Load Requirements

As shown in Table 3.7.1, the communications and housekeeping equipment require approximately 231 watts of power during daylight and 114 watts during eclipse. The bulk of this power has to be supplied at a variety of regulated voltages. Optimization analyses are necessary to decide whether the main power bus (or busses) should be regulated or not and whether voltage conversion is best performed at the individual equipments after power distribution or at one or more centralized converters prior to power distribution. The main parameters involved are efficiency, weight, reliability and interference suppression.

3.7.2.2 Solar Array Requirements

As the satellite loads require full power continuously, the solar array must be designed to provide a minimum of 231 watts plus battery recharge power at any season after 5 years in orbit.

The solar array power varies throughout a year because of the seasonal variations of the sun's intensity (due to the ellipticity of the earth's orbit), the satellite's inclination to the sun vector and the resultant stabilized solar array temperature. Superimposed on these variables is a slow reduction of array power due mainly to the effects of charged particle radiation. The main solar array design problem is to provide the required power under worst case conditions at the end of 5 years with a minimum array size. Since the satellite is the maximum diameter permitted by the launch vehicle shroud, only the array height can be varied to give the required size.

Regulation is needed to take care of the excess array power capability in addition to the needs of the regulated loads.

3.7.2.3 The Battery

The battery has to provide the spacecraft power during the periods of eclipse. The eclipse seasons last for two periods of 45 days each year (at the equinoxes). The duration of the eclipse varies up to a maximum of 72 minutes in mid-season.

Flight data and ground tests support the contention that the nickel-cadmium cell is the only energy storage element capable of providing the 5 year life. Critical qualifications to this claim are that the cells must be provided with suitable protection against excessive overcharge or over-discharge and that the battery operating temperature has to be maintained within fairly narrow limits, generally in the range 5°C to 35°C.

Because of the relatively small number of discharges the battery will experience, it can be operated at a high depth of discharge, thereby conserving weight. A practical maximum limit on the depth of discharge is about 70% in this application. In principle this depth and the eclipse load define the minimum battery weight directly. In practice this may be modified by other factors, such as:-

a. the desirability of using a cell of standard capacity with a good performance history.

b. the need to supply a battery voltage range at which the voltage conversion equipment can operate efficiently

c. the need to match the battery charging voltage to the solar array output at the end of life

d. mission reliability requirements and satellite and battery failure modes, which influence the degree of design conservatism adopted and the choice of using either several batteries of low capacity or one battery of high capacity but the same terminal voltage.

3.7.2.4 Basic Subsystem Configuration

A basic power subsystem configuration is set up as a standard for convenience in performing trade-off studies and in describing the detailed system problems. This configuration is shown in figure 3.38.

Each of the 6 transmitting TWT's is provided with an independent regulating DC-DC converter of the pulse-width modulating type and presents a constant power characteristic to the bus over the operating range of input voltage. Some of the loads in the housekeeping systems are also supplied with power from a regulating DC-DC converter which also presents a constant power characteristic to the bus. The remaining loads operate directly from the bus.

The solar array feeds the bus directly. A shunt regulator controls the dissipation of excess array power. The dissipative portion of the regulator may be connected across the bus or to a tap point on the array. As most of the loads have independent voltage regulation, the shunt regulator does not need to control the bus voltage very accurately. This is referred to as an "unregulated bus".

The charge control circuit permits the battery to be charged and overcharged at safe rates. The discharge control circuit connects the battery to the bus when the solar array is unable to provide the required load current. Charge and discharge control methods are unspecified for the moment. In the simplest form the charge control circuit may be a resistor or relay and the discharge control may be a diode or relay, the relays in either case being controlled by sensors and logic circuits.

3.7.3 System Configuration Trade-off Studies

3.7.3.1 Ground Rules

In the study made of power system configurations, the following ground rules were adopted:

a) Converter power supplies for output stage transmitting tubes must be internally regulated whether or not they are operated from a regulated supply

b) Housekeeping equipment converters with a regulation requirement of not less than $\pm$ 3% may be operated from a $\pm$ 1% regulated bus without further internal regulation

c) Converter efficiencies were assumed as in Table 3.7.2, based on available hardware.

d) Load requirements are defined in Table 3.7.1.

3.7.3.2 Configurations Studied

Total power required and system weight were calculated for three configurations:

1. The shunt-regulated system, as shown in figure 3.38.

2. The isolated battery charge system in which power is fed to the loads directly from one section of the solar array and to the battery from a separate section, as shown in figure 3.39

3. The series-regulated system, which employs a separate regulator for control of the main bus voltage, as shown in figure 3.40.

Configuration 1 was further divided into three alternatives, 1A, 1B and 1C, of varying efficiency and complexity by varying the method of charge and discharge control.

Configuration 1A (Figure 3.41)

In this version, the charge control sensor opens relay K1 upon attainment of full charge. K1 is closed when the battery is on discharge, and remains closed throughout discharge and during the early stages of charge when it is not desirable to limit charging current. The trickle charging resistor may be replace d by a crude constant current regulator if desired, without affecting the conclusions.

Configuration 1B (Figure 3.42)

In Configuration 1B, the operation is the same as 1A, except that the discharge diode is not bypassed when the battery discharges. This results in an efficiency penalty which is sufficiently small that it can be taken into account by a small increase in battery depth of discharge rather than by an increase in battery weight. No penalty is incurred in solar array size (as compared to configuration 1A).

Configuration 1C(Figure 3.43)

Configuration 1C is a much more complex power subsystem concept which has potential advantages in overall efficiency and consequently in solar array dimensions and overall weight. In this concept, the charge control is designed to control charging current at the magnitude required to maintain the bus voltage at a constant level. When the battery is fully charged, the charging current is reduced further, and the bus is then controlled by diverting current through the shunt regulator.

The discharge control consists of a boost converter which regulates the bus during battery discharge. The result is a continuously regulated bus, allowing operation of the housekeeping converter without preregulation, and of the TWT converters over a narrower input voltage range, thus improving the efficiency of both. A penalty in battery capacity results from the reduced efficiency of the discharge circuit.

Configuration 2 (Figure 3.39)

Configuration 2 seeks to simplify the power subsystem as much as possible by eliminating the charge controller. This is accomplished by utilizing a separate section of the solar array for charging the battery and taking advantage of the natural current limiting characteristics of the solar array to limit charging current to that which the battery will tolerate on a continuous basis. By introducing some additional complication into the solar array layout, it is possible to design the battery charging array to deliver pulses of energy to each of several batteries rather than sharing a lower continuous current between them. This configuration carries with it penalties in solar array size, and may also offer difficulties in control of noise due to switching transients at the transition between discharge and charge.

The voltage regulation of configuration 2 is superior to configurations 1A and 1B, and inferior to 1C. It is not adequate to permit elimination of the equipment converter input regulator.

Configuration 3 (Figure 3.40)

Configuration 3 utilizes a series regulator to achieve bus regulation. It has the advantage of having a relatively constant heat dissipation throughout its operating life, at a level much lower than the maximum possible heat dissipation of the shunt regulator. This simplifies the interface between the power control equipment and the thermal control subsystem. In the Cansat application, it carries a significant penalty in efficiency, since the efficiency of the communications converters is not adequately improved by the use of a central line regulator to justify its use.

3.7.3.3 Comparison of Configurations in Performance

Table 3.7.2 gives a summary of the main performance characteristics of each configuration, based on the available solar array power at equinox. The power at equinox is calculated from the known power requirement at summer solstice, when the spacecraft is in 100% sun but the array power is minimum.

It should be noted, however, that configuration 2 estimated solar array power requirements are based upon the minimum power required to recharge the battery in a period of 22.8 hours. This results in a charge rate approximately equal to $c/26$, or approximately a safe trickle charge. This is inadequate for effective battery charge unless the battery is divided into at least three parts which are charged sequentially or in a pulsed manner so as to increase the effective instantaneous charge rate. Since all other configurations utilize the increased output of the complete array at equinox for battery charging, they have available charge currents of approximately c/10.

3.7.3.4 Study of Charge Control Methods

Of the various methods of charge control available, four were selected as being sufficiently practical for further study.

1) Constant Current (Pulsed Charge Modification)

2) Limited voltage with a maximum temperature override

3) Auxiliary electrode charge control

4) Coulometric charge control.

Voltage switchdown methods were eliminated from consideration because of their extreme sensitivity to relatively wide range of operating temperature to which the battery is expected to be exposed.

Constant Current Charging

The constant current charge is a natural adjunct to configuration 2, using the current limiting characteristic of the solar array for control of charge. The pulsed charge modification is of particular interest, since the battery efficiency increases as a function of the instantaneous current, which is high, while the overcharge gas evolution rate is a function of the average current, which is maintained at a low level. In this method, the total battery capacity is divided into three or four modules, each of which receives a high pulse of current for a short period. The pulsed current waves are generated by the solar array (battery charge section) by appropriate arrangement of cells on the rotating cylindrical array. The advantages of this approach are as follows:

1) No electronic charge control is necessary

2) The battery charges efficiently, but cannot be overcharged at too high an average rate

3) The modular battery has an increased reliability for partial operation.

The main disadvantage of the method is that the battery weight is increased due to the decrease in cell size and increased packaging requirements.

The use of constant current charging with any of the other candidate configurations, or without the pulsed charging technique, is not recommended because any charging current capable of charging the cells efficiently will be too high for the cell to accept on continuous overcharge.

Limited Voltage with Maximum Temperature Override

This method can be used conveniently with configurations 1A, 1B and 1C, but not with configurations 2 and 3. The main bus voltage, and consequently the charging voltage applied to the battery, is limited to a level of approximately 1.45 volts/cell, which will not permit high rate overcharge of the battery at low temperatures, and consequently minimizes or prevents the irreversible evolution of hydrogen gas in the cell at low temperatures. A constant voltage limit applied to the cell normally results in a condition of thermal runaway due to the negative voltage-temperature characteristic of the cell at any constant current. The system uses a thermal override switch to reduce the charging current to the c/40 level at a preset temperature, thus interrupting the thermal runaway. This technique of charge control provides an additional advantage, in that it permits independent control of battery temperatures, easing the thermal control problems of the spacecraft somewhat.

The disadvantage of this method is that the battery is exposed to brief periods of high overcharge current (if such high currents are available from the primary power source) during the latter stages of charge. The thermal controls for the battery must be designed to dissipate sufficient heat to permit cooling with c/40 trickle currents being applied to the battery. Another disadvantage is that the charge control becomes ineffective in the event of a metal-to-metal short-circuit in any one cell of the battery. It is not normally disturbed by the usual cell failure mode, in which the charging voltage across the defective cell is almost normal.

This charge control method is also disturbed by the effects of use and aging of the cells over long periods of time. This is manifested in an increasing variation from cell to cell of the charging characteristics, causing an unequal distribution of voltages between cells when the voltage limit is applied across the battery. A similar inequality of cell voltage is caused by unequal distribution of temperatures throughout the battery pack. Should these inequalities in voltage distribution be additive,

one or more cells could enter the high voltage region which permits generation of hydrogen gas, leading to progressive pressure buildup and eventual failure of the cell with the highest voltage.

Auxiliary Electrode Charge Control (Figure 3.44)

Cells can be purchased containing auxiliary electrodes whose output voltage, referred to the negative electrode, is a function of the internal oxygen pressure of the cell and of the temperature. Since generation of oxygen within the nickel-cadmium cell occurs only near the end of charge, electrode output voltage (or current through a fixed load) may be used as an indicator of approaching full charge and used to initiate termination of charge or reduction of charge rate.

Because the oxygen pressure is a function of the generation rate and the recombination rate, both of which are non-linear functions of temperature, a more accurate estimate of the state of charge is obtained by compensating the switch-to-trickle point for variations in battery temperature. The output of the auxiliary electrode is of the order of 0.25V.

The most commonly employed circuitry for measurement of auxiliary electrode output is the magnetic amplifier current sensor which employs a small DC current in one winding to control the rectified AC output of the amplifier. AC excitation of the magnetic amplifier is required. A separate amplifier must be used for each cell containing an auxiliary electrode, but a single oscillator may be used for excitation.

The advantage of the auxiliary electrode charge control is that it measures directly a cell characteristic indicative of charge completion. The amount of charge energy restored to the cell may be varied by varying the operating point of the sensor with battery temperature, thus compensating for the lower efficiency and earlier start of gas evolution with increased temperature. The auxiliary electrode tends to terminate charge earlier than the temperature override of a voltage limited charge, leading to lower battery maximum temperatures, less overcharge at high rates, and generally longer life.

The disadvantages of the auxiliary electrode charge control are as follows:

1) Complexity of electronic implementation. The low output voltage of the auxiliary electrode makes a direct DC amplifier

impracticable. The use of AC requires an excitation oscillator and magnetic amplifier, with resulting reliability and weight penalties.

2) The auxiliary electrode gives a false full-charge signal for a brief period after switchover from discharge to charge. In a long charge-time application such as this, the impact of this disadvantage is negligible.

3) The auxiliary electrode is known to drift in sensitivity with aging, the rate of drift decreasing with increasing age.

4) No adequate reliability data are available on auxiliary electrodes.

Coulometric Charge Control (Figure 3.45)

Cadmium-Cadmium Coulometers have been used in controlling the charge of nickel-cadmium cells. The coulometer consists of paired parallel sets of cadmium electrodes which are charged and discharged as the battery current is put through the coulometer. As long as neither electrode set is exhausted, (either fully charged or fully discharged), the voltage drop across the coulometer is of the order of 50 mv. When the coulometer cathode is fully charged, however, the voltage rises rapidly to a level of 1 volt or more. It is necessary to limit the voltage developed across the coulometer to approximately 0.8 volts by using a diode bypass.

The ampere-hour efficiency of the Cd-Cd coulometer is approximately 100%, consequently it forms an accurate analog of cell performance only when the cell efficiency is 100%. The coulometer has been used to control cells on cycling at moderate depths of discharge and normal temperatures for several thousand cycles. However, at greater depths of discharge than 35%, results have not been uniformly successful. It is also probable that the coulometer will fail to control battery charge at high battery temperatures without some sort of current-temperature compensation for variation in battery efficiency. The weight of a coulometer is approximately that of 1 cell, and the addition of a coulometer requires provision in packaging for the addition of the coulometer cell, similar in size to one cell. The coulometer drifts in capacity with aging, the rate of drift falling to a negligible level after several hundred cycles. No adequate reliability data are available on coulometers.

3.7.3.5 Subsystem Weight Trade-offs

Table 3.7.3 shows trade-offs between the five candidate configurations, each considered with applicable versions of the four candidate charge control schemes. Subsystem models 1A, 1B and 1C are considered with the voltage limit, auxiliary electrode, and coulometer charge control schemes, each one implemented using the ground rule that no single part failure can cause mission failure. This results in the use of quad or majority voting redundancy for the power control functions, and causes replication of the number of components.

Other ground rules used in each of the systems are as follows:

1) All shunt regulators are of the majority voting logic type

2) Shunts are quad redundant

3) All batteries are equipped with bypass electronics designed so that the loss of one cell by shorting will not affect the ability of the battery to support all loads.

4) Charge control logic and components are majority voting redundant, including the auxiliary electrodes and coulometers.

Based upon the above ground rules, Configuration 1B is the lightest in weight, by a small margin, without additional charge control features. The addition of the third electrode charge control increases the weight by 1.8 pounds, but the additional weight is well spent for the improvement in performance of the power subsystem and the decreased heat generation in the battery. The lowered efficiency of utilization of stored energy due to inclusion of the diode in the discharge circuit results in a small penalty in depth of discharge.

3.7.3.6 Results of Trade-off Studies

On the basis of the analyses which have been made so far, the best system configuration is shown in detail in figure 3.46.

The battery contains 20 cells of nominal capacity 9 AH. Three of the cells are fitted with auxiliary electrodes. The battery is connected across the main solar array bus via relay K1 during the early portion of recharge. When the auxiliary electrode currents indicate that overcharge conditions are approaching, the majority voting logic circuits cause K1 to open and the charge current switches to a predetermined trickle value, typically about C/30. The auxiliary electrode current at which K1 is switched to trickle is modified by the three cell temperature sensors TS1, TS2 and TS3. A back up switch control is provided by the battery temperature override, with sensor TS4.

The shunt Electrical Assemblies (SEA 1-4) are connected across a control tap on the solar array to control the bus voltage limit. Tapping the array in this manner provides an improvement (as compared to an untapped control point) in thermal interface and array impedance. The maximum bus voltage is 30 volts. An undervoltage cut-out system is provided which disconnects the communications loads (but not the vital housekeeping loads) if the bus voltage falls below 18 volts, indicative of a fault condition such as a short on the bus.

When nickel-cadmium cells are cycled at high depths under monotonously repetitive conditions they display a gradual deterioration in capacity and discharge voltage. Exact values depend to some extent on the manufacturers as well as on the precise cycling conditions. Simulated tests of synchronous orbit conditions during the eclipse season indicate that almost all the capacity can be recovered by reconditioning the cells prior to each eclipse season. The reconditioning operation consists of 1 or more very deep discharges followed by a normal recharge. Relays K2 and K3 permit this operation to be performed. Resistor R1 acts as a dummy load on the battery during the discharge. The reconditioning cycles are activated by command.

3.7.4 Solar Array Analysis

3.7.4.1 Solar Cell Characteristics

In establishing the most suitable types of solar cells to be used the following factors were considered:

Cell material and type

Base resistivity

Cover glass thickness and material

Contact type and material

Cell efficiency

Glass-to-cell adhesive

The solar cells selected for this application are n-on-p silicon cells 2 x 2 cm in size and 0.010 inches thick, having a bulk resistivity of 2 ohm cm. The ohmic contacts on the silicon cells are of titanium-silver and are covered with a thin layer of solder.

Base Resistivity

The relatively low resistivity was selected after trade-off studies against 10 ohm-cm cells because of the higher end-of-life performance of the 2 ohm-cm ones. Whereas the 10 ohm-cm cells have a somewhat higher charged particle radiation degradation resistance than the 2 ohm-cm cells, the latter have higher power initially. It was found for the environment specified that the initial higher power output outweighed the advantage of higher radiation resistance for the 10 ohm-cm cells.

Area

Silicon solar cells can be obtained in 1 x 2, 2 x 2, 3 x 3 and 2 x 6 cm size. In general, cost per unit area of silicon solar cells decreases as the cell area increases. For the 3 x 3 cm cells, insufficient data and lack of experience in addition to possible increased handling costs, precludes their use at this time. 2 x 2 cm cells as well as 1 x 2 cm cells have been successfully used on several satellites. The cost advantage of the 2 x 2 cm cells relative to the 2 x 1 cm cells, therefore, dictates their use for this program. The cell dimensions are 0.788 x 0.788 inch and have an active area of 0.589 in^2 (3.80 cm^2). 2 x 6 cm cells have been eliminated due to the fact that they are not capable of being used with the imposed spacecraft diameter.

Thickness

Up to approximately 0.016", increased thickness results in increased power output due to the useful response of the added thickness to infrared radiation. This extra response is lost with a modest amount of radiation damage due to the decrease in diffusion length. Consequently thin cells with initially low output may have the same output as thick cells after some radiation damage. This condition has led to the selection of 0.010 inch thick cell for maximum power-to-weight effectiveness at end-of-life. In addition to the weight advantage gained, the selection of such cells results in a minimization of power output variation between the beginning and end-of-life. Cells much thinner than 0.010" present difficult manufacturing problems.

Contact Type and Material

Solderless cells with titanium-silver contacts show severe degradation when subjected to a combination of high temperature and humidity while completely solder covered cells exhibit hardly any degradation as a result of such exposure. However, conventional solder covered cells are obtained by dipping the cells into solder which results in

unnecessarily heavy cells. The amount of solder required for the humidity protection is much less. Cells have been developed with only a thin coating of solder, sufficient to make the cells humidity resistant without a noticeable weight increase. These cells are recommended for this project.

Efficiency

The n-on-p silicon cells are made in large quantities at air mass zero efficiencies of 10 to 11 percent at 28°C. For this program, solar cells with average conversion efficiency of 10.75 percent have been selected. The average cell E-I characteristic is shown in Table 3.7.4.

Cover Slides

The solar cells are covered with slides of 0.006 inch thick Microsheet for thermal reasons and to increase the resistance to proton and electron radiation encountered in orbit. The glass thickness was chosen consistent with weight limitations, since trade-off studies between cell area and cover-slide thickness have shown that for this orbit, maximization of the area rather than increasing cover slide thickness yields optimum power output. The available solar array area is limited by the satellite diameter.

Filters

The slides are coated with interference filters. One side contains an ultraviolet reflective filter and the other side an anti-reflective filter of magnesium fluoride. The ultraviolet reflective filter is located on the cell side of the cover slide and provides protection of the cell-to-glass adhesive. The selected cutoff wave length of the ultra-violet filter is 0.410 microns.

Glass-to-Cell Adhesive

The principal adhesives of interest for space use are epoxies and silicones because of their superior ability to withstand ionizing radiation for long periods without structural changes or changes in their optical transmittance. Dow Corning's silicone adhesive type XR-63489 has been selected since laboratory tests have shown this adhesive to have the least discoloration due to charged particle irradiation compared to other commonly used adhesives for solar arrays. Data from satellite experiments have shown that discoloration of this adhesive due to charged particle irradiation has not occurred for time integrated fluxes corresponding to 3 to 5 years at communication satellite orbits.

3.7.4.2 Detailed Design of Solar Array

A detailed design of the solar array has been made to ensure that the results of this study are based on realistic calculations of power system performance capability and satellite height.

The solar array consists of 20,480, 2 x 2 centimeter solar cells, with 0.006 inch fused silica cover slides, body mounted on a cylinder 79.00 inch long by 56 inch in diameter. The entire cylinder is covered with cells except for two 2 inch slots running the length of the cylinder and located 180 degrees apart, and thirty spaces 0.68 inch by 1.58 inch reserved for structural and protective cover attachments. The 20480 cells are divided between sixteen panels of 1280 cells each. Each panel is further divided into ten strings (five string-pairs) each of 64 cells in series by 2 cells in parallel. A schematic diagram of a solar cell string-pair is shown in Figure 3.47.

Blocking diodes are connected in series at the positive end and at the tap of each string-pair to isolate the string-pair from the output bus during periods of darkness.

Each string is formed from sixteen eight-cell (4S x 2P) modules connected in series to form a 64-series-cell string. The combination of modules and their relative position for each string differs depending upon the position of the string relative to the holes for panel and protective cover-mounting provisions. All cell and module interconnections within a string are redundant.

Negative, positive and tap connections are made with redundant feed-through connections at the back of the panel. The feedthrough connections are back-wired to turret terminals on a pre-fabricated terminal board assembly bonded to the back of the panel near the equipment platform. For fabrication simplicity, the feedthroughs are soldered to the module during panel assembly, thus limiting the module configuration to two types only.

Every two strings (64S x 2P) are bussed at each end and at the tap to form a string-pair. The panel specification provides for electrical output from each string-pair to meet a minimum output requirement. All wiring is made at the back of the panel except for the interconnection of modules at the end of each row. Such interconnections are short wires since the modules to be connected are adjacent. All sixteen panels are identical except two which are equipped with a temperature sensor located on the rear surface. The temperature sensors are located such that when used in conjunction with thermal analysis data, the array temperature can be

ascertained during launch and orbital conditions. The output from each panel will terminate in a connector located on the rear of the panel to plug into the spacecraft wiring harness. This harness will interconnect the positive, tap, and negative connections between the eight panels and power bus.

3.7.4.3 Solar Array Performance

The predicted electrical characteristics of the array at the beginning and end of life are shown in Table 3.7.5 for equinox, winter solstice and summer solstice. The variation of array power output (at a terminal voltage of 29 volts) is shown in Figure 3.48. These results were obtained using a computer program which takes into account the following factors:

a) Initial cell output (Table 3.7.4)

b) Temperature of each illuminated solar cell string.

c) Solar cell short-circuit current degradation due to charged particle irradiation.

d) Open-circuit voltage degradation due to charged particle irradiation.

e) Effect of angle of incidence on solar cell output and the variation due to charged particle irradiation.

f) Temperature coefficient of solar cell short-circuit current and its variation due to charged particle irradiation.

g) Temperature coefficient of the solar cell open-circuit voltage and its variation due to cell temperature.

h) Adhesive transmittance degradation due to charged particle and ultraviolet irradiation.

i) Coverglass transmittance degradation due to charged particle and ultraviolet irradiation, and micro-meteorite erosion.

j) Chromatic response shift of solar cells due to charged particle irradiation.

k) Distance to sun and sun angle.

l) Output losses of solar cells due to cover glass installation.

m) Solar cell output losses due to assembly.

n) Power losses due to isolation diodes and wiring.

o) Operation time.

p) Array configuration

The data used in the analysis of these factors are based on information from a wide variety of published sources, ground tests and flight experience. The radiation damage calculations are based on expected charged particle flux due to trapped electrons, trapped protons and solar flares, with a maximum of 12 transfer orbits in addition to the 5 years at synchronous altitude.

3.7.4.4 Solar Panel Construction

The solar panel consists of solar cell modules cemented directly to panels. The panel substrate consists of two face sheets bonded to aluminum honeycomb. The adhesive used to mount the solar cell modules to the solar panels is a room temperature vulcanizing silicone which allows for differential thermal expansion between modules and substrate. The solar panels will be subjected to temperature variations over the range of (+20°C to -129°C). The solar array utilizes one module configuration containing 2 parallel by 5 series cells as shown in Figure 3.49. Each panel weighs 3.27 lbs.

The cells are overlapped as shown in Figure 3.49 using interconnector strips of 0.001 inch Kovar. The interconnector strip provides interconnection between the two parallel connected cells as well as connection to the next pair of series connected cells. At the end of each module special interconnections are used. On the N terminal, a formed ribbon is used. On the P terminal, a special interconnector is used, having tabs designed to fit to the N terminal ribbon of the adjacent module. This interconnection scheme provides highly flexible modules which may easily be attached to a curved surface. The design has been used on previous spacecraft.

The triple redundancy between series connected cells results in very high reliability. An extensive statistically designed test program involving extended temperature cycling over a wide temperature range has shown the recommended assembly method to provide joints of high inherent strength. The manufacturing processes employed for assembly subjects the cells to minimum stresses and provides for 100 percent microscopic inspection by the operator.

Redundant isolation diodes are utilized to connect the positive output of each illuminated solar panel power bus and the tap point to the main control bus. These diodes provide low resistance paths for current flow from the illuminated strings of the solar array, while preventing leakage currents through the non-illuminated panels. At the positive, negative and shunt tap terminals of each string, redundant feedthrough connectors extend through the substrate to the panel back wiring.

It has recently been established that excessive power degradation can occur in solar cells if small edge areas are not completely shielded against low energy protons. The assembly method described here use techniques which ensure complete cell coverage. The effectiveness of this protection has been established by test programs on previous projects.

System	Power Required by System (watts)			
	Unregulated (from bus)		Regulated (from central converter)	
	Normal	Eclipse	Normal	Eclipse
High Level TWTs and Converters (8W RF, 28.4% efficiency)	169.2	56.4	-	-
TWT Driver	5	5	-	-
Receiver	-	-	5	5
Attitude Determination and Control	13.7	13.7	0.8	0.8
Position and Orientation	0.5	0.5	-	-
Tracking, Telemetry and Command	-	-	14.3	14.3
Electrical Integration Assembly	0.2	0.2	0.2	0.2
Wiring Losses	4.5	2.1	-	-
Power Conditioning and Control	10.8	10.8	-	-
TWT Heaters	-	5	-	-
Total	203.9	93.7	20.3	20.3

Note: In addition, 6.6 watts is required for battery trickle charge in solstice seasons. 5 watts is required for the heaters of the 4 TWTs which are turned off during eclipse.

Table 3.7.1 - Power Required by Each System

Configuration	1A	1B	1C	2	3	Units
TWT Converter Efficiency	86	86	89	86	89	%
Equipment Converter Efficiency	75	75	78	75	78	%
Power into TWT Converters						
Daylight (6 on)	169.2	169.2	163.5	169.2	163.5	watts
Eclipse (2 on)	56.4	56.4	54.5	56.4	54.5	watts
Power into equipment converter	27.1	27.1	26.1	27.1	26.1	watts
"Unregulated" Housekeeping power	27.9	27.9	27.9	27.9	27.9	watts
Battery Trickle Power	6.6	6.6	6.6	6.6	6.6	watts
Heater Power (eclipse only)	5.0	5.0	5.0	5.0	5.0	watts
Power required from array at solstices	230.8	230.8	224.1	$\begin{bmatrix}224.1\\+6.6\end{bmatrix}$	253.6	watts
Power required from array at equinoxes in sunlight	233.1	233.1	228.6	$\begin{bmatrix}224.1\\+9.9\end{bmatrix}$	257.5	watts
Min. power available from array at equinoxes, in sunlight	261	261	254	$\begin{bmatrix}254\\+9.9\end{bmatrix}$	286	watts
Min. excess power available for recharge, at equinoxes	26.9	26.9	25.4	9.9	28.5	watts
Minimum charge rate	$\frac{C}{10.2}$	$\frac{C}{10.2}$	$\frac{C}{10.8}$	$\frac{C}{29}$	$\frac{C}{9.7}$	A

Table 3.7.2 - Comparison of Candidate Configurations

Subsystem Configuration	Array	Battery	PCU	Equip. Conv.	Shunt	Syst. Status TLM	Total
1A	52.4	23	2.0	3.5	3.6	2.0	86.5
1A + 3rd electrode	52.4	23.2	3.6	3.5	3.6	2.0	88.3
1A + coulometer	52.4	26	3.2	3.5	3.6	2.0	90.7
1B	52.4	23	1.9	3.5	3.6	2.0	86.4
1B + 3rd electrode	52.4	23.2	3.5	3.5	3.6	2.0	88.2
1B + coulometer	52.4	26	3.1	3.5	3.6	2.0	90.6
1C	50.5	23	10.2	3.5	3.6	2.0	91.8
1C + 3rd electrode	50.5	23.2	11.5	3.5	3.6	2.0	94.3
1C + coulometer	50.5	26	11.1	3.5	3.6	2.0	94.7
2	52.6	32.4	1.5	3.5		2.0	92.0
3 + 3rd electrode	57.4	23.2	12.8	3.5		2.0	96.9
3 + coulometer	57.4	26.0	12.4	3.5		2.0	101.3

Table 3.7.3 - Subsystem Weight Trade-offs

Voltage (V)	Current (mA)
0	128
0.1	127.99
0.2	127.99
0.3	127.93
0.40	127.04
0.42	126.4
0.44	125.1
0.46	122.9
0.475	120
0.48	118.1
0.50	111.9
0.52	99.4
0.54	79.3
0.56	43.35
0.5715	0

Table 3.7.4 - Average Electrical Characteristic of Solar Cell

Condition	Equilibrium Temperature °C		Distance From Sun	Sun Angle	Average Power at 29 V		Average Short-Circuit Current		Open-Circuit Voltage		Current at 29V (Average)	
	0 YR Min	5 YR Max	Au	Deg.	0 YR W	5 YR W	0 YR amp	5 YR amp	0 YR V	5 YR V	0 YR amp	5 YR amp
Equinox	10	19.5	1.0000	90	329	263.3	11.644	10.04	37.5	34.5	11.35	9.0
Winter Solstice	8.3	17.2	0.9837	66.5	312.8	251.7	11.04	9.48	37.5	35.0	10.79	8.68
Summer Solstice	1.5	12.2	1.0163	66.5	293.9	239.7	10.29	8.82	38.5	35.5	10.13	8.27

Table 3.7.5 - Electrical Characteristics of Solar Array

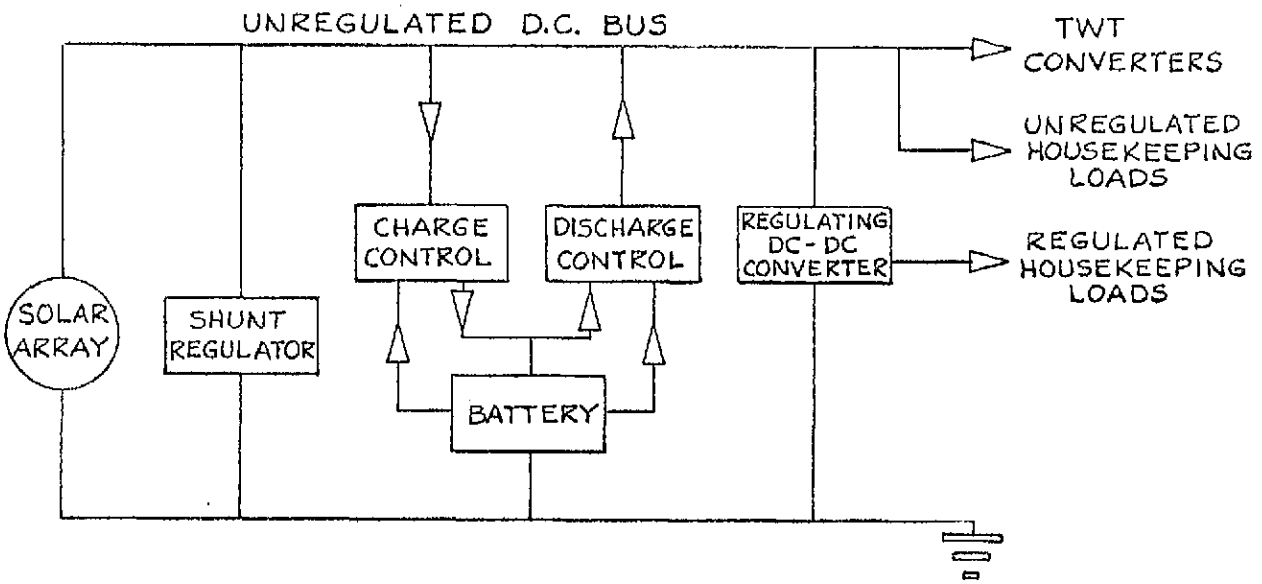

FIG. 3·38

BASIC POWER SYSTEM, CONFIGURATION 1.

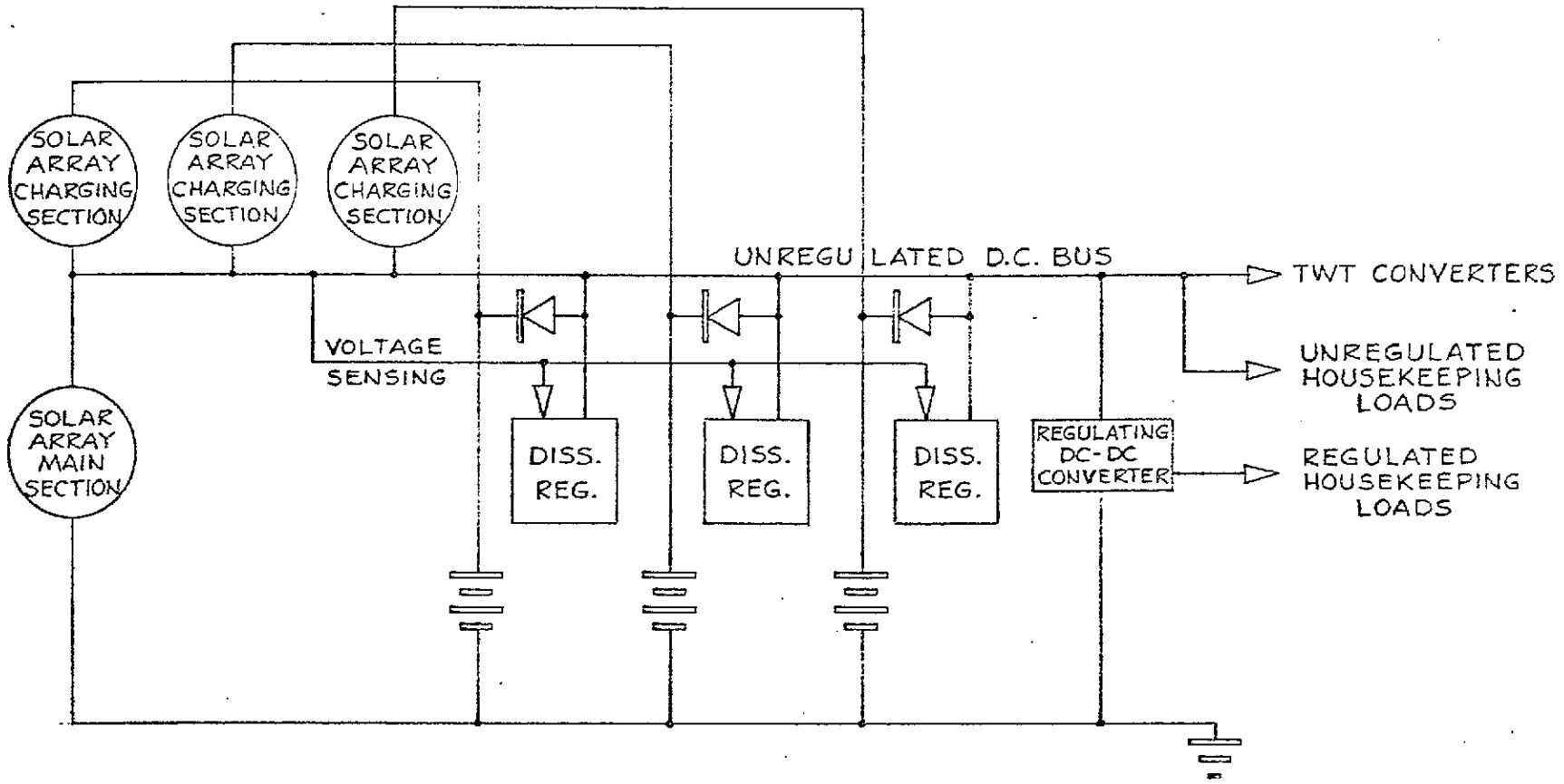

FIG. 3·39

ISOLATED BATTERY CHARGE SYSTEM CONFIGURATION 2.

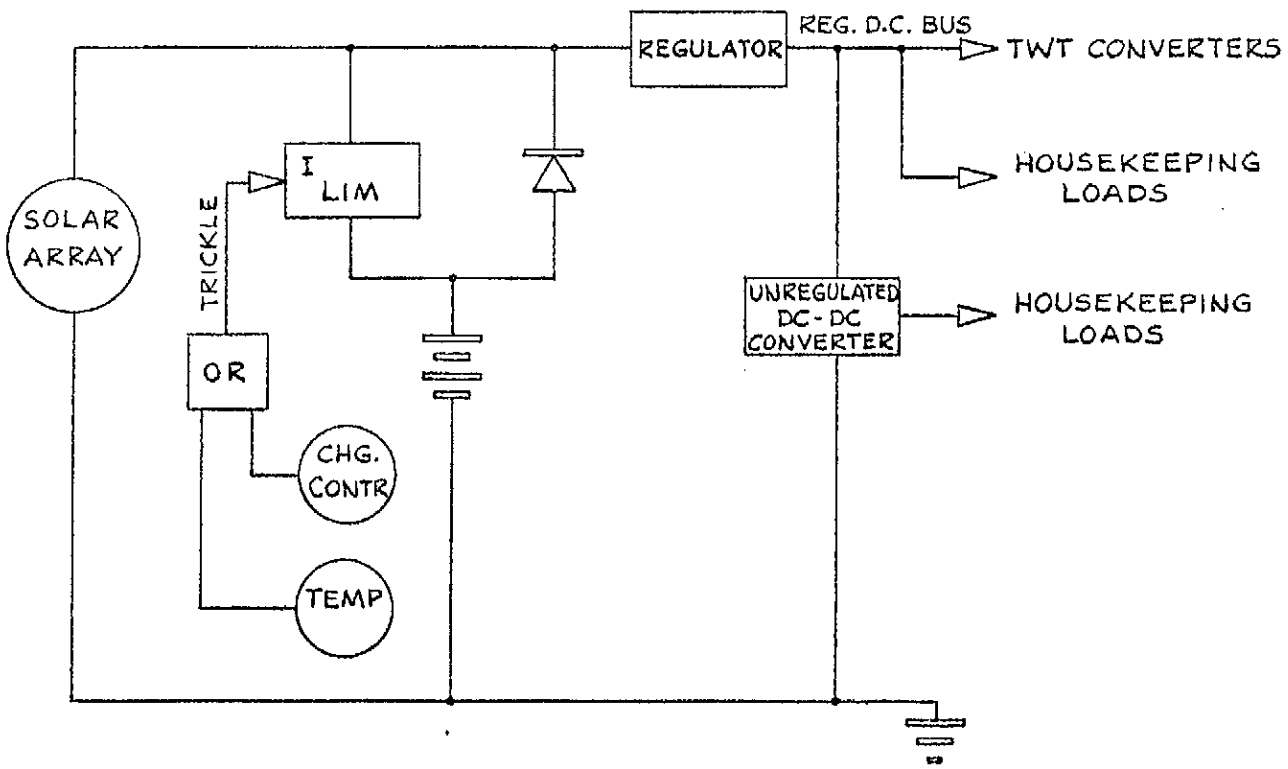

FIG. 3·40
SERIES REGULATED SYSTEM
CONFIGURATION 3.

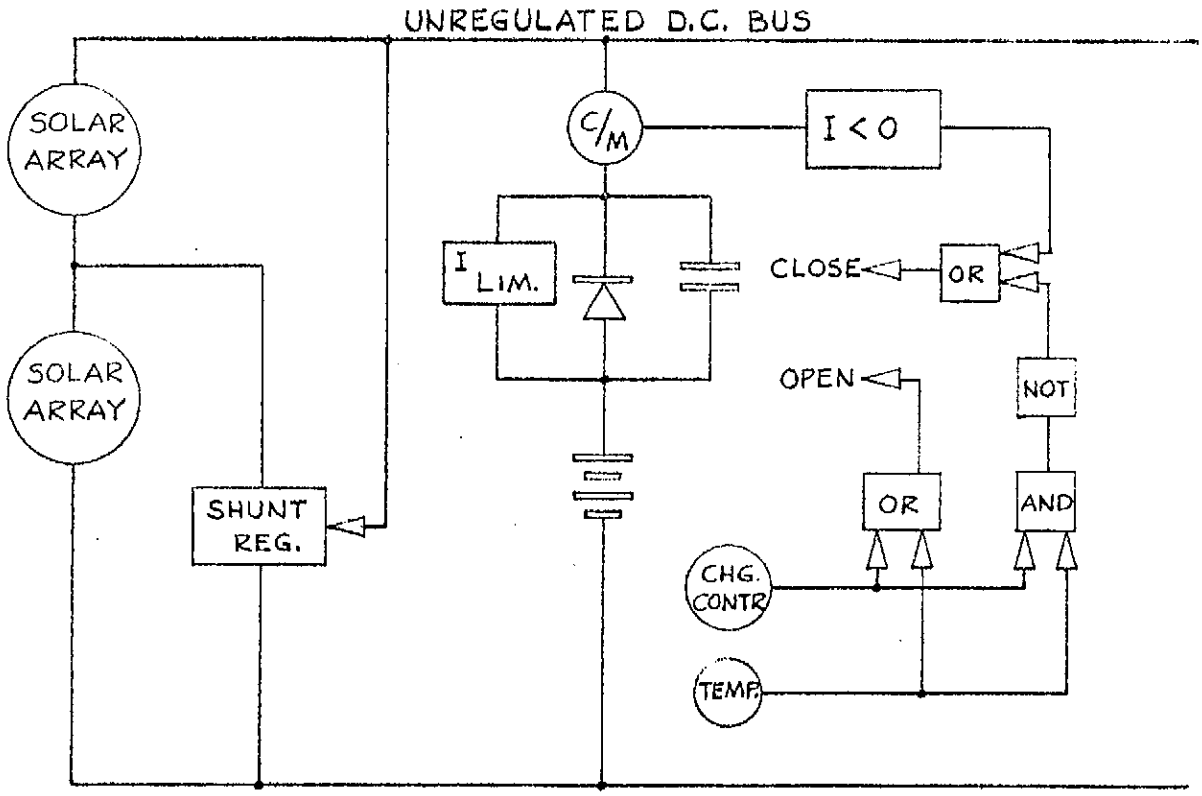

FIG. 3·41
BASIC POWER SYSTEM
CONFIGURATION 1A.

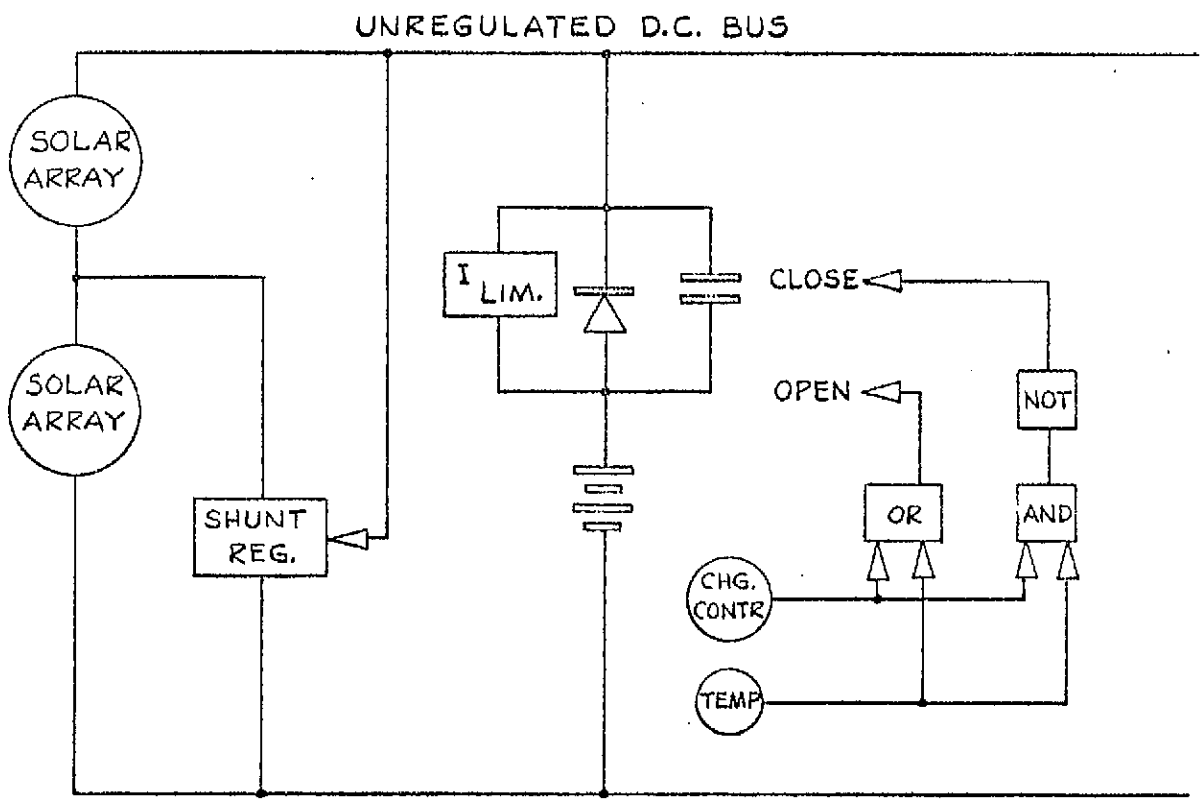

FIG. 3·42
BASIC POWER SYSTEM
CONFIGURATION 1B.

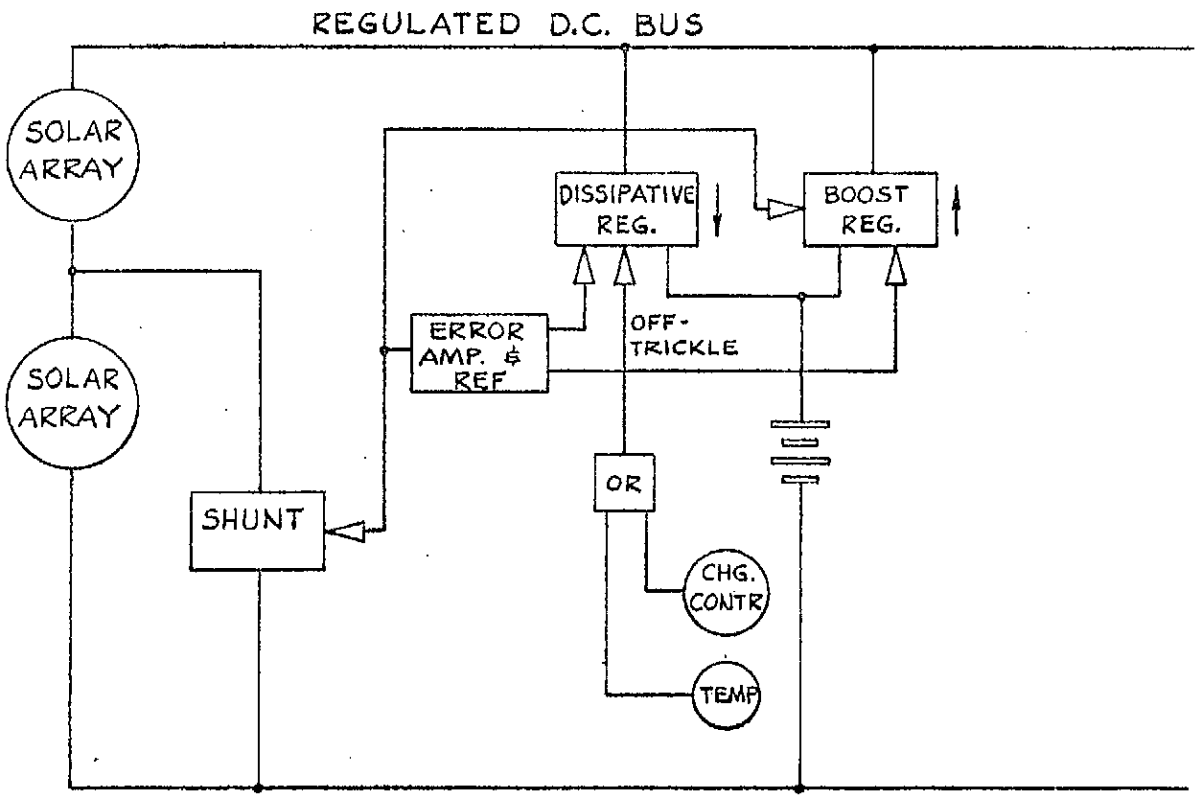

FIG. 3·43
BASIC POWER SYSTEM
CONFIGURATION 1C.

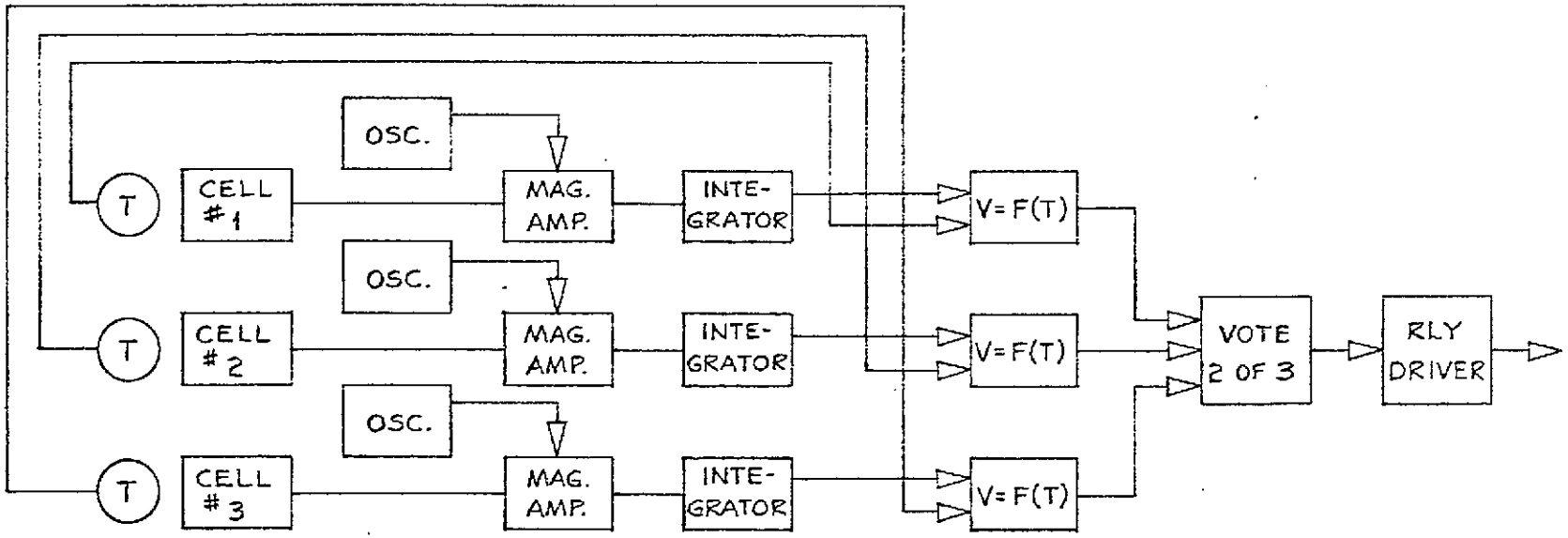

FIG. 3·44

AUXILIARY ELECTRODE CHARGE CONTROL

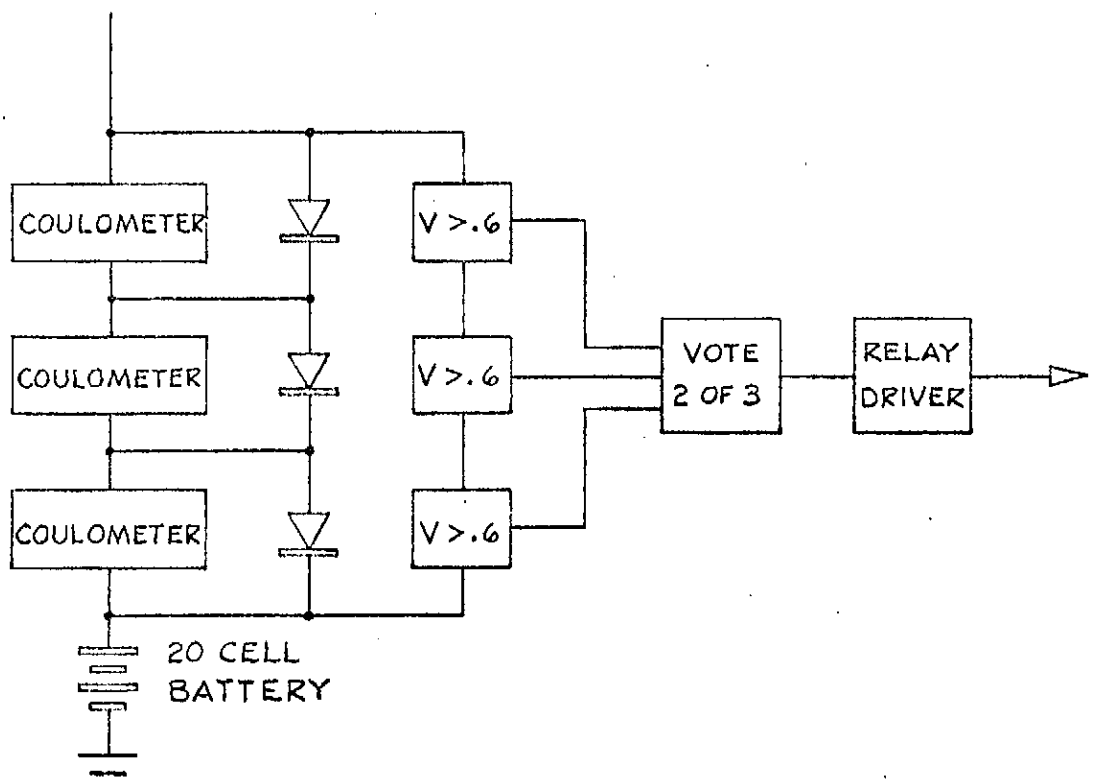

FIG. 3·45
COULOMETRIC CHARGE CONTROL

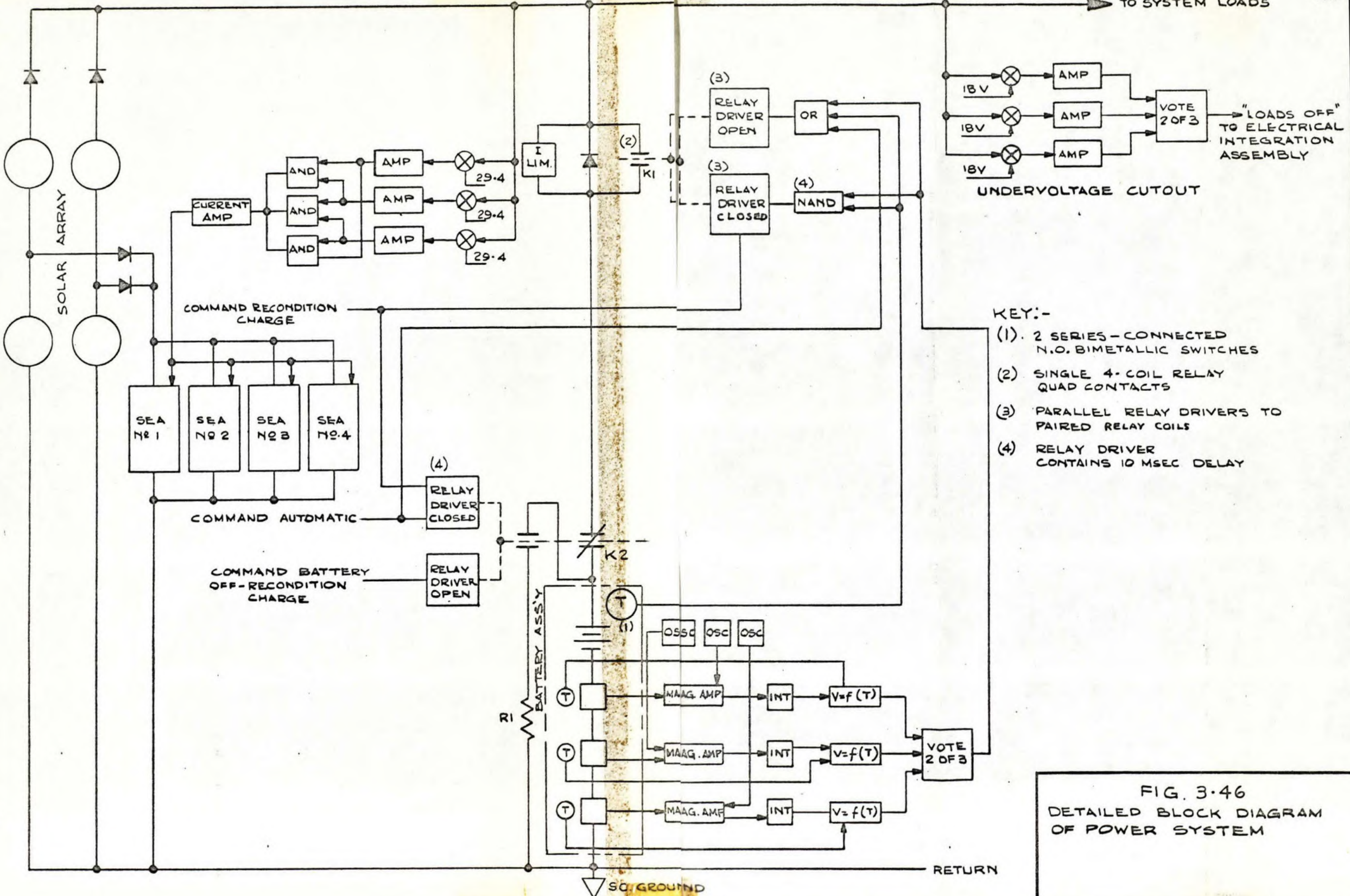

KEY:-

(1). 2 SERIES-CONNECTED N.O. BIMETALLIC SWITCHES

(2) SINGLE 4-COIL RELAY QUAD CONTACTS

(3) PARALLEL RELAY DRIVERS TO PAIRED RELAY COILS

(4) RELAY DRIVER CONTAINS 10 MSEC DELAY

FIG. 3·46
DETAILED BLOCK DIAGRAM OF POWER SYSTEM

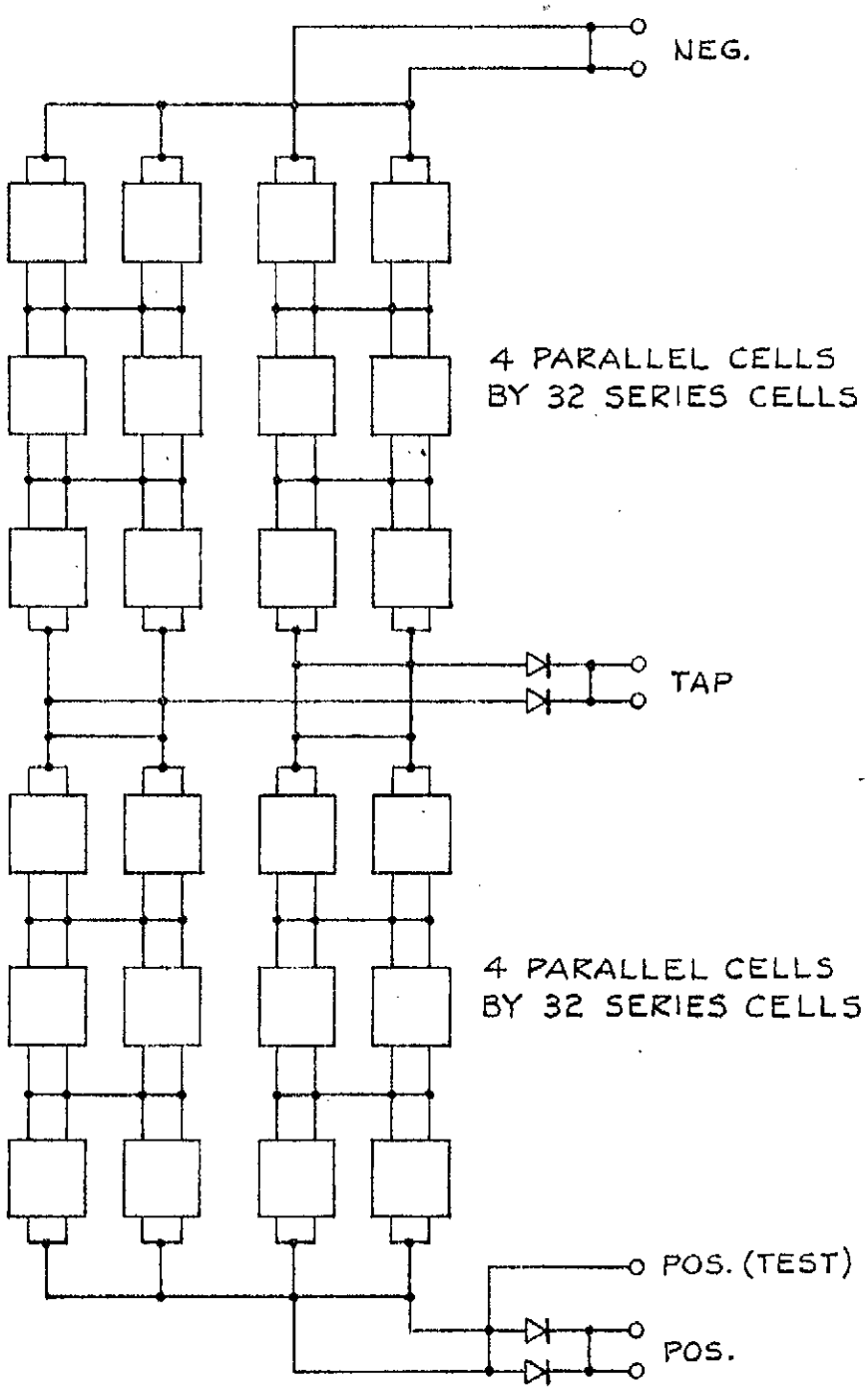

FIG. 3·47

SOLAR CELL STRING PAIR SCHEMATIC

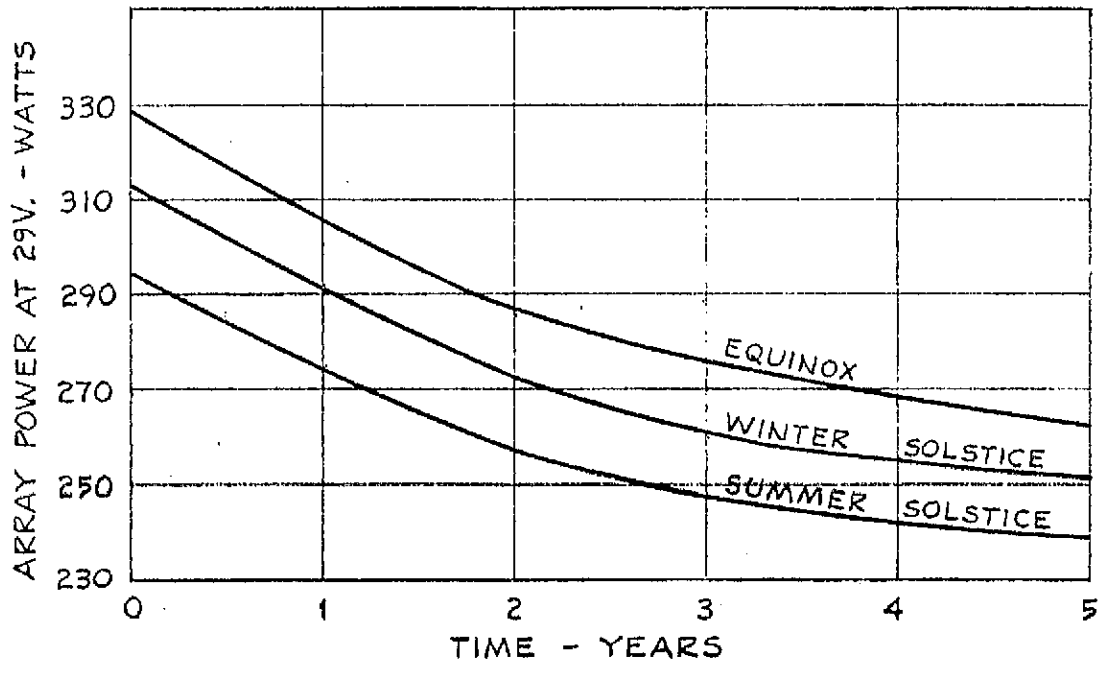

FIG. 3·48

SOLAR ARRAY POWER OUTPUT (AT 29V.)

THREE SEASONS

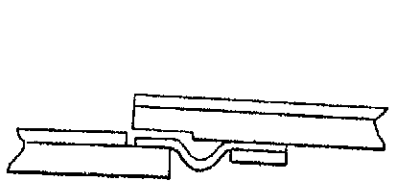

INTERCONNECTION DETAIL

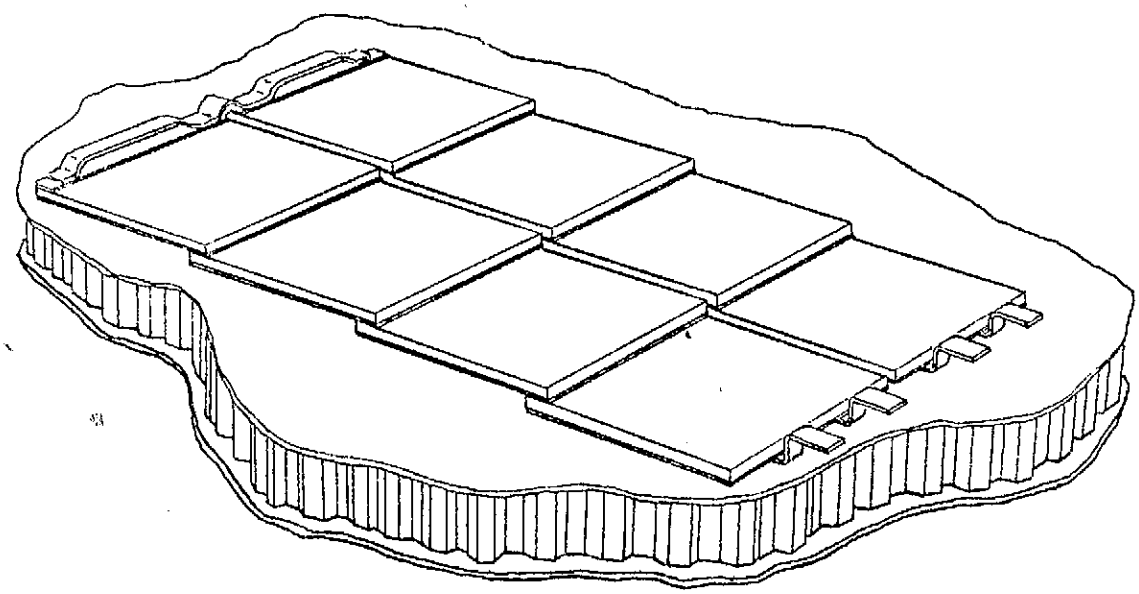

FIG. 3·49

SOLAR CELL MODULE CONSTRUCTION

3.8 Apogee Motor

Table 3.8.1 presents a summary of information currently available regarding apogee motors applicable to the Canadian domestic communications satellite program. It should be noted that the data presented are based on preliminary velocity increments and total satellite weights available from the study at the time that the apogee motor manufacturers were contacted. Subsequently, a letter formally requesting apogee motor data was prepared and forwarded to four organizations: Thiokol Chemical Corp., Hercules, Inc., Aerojet-General Corp. and United Techology Center (a division of United Aircraft located in Sunnyvale, California). Responses to this letter were requested by mid August.

It is anticipated that this information will provide an adequate basis for evaluation of the state-of-the-art of apogee motor technology, determining the optimum design approach, and determining budgetary costs for the Canadian domestic communications satellite apogee motor program.

TABLE 3.8.1

CANDIDATE APOGEE MOTORS FOR CANADIAN COMSAT PROGRAM

MOTOR MANUFACTURER &	THIOKOL CHEMICAL CORP.		HERCULES, INC. WILMINGTON, DEL.		AEROJET GENERAL CORP. SACRAMENTO, CALIF.
MOTOR DESIGNATION	TE-M-442	--	X-258E6	--	--
Status	Qualified for Sandia Corp. Application, offloaded	New motor, similar to TE-M-442	Production for Scout, other Applications, offloaded	New motor, similar to X-258	New motor, based on Intelsat II and III technology
Design V (ft/sec)	6100	6335	6100	6100	6100
Total S/C Weight (lb)	950	906	906	906	906
Total Impulse (in sec)	130,000	130,340	125000	--	126,400
Average Thrust (lb)	6420	--	5600	--	5660
Specific Impulse (sec)	278	289	282	--	292
Average Burn Time (sec)	20	--	22	17	22.3
Total Weight (lb)	538	516	503	486	502
Propellant (lb)	467.4	450	443	432	433
Inerts (lb)	70.6	66.0	60	54	69
Mass Fraction, f	.869	.870	.88	.89	.863
Expansion Ratio	18.7:1	53:1	28:1	28.5:1	50:1
Case Material	Steel	Titanium	Fiberglass	Fiberglass	Fiberglass
Throat Area (in^2)	6.55	6.55	6.9	8.5	5.96
Overall Length (in)	33.0	44.0	55.2	58.6	41.0
Case Diameter (in)	26.0	26.0	18.0	18.0	27.0
Nozzle Diameter (in)	12.92	20.2	15.8	17.6	20.0
NOTES	Electromechanical safe and arm not included, motors based on scale down of Surveyor		Electromechanical S & A not included, case length of motors reduced		S & A included

3.9 Thermal Control System

3.9.1 System Description

3.9.1.1 General

The thermal control system for CANSAT is designed to be completely passive. Fluctuations in the total internal heat load are minimized and a radiative heat balance is established between absorbed solar, internal dissipation, and emitted energy to maintain components within allowable temperature limits during steady state sunlit operation. The heat capacity of the spacecraft aids in maintaining allowable temperatures during transient eclipse conditions. Surface thermal radiation property requirements, insulation, structural coupling, and component grouping are the passive techniques utilized to obtain thermal control. The materials, finishes and coatings specified, when critical, are the most stable materials now available for spacecraft use based on exposure to combined vacuum, ultraviolet, and charged particle environments. The details of the above are given in Table 3.9.1.

The thermal control subsystem is designed to meet the following five conditions:

Synchronous Orbit - Sunlit and Eclipse

Transfer Orbit - Sunlit

Parking Orbit - Sunlit and Eclipse

Boost

Ground Hold

Thermal control concepts for the despun and spinning section of the spacecraft will be discussed separately in the following sections.

3.9.1.2 Despun Section

Despin Mechanical Assembly

The despin mechanical assembly can be described thermally as an outer aluminum vertical spinning cylinder, inner steel vertical despun shaft having an aluminum spinning interface adapter and rotary counter assembly aft. The outer cylinder internal surfaces and the external surface of the inner shaft will be coated with black Cat-a-lac paint ($\varepsilon = .86$) to thermally couple the two to minimize temperature differentials that might cause interference. The external surface of the cylinder will also be coated with black paint to thermally couple the despin assembly with the upper platform. The structural attachments

Cansat Thermal Control System Description

Description	Material	ε	α
Omni and Biconical Antenna Coating	White Paint - Dow Corning 092-007	.85	.2/.5*
Elliptic Antenna Reflector Concave Caating	White Paint - Dow Corning 092-007	.85	.2/.5
Elliptic Antenna Reflector Convex Coating	Vacuum Deposited Aluminum	.04	.12
Elliptic Antenna Feed and Reflector Support Insulation	10 Layer Aluminized Kapton	.60	.30
Antenna Thermal Insulators	Fiberglass	-	-
Forward Platform Radiating Surfaces	Second Surface Mirrors	.80	.10
Forward Platform Insulation	10 layer Aluminized Kapton	.6	.3
Forward Platform and Component Surface Coating	Black Paint - Cat-a-lac	.86	-
TWT Base Plate and Thermal Filler Material	.060" Aluminum, RTV-11 Adhesive	-	-
Despin Mechanical Assy External and Internal Surface Coating	Black Paint - Cat-a-lac	.86	-
Despin Mechanical Assy Thermal Insulator	Fiberglass	-	-
Central Cylinder Internal and External Surface Coating	White Paint - Dow Corning 092-007	.85	-
Solar Array Substrate Internal Surface Coating	White Paint - Dow Corning 092-007	.85	-
Propellant Tank and Line Thermal Insulators	Fiberglass	-	-
Propellant Tank and Line Surface Finish	Vacuum Deposited Aluminum	.04	-
Propellant Tank and Line Insulation	10 Layer Aluminized Mylar	.04	-
Aft Platform and Component Surface Coating High Heat	White Paint - Dow Corning	.85	
Low Heat	VDA Tape	.04	
Apogee Motor Insulation	Aluminum Foil and Dexiglass Insulation	.04	-
Apogee Motor Thermal Insulators	Fiberglass	-	-
Apogee Motor Nozzle Closure	Aluminized Mylar	.6	.3
Aft Closure Fwd	Stainless Steel	.15	-
Aft	White Paint - Dow Corning	.8	.2/.5
Axial Thruster Solar Collector	Incoloy	.11	.56
Beryllium Heat Sink	Beryllium	.08	-
Axial Thruster Thermal Insulator	Gold Coated Stainless Steel Foil and Micro Quartz	.08	-
Solar Array External Surface	----	.82	.79

* α = .2 New/α = .5 Degraded

Table 3.9.1

of the outer cylinder to the upper platform will also provide good thermal coupling. The antenna support adaptor forward and central cylinder adaptor aft will be thermally decoupled from the despin mechanical assembly by means of fiberglass insulators to minimize longitudinal temperature gradients in the assembly and heat leaks from the spacecraft.

The drive motors and cabling dissipate 4 watts under normal operating conditions. The aluminum spinning shaft will tend to minimize temperature gradients along the shaft due to its good thermal conductivity. The heat generated in the drive motors on the spinning cylinder will be transmitted radiatively to the despun platform by good radiative coupling.

Antennae

The despin mechanical assembly supports three despun antennae as shown in Figure 3.55. All the antennae are maintained within maximum and minimum allowable temperature limits by the selection of thermal coatings. The antennae will experience temperature gradients in the longitudinal and transverse directions as well as wide variations in average temperature levels due to various sun angles and shadowing. The two telemetry and command antennae will be covered with white paint (Dow Corning 092-007 Zinc Oxide Pigment, Silicone base, $\alpha_{initial} = .2$, $\alpha_{degraded} = .5$, $\varepsilon = .85$) and will be thermally decoupled from the elliptical antenna support by fiberglass insulators. The solar absorptivity degradation will not influence the performance of these antennae. Only the elliptical communications antenna has pointing accuracy requirements that require a detailed examination of thermally induced distortions.

The reflector portion of the elliptical antenna will be contoured aluminum honeycomb with aluminum face sheets. Different surface coatings will be applied to the reflector external surfaces to reduce longitudinal and transverse temperature gradients and thereby reduce thermally induced antenna pointing errors. White paint will be used on the concave surface to produce as low a solar absorptivity value as possible and still provide diffuse solar reflection to prevent specular focusing of solar energy on the antenna feed. Vacuum deposited aluminum VDA($\alpha = .12$, $\varepsilon = .04$) on the convex surface of the reflector will reduce transverse thermal gradients at the expense of somewhat higher average reflector temperatures for the various sun angles.

The elliptical antenna feed and reflector supports will be wrapped with multilayer aluminized Kapton insulation blankets (aluminized side facing inward) and painted with black epoxy paint ($\varepsilon = .92$) internally to minimize circumferential thermal gradients in the supports that would cause antenna pointing error. The multilayer aluminized Kapton insulation blanket will consist of 10 layers of 1/4 mil Kapton sandwiched between two layers of 2 mil Kapton. Aluminized Kapton was selected over aluminized Mylar because of its thermal property stability.

Nutation Damper

The nutation damper will be attached to the communications antenna support structure. The damper allowable temperature limits and hence the thermal design depends upon the temperature sensitivity of the damping fluid, the latter yet to be chosen. It may involve insulation from the antenna support and/or the use of a thermal blanket. The cooling effect of the approximate 12 hour shadow period caused by the communications antenna support reflector can be minimized by providing a pattern of holes through the reflector adjacent to the damper to allow incident solar radiation to be directly transmitted through the reflector to the damper.

3.9.1.3 Spinning Section

Upper Equipment Platform and Components

The high power density and high allowable temperature components in the communication subsystem (TWT's) are grouped in three patterns and mounted on the inside of the upper platform as shown in Figure 3.54. Heaters are located between each pair of TWT's to dissipate excess power caused by adjacent TWT failures and to maintain constant heat dissipation and resultant equipment temperatures on the platform during sunlit conditions.

A local increase in the platform internal face sheet thickness is provided in the TWT area by means of a .060" aluminum mounting plate (4.8 ft^2 total). The TWT's will be thermally coupled to the mounting plate, and the mounting plate to the platform face sheet by RTV-11 interface material. The .060" mounting plate serves to distribute heat laterally to be conducted through the platform and radiated to space. The lateral conduction of heat lowers operating baseplate temperatures and aids in maintaining non-operating TWT's within allowable temperature limits during eclipse conditions. Second surface mirrors ($\alpha = .1$, $\varepsilon = .8$) are mounted on the external face sheet of the platform in the high TWT power density mounting plate area (4.8 ft^2 total) to minimize absorbed solar radiation while maximizing the radiating ability of the platform. Second surface mirrors consist of vapor deposited silver on fused silica with an inconel flash coating for protection. Second surface mirrors have been utilized on several TRW spacecraft with a maximum total radiating area of 7 ft^2 on one spacecraft.

With second surface mirrors to reduce temperature fluctuations due to varying solar heat loads, and component heat load fluctuations minimized by TWT heaters, the upper component mounting platform may be decoupled from the array heat sink so that the external surface may see space directly without an intermediate surface. This allows the required radiating plate area to be reduced by a factor of two compared to a lower platform TWT installation concept. The net effect of the mounting platform seeing space directly and grouping the higher allowable temperature TWT's together is a weight reduction of approximately

15 pounds compared to a lower platform installation concept with high and low allowable temperature components intermingled.

The remaining low power density components in the communications, and possibly the telemetry and command systems are mounted directly to the inside face sheet of the platform. The external face sheet of the platform in this area is covered with multilayer aluminized Kapton insulation except for several small areas having second surface mirrors (TWT drivers (11 in^2 each) telemetry transmitter (56 in^2) and command receiver (19 in^2)).

The entire inside surface of the platform, and the external surfaces of the components will be coated with black paint (ε = .86) to equalize temperature differentials on the platform. An aluminized Mylar insulation blanket consisting of ten layers of 1/4 mil Mylar sandwiched between 2 layers of 2 mil Mylar will enclose the entire inside portion of the platform to distribute heat around the platform. The insulation also thermally decouples the upper platform from the solar array heat sink which would tend to decrease upper platform component temperatures below allowable temperature limits during reduced power eclipse conditions. Lower cost aluminized Mylar insulation is utilized in this area since it will not be exposed to ultraviolet and charged particle environments.

Lower Equipment Platform/Central Column

The equipment platform will be thermally decoupled (conductively) from the solar arrays and central column similar to the INTELSAT III design in order to maintain acceptable platform temperatures during eclipse when the arrays and cylinder cool appreciably. The surface coating on the forward and aft side of the platform will be painted white (ε = .85) or covered with VDA tape (ε = .04) as required to maintain platform temperature within acceptable limits.

The central column will be thermally decoupled (conductively) from the spinning section of the despin mechanical assembly by means of fiberglass insulators to minimize longitudinal temperature gradients in the assembly. The central column will be painted white (ε = .85) on the internal and external surfaces to distribute heat internally and dissipate soak back heat from the apogee motor.

Components (Figure 3.54) will be located above and below the platform. The battery, and PCU are the major sources of heat, and will be radiatively coupled with the solar arrays by white Cat-a-lac paint on the component surfaces to maintain acceptable temperatures during sunlit periods. The battery will be conductively decoupled from the equipment platform with honeycomb standoffs similar to INTELSAT III to minimize battery cooldown during eclipse by limiting heat conducted to the platform.

Thermal balance of the other components will be maintained by specifying surface coatings such as VDA tape (ε = .04) on low heat components and white paint (ε = .85) on high heat components surfaces. Thermal coupling by means of RTV-11 interface fillers on high heat components and thermal decoupling by means of fiberglass standoffs on low heat components will also be specified between the component baseplates and platform.

Solar Array and Aft Closure

The solar array substrate internal surface will be painted with white paint (ε = .85) to distribute heat within the enclosed portion of the spacecraft. White paint is selected to provide increased personnel visibility during assembly and checkout.

The aft closure will consist of a .005" stainless steel foil (bare on the internal surface ε = .15) coated with .003" of ($a = .2_{new}$, $a = .5_{degraded}$, ε = .85) high temperature white paint on the external surface similar to the INTELSAT III aft closure. The aft closure will be attached to, but insulated from, the solar array substrate aft stabilization ring, central cylinder, and apogee engine nozzle in a horizontal plane at least 5-1/2" forward of the apogee engine nozzle exit plane to minimize incident plume radiation. The high temperature white paint has a low absorptivity (a_p = .5) to the incident plume radiation as well as incident solar radiation to minimize absorbed heat while the high emissivity maximizes reradiation to maintain acceptable temperatures when heated externally. The low emissivity internal surface minimizes heat leak into or out of the spacecraft and can be coated with selected emissivity material to adjust spacecraft temperatures if required.

Apogee Motor

The apogee motor will be insulated with multilayer insulation to maintain apogee motor allowable temperatures during extended transfer orbit conditions. In order to withstand apogee motor case temperatures at the end of firing an aluminum foil and dexiglass multilayer insulation similar to that on INTELSAT III will be used. The insulation will be attached to the apogee motor. A sheet of aluminized Mylar will be installed across the nozzle exit cone to limit heat losses from the throat and nozzle prior to the motor being fired.

The thermal coupling between the apogee motor and the central column supporting the motor is minimized by means of fiberglass insulators. The decoupling requirement is necessary to reduce heat soak back from the apogee motor after firing.

Positioning and Orientation Subsystem Components

The propellant storage tanks will have a low emissivity surface finish, multilayer aluminized Mylar insulation blankets, and fiberglass structural attachment insulators to thermally decouple the tanks from varying surrounding temperatures caused by internal power variations and eclipse conditions. The propellant feed lines to the thrusters will be wrapped with multilayer aluminized Mylar insulation and attached to the surrounding structure with insulators. The axial thruster valve assembly will have a beryllium heat sink in contact with a high α/ε solar collector window in the solar array substrate to maintain propellant temperatures within allowable limits during eclipse conditions. A low emissivity beryllium surface finish (ε = .08) will minimize radiation away during eclipse, while the high α/ε incoloy solar collector (α = .56, ε = .11) will maximize temperatures prior to eclipse and minimize radiation away during eclipse.

Two radial thrusters will extend through the solar array to control longitudinal position and will operate in a pulsed mode. The plume will not impinge directly on the surrounding structure precluding local convective heating. Since the thrusters operate in a pulse mode only, local radiant heating from the thruster body will not be a problem. The axial thrusters extend through the end closures such that convective and radiant heating to the aft closure from the plume is insignificant. Insulation to limit radiant heating of the surrounding structure by the hot thruster body during extended axial mode firing and cool down will consist of alternating layers of stainless steel foil and microquartz separators with a gold coated stainless steel cover.

3.9.2 System Performance

3.9.2.1 Synchronous Orbit

The spacecraft will be oriented toward the sun during synchronous orbit. The spacecraft will experience a maximum eclipse time of 72 minutes every 24 hours when the sun angle is normal to the spin axis. As the sun angle with the normal to the spin axis increases in a positive or negative direction, the eclipse time will decrease reaching zero at a $\pm$ 8° angle. The spacecraft will encounter the following four synchronous orbit limit sun conditions. The maximum and minimum solar constants used for the limit cases are also given taking into account 3σ and seasonal variations.

	Solar Constant	
	Maximum (Btu/hr-ft^2)	Minimum (Btu/hr-ft^2)
Case 1 sun 0° off normal to spin axis - steady state	460	420
Case 1E eclipse transient - 72' using Case 1 as initial conditions	---	---
Case 2 sun +23-1/2° off normal to spin axis - steady state	440	400
Case 3 sun -23-1/2° off normal to spin axis - steady state	480	440

Two major spacecraft internal heating conditions will affect temperatures in addition to the solar heating and sun angles. The extent of solar array degradation will influence the amount of excess solar array power that is dissipated as heat in the shunts, while the number of TWT's operating will determine the amount of heat that is dissipated on the upper component mounting platform. Six TWT's not transmitting but operating will present maximum steady state heat conditions. Six TWT's transmitting will present minimum steady state heat conditions while two TWT's transmitting during eclipse will present minimum transient heat conditions. The TWT heaters that dissipate excess power for the three TWT failure case will prevent the upper equipment platform heat dissipation from falling below the minimum steady state condition.

3.9.2.2 Transfer Orbit

The spacecraft will be injected into a synchronous orbit transfer from a 100 n.m. parking orbit. Several transfer orbits may be required before the apogee motor places the spacecraft into synchronous orbit. To maintain spacecraft temperatures within allowable limits with a passive design during extended transfer orbit times, equipment will have to operate at near full power levels. Figure 3.50 presents a plot of spacecraft/sun angles experienced during transfer orbit for the three seasonal sun/earth angle conditions (summer solstice, spring and fall equinox, and winter solstice). The horizontal hour scale indicates the relative time at which the spacecraft is injected into the transfer orbit. The horizontal dotted lines represent spacecraft/sun angles of $\pm$ 23-1/2° off the normal to the spin axis similar to the sun angles experienced during synchronous orbit. It can be seen that by limiting the launch and parking orbit times, the spacecraft will see transfer orbit sun angles within the range seen during synchronous orbit.

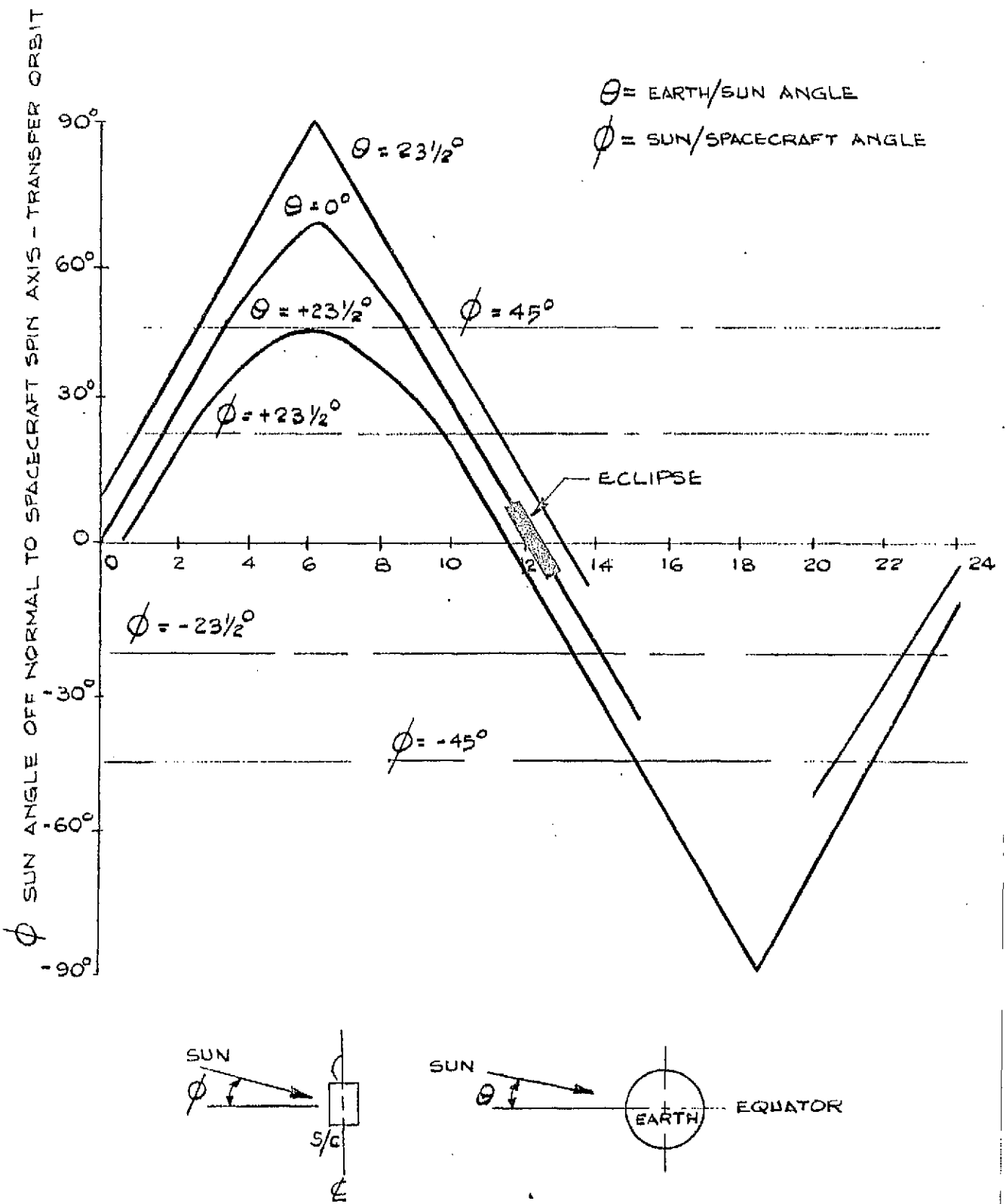

FIG. 3.50

LAUNCH TIMES TO OBTAIN GIVEN SPACECRAFT/SUN ANGLES DURING TRANSFER ORBIT.

Spacecraft sun angles up to ± 45°, which would still allow sufficient power output due to the excess array capacity at this time, are acceptable. Due to the low solar absorptivity thermal design features incorporated for optimum synchronous orbit performance, the increased solar load on the end closure and upper platform with even greater sun angles would not compensate for the loss of array power and internal component heating.

The ± 23-1/2° transfer orbit spacecraft/sun angle can be achieved by limiting launch times to approximately 4 hours out of every 24 while the ± 45° spacecraft/sun angle limits launch times to 12 hours out of every 24. Eclipse at apogee in the transfer orbit could exceed 2 hours for equinox conditions which would be excessively long to maintain temperature control even at full power. Figure 3.50 indicates this possibility by a dark line on the 0° sun/earth angles line. Proper selection of launch times during eclipse seasons can prevent such an eclipse from occurring. This consideration only applies four months of the year for near equinox launches with no restriction during the rest of the year.

Since the transfer orbit spacecraft/sun angles, eclipse times, and internal power levels can be maintained within synchronous orbit limits, the synchronous orbit performance will apply and be quite similar up to ± 45° spacecraft/sun angles. The apogee motor minimum temperature limit prior to firing, apogee motor radiant plume heating and soak back, associated specifically with transfer orbit conditions, have been discussed in the synchronous orbit section.

3.9.2.3 Earth Orbit

The spacecraft will be launched into earth orbit and remain attached to the booster. The spacecraft and booster will not be spinning, and the aerodynamic shroud will be removed. Due to the limited battery power, electrical components will not be operating and dissipating heat during earth orbit.

Spacecraft component temperatures might cool or warm slightly depending on whether launch is followed by earth eclipse or sun conditions. In either case temperatures will not change appreciably due to the heat capacity of the spacecraft and the limited earth orbit time. The earth orbit time will be limited to the first or second crossing of the equator (15 to 45 minutes).

3.9.2.4 Boost

The spacecraft will be protected by a shroud during boost that will not exceed 300°F based on past experience. Analysis of similar fairings indicates that the maximum radiant heat rate (.1 Btu/ft^2) from the shroud will be insignificant.

The shroud is normally separated when the external aerodynamic stagnation heating rate is below a level determined by spacecraft external material temperature limits and response times. A temperature limit in the order of 500°F, would require an aerodynamic free molecular stagnation heating rate of .35 Btu/ft-sec or less must exist before the shroud is separated.

The spacecraft will not be dissipating appreciable heat internally due to component operation in order to conserve battery power. The heat capacity of the spacecraft will limit significant temperature excursions during boost.

3.9.2.5 Ground Hold

When the spacecraft is enclosed in the shroud during ground hold, internal component heating must be limited or cooling air must be supplied to maintain components within allowable temperature limits. For example, 50 cfm of 70°F air directed over the external surface of the upper platform, would allow operation of the upper platform components. Natural convection cooling internal to the spinning section of the spacecraft in conjunction with the air being circulated in the shroud, would allow operation of lower platform components.

3.10 STRUCTURE

3.10.1 Spacecraft Structure

The spacecraft structure is between 13 and 14 ft. high and 55.4 inches in diameter. The maximum diameter is dictated by the shroud diameter and the allowable 55.4 inches is used. This leaves four inches clearance to the shroud. The solar array height is determined by the power requirement and is presently estimated at 74 inches. Above the array is the despun section consisting mainly of the communications antenna and its support and as presently conceived, it extends to between 70 and 80 inches above the array. Above this extends further the bicone antenna and protruding upwards from this is a VHF whip approximately 12 inches long. Hence overall height without the telemetry and command antenna is between 12 and 13 feet with an additional foot for the latter.

The satellite structural concept is as shown in Figures 3.53 and 3.55. The main load carrying central member consists of a series of cylinders and conical frustrums. This main member transmits the load down to the spacecraft adapter. Connected to the inside of this central member in the bottom half is the apogee motor which dictates the diameter of the lower section. Two equipment decks are mounted to the outside of this central member, one at about mid-height and the other near the top. They are supported on it by brackets and struts. The solar panels are supported at the outside of the bottom one of these decks and are stiffened by four rings around the inside of the panels. The despin mechanism is connected at the top of the central member.

The largest quasistatic longitudinal load on the central member occurs during apogee motor firing and could be as high as 15g. However a larger load will probably be placed on this member during random vibration. To design for this case the pessimistic assumption is made that the maximum longitudinal g levels at the resonances of the various components all occur together and in addition a 3g cross-talk occurs. The components considered are the antennas, the solar array, the upper equipment deck, the lower equipment deck, the despin mechanism, the apogee motor and the central cylinder. The g levels at the resonances of the various components are estimated from analyses carried out on similar structures. The first failure mode is buckling of the walls of the central member under combined axial compression and bending. Investigations carried out for these loads indicate that a cylinder

of wall thickness 0.060" of 6061 aluminum is required for the section at the bottom supporting the heavy apogee motor. A section of thickness 0.040" of 6061 aluminum is required for the section above this supporting the lower deck and for the section above this a section having 0.040" wall thickness of magnesium is required. It is considered preferable for ease of manufacturing, to have a section of 0.040" wall thickness of magnesium rather than use a thinner section of aluminum. The weight of the central member for a 74 inch height of solar panel is about 21 lb.

There are rings distributed along the central member providing direct support for the apogee motor, the decks, the struts from the decks and also the interface with the spacecraft adapter. These rings weigh a total of about 11 lb.

The top deck carries the communications equipment thus ensuring short lead lengths to the rotary joint inside the central member. It also supports auxiliary heaters which are turned on in sunlight if one or more of the TWT's are off. This ensures that the power dissipation on this deck is relatively constant in sunlight and level temperatures can be maintained. The telemetry and command system components may also be placed on this deck. The deck is relatively lightly loaded compared to the bottom deck and one inch thick aluminum honeycomb with 0.012" thick aluminum face sheets are considered satisfactory. The weight of this deck is about 9 lb.

The bottom deck carries the propulsion equipment, the batteries, the power control electronics and possibly the telemetry and command system. Also on its outside edge is supported the solar array by means of a fibreglass array support ring. The bottom deck is thus relatively heavily loaded and one inch thick aluminum honeycomb with 0.020 inch thick aluminum face sheets are considered necessary. The weight is between 11 and 12 lb.

Each deck is supported by eight struts towards the outer edge, the struts sloping at about 45° to the spacecraft longitudinal axis down to the central member. Brackets at two ends of these struts can be made of magnesium, thus reducing their weight. The solar panels are stiffened at both ends and at two intermediate positions with rings.

The total weight of the spacecraft structure for a 74 inch high solar array is 73.5 lb. More detailed stress analyses may indicate that savings can be made but the present weight does seem to be reasonable when compared with other communications satellites having the same structural concept.

3.10.2 Antenna Structure

3.10.2.1 Primary Reflector

The primary reflector is presently considered to be $\frac{1}{4}$" thick aluminum honeycomb with 0.006" aluminum facing skins. The antenna face is very approximately elliptical and measures 92" x 31" along each axis measured along the surface. It is highly curved in the vertical direction but maximum curvature in the horizontal direction gives a depth of about 1.5 inches. The estimated weight is between 4 and 4.5 lb. It is expected that when the actual shape is determined a detailed stress and dynamic analysis will indicate the required overall thickness and the skin thickness. The reflector can be stiffened by a factor of 4 if necessary by increasing its thickness with a weight penalty of only 0.75 lb. It is planned to paint the concave surface of the reflector with white paint and to have highly emissive evaporated aluminum on the convex surface. Such a reflector will have a very low temperature differential between surfaces (estimated as less than 2°F). These temperature differentials along the surface have been computed to cause acceptably small temperature deformations.

3.10.2.2 Antenna Support Structure

Because of the probable shallow curvature of the primary reflector in the horizontal direction, it has been assumed that there is no inherent 'shell-type' stiffness but simply that due to its own thickness.

The antenna tip is about 80 to 85 inches above the solar array which is 76" above the separation plane. Because of this great height then it will be subject to high g levels during lateral vibration qualification testing (estimated at between 30 and 60 g) and it is important that the antenna support structure be strong enough to withstand these levels. Also, the antenna support structure must be still enough to give a reasonably high (say above 25 cps) resonant frequency. This means that the structure must be stiff in both bending and torsion. A further requirement of the antenna support structure is for it to have small thermal deformations for all sun orientations. Thermal deformations effect both the absolute direction in which the antenna points and the relative positioning of the feed, the secondary reflector (if there is one) and the primary reflector.

A number of support structures for the antenna have been considered. These have included structures with different stiffener patterns up the back, many truss type configurations and also many pipe support configurations. Several combinations have also been

considered. A truss type structure running up the back of the primary reflector has the advantage of being relatively light in weight but much bracing is needed to make it very stiff in all directions. A multitude of such bracing could also lead to manufacturing difficulties with much weight being used up with brackets at the joints. A more severe disadvantage is that under particular sun orientations the elements of the truss will be at widely different temperatures. It has been estimated that the temperature difference which would occur for unfavourable sun orientations in legs of the same truss would be 50°F whereas if a two tower support structure were used (one tower on each side of the antenna) then there could be as much as 150°C between towers. These temperature differentials cause truss and antenna deformations resulting in significant antenna pointing errors. This effect could be reduced by placing a thermal insulation tent over the tower but it is expected that the pointing errors would still be substantial.

A support structure consisting of a series of pipe sections has the advantage of having a much smaller temperature deformation resulting in acceptably small pointing errors, it being calculated that the maximum possible error is less than 0.05°. It also is a structure that is inherently stiff in both bending and torsion. In addition adjustable attachment points to the main reflector can be readily integrated with it. It is a little heavier than most truss structures but it is considered that the extra weight is worth the above advantages. The presently designed primary reflector support weighs 8.5 lb. This is a first estimate based on tentative stress and structural dynamics computations. It is felt that it may be a little pessimistic and more detailed stressing will probably show that weight reductions can be made. Such a detailed analysis of course is also dependent on the physical shape of the final antenna. The pipe support structure consists of four equal diameter pipe sections welded together. Each of the sections are of uniform wall thickness with the wall thickness diminishing towards the top of the structure. This ensures that they can be bought off the shelf and will be relatively inexpensive. Weight savings could be made with tapered sections but these would be more costly.

The details of the attaching points may be different to that shown on figure 3.55 but the necessary support will be determined by stress and dynamic analysis on the final design. It is planned to use 6061 Aluminum for the support structure. Other materials including magnesium, magnesium lithium alloy, titanium and beryllium have been considered. Beryllium is the only one appearing to have significantly better physical parameters than aluminum. It

is two thirds the density of aluminum and is four times as stiff. From this it can be determined that the weight of the beryllium support structure giving the same resonant lateral frequency of the overall despun structure would be about 60% that of aluminum. However manufacturing would be costly due to the difficulties of working with beryllium. If the spacecraft weight becomes extremely critical then the potential 3 lb. saving may be considered worth the cost but it is not expected that this will be so.

The bicone antenna will be supported on top of the support structure as shown in Figure 3.5.3, the coaxial cable running from the rotary joint up inside the pipe support. The VHF whip antenna will protrude from the centre of the bicone. The damper will be connected to the pipe support (see Section 3.11).

The antenna may be offset as shown in Figure 3.51 or center fed as shown in Figure 3.52. A larger support would be required for the offset antenna.

3.11 Weight and Dynamic Stability

3.11.1 Spacecraft Weight

The spacecraft weight estimate is detailed in Table 3.11.1. This configuration will be capable of giving six channel operation in sunlight and two channel operation in eclipse. The required solar array height is 74.0".

Since many of the subsystem weights are based on similar previous designs the estimate is expected to be quite realistic. The communications system and the structure are the ones that are most likely to change. The contingency of 37.1 lb. appears to be adequate in that it compares favourably with accepted levels of 10% of spacecraft dry weight (39.6 lb.) or 3.5% of transfer orbit weight (32.5 lb.). The apogee motor weight was calculated for a spacecraft weight of 965 lbs. and a velocity increment of 6040 ft./sec. The hydrazine propellant was calculated for a total velocity increment of 1144 ft./sec.

The configuration on which the weight estimate is based gives adequate contingency in both EIRP and weight. However, either one can be increased at the expense of the other. The beam edge EIRP could be reduced 0.5 db by reducing the solar array to 67.0" in height. This would decrease the solar panel weight by 4.2 lb. and the structure weight by 2.4 lb., thus increasing the weight contingency to 43.7 lb.

3.11.2 Dynamic Stability

Assuming the full launch vehicle capability of 965.0 lb. is used then the spacecraft weight after apogee motor burn will be 507 lb. and the end of mission weight will be 438 lb. (it being assumed that 69 lb. of the propellant will be used, the remaining 2 lb. being unavailable). The spin axis moment of inertia of the spinning spacecraft section will be approximately 40 slugs ft^2 at booster separation, 34 slug ft^2 after apogee motor burn and 30 slug ft^2 at the end of mission. The transverse moment of inertia of the complete spacecraft will be approximately 130 slug ft^2 at booster separation, 90 slug ft^2 after apogee motor burn and 88 slug ft^2 at the end of mission. The ratio at all three stages will then be approximately 1:3. Because this is less than one then, for dynamic stability, the damper will need to be positioned on the spacecraft despun section. Also, because the ratio is low it indicates that any disturbance torque on the spacecraft will cause a relatively low amplitude coning motion.

Table 3.11.1

Spacecraft Weight Estimate

6 Channel Sunlight Operation
2 Channel Eclipse Operation

Subsystem		Weight (lb.)
Communications		51.3
Communications Antenna and Support		16.3
Telemetry and Command		18.0
Telemetry and Command Antennae and Support		1.6
Electrical Power		81.9
Solar Array	49.5	
Batteries	21.0	
Power Electronics	11.4	
Electrical Integration		17.2
Attitude Determination and Control		32.1
Structure ;		73.5
Thermal Control		16.4
Positioning and Orientation		85.6
Dry System	14.6	
Propellant	71.0	
Apogee Motor		531.0
Inert Motor	73	
Propellant	458	
Balance Weights		3.0
Contingency		37.1
Total Spacecraft		965.0 Lb.

The damper will need to be placed far enough from the spacecraft principal axis that the centrifugal field will force it against the stop and thus prevent damping in the failure condition when the complete body is spinning at the one rate. However, it must be positioned such that, in the idling mode, it will not be forced against its stop, and damping will occur. Also, the further it is placed above the spacecraft centre of gravity, the more quickly it will damp out nutation. However, the latter is not critical in that satisfactory damping will occur for most positions on the despun section. The type of attachment as shown in Figure 3.53 will give enough flexibility to locate the damper within the above limitations.

3.12 Reliability Assessment

A preliminary reliability assessment is shown in Table 3.12.1. The reliability numbers were calculated in most cases by comparison with similar type equipment used in Intelsat III. Where no similar equipment presently exists, the reliability was arrived at by a part count assessment. The following equipment is completely redundant:

1) All the electronics in the antenna despin system and the attitude determination system,

2) The telemetry and command system,

3) The hydrazine propulsion system, and

4) All the electronics in the communication system except for the output TWT's.

No attempt has yet been made to optimize the overall system reliability versus cost, weight, and performance. In the second phase of the study, a detailed reliability sensitivity matrix will be developed which will be used to optimize the system reliability.

Table 3.12.1

Reliability Assessment

	Equipment	Reliability (5 Years)	
1.	Attitude Control	.917	
	Despin Antenna		.9484
	Attitude Determination		.9729
2.	Propulsion	.983	
	Apogee Motor		.994
	Positioning & Orientation		.9833
3.	Electrical Distribution	.9989	
	Electrical Integration		.999
	Harness		.9999
4.	Structure	.9995	
5.	Electrical Power	.943	
	Solar Array		.9985
	Battery		.985
	Power Control Unit		.964
	Converter		.995
6.	Telemetry & Command	.910	
	Satellite Reliability less Communications		0.771
7.	Communications		
	4 out of 6 for 5 years	.975	
8.	Overall	.723	

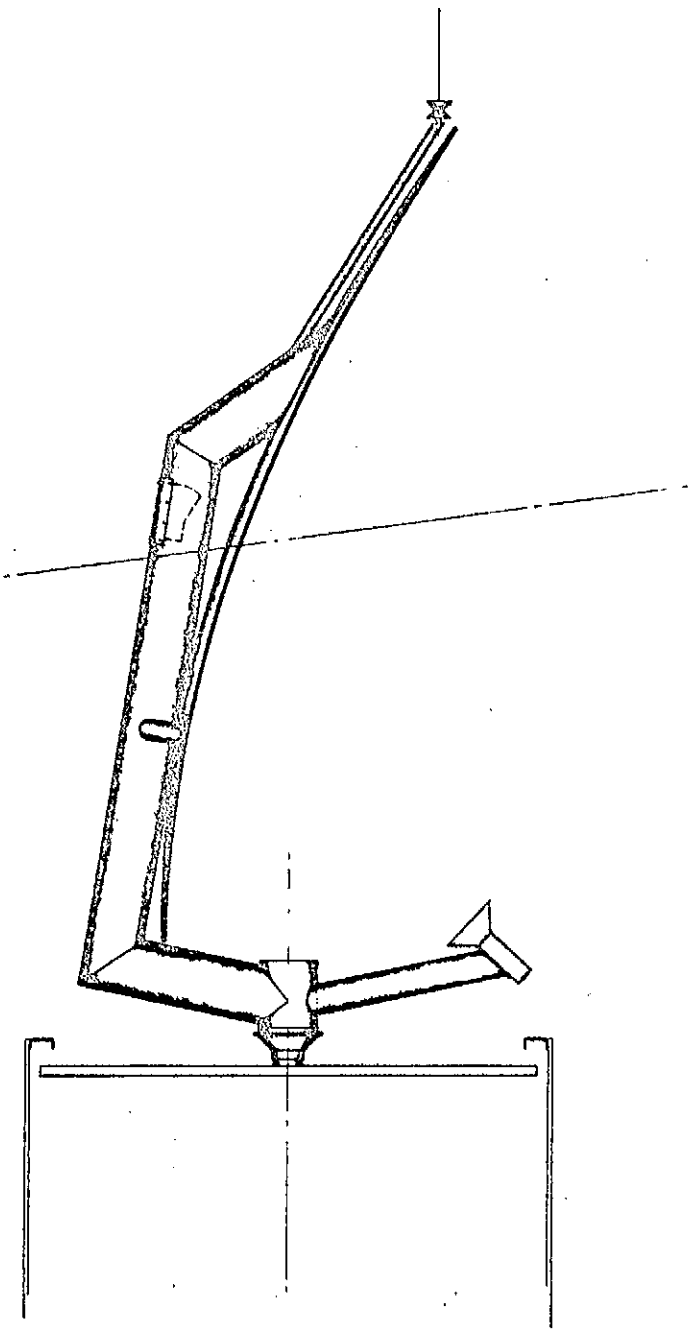

FIG. 3-51

OFF-SET FEED SYSTEM
COMMUNICATIONS ANTENNA

DWG. CDCS-SK-108 JAF 2 AUG. 68

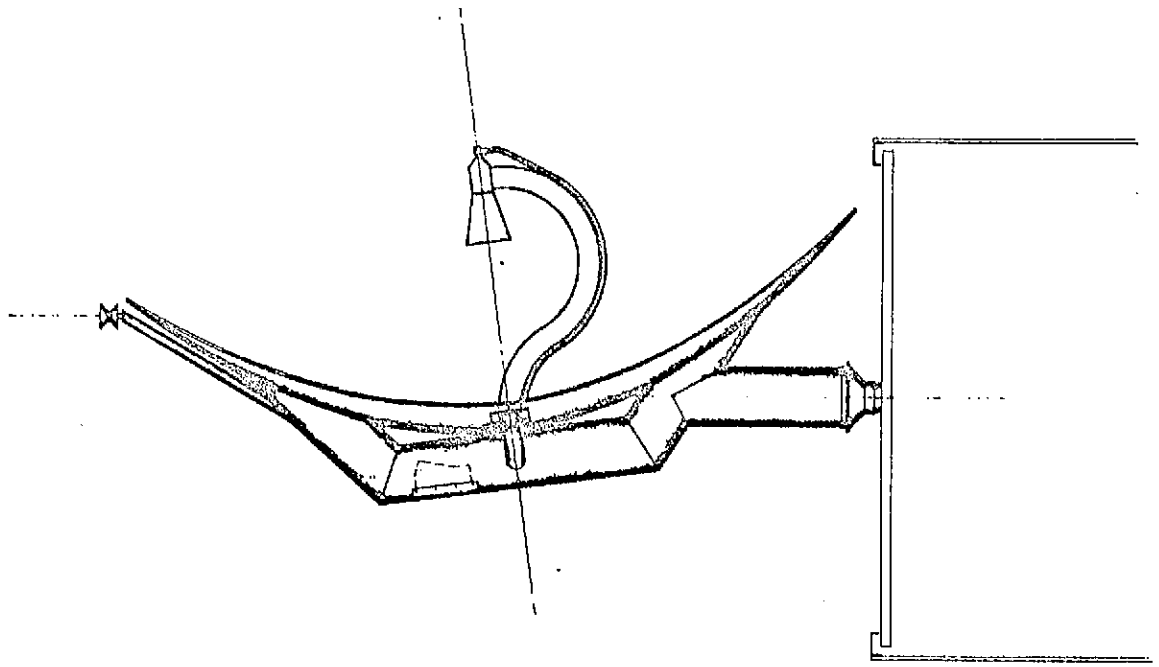

DIRECT FEED
20·0 FOCUS

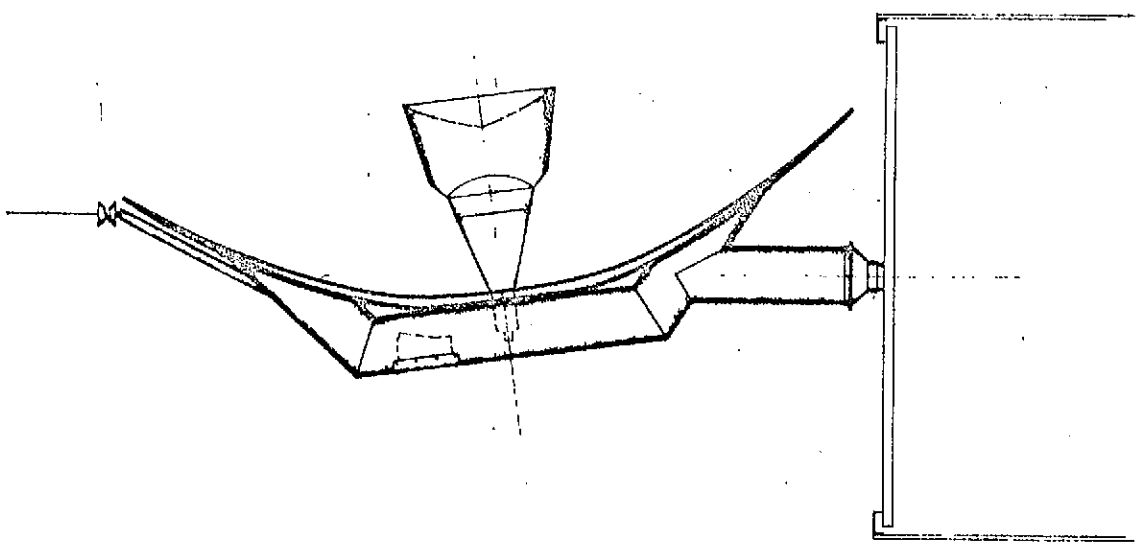

SUB-REFLECTOR FEED
24·1 FOCUS

FIG. 3·52
ALTERNATE FEED SYSTEMS
COMMUNICATIONS ANTENNA

DWG. CDC5-5K-105 JAF 1 AUG. 68

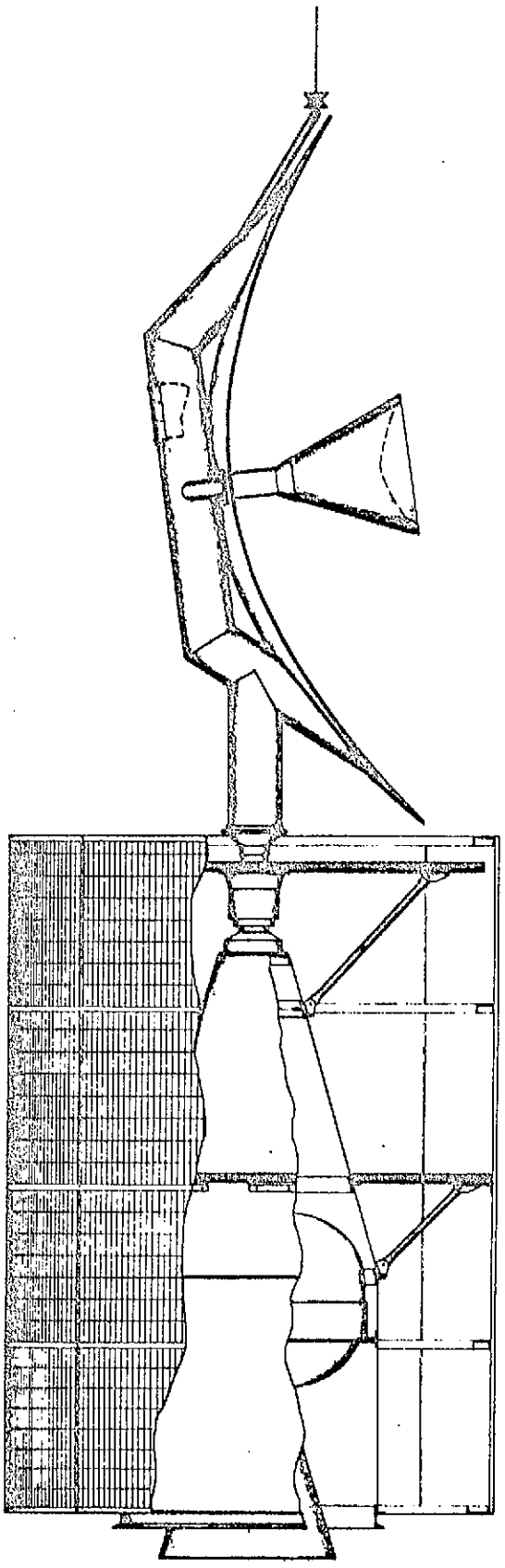

FIG. 3·53

SPACECRAFT
STRUCTURAL ARRANGEMENT

DWG. CDCS-SK-107 JAF 2 AUG.68

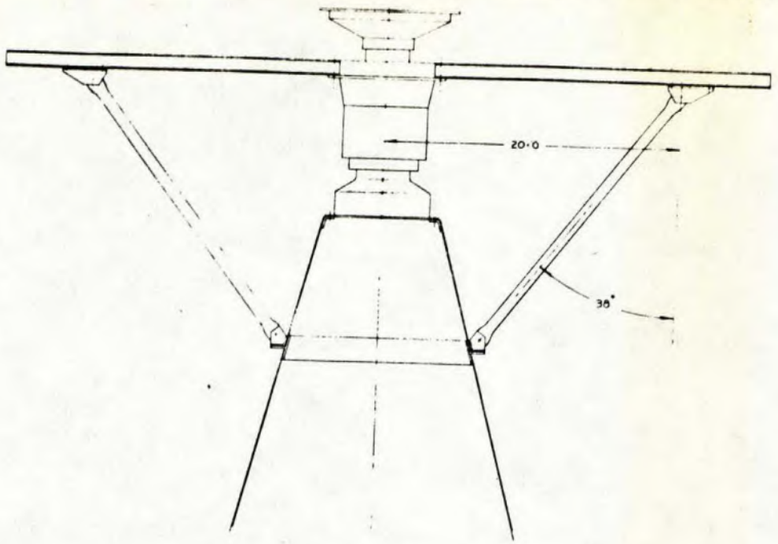

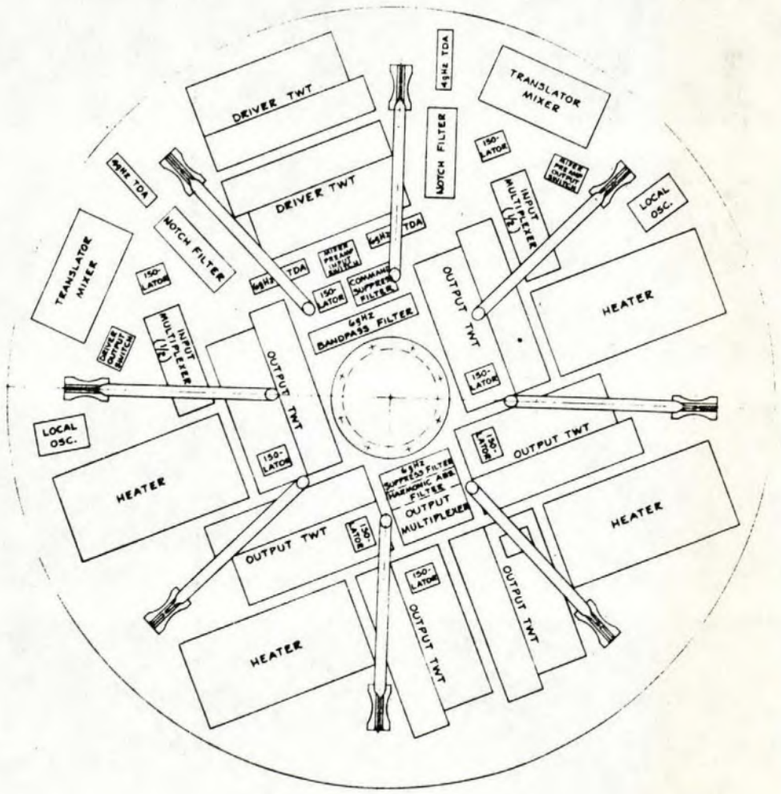

PAYLOAD ARRANGEMENT
FORWARD DECK - AFT SIDE

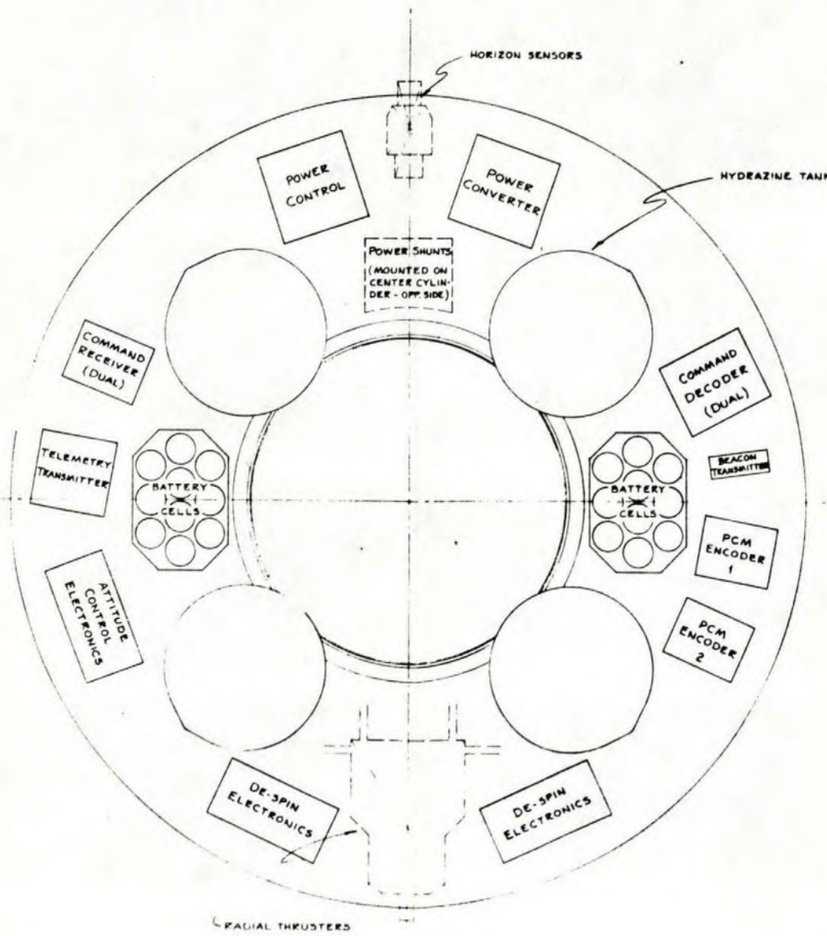

PAYLOAD ARRANGEMENT
AFT DECK - FORWARD SIDE

FIG. 3·54

PRELIMINARY
PAYLOAD ARRANGEMENT
FORWARD AND AFT DECKS
DWG CDCS-SK-103 JAF 12 JULY 68

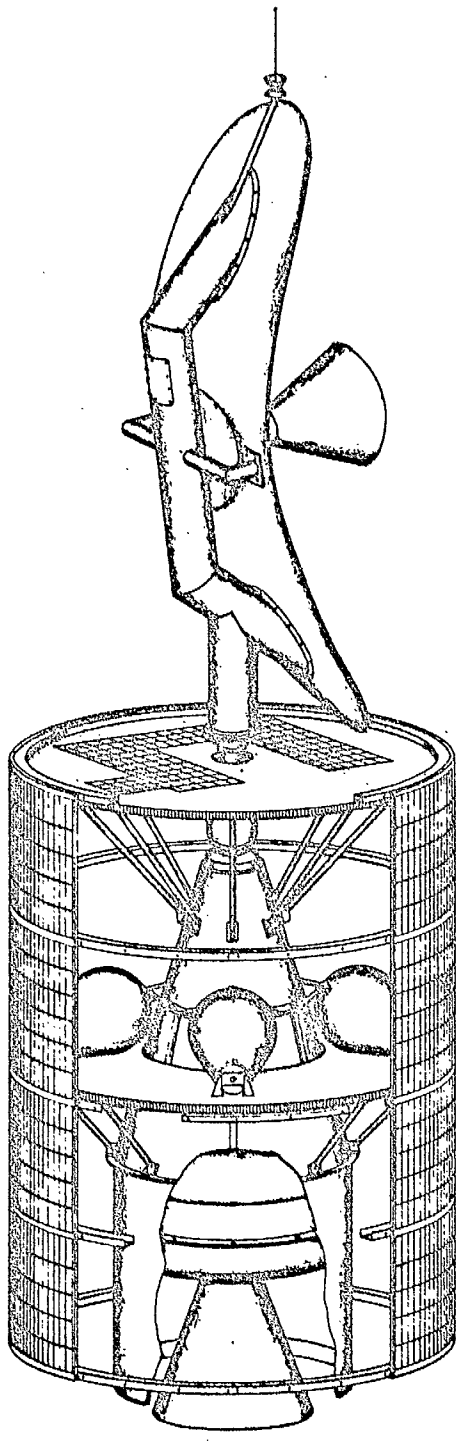

FIG. 3·55